THE ASTROPHYSICAL JOURNAL

An International Review of Spectroscopy and Astronomical Physics

FOUNDED IN 1895 BY GEORGE E. HALE AND JAMES E. KEELER

EDITORS

PAUL W. MERRILL
Mount Wilson Observatory of the Carnegie Institution of Washington

HARLOW SHAPLEY
Harvard College Observatory Cambridge, Massachusetts

J. H. MOORE
Lick Observatory University of California

OTTO STRUVE
Yerkes Observatory of the University of Chicago

COLLABORATORS

S. B. NICHOLSON, *Mount Wilson Observatory;* D. B. MCLAUGHLIN, *University of Michigan;* J. A. PEARCE, *Dominion Astrophysical Observatory, Victoria;* S. A. MITCHELL, *Leander McCormick Observatory;* LYMAN SPITZER, JR., *Yale University;* W. W. MORGAN, *Yerkes Observatory;* CECILIA H. PAYNE GAPOSCHKIN, *Harvard College Observatory;* H. N. RUSSELL, *Princeton University;* F. H. SEARES, *Mount Wilson Observatory*

VOLUME 100

JULY–NOVEMBER 1944

THE UNIVERSITY OF CHICAGO PRESS
CHICAGO, ILLINOIS

THE CAMBRIDGE UNIVERSITY PRESS, LONDON

PUBLISHED JULY, SEPTEMBER, NOVEMBER, 1944

COMPOSED AND PRINTED BY THE UNIVERSITY OF CHICAGO PRESS
CHICAGO, ILLINOIS, U.S.A.

CONTENTS

NUMBER 1

PAGE

BN Monocerotis: An N-Type Variable. Frank K. Edmondson and Henry Giclas . 1

The Spectroscopic Binary 31 Cygni. Julie M. Vinter Hansen 8

Spectroscopic Observations of 48 Librae. Paul W. Merrill and Roscoe F. Sanford . 14

Investigations on Proper Motion. XXIII. The Proper Motion of the Cluster *h* Persei. Adriaan van Maanen 31

The Photographic Determination of Stellar Parallaxes with the 60- and 100-Inch Reflectors. Nineteenth Series. Adriaan van Maanen 55

Orbit of the Ninth Satellite of Jupiter. Seth B. Nicholson 57

The Spectrographic Orbit and Light-Variations of η Geminorum. Dean B. McLaughlin and Suzanne E. A. Van Dijke 63

Comparison of the λ 3883 *CN* Band in the Spectra of Comets 1940c and 1942g. Andrew McKellar 69

On the Radiative Equilibrium of a Stellar Atmosphere. II. S. Chandrasekhar . . 76

On the Absorption Continuum of the Negative Oxygen Ion. Rupert Wildt and S. Chandrasekhar 87

Studies of Faint B-Type Stars. II. Daniel M. Popper 94

Recent Progress in Astrophysics

An Upper Limit for the Mass of the Lunar Atmosphere. Otto Struve 104

A. Unsöld's Work on the Spectrum of the B0 Star τ Scorpii. Otto Struve . . . 105

Notes

Note on the Epoch of the Next Sunspot Maximum. W. Gleissberg 114

Reviews 115

NUMBER 2

On the Radiative Equilibrium of a Stellar Atmosphere. III. S. Chandrasekhar . 117

Effect of Temperature on the Wave Length of a Transmission Band of the Interference Polarizing Monochromator. Edison Pettit 128

Doubly Ionized Rare Earths in α^2 Canum Venaticorum. P. Swings 132

The Resolution of Messier 32, NGC 205, and the Central Region of the Andromeda Nebula. W. Baade 137

NGC 147 and NGC 185, Two New Members of the Local Group of Galaxies. W. Baade 147

The Helium Anomaly in ϕ Persei. J. A. Hynek 151

Partially Degenerate Stellar Models. Gordon W. Wares 158

Some Remarks on the Negative Hydrogen Ion and Its Absorption Coefficient. S. Chandrasekhar 176

PAGE

THE SPECTROSCOPIC ORBIT OF BD VIRGINIS. Otto Struve, Carlos U. Cesco, and Jorge Sahade 181

THE ECLIPSING STAR BD VIRGINIS. Cecilia Payne Gaposchkin 186

RADIAL VELOCITIES OF TWENTY STARS OF EARLY TYPE IN AND NEAR THE GALACTIC CLUSTER NGC 6231. O. Struve 189

NOTE ON THE DOUBLE WHITE DWARF L 462-56 = LDS 275. W. J. Luyten 202

A STUDY OF THE WOLF-RAYET ECLIPSING BINARY HD 193576 = V 444 CYGNI. Zdeněk Kopal 204

PROVISIONAL ELEMENTS OF THE ECLIPSING BINARY V 444 CYGNI. Henry Norris Russell . 213

NOTES

NOTE ON THE LATITUDE VARIATION OF THE SUNSPOT BELTS. W. Gleissberg 219

NUMBER 3

THE ECLIPSING SYSTEM SX CASSIOPEIAE. Sergei Gaposchkin 221

THE ECLIPSING SYSTEM RX CASSIOPEIAE. Sergei Gaposchkin 230

THE WOLF-RAYET ECLIPSING VARIABLE HV 11086 = HD 214419. Sergei Gaposchkin . 242

THE ECLIPSING STAR AR MONOCEROTIS. Cecilia Payne Gaposchkin 251

REGRESSION LINES AND THE FUNCTIONAL RELATION. Frederick H. Seares 255

RELATION BETWEEN COLOR INDEX AND EFFECTIVE WAVE LENGTH FROM THE OBSERVATIONS OF HERTZSPRUNG AND VANDERLINDEN. Frederick H. Seares and Mary C. Joyner 264

COSMIC STATIC. Grote Reber 279

ON THE ORIGIN OF SMOKE PARTICLES IN THE INTERSTELLAR GAS. D. ter Haar . . . 288

SOLAR CONCENTRATIONS OF THE HYDROXYL RADICAL. Robert J. Dwyer 300

A REPORT ON NEW SPECTROGRAPHIC MATERIAL OF 13 CETI. Carl August Bauer . . 302

THE INTERACTION OF A PROTON AND A HYDROGEN ATOM IN ITS EXCITED STATES. Margaret K. Krogdahl 311

THE INTERACTION OF A PROTON AND A HELIUM ATOM IN ITS EXCITED STATES. Margaret Kiess Krogdahl 333

THE GENERALIZED COWLING MODEL. Marjorie Hall Harrison 343

AN APPROXIMATE SOLAR MODEL ON BETHE'S LAW OF ENERGY GENERATION. N. R. Sen and U. R. Burman 347

ON THE RADIATIVE EQUILIBRIUM OF A STELLAR ATMOSPHERE. IV. C. U. Cesco, S. Chandrasekhar, and J. Sahade 355

THE RADIAL VELOCITIES OF THE PLEIADES. Burke Smith and Otto Struve 360

THE SPECTROSCOPIC ORBIT OF AR MONOCEROTIS. Jorge Sahade and Carlos U. Cesco . 374

TITAN: A SATELLITE WITH AN ATMOSPHERE. Gerard P. Kuiper 378

THE WOLF-RAYET TYPE SPECTROSCOPIC BINARY HD 152270. Otto Struve 384

RECENT PROGRESS IN ASTROPHYSICS

"PHYSICAL CHARACTERISTICS OF THE ATMOSPHERES OF SUPERGIANTS OF CLASSES cB5 TO cA3" BY G. A. SHAJN. O. Struve 388

NOTES

A CHANGE IN THE SPECTRUM OF 39ϵ CAPRICORNI. O. Struve and A. J. Deutsch . . 390

INDEX 391

THE ASTROPHYSICAL JOURNAL

AN INTERNATIONAL REVIEW OF SPECTROSCOPY AND ASTRONOMICAL PHYSICS

VOLUME 100 JULY 1944 NUMBER 1

BN MONOCEROTIS: AN N-TYPE VARIABLE

FRANK K. EDMONDSON AND HENRY L. GICLAS

Kirkwood Observatory, Indiana University

and

Lowell Observatory, Flagstaff, Arizona

Received April 4, 1944

ABSTRACT

Photographic, photovisual, and photo-red observations made with seven different telescopes at the Kirkwood, Lowell, and Harvard observatories are used to study the light and color variation of this N-type variable.

Sequences based on polar comparisons are given for the three colors.

The photographic light-curve, based on 154 observations, covers an interval of nearly 19 years. It shows a semiregular type of variation with an amplitude of 3 mag. *The photovisual light-curve*, based on 80 observations, is in phase with the photographic light-curve, but the amplitude is only 1 mag. *The photo-red light-curve*, based on 30 observations, has a still smaller amplitude. The variation seems to take place in cycles of 500 days; but smaller fluctuations of shorter period are also present.

The color index varies from $+4^m$ to $+6^m$. It is strongly correlated with the photographic magnitude and only slightly correlated with the photovisual magnitude.

The red index varies from $+5^m5$ to $+7^m5$ and is strongly correlated with the photographic magnitude. There is little or no correlation with the photo-red magnitude.

INTRODUCTION

BN Monocerotis is No. 18 in the list of red stars published by Merrill, Sanford, and Burwell.[1] The spectral class was given as N, and this was later confirmed by Sanford,[2] who also found the radial velocity to be +28 km/sec. This star also appears as No. 1529 in the recent Dearborn list of red stars[3] and as No. 41 in an earlier list.[4]

The variability of BN Monocerotis was discovered at the Lowell Observatory by Edmondson and Rogers,[5] who published provisional photographic and photovisual sequences and found a mean color index of nearly 5 mag. Photographic and photovisual observations have been continued at Flagstaff by Giclas and at Indiana by Edmondson. In addition to this, a photo-red sequence has been set up and photo-red observations

[1] *Pub. A.S.P.*, **45**, 306, 1933.

[2] *Pub. A.S.P.*, **47**, 273, 1935; also *Ap. J.*, **82**, 202, 1935.

[3] *Dearborn Ann.*, **5**, Part IA, 1943.

[4] *Dearborn Ann.*, **4**, Part 16, 1940.

[5] *Pub. A.S.P.*, **47**, 191, 1935.

made regularly since September, 1939. Photographic magnitudes have also been estimated by Edmondson on plates in the Harvard collection. The desire to accumulate additional observations has caused several postponements of the publication of this paper; but it now appears that no useful purpose will be served by further delay.

THE OBSERVATIONS

The observations published in Table 5 were made with seven different telescopes. These instruments and the symbols used for identifying them are given in Table 1, together with the systematic corrections that were applied to the measured magnitudes to reduce them to a uniform system.

TABLE 1

Symbol	Instrument	Δm_{pg}	Δm_{pv}	Δm_{pr}
a	8-inch reflector, Kirkwood	-0^m4	0.0	0.0
b	24-inch reflector, Kirkwood	− .4	.0	.....
c	13-inch refractor, Lowell	.0	0.0	0.0
d	8-inch (I) refractor, Harvard	.0	.....	.....
e	8-inch (IR) refractor, Harvard	.0	.....	.....
f	10-inch (MF) refractor, Harvard	− .6 near center	.....	.....
		− .4 near corner	.....	.....
g	16-inch (MC) refractor, Harvard	+0.5	.....	.....

TABLE 2

Star	m_{pg}	Star	m_{pg}	Star	m_{pg}	Star	m_{pg}
8	12.55:	2	13.80	4	15.15	6	15.75
1	13.45	3	14.30	5	15.50	7	15.50:

a) PHOTOGRAPHIC MAGNITUDES

The possibility of systematic errors in the magnitudes of red stars derived from comparison with stars of small color index is well known, and one usually tries to select comparison stars of the same color as the variable. This is not possible in the present case, nor has it seemed advisable to extrapolate the known color corrections of the various instruments. Instead, an attempt has been made to reduce the magnitudes to the system of the 13-inch Lawrence Lowell telescope by application of corrections derived from the various overlapping series of observations. For example, c and d can be compared by means of the observations in March and April, 1935; a and c by means of the observations in March and October, 1939; etc.

The comparison stars and magnitudes used are the same as those given by Edmondson and Rogers.[5] For convenience, they are repeated here in Table 2 and Plate I, *a*.

The comparison stars are close to the variable; and Edmondson has derived magnitudes by direct visual estimates, except for the early Flagstaff plates, which were measured originally with a scale plate and later checked by direct visual estimates. Giclas has used a Stetson-type photometer for the measurement of his plates.

b) PHOTOVISUAL MAGNITUDES

The photovisual sequence has been revised by Giclas, and the new magnitudes are given in Table 3. The stars can be identified with the aid of Plate I, *b*.

PLATE I

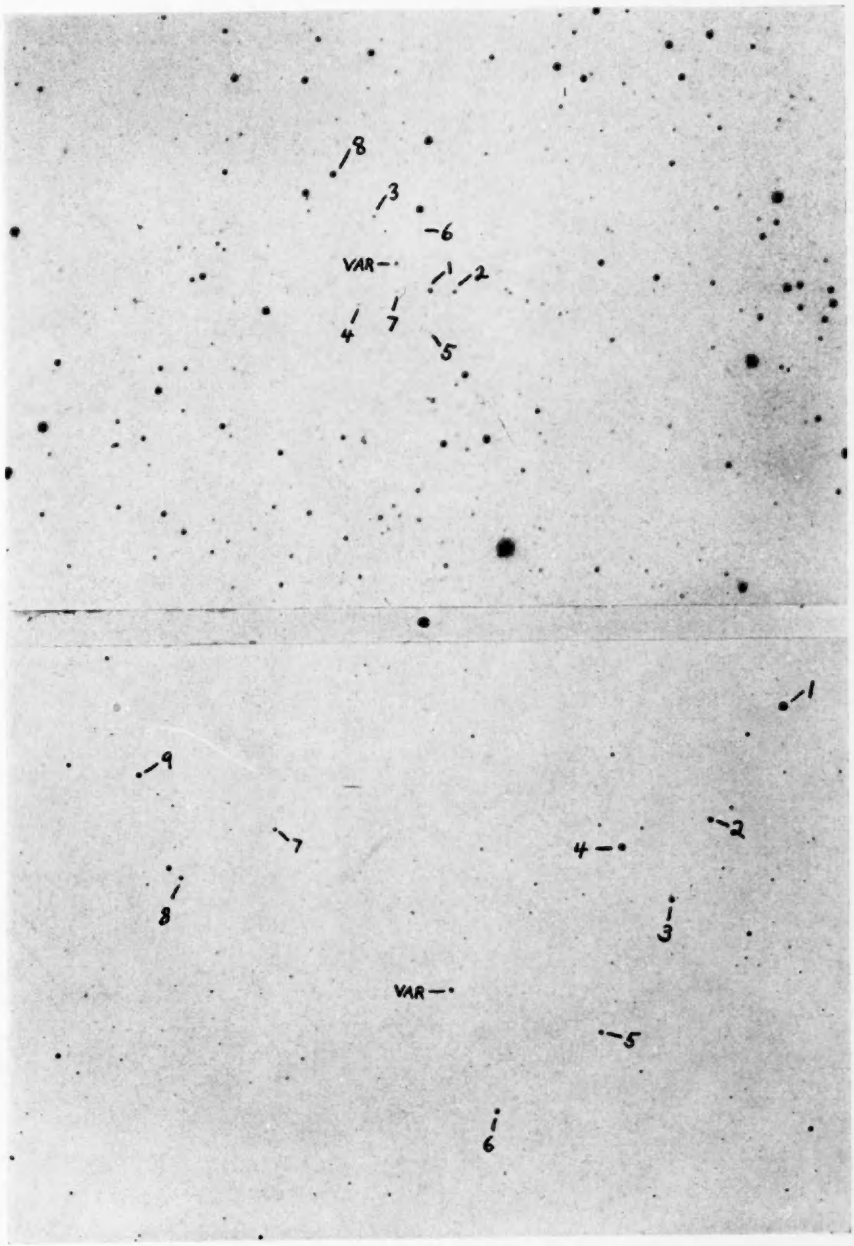

(*a*) PHOTOGRAPHIC SEQUENCE; (*b*) PHOTOVISUAL AND PHOTO-RED SEQUENCE
The scale of (*a*) is 14″.0 per mm; that of (*b*), 33″.4 per mm

Observations of the photovisual magnitude have been made only at the Lowell and Kirkwood observatories. Edmondson has measured the Indiana photovisual plates with a Ross-type photometer,[6] and Giclas has measured the Flagstaff plates with a Stetson-type photometer. There is some indication that comparison star No. 3 is variable.

c) PHOTO-RED MAGNITUDES

The adopted photo-red sequence is based on three polar comparisons made by Giclas and has been checked by two additional polar comparisons made by Edmondson. The magnitudes are given in Table 4, and the stars can be identified with the aid of Plate I, *b*.

Photo-red observations have been made at Indiana and Flagstaff, and the method of measurement is the same as for the photovisual plates. Comparison star No. 3 seems to be variable, in agreement with the photovisual observations.

TABLE 3

Star	m_{pv}	Star	m_{pv}	Star	m_{pv}	Star	m_{pv}
1	6.75	3	(8.30)	5	9.10	7	9.65
2	8.45	4	7.55	6	8.45	8	9.60

TABLE 4

Star	m_{pr}*	Star	m_{pr}*	Star	m_{pr}*	Star	m_{pr}*
1	6.75	4	7.45	6	8.10	8	9.15
2	8.15	5	8.50	7	9.25	9	7.70
3	(7.85)						

* System of *Harvard Ann.*, Vol. **89**, No. 5.

Thanks are due to Herbert S. Gutowsky and J. Lynn Smith for taking most of the Kirkwood Observatory 8-inch reflector plates (indicated by a in Table 5). Gutowsky took 41 plates and Smith took 11 in 1939 and the early part of 1940. Smith continued through the early part of 1942 and added 62 more plates to the series.

DISCUSSION

a) THE LIGHT-CURVES

The observations listed in Table 5 are shown graphically in Figure 1. The photographic light-curve covers an interval of nearly nineteen years and shows a semiregular type of variation. During the period between 1925.2 and 1934.0 the magnitude varied over a range of 3 mag. in what appear to be cycles of about 1000 days. This large-range variation seems to have stopped during the interval between 1934.0 and 1940.0; and a noteworthy feature of this part of the light-curve is the short-period variation near 1937.0. The large-range variation returned following the 1940.0 maximum and has continued in cycles of about 500 days. This suggests that the earlier large-amplitude cycles were also 500 days, since it is impossible to observe BN Monocerotis during the middle third of the

[6] Grateful acknowledgment is made to the American Academy of Arts and Sciences and the Society of Sigma Xi for grants-in-aid to help defray the cost of this instrument, which was constructed in the Yerkes Observatory shop by Mr. Charles Ridell.

TABLE 5

U.T.	JD	m_{pg}	m_{pv}	m_{pr}
1900, Oct. 17.4	2415309.9	14.2 d	.....	.....
1901, Mar. 20.0	5463.5	14.0 d	.....	.....
1925, Mar. 21.1	2424230.6	14.9: g	.....	.....
Dec. 14.3	4498.8	16.:: g	.....	.....
1926, Dec. 13.3	4862.8	16.:: g	.....	.....
1927, Oct. 30.4	5183.9	14.9 g	.....	.....
1928, Feb. 17.8	5294.3	13.7 f	.....	.....
Feb. 22.8	5299.3	14.1 f	.....	.....
Mar. 12.8	5318.3	14.4 f	.....	.....
Mar. 18.8	5324.3	14.1 f	.....	.....
Mar. 22.7	5328.2	13.9 f	.....	.....
Dec. 18.0	5598.5	15.2: f	.....	.....
1929, Jan. 4.9	5616.4	15.4: f	.....	.....
Jan. 16.2	5627.7	15.2: g	.....	.....
Mar. 15.8	5686.3	15.2 f	.....	.....
Mar. 27.7	5698.2	15.1: f	.....	.....
Nov. 29.0	5944.5	15.4: f	.....	.....
Dec. 26.0	5971.5	15.2 f	.....	.....
1930, Jan. 1.1	5977.6	14.7 c	.....	.....
Jan. 7.9	5984.4	14.9 f	.....	.....
Apr. 22.7	6089.2	14.5 f	.....	.....
Nov. 24.3	6304.8	13.9 g	.....	.....
1931, Jan. 17.1	6358.6	13.0 c	.....	.....
1932, Jan. 7.0	6713.5	15.3 f	.....	.....
Jan. 15.9	6722.4	15.3 f	.....	.....
Mar. 3.1	6769.6	14.8 g	.....	.....
Mar. 3.8	6770.3	15.2 f	.....	.....
Mar. 7.1	6773.6	15.3 c	.....	.....
Nov. 28.3	7039.8	15.2 c	.....	.....
Dec. 2.3	7043.8	14.5: d	.....	.....
Dec. 21.2	7062.7	14.5: d	.....	.....
1933, Jan. 23.8	7096.3	14.9: f	.....	.....
Nov. 20.3	7396.8	14.2 c	.....	.....
Dec. 19.2	7425.7	14.2 d	.....	.....
1934, Jan. 8.1	7445.6	13.9 c	.....	.....
1935, Jan. 27.1	7829.6	14.3 c	.....	.....
Feb. 26.1	7859.6	13.8 c	.....	.....
Feb. 27.1	7860.6	.....	8.8 c	.....
Mar. 23.0	7884.5	14.1 d	.....	.....
Mar. 26.0	7887.5	14.0 d	.....	.....
Mar. 27.0	7888.5	14.1 d	.....	.....
Mar. 28.0	7889.5	14.0 d	.....	.....
Mar. 28.1	7889.6	.....	8.7 c	.....
Mar. 29.1	7890.6	14.0 c	8.8 c	.....
Mar. 30.2	7891.7	.....	9.0 c	.....
Mar. 31.0	7892.5	14.1 d	.....	.....
Mar. 31.1	7892.6	.....	8.8 c	.....
Apr. 1.2	7893.7	13.9 c	.....	.....
Apr. 3.0	7895.5	14.0 d	.....	.....
Apr. 4.0	7896.5	13.9 d	.....	.....
Apr. 7.0	7899.5	14.0 d	.....	.....
Apr. 24.2	7916.7	13.9 c	.....	.....
Nov. 25.3	8131.8	14.4 d	.....	.....
1936, Jan. 12.1	8179.6	13.6 c	.....	.....
Jan. 25.1	8192.6	.....	9.3 c	.....
Oct. 13.4	8454.9	13.3 d	.....	.....
Nov. 11.3	8483.8	12.7 c	8.4 c	.....
Nov. 12.4	8484.9	13.0 e	.....	.....
Nov. 14.3	8486.8	12.8 c	8.4 c	.....
Nov. 15.3	8487.8	.....	8.5 c	.....
Nov. 17.3	8489.8	12.9 c	8.5 c	.....
Dec. 19.3	8521.8	13.8 d	.....	.....
1937, Jan. 12.2	8545.7	13.1 c	8.8 c	.....
Mar. 7.2	8599.7	13.6 c	9.0 c	.....
Apr. 2.2	8625.7	13.5 c	9.2 c	.....
1938, Jan. 28.2	8926.7	13.9 a	.....	.....
Feb. 1.2	8930.7	13.9 b	.....	.....
Mar. 22.1	8979.6	13.2 b	.....	.....
1938, Mar. 25.1	2428982.6	13.3: b	8.9 b	.....
Mar. 28.1	8985.6	13.3 b	.....	.....
Apr. 21.1	9009.6	13.3 a	.....	.....
Apr. 23.1	9011.6	13.4 a	.....	.....
Apr. 23.1	9011.6	13.3: b	.....	.....
Oct. 6.5	9178.0	13.5 c	9.5 c	.....
Oct. 22.5	9194.0	13.4 c	9.4 c	.....
Oct. 24.4	9195.9	13.4 c	.....	.....
Oct. 26.3	9197.8	13.4 c	9.3 c	.....
Nov. 27.3	9229.8	13.4 c	.....	.....
1939, Jan. 18.2	9281.7	13.6 c	.....	.....
Feb. 14.2	9308.7	13.9 a	.....	.....
Feb. 16.1	9310.6	13.9 a	.....	.....
Feb. 18.1	9312.6	13.9 a	.....	.....
Mar. 9.1	9331.6	13.4: a	.....	.....
Mar. 14.1	9336.6	13.9 a	.....	.....
Mar. 14.2	9336.7	13.9 c	.....	.....
Mar. 17.1	9339.6	13.4 a	.....	.....
Mar. 18.1	9340.6	13.8: a	.....	.....
Mar. 21.1	9343.6	13.6 a	.....	.....
Mar. 24.2	9346.7	13.6 c	.....	.....
Apr. 9.2	9362.7	13.7 c	.....	.....
Apr. 22.2	9375.7	13.5 c	8.8 c	.....
May 12.0	9395.5	13.5: c	.....	.....
Aug. 27.4	9502.9	13.3 a	.....	.....
Sept. 2.5	9509.0	13.5: c	.....	7.5 c
Sept. 3.5	9510.0	13.8 c	8.9 c	7.7 c
Sept. 9.4	9515.9	13.3: a	.....	.....
Sept. 9.5	9516.0	.....	9.1 c	.....
Sept. 22.4	9528.9	13.9: c	.....	.....
Sept. 23.4	9529.9	13.6 a	.....	.....
Oct. 8.4	9544.9	13.5 a	.....	.....
Oct. 14.3	9550.8	13.4 a	.....	.....
Oct. 14.4	9550.9	13.3 c	8.6 c	.....
Oct. 21.3	9557.8	13.4 a	.....	.....
Oct. 21.4	9557.9	13.5 c	8.9 c	7.3 c
Nov. 4.3	9571.8	13.0 c	8.5 c	.....
Nov. 5.3	9572.8	13.4 a	8.9 a	.....
Nov. 11.3	9578.8	13.1 a	8.9 a	.....
Nov. 15.2	9582.7	13.1 a	9.0 a	.....
Nov. 18.2	9585.7	12.9 a	.....	.....
Nov. 21.3	9588.8	12.8 c	8.8 c	.....
Dec. 5.3	9602.8	13.0 c	8.7 c	7.5 c
Dec. 6.1	9603.6	12.8 a	8.9 a	.....
Dec. 7.2	9604.7	13.0 a	8.7 a	.....
Dec. 8.2	9605.7	13.1 a	8.7 a	.....
Dec. 9.1	9606.6	13.0 a	8.8 a	.....
Dec. 10.1	9607.6	13.1 a	8.8 a	.....
Dec. 12.1	9609.6	13.1 a	8.8 a	.....
Dec. 15.2	9612.7	.....	8.6:: a	.....
Dec. 17.1	9614.6	13.0 a	8.7 a	.....
Dec. 17.3	9614.8	13.0 c	9.1 c	7.5 c
Dec. 22.2	9619.7	.....	8.9 a	.....
1940, Jan. 2.1	9630.6	13.1 a	8.8 a	.....
Jan. 2.3	9630.8	13.2 c	8.9 c	7.5 c
Jan. 6.1	9634.6	13.4 a	8.8 a	.....
Jan. 9.3	9637.8	.....	8.7 a	.....
Jan. 15.3	9643.8	13.1 c	8.7 c	.....
Jan. 30.2	9658.7	13.2 c	9.1 c	7.4 c
Feb. 10.2	9669.7	.....	.....	7.3 c
Feb. 12.0	9671.5	13.4 a	9.5: a	.....
Feb. 15.0	9674.5	13.1 a	9.1 a	.....
Feb. 16.1	9675.6	13.1 a	.....	.....
Mar. 10.2	9698.7	13.4 c	.....	.....
Mar. 13.1	9701.6	13.7 c	9.0 c	.....
Mar. 26.1	9714.6	13.5 a	9.3 a	8.0 c
Apr. 4.1	9723.6	13.9 a	9.6 a	.....
Apr. 7.1	9726.6	14.1 c	.....	.....

TABLE 5—*Continued*

U.T.	JD	m_{pg}	m_{pv}	m_{pr}	U.T.	JD	m_{pg}	m_{pv}	m_{pr}
1940, Apr. 8.0	2429727.5	.....	9.2 c	.....	1941, Apr. 26.1	2430110.6	13.6: a	.....	.....
Apr. 13.1	9732.6	.....	.....	7.8 c	Apr. 27.1	0111.6	.....	.....	7.5 a
Apr. 27.1	9746.6	13.9: a	.....	.....	May 4.1	0118.6	.....	8.8 a	7.4 a
May 4.1	9753.6	14.7: c	.....	.....	Sept. 23.4	0260.9	15.1:: a	9.4: a	7.9 a
May 7.0	9756.5	.....	9.3 c	.....	Nov. 14.2	0312.7	14.6:: a	.....	.....
May 9.1	9758.6	14.5: c	.....	.....	Nov. 17.2	0315.7	15.1:: a	9.2: a	7.9: a
Dec. 2.2	9965.7	15.1 a	9.3 a	.....	1942, Jan. 11.2	0370.7	.....	.....	7.9 c
Dec. 9.2	9972.7	.....	9.1 a	.....	Jan. 15.1	0374.6	15.1: a	9.6: a	7.4: a
1941, Jan. 6.1	2430000.6	.....	9.4 a	.....	Jan. 16.2	0375.7	.....	9.3 c	7.8 c
Jan. 31.1	0025.6	15.1 a	9.4 a	.....	Jan. 18.2	0377.7	15.6 c	.....	.....
Feb. 1.2	0026.7	15.3 a	9.6 a	.....	Feb. 10.2	0400.7	.....	.....	7.6 c
Feb. 19.1	0044.6	15.4 a	9.6:: a	.....	Mar. 10.1	0428.6	15.3 a	9.6: a	8.3: a
Feb. 20.1	0045.6	15.2 a	9.5 a	.....	Mar. 21.1	0439.6	.....	.....	7.6 c
Feb. 22.1	0047.6	15.1 a	9.4 a	.....	Apr. 17.2	0466.7	15.3:: a	.....	.....
Mar. 1.2	0054.7	15.1 a	9.6:: a	.....	Oct. 20.5	0653.0	13.4 c	8.9 c	7.6 c
Mar. 9.1	0062.6	.....	9.4 a	.....	1943, Jan. 12.3	0736.8	13.8 c	.....	.....
Mar. 18.1	0071.6	.....	9.1 a	7.8 a	Feb. 7.2	0762.7	13.8 c	9.0 c	7.6 c
Mar. 20.1	0073.6	14.8 a	9.2 a	7.8: a	Mar. 25.1	0808.6	14.4 c	9.3 c	7.6 c
Mar. 22.1	0075.6	14.9: a	9.3 a	7.9 a	May 6.2	0850.7	15.2 c	.....	.....
Mar. 26.1	0079.6	.....	9.3 a	7.9 a	Nov. 3.4	1031.9	14.4 c	9.1 c	7.4 c
Mar. 29.2	0082.7	.....	9.1:: a	8.0 a	Nov. 4.3	1032.8	.....	9.1 c	.....
Mar. 30.1	0083.6	14.8 a	9.3 a	7.9 a	Dec. 1.3	1059.8	14.5 c	9.0 c	7.4 c
Apr. 21.1	0105.6	13.9: a	8.7 a	7.5 a	1944, Mar. 25.1	1174.6	14.0 c	.....	.....
Apr. 22.1	0106.6	.....	.....	7.7 a					

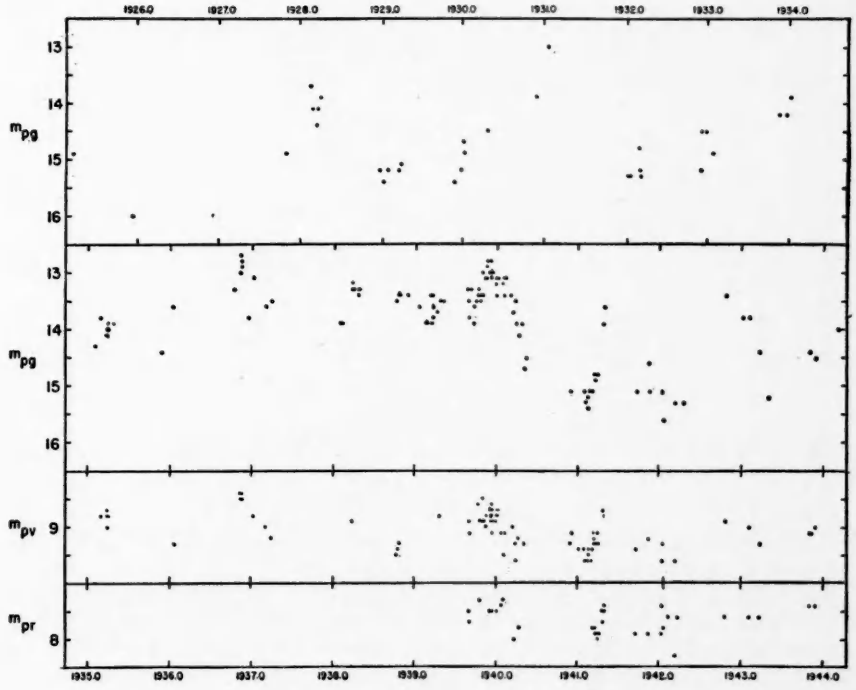

FIG. 1.—Photographic, photovisual, and photo-red light-curves of BN Monocerotis

year and alternate maxima could have been missed. In this connection it should be noted that the discovery of the 500-day cycle depends on two observations (1941, April 21.1 and 26.1) and that without them the recent variation would have seemed to be in a 1000-day cycle.

The photovisual light-curve is in phase with the photographic light-curve, but the amplitude is only about one-third as great.[7] The amplitude of the photo-red light-curve is still smaller.

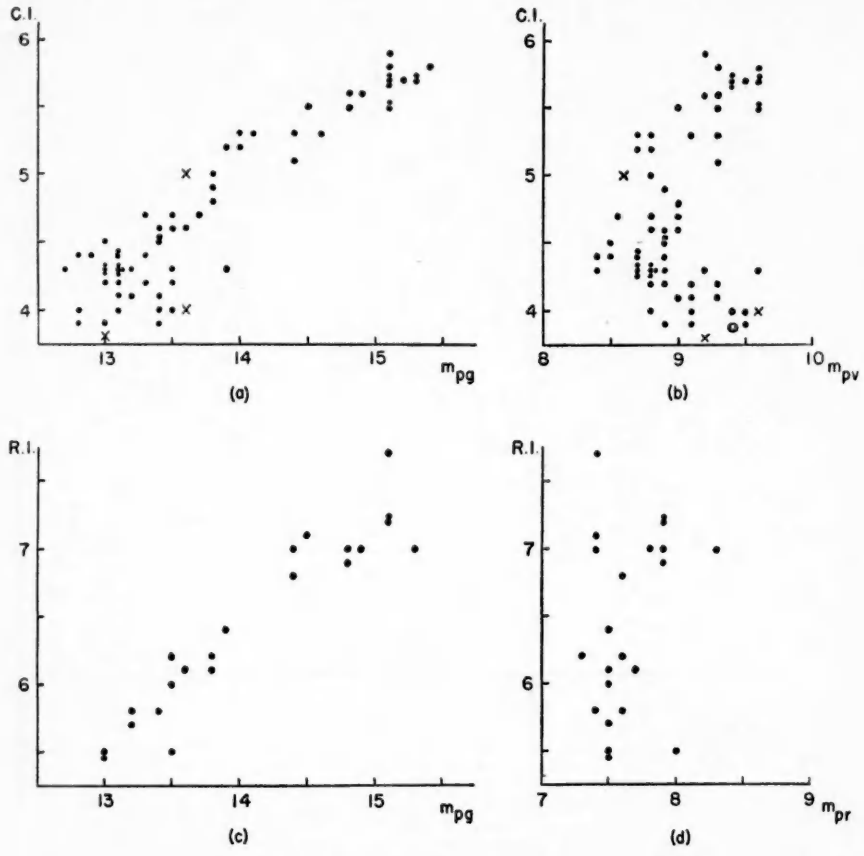

FIG. 2.—Relationship of color to magnitude (XZ Aurigae shown by *x*'s for comparison)

b) COLOR CHANGES

The color index is plotted against the photographic magnitude in Figure 2, *a* and against the photovisual magnitude in Figure 2, *b*. The color index changes from $+4^m$ to $+6^m$, while the photographic magnitude drops from 12^m8 to 15^m5. In sharp contrast, as the color index increases from $+4^m$ to $+5^m$, the photovisual magnitude gets brighter; and as the color index increases further, from $+5^m$ to $+6^m$, the photovisual magnitude gets fainter. There is a strong correlation between red index and photographic magnitude and little or no correlation between red index and photo-red magnitude, as shown in

[7] Compare with: S Cephei, *Harvard Circ.*, No. 188, 1915; and RV Centauri, *Harvard Bull.*, No. 875, 1930.

Figures 2, *c* and 2, *d*. This is in accord with the spectral changes that have been observed in other stars of this class, namely, the band absorption at minimum decreases the light from the blue end of the spectrum and accentuates the change in relative energy.

The observations of XZ Aurigae by Alter and Edwards[8] are sufficient to indicate that it must be similar to BN Monocerotis. Their three determinations of color index are plotted as *x*'s in Figure 2, *a* and *b*, after subtracting a zero-point correction of $1^m.3$ from both the photographic and the photovisual magnitudes. The similarity of behavior is especially striking in Figure 2, *b*.

The mean color index of nearly 5 mag. and the period of approximately 500 days are in agreement with the general relationship found by Gerasimovič and Shapley;[9] and their results also indicate that the spectral class is probably late N type.[10]

We are indebted to Dr. Harlow Shapley for the opportunity to make use of the Harvard plate collection. We also wish to thank Dr. V. M. Slipher and Professor W. A. Cogshall for permission to pool our resources in this joint publication.

[8] *M.N.*, **101**, 295, 1941. [9] *Harvard Bull.*, No. 872, 1930.

[10] In a letter dated October 18, 1939, Dr. Sanford writes:
"I have two plates of BN Monocerotis. . . . The second plate has nearly twice the dispersion, is of good quality, and points to a fairly late class N star, although I had tentatively called it (N2) in my catalog." The plate was taken on November 10, 1933.

THE SPECTROSCOPIC BINARY 31 CYGNI*

JULIE M. VINTER HANSEN
Lick Observatory
Received March 22, 1944

ABSTRACT

The orbital elements of the brighter component of the spectroscopic binary, 31 Cygni, a class K0 supergiant, were derived from the radial velocities given by the measurement of 75 spectrograms taken with the three-prism Mills spectrograph in the interval 1899–1943. On a few spectrograms obtained in the ultraviolet with a one-prism spectrograph, the spectrum of the fainter B-type component is visible. From the approximate velocities yielded by the measures of these plates, the mass ratio of the brighter to the fainter component is estimated to be 1.7.

The star 31 Cygni ($\alpha = 20^h10^m.5$; $\delta = +46°26'$ (1900); vis. mag. = $4^m.0$) was announced as a spectroscopic binary in 1901 by W. W. Campbell.[1] It is listed in the *Henry Draper Catalogue* as having a composite spectrum; the brighter component is a supergiant of spectral class K0, while the fainter component is of spectral class B8. The Mount Wilson Observatory designates the star as of spectral class cK1, with the remark that the spectrum of the primary is veiled by that of the companion.[2] W. H. Christie[3] has given the following provisional elements, deduced from 23 observations, mostly from the Lick Observatory:

$$T = 2414400 \text{ JD}$$
$$\omega = 200°$$
$$e = 0.3$$
$$K = 20.0 \text{ km/sec}$$
$$V = \text{var. (?)}$$
$$P = 4000 \text{ days}$$

Christie found some evidence of a change in the velocity of the system amounting to +0.66 km/sec per 1000 days.

Since the Lick Observatory had collected a series of spectrograms of this binary covering an interval of 44 years, it was decided to compute new elements. There were available, in all, 75 spectrograms, taken between June, 1899, and July, 1943. The first 10 of these were obtained with the original Mills three-prism spectrograph ($H\gamma$ central) and the remaining ones with the new Mills three-prism instrument (λ 4500 central). All the plates were measured by the writer on the Hartmann spectrocomparator against standard plates of α Boötis. The results are listed in Table 1, in which, in the second column, is given the Universal Time of the observations, the first 16 having been reduced to this time. In the third column are listed the Julian days and decimals of a day, in heliocentric Greenwich Mean Astronomical Time; and in the fourth column are tabulated the measured velocities.

From a plot of the velocity data, an approximate value for the period of 3820 days

* *Contributions from the Lick Observatory*, Ser. II, No. 9.

[1] *Lick Obs. Bull.*, **1**, 22, 1901.

[2] *Ap. J.*, **81**, 274, 1935.

[3] *Ap. J.*, **83**, 433, 1936.

TABLE 1

No.	Date U.T.	Julian Day	Velocity Km/Sec	O−C Km/Sec	Phase (Days)	Photographed by
		2410000+				
1	1899 June 21	4826.841	−11.1	+1.0	368	Campbell
2	July 3	4838.855	−12.5	−0.7	380	Campbell
3	1900 July 31	5231.901	− 3.5	−1.5	773	Campbell, Wright
4	Aug. 13	5244.922	− 1.8	0.0	786	Campbell, Wright
5	Oct. 8	5300.695	− 2.2	−1.5	842	Campbell, Reese
6	1901 June 6	5541.944	+ 2.6	−0.3	1083	Reese
7	Oct. 14	5671.784	+ 4.8	+0.6	1213	Campbell
8	1902 May 28	5897.918	+ 4.1	−1.2	1439	Wright
9	Sept. 10	6002.801	+ 3.9	−1.4	1544	Reese
10	1904 Nov. 23	6807.643	− 3.3	−1.1	2349	Moore
11	1912 May 10	9532.989	+ 5.8	+1.2	1271	Moore, Reese
12	June 17	9570.834	+ 4.4	−0.5	1309	R. E. Wilson
13	July 8	9591.748	+ 4.7	−0.2	1330	Kiess
14	July 21	9604.963	+ 4.8	−0.2	1343	Pitman
15	Oct. 21	9696.665	+ 6.0	+0.7	1435	R. E. Wilson
		2420000+				
16	1923 June 6	3576.905	+ 6.3	+1.0	1512	Neubauer
17	1928 Oct. 10	5529.700	−22.1	−0.1	3465	Paddock
18	1930 June 6	6133.894	−14.7	+0.2	266	Paddock
19	1931 July 13	6535.935	− 3.8	+0.6	668	Moore
20	July 22	6544.353	− 3.4	+0.7	677	Paddock
21	Oct. 5	6619.700	− 4.0	−1.6	752	Neubauer
22	Nov. 24	6669.649	− 1.4	+0.1	802	Moore
23	1932 June 24	6882.877	+ 2.1	0.0	1015	Paddock
24	July 15	6903.906	+ 3.9	+1.4	1036	Paddock
25	1933 July 4	7257.844	+ 6.2	+1.0	1390	Paddock
26	July 28	7281.944	+ 7.0	+1.8	1414	Paddock
27	Aug. 30	7314.802	+ 7.0	+1.7	1447	Moore
28	Oct. 18	7363.730	+ 6.1	+0.8	1496	Paddock
29	1935 May 6	7928.959	+ 1.8	−0.1	2053	Moore
30	May 12	7934.959	+ 2.0	+0.2	2067	Paddock
31	Sept. 13	8058.746	+ 0.1	−0.1	2191	Moore
32	Sept. 18	8063.809	+ 0.2	+0.1	2196	Moore
33	Oct. 9	8084.717	− 0.9	−0.7	2217	Moore
34	Oct. 26	8101.656	− 0.1	+0.1	2234	Wyse
35	1936 June 17	8336.977	− 4.5	−0.2	2470	Paddock
36	June 26	8345.842	− 2.2	+2.3	2478	Paddock
37	July 30	8379.943	− 4.5	+0.5	2512	Paddock
38	Aug. 1	8381.966	− 5.1	0.0	2514	Paddock
39	Aug. 5	8385.935	− 5.4	−0.2	2518	Paddock
40	Aug. 25	8405.965	− 6.0	−0.4	2538	Paddock
41	Oct. 23	8464.689	− 8.1	−1.4	2597	Paddock
42	Nov. 9	8481.636	− 7.9	−0.8	2614	Moore
43	1937 Aug. 7	8752.929	−12.1	+0.6	2885	Moore
44	Aug. 12	8757.915	−13.3	−0.5	2890	Paddock
45	Aug. 19	8764.970	−14.0	−1.0	2897	Paddock
46	Aug. 23	8768.888	−13.0	0.0	2901	Paddock
47	1938 June 15	9064.986	−18.2	+0.6	3198	Paddock
48	Aug. 4	9114.938	−19.1	+0.4	3248	Stillwell, Baum
49	Aug. 7	9117.951	−20.3	−0.7	3250	Stillwell, Baum
50	Aug. 15	9125.922	−20.1	−0.3	3258	Stillwell, Mowbray
51	Sept. 2	9143.909	−18.8	+1.3	3276	Moore
52	Sept. 12	9153.784	−20.5	−0.3	3286	Moore
53	Oct. 17	9188.689	−19.8	+0.8	3321	Paddock
54	Oct. 20	9191.687	−19.7	+1.0	3324	Moore
55	Nov. 17	9219.636	−19.8	+1.2	3352	Paddock
56	1939 Aug. 1	9476.967	−23.4	−1.3	3609	Moore
57	Aug. 2	9477.910	−23.8	−1.7	3610	Moore

TABLE 1—*Continued*

No.	Date U.T.	Julian Day	Velocity Km/Sec	O−C Km/Sec	Phase (Days)	Photographed by
58	1939 Sept. 7	9513.821	−21.4	+0.6	3646	Moore
59	Oct. 17	9553.653	−21.4	+0.3	3686	Neubauer
60	Nov. 4	9571.699	−21.9	−0.3	3704	Paddock
61	Nov. 8	9575.688	−21.4	+0.2	3708	Paddock
62	1940 May 26	9775.945	−18.8	−0.2	106	Paddock
63	July 10	9820.931	−16.7	+0.9	151	Paddock
64	July 14	9824.970	−16.7	+0.8	155	Paddock
65	Sept. 10	9882.771	−16.6	−0.5	212	Paddock
66	Oct. 11	9913.724	−16.6	−1.2	243	Paddock
		2430000+				
67	1941 Aug. 9	0215.893	− 5.6	+1.8	546	Moore
68	Sept. 7	0244.809	− 6.3	+0.3	574	Moore
69	Nov. 7	0305.681	− 4.4	+0.8	635	Moore
70	1942 July 6	0546.949	+ 0.2	+0.2	877	Paddock
71	Aug. 3	0574.880	+ 0.5	+0.1	904	Paddock
72	Oct. 18	0650.641	+ 0.2	−1.4	980	Gordon
73	1943 June 18	0893.962	+ 2.4	−2.0	1224	Nagtegaal
74	June 20	0895.835	+ 3.3	−1.0	1226	Nagtegaal
75	July 17	0922.824	+ 3.2	−1.3	1252	Moore

was found; and, on the basis of the corresponding velocity-curve, the following preliminary elements were derived by the method of Lehmann-Filhés:

$$T = 2422072 \text{ JD}$$
$$\omega = 213.13°$$
$$e = 0.12$$
$$\mu = 0.09424°$$
$$K = 14.9 \text{ km/sec}$$
$$V = -7.1 \text{ km/sec}$$

With these elements an ephemeris was computed. This was compared with the observed velocities, and the resulting residuals were used for deriving differential corrections to the elements by the method of least squares. The observations were grouped into 35 normal places, only those of the same epoch being combined to form a normal place, since a correction to the period was to be included among the unknowns. The solution resulted in the following elements with their probable errors:

FINAL ELEMENTS

$$T = 2422064.7 \text{ JD} \pm 27^d.8$$
$$\omega = 209.65° \pm 2.61°$$
$$e = 0.131 \pm 0.006$$
$$K = 13.78 \pm 0.08 \text{ km/sec}$$
$$V = -6.87 \text{ km/sec}$$
$$\mu = 0.094666° \pm 0.000067°$$
$$P = 3802.84 \pm 2.69 \text{ days}^4$$
$$a_1 \sin i = 720 \times 10^6 \text{ km}$$
$$\frac{m_2^3 \sin^3 i}{(m_1 + m_2)^2} = 1.007 \odot$$

The probable error of a single observation of unit weight is ±0.50 km/sec.

[4] This is the apparent period; the true period = 3802.93 days.

The solution reduced the sum of the squares of the residuals from 110.340 to 39.160; this fact shows that the new elements are considerably more satisfactory than were the preliminary ones. A complete check on the solution is furnished by the circumstance that the differences between the residuals derived from the ephemeris based upon the new elements and those derived by substitution of the unknowns into the 35 equations of condition in no case exceed 0.1 km/sec. The residuals from the ephemeris are listed in the fifth column of Table 1. Figure 1 shows the velocity-curve corresponding to the final elements. The observations are marked as vertical lines, the half-length of which corresponds to the probable error; the periastron is denoted by the letter *P*.

To test whether there is any evidence that the velocity of the system is variable, as suggested by Christie, the residuals of the individual observations were plotted against the time. No evidence of such a variability in systemic velocity was revealed by the present material.

Attempts were made by Dr. Moore to secure spectra of the class B companion. For this purpose a light-flint, one-prism spectrograph (equipped with a 12-inch camera) was

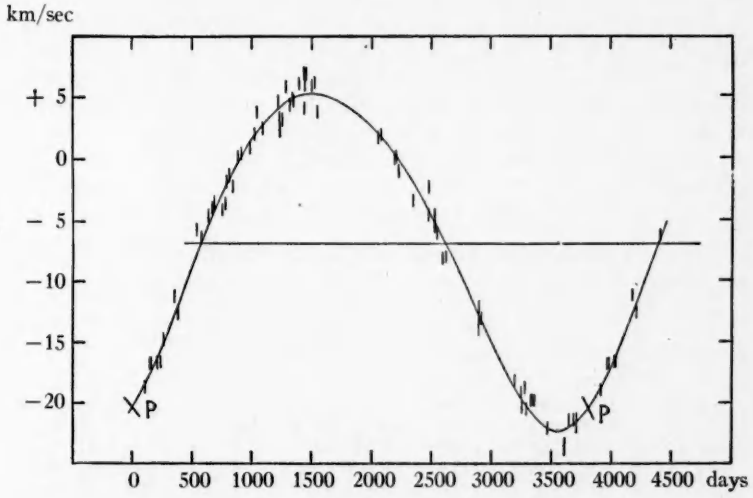

FIG. 1.—Velocity-curve of 31 Cygni

used in conjunction with the 36-inch refractor. The plates employed were Eastman 103a0 and Cramer Hi-Speed; and the exposures ranged from 30^m to 150^m. On account of the strong absorption of ultraviolet light by the telescopic objective, it was not possible to obtain measurable lines lying to the violet of λ 3750 A, even with an exposure of 150^m, although in the usual photographic region ($H\beta$ to $H\delta$) of the spectrum an exposure of 5^m was sufficient to produce a measurable spectrum of the K-type star.

The spectra showed a number of lines in the region λλ 3700–4100, a few strong lines belonging to the B-type component, and several fainter lines, due to the supergiant class K star. All the lines were difficult to measure; but on each of 7 plates, taken near the date of the nodal passage in 1943, it was possible to measure 2 to 4 lines belonging to the B-type star. The wave lengths and the identifications of the 7 lines in the spectrum of the class B star, which were utilized, are listed in Table 2. Data relating to the radial velocities and the number of lines upon which the measurement depends are given in Table 3.

The weighted mean of the velocities is −22 km/sec, which, with the systemic velocity

and orbital eccentricity as herein derived, yields the value of $K_2 = 17$ km/sec. Thus, for $K_1 = 13.8$ km/sec and $K_2 = 17$ km/sec, we obtain a mass ratio of

$$\frac{m_1}{m_2} = 1.2$$

The foregoing value of K_2 must be considered as being very uncertain, not only because the diffuseness of the spectral lines makes the measurements inaccurate, but also because this value has been derived from velocities determined at only one nodal passage. The uncertainty in the value of K_2 arising from the latter circumstance cannot properly be removed except by observations made near the other node or in other parts of the velocity-curve, since, for its derivation, the velocity of the system, as given by the three-prism velocities of the bright component, was used. Thus, if there is a systematic differ-

TABLE 2

SPECTRAL LINES OF THE B-TYPE COMPONENT

λ	Element	λ	Element
3770.6	*H* (*H*11)	3856.12	*O*+
3797.86	*H* (*H*10)	3889.12	*H* (*H*8)
3819.68	*He*	3970.13	*H* (*H*ε)
3835.34	*H* (*H*9)		

TABLE 3

RADIAL VELOCITIES OF THE B-TYPE COMPONENT

No.	U.T. 1943	JD 2430000+	Rad. Vel. Km/Sec	Lines Measured	Weight	Plate	Exposure Time (In Minutes)
76	Aug. 21	0957.762	−20	*O*+, *H*8, *H*ε	1	East. 103aO	30
77	31	0967.683	−22	*H*11, *He*, *H*8, *H*ε	1	Cr. H. Sp.	120
78	Oct. 8	1005.765	−11	*H*11, *He*	½	Cr. H. Sp.	150
79	Nov. 29	1057.608	−32	*He*, *H*9, *H*8	1	Cr. H. Sp.	120
80	Dec. 4	1062.586	−41	*He*, *H*8	½	Cr. H. Sp.	50
81	4	1062.637	−20	*H*11, *He*, *O*+, *H*8	1	Cr. H. Sp.	90
82	14	1072.594	− 9	*H*11, *He*, *H*8	1	Cr. H. Sp.	90

ence between the measures made with the two instruments, an erroneous value of K_2 would be obtained. In the absence of the required observations, an attempt was made to test for the presence of such a systematic difference by measuring 5 or 6 of the stronger lines of the K-type star that were visible in the ultraviolet on the 7 one-prism spectrograms. The identifications and wave lengths used for these lines were those given by Miss Dorothy Davis[5] for the spectrum of Antares. Although the lines were comparatively well defined, their measurement and identification were rendered difficult on account of the small dispersion and their faintness, which was due to the veiling of the spectrum by the B-type component. The velocities of the K-type star given by the measurements of the 7 spectrograms, when compared with the values predicted by the three-prism velocity-curve, indicated a systematic difference of the order of −5 km/sec in the sense three-prism *minus* one-prism. Thus, if we assume that this is an instrumental correction,

[5] *Ap. J.*, **89**, 41, 1939.

the one-prism velocities should be corrected by this amount, and we obtain $K_2 = 23$ km/sec. From this value it follows that

$$\frac{m_1}{m_2} = 1.7$$

and

$$m_1 \sin^3 i = 12\odot$$
$$m_2 \sin^3 i = 7\odot$$
$$a_2 \sin i = 1224 \times 10^6 \text{ km}$$

As far as the available evidence goes, we appear to be justified in assuming that the mass ratio is of the order of 1.7, although, on account of the uncertainty referred to previously, this value must be regarded as little more than a rough estimate.

The trigonometric parallax of 31 Cygni is given in Schlesinger's *General Catalogue of Stellar Parallaxes* (1935) as $-0''.006 \pm 0''.007$, while the spectroscopic parallax corresponding to the Mount Wilson[6] absolute magnitude of $-1^m.8$ is $0''.005$. With the spectroscopic parallax and the values of $a_1 \sin i$ and $a_2 \sin i$ given previously for $m_1/m_2 = 1.7$, we obtain, for the maximum angular separation of the two components of the binary, $d = 0''.074$, a value which is below the visual limit of resolution of the 36-inch refractor. It may be worth while, however, to examine the star for duplicity with one of the larger reflectors at or near the time of apastron passage, which will occur in April, 1945. Since the apparent major axis of the orbit of the B-type companion is $0''.082$ and that of the K-type star is $0''.048$, it may be possible to measure the displacements of either component with reference to neighboring stars on photographs taken with an ultraviolet filter for the class B star and with a yellow or red filter for the K-type star, and thus to determine their absolute orbits.

This investigation was proposed by Dr. J. H. Moore, to whom I wish to express my hearty thanks for many helpful suggestions during its course.

[6] *Ap. J.*, **81**, 57, 1935.

SPECTROSCOPIC OBSERVATIONS OF 48 LIBRAE*

PAUL W. MERRILL AND ROSCOE F. SANFORD
Mount Wilson Observatory
Received March 16, 1944

ABSTRACT

Radial velocity.—Between 1904 and 1931, spectrograms at various observatories indicated a nearly constant velocity; but between 1935 and 1944 a fluctuation of considerable amplitude occurred. At the extreme velocities a progression in displacement from line to line along the Balmer series was observed. Microphotometer tracings showed the bright *Hα* line to be more nearly stationary than its dark core. Velocities from metallic lines agree with those of *H* lines near the head of the series. Lines of *Na* I and *Ca* II have stationary components which are possibly partly circumstellar.

Intensities of lines.—The dark lines of *H* and of metals—notably lines of *Fe* II, *Cr* II, *Ni* II, and *Ca* II—became stronger from 1938 to 1943. In certain typical lines the equivalent widths more than doubled. The absorption in *H* 15 increased from 38 to 87 per cent. In the dark core of *Hα* the absorption became more than 90 per cent, showing that absorbing atoms lay in front of most of the emitting atoms. In 1943 the dark Balmer lines were measured to *H* 41. The *H* cores and the metallic lines are narrow but at times asymmetrical. The change in structure does not explain the measured displacements.

Discussion.—Displacements of the lines are probably due to motions in the stellar atmosphere. The amplitude of the fluctuations seems to increase from the photosphere outward. Several facts suggest that the bright *H* lines may come from a layer of hydrogen just above the photosphere. This hypothesis may be applicable to other Be stars with shell spectra.

The Harvard objective-prism survey showed that the spectrum of 48 Librae[1] "is peculiar in combining sharply defined hydrogen lines with very wide and ill-defined helium lines."[2] Miss Annie J. Cannon considered the spectrum composite and suggested that the star might be a binary.

The *Hα* line was found to be bright on an objective-prism photograph taken at Mount Wilson[3] on March 20, 1928. Slit spectrograms later showed this line to have a very strong absorption core.[3,4] Strong, well-defined cores with a slow decrement in intensity characterize the whole Balmer series. Weak emission is sometimes present on the edges of *Hβ*. Narrow dark lines of *Ca* II, of *Fe* II, and of other ionized metals are present in moderate (and variable) intensity. Lines of *He* I are weak and very diffuse.

Numerous slit spectrograms taken from 1904 to 1931 at various observatories indicated a nearly constant radial velocity. It was a surprise, therefore, to find that between 1935 and 1939 the velocity derived from the metallic lines and from the ultraviolet members of the Balmer series decreased about 100 km/sec and then returned to its previous value.[5] The Balmer lines *Hβ*, *Hγ*, and *Hδ* were displaced only about half as much. This remarkable occurrence and the behavior of the spectrum from 1939 to 1944 are discussed in some detail in the present *Contribution*. A summary of early observations is included.

OBSERVATIONS, 1904–1931

Yerkes Observatory.—Two spectrograms[6] obtained in 1904 and four in 1915 were forwarded to us through the kindness of Dr. O. Struve. Our measures of the lines *Hβ*, *Hγ*,

* *Contributions from the Mount Wilson Observatory, Carnegie Institution of Washington*, No. 690.

[1] HD 142983, BD −13°4302: 1900 α 15^h52^m6, δ −13°59′; mag., 4.7.

[2] *Harv. Ann.*, **96**, 229, 1921.

[3] Merrill, Humason, and Burwell, *Mt. W. Contr.*, No. 456; *Ap. J.*, **76**, 156, 1932.

[4] P. W. Merrill, *Mt. W. Contr.*, No. 432; *Ap. J.*, **74**, 188, 1931.

[5] Merrill and Sanford, *Pub. A.S.P.*, **52**, 279, 1940.

[6] *Ap. J.*, **76**, 210, 1932.

and $H\delta$ on the 1904 plates yield the mean velocity -5 km/sec. The published[7] mean velocity from the 1915 plates is -10 km/sec (*Ca* II, -7 km/sec).

Lick Observatory.—Four spectrograms obtained in 1922 at the Chile station and one in 1924 at Mount Hamilton[8] yielded the mean velocity -14 km/sec.

Mount Wilson Observatory.—Three low-dispersion plates were obtained in July, 1910, with a temporary form of spectrograph. The mean velocity, $+3$ km/sec, from $H\beta$, $H\gamma$, and $H\delta$ is not very reliable. No other lines are measurable. One plate of the blue-violet region was obtained with a better spectrograph in each of the years 1925, 1926, and 1928. One or two plates of the visual region were obtained in each of the years 1928, 1929, and 1930. The measured velocities from these early Mount Wilson plates (Table 1) are not

TABLE 1

RADIAL VELOCITIES: 1904–1931
(One-Prism Spectrograms unless Noted; Representative Dispersion, 35 A/Mm at $H\gamma$)

Date	Observatory	Rad. Vel.	Normal Places	
			J.D.	Rad. Vel.
		km/sec		km/sec
1904 June 10	Yerkes	− 4	2416646	− 5
18	Yerkes	− 7		
1910 July 16	Mt. Wilson	(+ 3)*	2418869	(+ 3)
1915 Mar. 29	Yerkes	+ 3	2420589	−10
30	Yerkes	−13		
Apr. 2	Yerkes	−11		
5	Yerkes	−20		
1922 Mar. 18	Lick (Chile)	−19	3160	−15
Apr. 17	Lick (Chile)	−14		
26	Lick (Chile)	−11		
30	Lick (Chile)	−15		
1924 Apr. 9	Lick (Mt. H.)	− 9	3886	− 9
1925 Apr. 7	Mt. Wilson	− 3	4248	− 3
1926 May 2	Mt. Wilson	−25	4638	−25
1928 May 18	Mt. Wilson	(− 7)	5423	− 2
Aug. 2†	Mt. Wilson	(+ 5)		
1930 July 11†	Mt. Wilson	(+ 2)	6170	+ 5
12†	Mt. Wilson	+ 6		
1931 June 5†	Mt. Wilson	(− 7)	6498	(− 7)

* Mean of three plates.
† Visual region; small grating spectrograph, dispersion 65 A/mm.

very accurate; with the possible exception of the result for 1926, they appear to agree within the uncertainties of measurement. In fact, most of the range in the whole of Table 1 could probably be considered observational rather than intrinsic. The early velocities are plotted in Figure 1. The velocity adopted in J. H. Moore's *Catalogue of Radial Velocities*[9] is -12.1 km/sec.

OBSERVATIONS, 1935–1936

Spectrograms obtained at Yerkes[10] and at Mount Wilson in 1935 (Table 2) yielded interesting results. Velocities from the *H* lines were slightly lower (algebraically) than

[7] *Ap. J.*, **64**, 60, 1926.
[8] *Pub. Lick Obs.*, **16**, 233, 1928.
[9] *Pub. Lick Obs.*, **18**, 125, 1932.
[10] Kindly forwarded to us by Dr. Struve.

those measured in previous years, while velocities from metallic lines were still lower. In 1936 these discrepancies were more striking. On the last plate of Table 2 the velocity derived from $H\beta$ was -42 km/sec; that from $H\zeta$, -60 km/sec. This curious progression in measured displacement of successive members of the Balmer series, as well as the duplicity of the sodium D lines on the preceding plate, will be discussed in following sections in connection with related results in other years.

Observations, 1938–1944

Since 1938, when we began to observe 48 Librae more assiduously, we have obtained numerous spectrograms each year, an increasing proportion of them having a dispersion

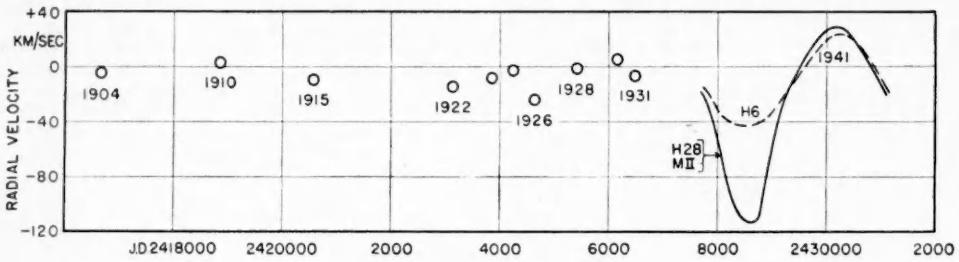

Fig. 1.—Radial velocities, 1904–1944

TABLE 2

Radial Velocities: 1935–1936

Date	J.D.	Observatory	Radial Velocity (Km/Sec)					
			H 6	*Ca* II	*Fe* II	*Si* II	*Na* I	Mean Metals
1935 Apr. 13...	2427906	Yerkes	−26	.....	− 35	.....	.....	− 35
June 8...	7962	Yerkes	−29	.....	− 50	.....	.....	− 50
July 15...	7999	Mt. Wilson	−30	−41	− 60	.....	.....	− 50
1936 June 10...	8330	Mt. Wilson	.....	.....	(−106)	−91	{−104, − 22}	−100
June 29...	8349	Mt. Wilson	−53	−97	−108	.....	.....	−104

of 10 A/mm, a scale three or four times that of the earlier plates. (See Table 3.) We are indebted to W. S. Adams for two plates with a dispersion of 2.9 A/mm. Normal places obtained from the velocities in Table 3 are collected in Table 4 and are plotted in Figure 2. The relative displacements of various lines will be discussed in following sections.

Results obtained from numerous spectrograms taken in the years 1941–1943 at the Yerkes and McDonald observatories have been reported by O. Struve[11] and by W. A. Hiltner.[12] Normal places obtained from Struve's velocities are collected in Table 5. Comparison with the Mount Wilson curve, Figure 2, shows small but consistent residuals. The systematic differences may arise in various ways from the slight asymmetry of the lines. Curves plotted from the Yerkes and from the Mount Wilson results are closely parallel.

[11] *Ap. J.*, **98**, 98, 1943.

[12] *Ap. J.*, **99**, 103, 1944.

TABLE 3

RADIAL VELOCITIES: 1938–1944

DATE	J.D.	PLATE	RADIAL VELOCITY (KM/SEC)		
			H 6	*H* 28	*M* II
1938 Mar. 14	2428972	V 2174	−37	.....	−61
17	8975	Ce 1638	−44	−76	−72
Apr. 18	9007	V 2205	−40	.....	−43
May 17	9036	Ce 1679	−30	.....	−52
20	9039	V 2227	−38	.....	−47
June 11	9061	Ce 1688	−30	.....	−48
12	9062	Ce 1689	−26	−49	−50
14	9064	V 2293	−33	.....	−44
16	9066	V 2303	−33	.....	−41
16	9066	V 2305	−34	.....	−46
17	9067	V 2309	−33	.....	−47
17	9067	V 2310	−32	.....	−48
July 13	9093	V 2336	−33	.....	−38
Aug. 16	9127	V 2379	(−33)	.....	−26
16	9127	V 2380	−31	.....	−29
1939 Mar. 4	9327	Ce 1926	−16	−16	−16
5	9328	Ce 1931	−15	−16	−14
6	9329	Ce 1937	−17	−16	−15
11	9334	V 2415	−14	.....	−14
May 4	9388	Ce 2021	−12	.....	(− 7)
4	9388	Ce 2022	−15	− 8	− 9
June 6	9421	Ce 2048	− 9	0	− 2
July 31	9476	Ce 2063	− 8	0	0
Aug. 30	9506	γ 22110	+ 1	.....	+ 2
1940 Feb. 27	9687	Ce 2275	+ 2	+11	+16
Mar. 24	9713	Ce 2300	+ 7	+16	+20
July 25	9836	Ce 2379	+11	+20	+23
25	9836	Ce 2380	+11	.....	+23
1941 May 12	2430127	Ce 2571	+20	+28	+28
16	0131	C 7679	+24	.....	+31
July 14	0190	C 7682	+26	.....	+30
15	0191	C 7687	+23	.....	+29
Aug. 8	0215	C 7694	+26	.....	+33
9	0216	Ce 2597	(+20)	.....	.....
12	0219	Ce 2601	+19	.....	+25
1942 Mar. 1	0420	Ce 2731	+20	+23	+22
2	0421	Ce 2736	+19	+24	+21
May 30	0516	Ce 2794	+20	.....	+19
June 28	0539	Ce 2808	+17	+17	+13
July 27	0568	Ce 2822	.....	.....	+17
1943 Feb. 25	0781	Ce 2960	+ 6	+ 4	+ 4
May 18	0863	Ce 3031	+ 2	0	+ 1
19	0864	Ce 3034	− 1	− 2	0
20	0865	Ce 3039	+ 1	+ 1	+ 1
June 16	0892	Ce 3070	.....	.....	− 1
23	0899	Ce 3079	− 2	− 2	− 5
Aug. 17	0954	Ce 3147	− 3	.....	− 7
1944 Feb. 10	1131	Ce 3391	−18	−23	−23

NOTES TO TABLE 3

The V plates were taken with a three-prism spectrograph, dispersion at $H\gamma$, 35 A/mm. The γ and C plates were taken with one-prism spectrographs attached to the 60-inch and 100-inch telescopes, respectively; dispersion at $H\gamma$, about 40 A/mm. The Ce plates were taken with the coudé spectrograph at the 250-foot focus of the 100-inch telescope; dispersion 10 A/mm except Nos. 2794, 2822, and 3070, on which it was 2.9 A/mm.

Hydrogen Lines

The Balmer series of hydrogen is exceptionally well developed in the spectrum of 48 Librae, being remarkable for the intensity, sharpness, and number of its lines. (See

TABLE 4

Radial Velocities: Normal Places

J.D.	Wt.	*H* 6	*H* 28 and *M* II	J.D.	Wt.	*H* 6	*H* 28 and *M* II
		km/sec	km/sec			km/sec	km/sec
2428974	3	−41	−71	2430128	3	+21	+29
9007	1	−40	−43	0190	2	+24	+30
9037	3	−33	−50	0217	3	+21	+28
9064	9	−32	−47	0420	4	+20	+23
9093	1	−33	−38	0510	2	+20	+19
9127	2	−32	−28	0539	2	+17	+15
9329	9	−16	−16	0568	2	.....	+17
9388	3	−14	− 8	0781	2	+ 6	+ 4
9421	2	− 9	− 1	0864	6	+ 1	0
9476	2	− 8	0	0897	3	− 2	− 3
9506	1	+ 1	+ 2	0954	2	− 3	− 7
9687	2	+ 2	+13	1131	2	−18	−23
9713	2	+ 7	+18				
9836	4	+11	+22				

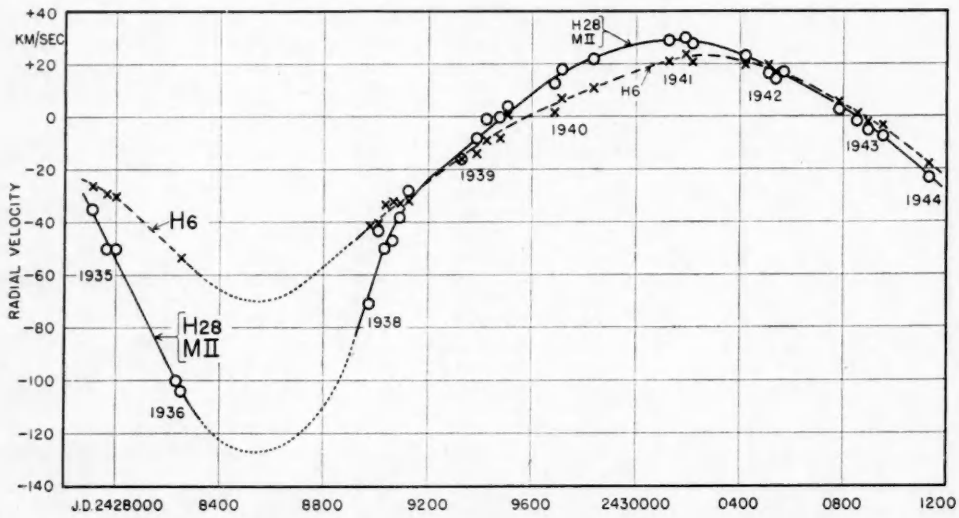

Fig. 2.—Radial velocities, 1935–1944. Circles and solid line represent velocities derived from *H* 28 and lines of ionized metals; crosses and dashed line, velocities from *H* 6. See text.

Pls. II and III and Fig. 3.) At *Hα* a strong emission line about 28 A wide is divided by an absorption core about 2 A wide which undergoes marked changes in intensity. The structure of *Hβ* is somewhat similar, but the emission is very much weaker. At *Hγ*, little if any emission remains. This rapid decrement in the intensity of the bright *H* lines is

PLATE II

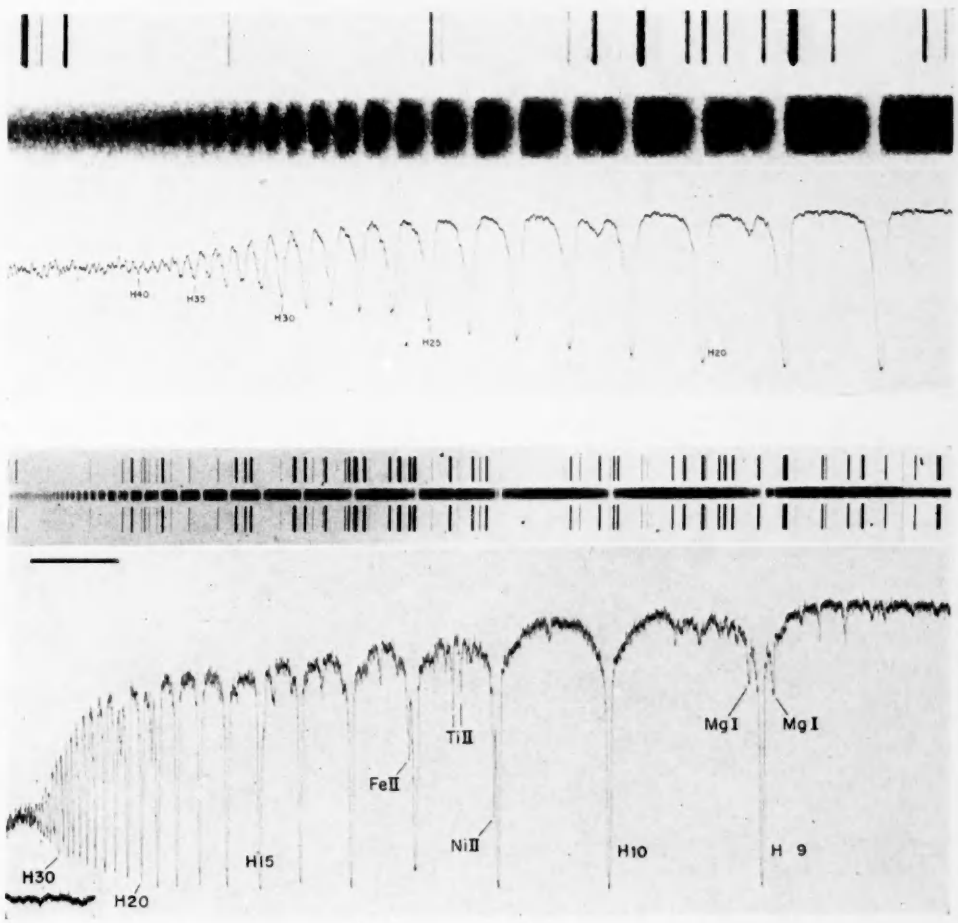

THE HEAD OF THE BALMER SERIES IN THE SPECTRUM OF 48 LIBRAE

Above: Plate Ce 3031, May 18, 1943
Below: Plate Ce 3034, May 19, 1943

PLATE III

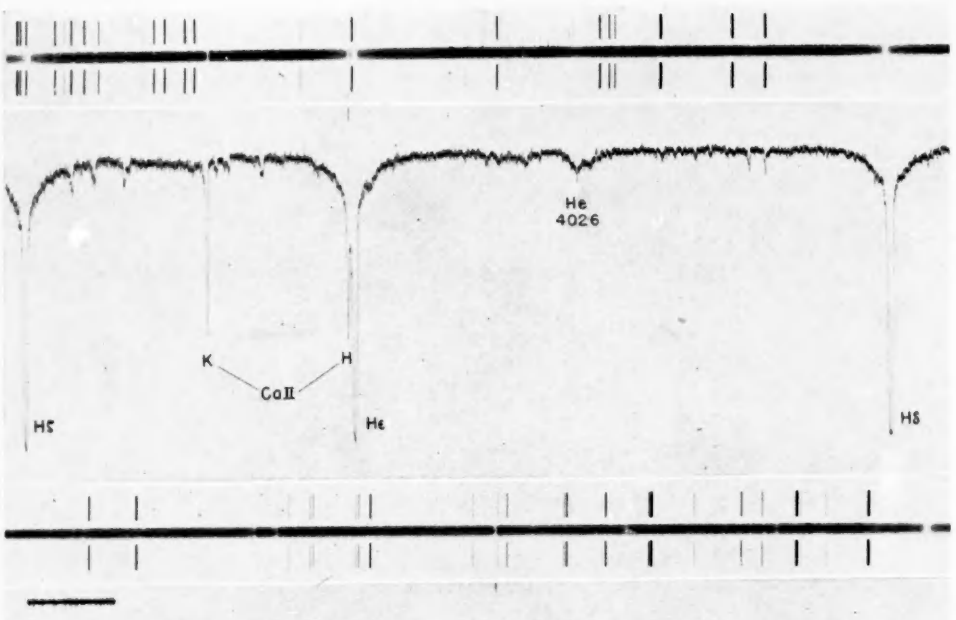

THE SPECTRUM OF 48 LIBRAE WITH MICROPHOTOMETER TRACINGS

Plate Ce 3034, May 19, 1943

characteristic of spectra of types B8e and Ae. The well-defined dark cores, on the other hand, weaken but slowly toward the ultraviolet. Because they remain narrow, they are resolved well toward the head of the series. On a plate of 48 Librae taken in 1943, lines

TABLE 5

RADIAL VELOCITIES: NORMAL PLACES FROM YERKES AND MCDONALD OBSERVATIONS

J.D.	Wt.	*H*		*M* II	
		Y	Y *minus* Mt. W.	Y	Y *minus* Mt. W.
		km/sec	km/sec	km/sec	km/sec
2429748.....	0.5	+ 5	−4	.....	.....
2430080.....	5	+16	−3	+24	− 5
0494.....	7	+15	−4	+11	− 9
0787.....	8.5	+ 2	−4	− 5	− 9
0821.....	8	0	−4	−10	−12
0872.....	8.5	− 4	−5	−11	− 9

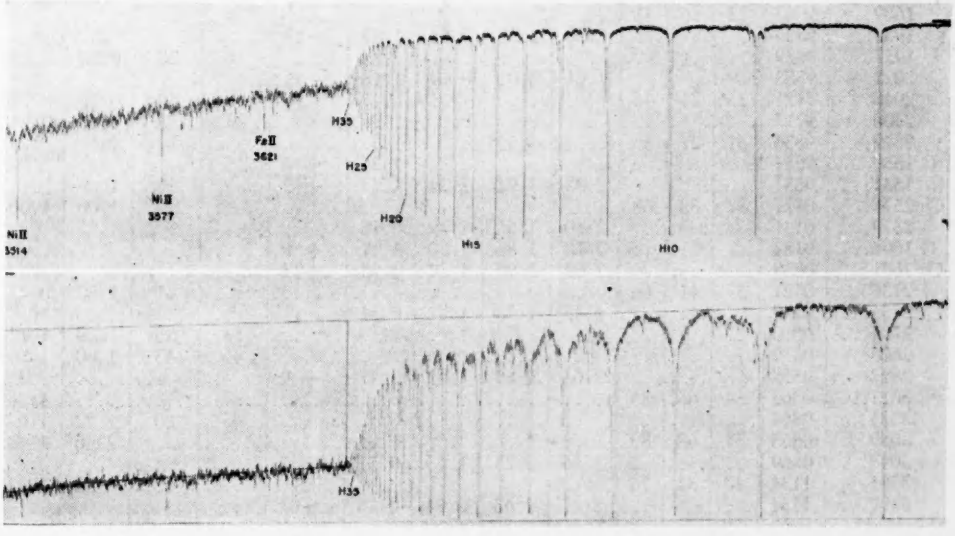

FIG. 3.—Continuous absorption at the head of the Balmer series. *Above:* Ce 3031, May 18, 1943. *Below:* Ce 3034, May 19, 1943. The difference in the appearance of the two tracings is due to the difference in density of the original spectrograms.

up to *H* 41 were measured. Variation from year to year in the intensity and structure of the *H* lines is apparent upon inspection of the spectrograms.

Photometric observations of hydrogen lines.—Measurements of microphotometer tracings show that the equivalent widths of the dark lines of the Balmer series more than doubled from 1938 to 1943. The absorption of the continuous spectrum near the head of the series, measured in the manner indicated in Figure 3, increased from 17 to 54 per

cent. During the same interval the maximum absorption in the line *H* 25 increased from 26 to 66 per cent; in *H* 15, from 38 to 87 per cent. In February, 1944, the absorption was somewhat less than in 1943. (See Table 6, cols. [3], [4], and [5], and Figs. 4 and 6*a*, *b*, *c*.)

The dark core of *Hα* gradually became stronger from 1938 to 1944. Its residual intensity, in terms of the continuous spectrum outside of the emission components, decreased from 1.5 to 0.3 (Table 6, col. [9], and Figs. 5 and 7). Referred to the highest in-

TABLE 6

DATA FROM MICROPHOTOMETER TRACINGS

		Percentage of Absorption			Emission *Hα*			Absorption *Hα*		Percentage of Absorption		Asymmetry	
Plate	J.D.	Bal. Head	*H* 25	*H* 15	*V*	*R*	*V*/*R*	Percentage of Cont. Spect.	Vel.	*Ca* II λ 3933	*Fe* II λ 4233	*Fe* II λ 4233	Hydrogen
(1)	(2)	(3)	(4)	(5)	(6)	(7)	(8)	(9)	(10)	(11)	(12)	(13)	(14)
	242								km/sec				
Ce 1638	8975	17	26	38	.....	.....	0.63	1.48	−41	.....	.....	.....	1.22
1688	9061	.....	.....	.....	.....	.....	.....	.....	.....	.....	26	.....	.....
1689	9062	22	16	31	.....	.....	.....	.....	.....	26	.....	.....	.....
1930	9328	.....	.....	.....	2.00	2.38	0.84	1.43	−13	.....	.....	.....	.....
1937	9329	.....	.....	.....	.....	.....	.....	.....	.....	26	28	0.70	1.15
2022	9388	.....	.....	.....	1.61	2.04	0.79	1.18	−11	.....	.....	.....	.....
2048	9421	25	24	46	.....	.....	.....	.....	.....	.....	40	0.85	0.73
2300	9713	.....	.....	.....	.....	.....	.....	.....	.....	33	28	0.40	0.74
2379	9836	31	27	56	.....	.....	.....	.....	.....	.....	.....	.....	.....
G 1530	9857	.....	.....	.....	.....	.....	.....	1.25	+ 4	.....	.....	.....	.....
1531	9857	.....	.....	.....	2.38	1.92	1.24	1.23	+ 2	.....	.....	.....	.....
Ce 2571	0127*	37	38	60	.....	.....	.....	.....	.....	.....	.....	1.00	1.00
2579	0131	.....	.....	.....	2.50	1.68	1.49	0.75	.....	.....	.....	.....	.....
G 1608	0184	.....	.....	.....	2.78	1.86	1.50	1.11	+ 9	.....	.....	.....	.....
Ce 2601	0219	.....	.....	.....	2.50	1.90	1.32	0.75	+12	.....	.....	.....	.....
2736	0421	37	41	66	.....	.....	.....	.....	.....	.....	41	1.50	0.92
2755	0448	.....	.....	.....	2.45	1.73	1.42	0.51	.....	.....	.....	.....	.....
2794	0510	.....	.....	.....	.....	.....	.....	.....	.....	53	48	1.09	1.72
2808	0579	.....	.....	.....	.....	.....	.....	.....	.....	46	43	1.00	1.50
2822	0568	.....	.....	.....	2.63	1.85	1.42	0.47	+ 9	.....	.....	.....	.....
3031	0863	54	65	85	.....	.....	.....	.....	.....	.....	.....	.....	1.95
3034	0864	.....	.....	.....	.....	.....	.....	.....	.....	65	60	1.22	1.97
3039	0865	54	68	89	.....	.....	.....	.....	.....	.....	.....	2.46	1.89
3048	0869	.....	.....	.....	2.56	2.23	1.15	0.51	+ 7	.....	.....	.....	.....
3391	1131	40	54	74	.....	.....	.....	.....	.....	.....	.....	1.50	1.22
3399	1134	.....	.....	.....	2.47	2.63	0.94	0.26	− 1	.....	.....	.....	.....

* JD 2430127.

tensity of the emission borders on either side, these values become 0.7 and 0.1, respectively. Since the intensity of the center of the original emission line was undoubtedly higher than that recorded on the plate at either side of the dark core, the actual absorption at the center of the line must have varied from more than 30 per cent to more than 90 per cent. The absorbing atoms must have been not only in front of the photosphere but also in front of most of the *H* atoms emitting light near the center of the *Hα* line. The significance of this conclusion is discussed in another section.

In 1942 and 1943 the dark *H* lines appeared slightly unsymmetrical, the violet edges

being less sharp than the red edges. Accordingly, the asymmetry of lines H 6 to H 9 in the years 1938 to 1944 has been studied by means of microphotometer tracings of suitable spectrograms. The total area of a given line as it appeared on a tracing was divided into two parts by a vertical line through the point of maximum absorption. The ratio of the violet to the red area serves as a measure of the asymmetry. The line is

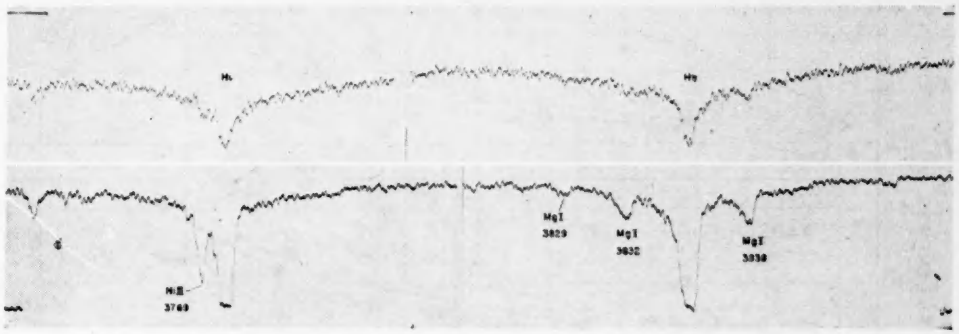

FIG. 4.—$H\iota$ and $H\eta$ in 1939 (*above*) and in 1943 (*below*)

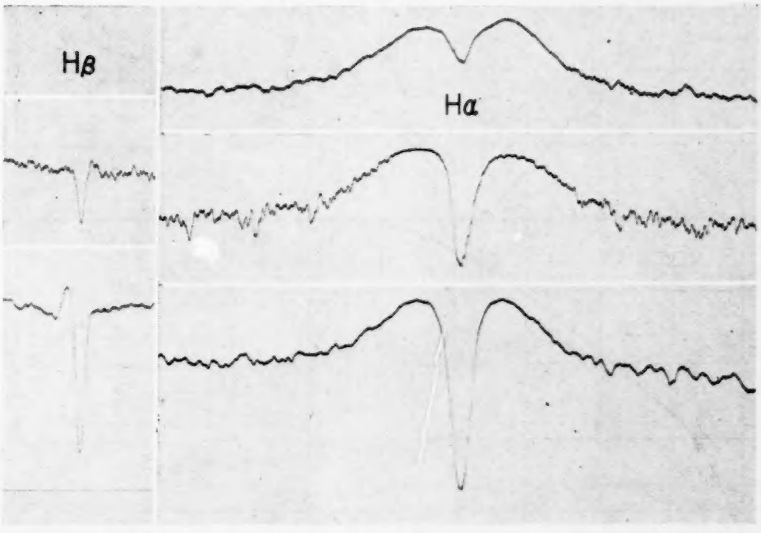

FIG. 5.—$H\beta$ in 1938 (*above*) and in 1941 (*below*); low dispersion. $H\alpha$ in 1938 (*above*), in 1941 (*center*), and in 1944 (*below*).

shaded toward the red when the ratio is less than unity and to the violet when it is greater than unity. The decided changes from year to year are shown by Table 6, column (14), and by Figure 6*f*.

The broad emission wings on either side of the dark core of $H\alpha$, shown in several tracings (Fig. 5), may or may not be symmetrical with respect to the core. The intensity of the highest point of each wing on various plates is recorded in Table 6, columns (6) and (7). The unit employed is the intensity of the adjacent continuous spectrum. To

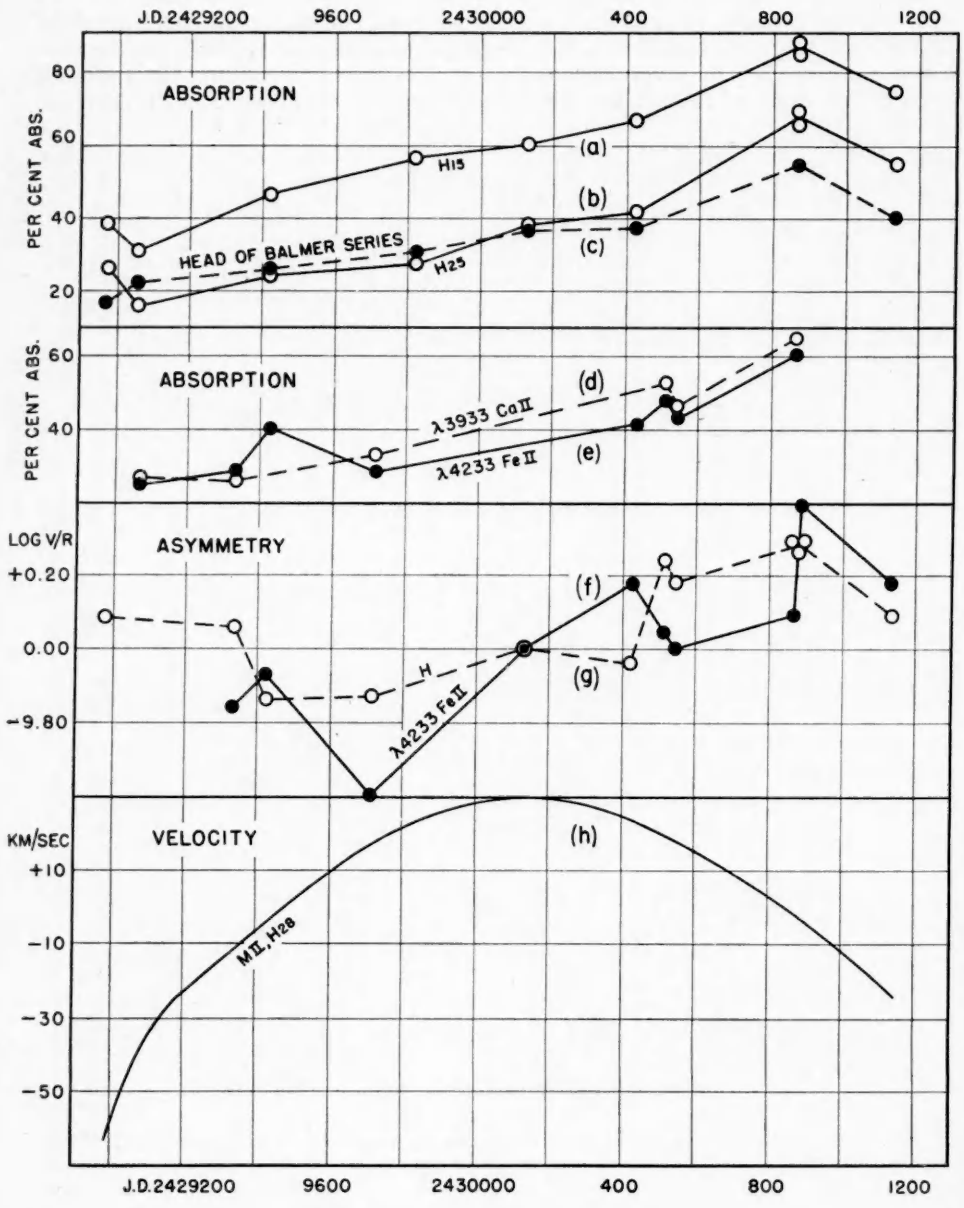

FIG. 6.—Photometric data. See text

obtain the intensity of the emission alone, subtract 1.00 (or a somewhat smaller value if allowance is to be made for a broad underlying absorption line).

The ratio V/R, Table 6, column (8), of the intensities of the two emission components provides a fairly sensitive indication of the relative position of the absorption core with respect to the maximum of the original broad emission line. As shown by Figure 7, the curve of V/R plotted against time runs nearly parallel to the curves for the displace-

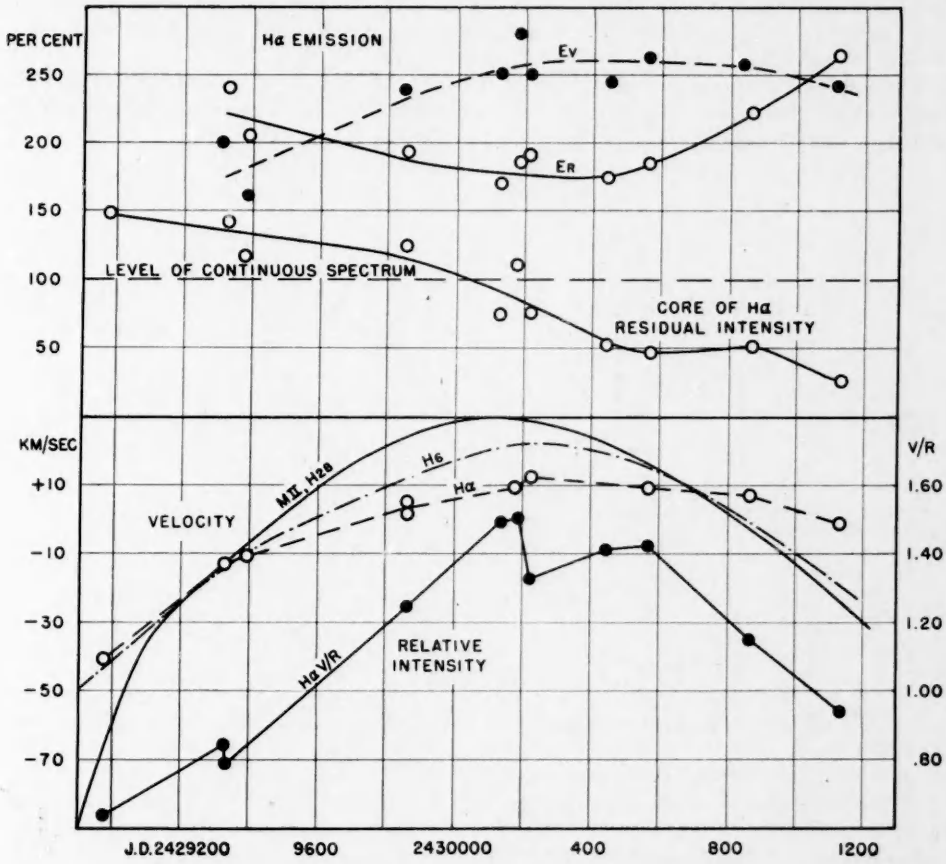

FIG. 7.—Data concerning the $H\alpha$ line. *Above:* Intensities of bright and dark components in percentage of the continuous spectrum. *Below:* Radial velocities (*scale on left*) and relative intensity of the two bright components (*scale on right*).

ments of the dark lines. Similarly, Figure 8 shows the values of V/R to be correlated with the displacements of dark $H\alpha$. The facts indicate that the emission line had smaller displacements than the absorption core. In other words, the dark core seems to have moved back and forth on a stationary or nearly stationary bright line whose position would correspond to a radial velocity of about -2 km/sec. Similar behavior has been observed in other Be stars and may perhaps be characteristic of bright-line stars with shell spectra.

Displacements of hydrogen lines.—The slight asymmetry of the H lines is not sufficient to interfere seriously with measurement of their displacements. On some of the later

coudé plates (dispersion, 10 A/mm) the probable error of measurement of a single line from *H* 5 to *H* 25 or *H* 30 is about 0.7 km/sec. Because in certain years the measured displacements of the lines have exhibited a well-marked progression from *Hβ* or *Hγ* toward the head of the series, the results from individual lines on numerous plates have been compared. The behavior of the lines from 1938, when the average displacement was about −60 km/sec, to 1941, when it was +24 km/sec, is shown in Figure 9. Similarly, the decreasing displacements from 1941 to 1944 are shown in Figure 10. As representative points in the series we have chosen *H* 6 and *H* 28. The corresponding values for each plate (Table 3) were read from smooth curves like those in Figures 9 and 10, drawn through the plotted values for individual lines.

The displacements seem to have no significant relationship to wave length. See Figure 11, in which are plotted smoothed curves for the *H* lines measured on plates Ce 1638 (negative displacement) and Ce 2571 (positive displacement).

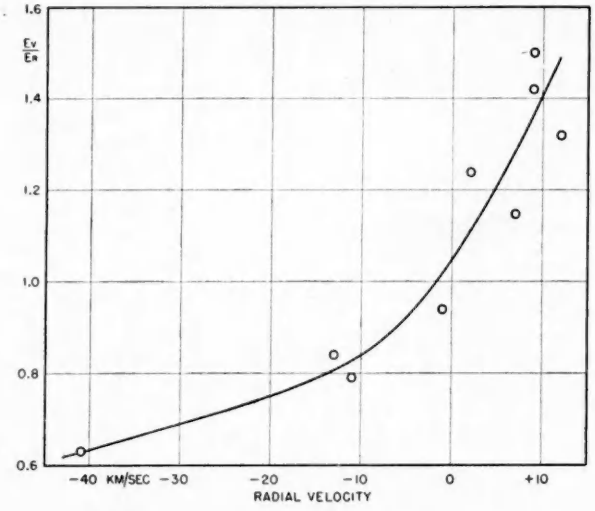

FIG. 8.—Relative intensity of the emission components of *Hα* plotted against the radial velocity from the dark lines.

If the velocities continue their present trend, the next year or two may present an opportunity of studying more thoroughly the interesting phase of large negative displacements with a rapid progressive shift from line to line of the Balmer series.

METALLIC LINES

Numerous metallic lines—notably those of *Fe* II, *Cr* II, *Ti* II, *Ni* II, and *Ca* II—have been quite prominent since 1942. The metallic spectrum is well exhibited by Struve's list,[11] which contains about four hundred metallic lines between λ 3289 and λ 4823, more than one hundred of which are below the head of the *H* series, λ 3645. On one of our plates (Ce 3039, May 20, 1943), taken especially for the extreme ultraviolet, measurable lines extend to λ 3168. (See Fig. 12.) Beyond Struve's limit of λ 3289 we have measured 33 lines, at least two-thirds of them due to *Fe* II.

The increase in intensity of the metallic lines since 1938 is illustrated by measurements of the percentage of absorption at the bottoms of the lines λ 3933 *Ca* II and λ 4233 *Fe* II

(Table 6, cols. [11] and [12]; Figs. 6*d*, *e*, and 13). The equivalent width of λ 4233 was about 0.8 A in 1938; 1.8 A in 1943.

Although the lines are narrow, many are at times definitely unsymmetrical, the long-wave-length edge usually being the sharper. The asymmetry of λ 4233 *Fe* II (Table 6, col. [13]; Figs. 6*f*, *g*, and 14) exhibits somewhat the same general behavior as that of the Balmer lines, but the extremes are more pronounced. Lines of *Ti* II, *Fe* I, and *Mg* I tend to be slightly hazy, as compared with those of *Fe* II, *Ni* II, and *Ca* II. The line

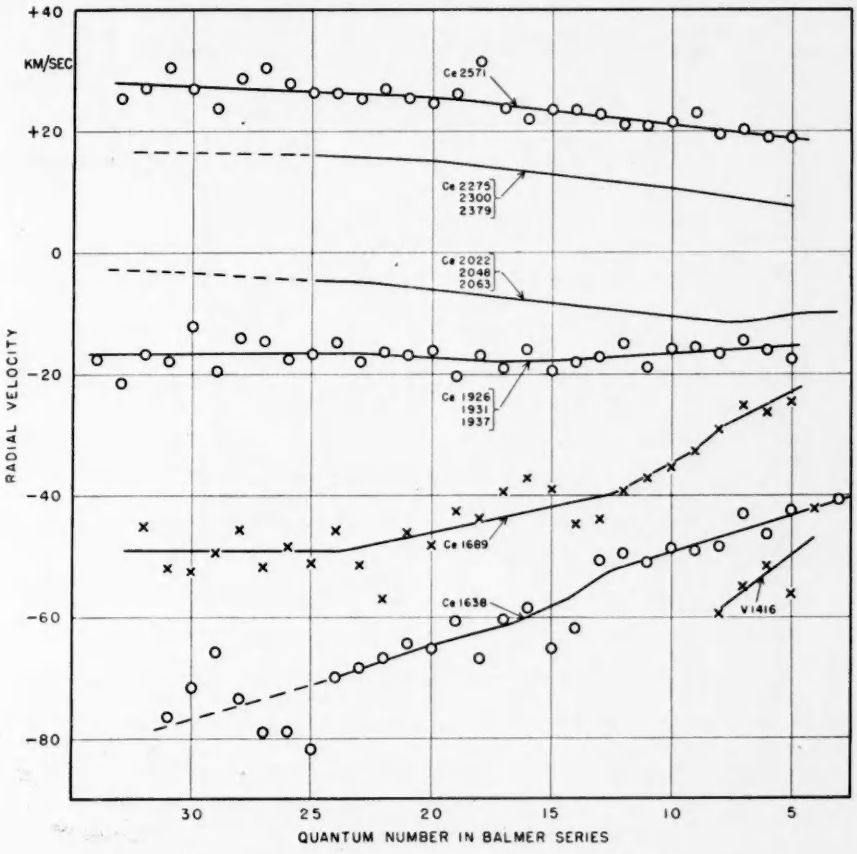

FIG. 9.—Displacements of *H* lines, 1936–1941. Ascending series

Mg II λ 4481 is wide and weak. Our results for 1943 are in substantial agreement with those of Struve[11] and of Hiltner.[12]

Displacements of metallic lines.—On most plates the velocities from lines of *Ca* II, *Fe* II, *Ti* II, and *Cr* II are in good agreement. The weak *Mg* I triplet λλ 3829, 3832, and 3838 (Fig. 4) is regularly displaced about −10 km/sec. On a few plates, lines of *Ti* II and especially of *Cr* II have residuals of −6 or −8 km/sec. Lines with negative displacements are often slightly diffuse.

A fact clearly shown by Tables 2 and 3 is that, when there is a progression in the velocities derived from successive lines of the Balmer series, the metallic-line velocities

(which show little or no dependence on wave length) agree with those of *H* lines near the head of the series. In Tables 3, 4, and 5 we have used the symbol *M* II to represent the mean displacements of lines of ionized metals.

Stationary Lines

The D lines of sodium are formed of two narrow components which are usually closely blended but on several plates are separated well enough for fairly reliable measurement. (See Fig. 15.) The stronger component is stationary, with a velocity displacement of

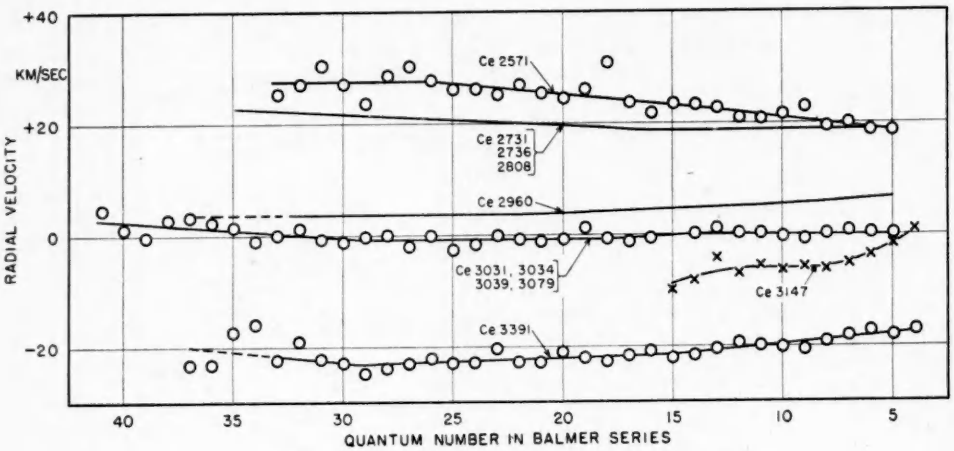

Fig. 10.—Displacements of *H* lines, 1941–1944. Descending series

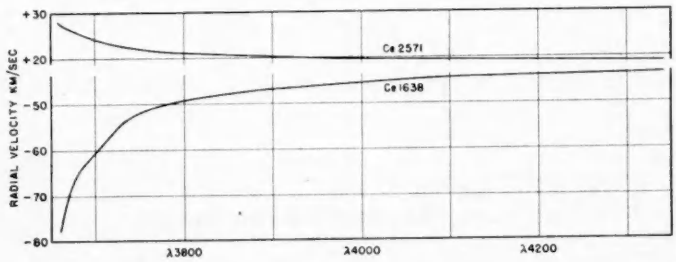

Fig. 11.—Displacements of *H* lines plotted against wave length. Smoothed curves

−14 km/sec; the other component yields a variable velocity agreeing with that from other metallic lines.

The K line of ionized calcium has the same structure and behavior except that the stationary component, instead of being stronger than the stellar component, is much weaker (Figs. 14 and 15). Measured on five spectrograms, the weak component yields a velocity of −15 km/sec.

Several facts suggest that the stationary lines may be at least partly circumstellar rather than wholly interstellar. The radial velocity from the fixed components is about the same as that of the star before 1935, when the abnormal displacements were first

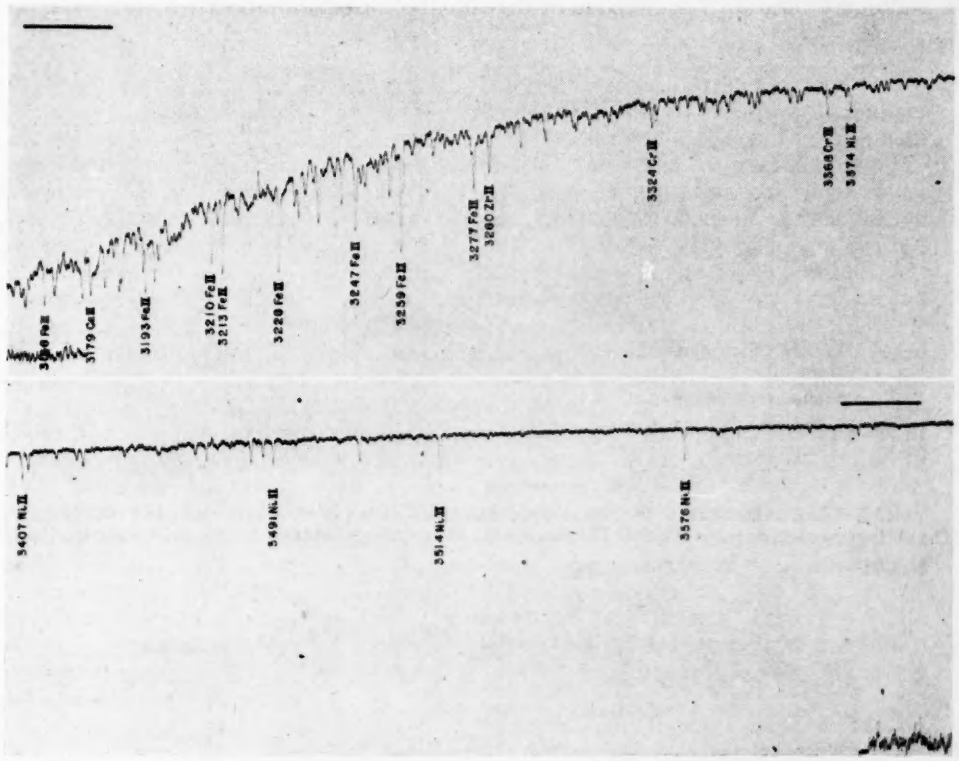

FIG. 12.—Extreme ultraviolet portion of the spectrum. Ce 3039, May 20, 1943

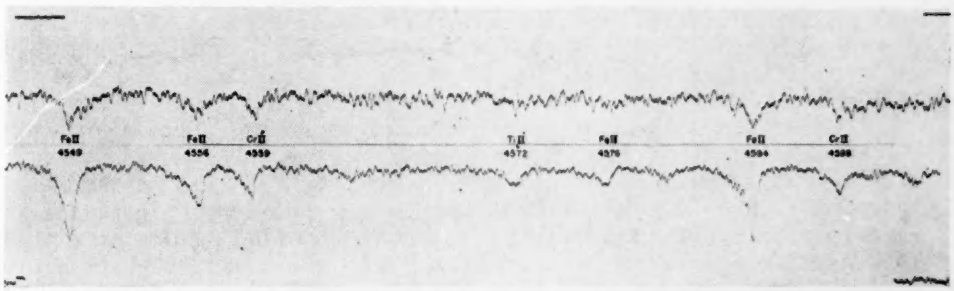

FIG. 13.—The spectrum from λ 4545 to λ 4590 in 1939 (*above*) and in 1943 (*below*)

measure[1]. The velocity, however, is not sufficient to distinguish between the two types of stationary lines. In the direction of the star the correction for solar motion is +12

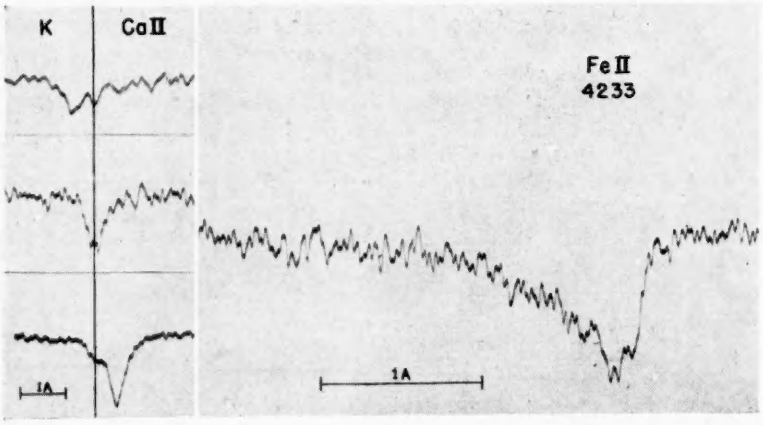

FIG. 14.—Two components of the K line of *Ca* II in 1938 (*above*), in 1939 (*center*), and in 1942 (*below*). The stationary component is aligned. The line λ 4233 *Fe* II with high dispersion; Ce 3070, June 16, 1943.

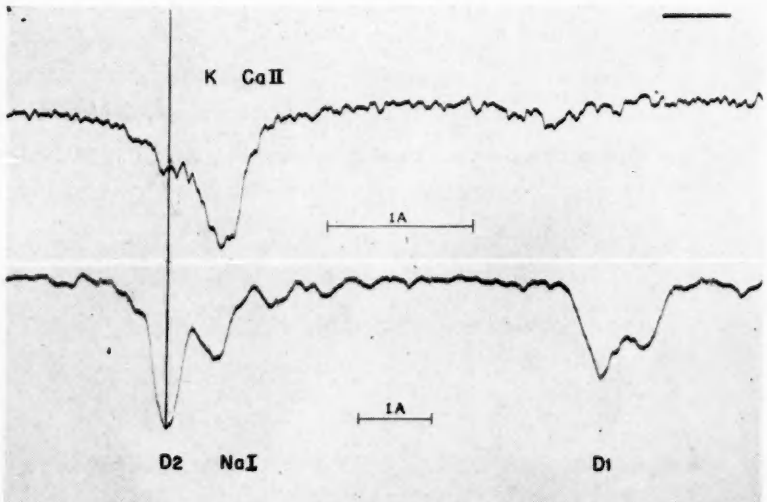

FIG. 15.—Components of *Ca* II and of *Na* I in 1942. Stationary components are aligned

km/sec. Thus the residual velocity is about −3 km/sec, a value not at all impossible for interstellar lines in this longitude. The mean equivalent width of stationary D1 and D2 is 0.34 A, a larger value than would be expected from the star's probable distance and

high galactic latitude, +27°. The K line is much weaker, its equivalent width being about 0.11 A; hence the probability that it is wholly interstellar is somewhat greater.

Discussion

Cause of the displacements.—The unusual behavior of the displacements of the Balmer lines and the shape of the velocity-curve in Figure 1 show that we are not dealing with an ordinary spectroscopic binary. From 1922 to 1931, preceding the well-marked minimum, the curve was nearly flat. Hence the changes in velocity, if periodic at all, must have had a strange, complex form. The data afford no evidence of a previous fluctuation like that which occurred between 1935 and 1944, but they do not exclude one with a minimum about 1913 and a maximum about 1918. In any event, it seems probable that the origin of the recent fluctuations was chiefly atmospheric, although the approach of a companion star may, of course, have had some important effect.

Since the lines were at times unsymmetrical, it might be supposed that the measured displacements merely reflect the strengthening of wings on one edge or the other of the lines. Examination of the data, however, does not support this view but seems rather to indicate that the lines suffered bodily displacements. In the first place, the lines are at all times fairly narrow. Hence, no very large displacements in the measured "centers of gravity" could be caused by variable wings. Moreover, the largest displacements occurred when the lines were nearly symmetrical. According to Figure 6*f*, *g*, *h*, the lines were most unsymmetrical at intermediate velocities. A significant fact is that when the velocity was about 0 km/sec in 1940 the lines were winged toward the red, whereas at the same velocity in 1943 they were winged toward the violet.

Origin of hydrogen lines.—The displacements of the dark Balmer lines (Figs. 9, 10, and 11) suggest that two blended series are involved—one with a slow decrement (S.D.) and large changes in velocity, the other with a rapid decrement (R.D.) and relatively small changes in velocity.

The S.D. series prevails near the head of the series; the other becomes increasingly important from line to line toward $H\alpha$. According to the formula used by F. L. Mohler,[13]

$$\log N_e = 23.06 - 7.5 \log n_m ,$$

where N_e is the number of electrons per cubic centimeter and n_m is the quantum number of the last observable line in the H series. For the S.D. series in 1943, $\log N_e = 11.0$. If the temperature is assumed to be 10,000°, $\log P_e = -6.9$, where P_e is the electron pressure in atmospheres. The S.D. series and the associated metallic lines, produced at a high atmospheric level, form the so-called "shell" spectrum.[14] The R.D. series is produced at a lower level, where the pressure is greater.

The probable place of origin of the H emission presents an interesting problem. It has usually been assumed that bright lines in stellar spectra originate in an atmosphere extending far above the normal reversing layer. In many bright-line objects this assumption is clearly correct. In Me stars, however, the reversing layer probably overlies the source of the bright lines. In 48 Librae, similarly, the emission may come from an intensely bright stratum of hydrogen just above the photosphere. Facts which seem to support this hypothesis are:

1. Great width of emission lines (probably caused by Stark effect).
2. Rapid decrement of emission lines from $H\alpha$ to $H\gamma$.
3. Relatively small displacements of $H\alpha$ and $H\beta$ emission.
4. Nearly complete absorption in the dark core of $H\alpha$.

[13] *Ap. J.*, **90**, 429, 1939.

[14] O. Struve, *Proc. Amer. Phil. Soc.*, **81**, 211, 1939.

On this hypothesis the following sequence would apply to the increasing range of displacements as well as to height in the atmosphere:

1. Photosphere.
2. *H* emission.
3. *H* absorption R.D. series.
4. *H* absorption S.D. series. Metallic absorption.

As a working hypothesis alternative to that of an extended emitting envelope, we suggest that in some Be and Ae stars, particularly in those with shell spectra, a special supply of *H* atoms or protons is released just above the photosphere. This cloud of hydrogen pushes part of the reversing layer upward to a level where it is cooler and less dense than normal and thus may produce a shell spectrum. The hydrogen may be produced by the disintegration of an unstable atomic nucleus of an unfamiliar type coming from the stellar interior. If the supply is cut off, the bright lines disappear, as they did in μ Centauri and Pleione, to reappear upon re-establishment of the special mechanism of hydrogen release.

INVESTIGATIONS ON PROPER MOTION. XXIII. THE PROPER MOTION OF THE CLUSTER *h* PERSEI*

ADRIAAN VAN MAANEN
Mount Wilson Observatory
Received April 19, 1944

ABSTRACT

On two pairs of plates, taken at the 80-foot focus of the 60-inch reflector, with intervals of 29 and 17 years, 800 stars in the central part of *h* Persei were measured for proper motion. The probable error of the motions is 0".00067 in each co-ordinate. Over a hundred stars were found not to belong to the cluster, including practically all the field stars brighter than magnitude 15; for the fainter stars it is more difficult to decide about possible membership in the cluster.

"On revient toujours à ses premières amours." In this paper are presented the results of a study of the proper motion of the cluster in Perseus, which was the subject of the investigation[1] with which I started my astronomical career. In 1908, J. C. Kapteyn suggested to me the measurement of some plates of the clusters *h* and χ Persei which had been taken at Helsingfors and Pulkovo with instruments of the *Carte du ciel* type. It was hoped that the proper motions might enable us to find which stars belonged to the clusters and which were foreground stars; we would then be able to determine the proper motion of the clusters as well as the distribution of the motions of the noncluster stars; finally, we might be able to derive the parallax of the clusters. Kapteyn and de Sitter[2] had measured the parallaxes of 178 stars in this region of the sky and had made the statement:

> In conclusion, attention may be drawn to the fact that the foregoing discussion affords the material from which the parallaxes of the clusters *h* and χ Persei relative to the surrounding stars may be derived with extreme accuracy, as soon as we will be able (by a discussion of the proper motions) to decide with certainty, for each of the stars on the plates, whether it belongs to either of these clusters or not.

This optimistic view is hardly realized by the present results. Of the 34 stars common to the two investigations, 7 are definitely or probably not members of the cluster. The 27 cluster stars have a mean parallax of $+0''.0033 \pm 0''.0068$. If we exclude 5 stars whose parallaxes are marked as uncertain in *Groningen* **10**, we find a mean parallax of $-0''.0027 \pm 0''.0062$.

The probable errors of these values are so large as to make the mean parallaxes quite illusory. The probable error of a final proper μ_α or μ_δ derived in *Utrecht* V was 0".0057; since the motion of the cluster with respect to the other stars is only a few thousandths of a second of arc, the results were not accurate enough to indicate definitely which stars belonged to the cluster and which did not. As recent results from plates taken at the 80-foot focus of the 60-inch reflector had, however, given results of a very high accuracy,[3] and as two pairs of plates of *h* Persei with intervals of 29 and 17 years, respectively, were available, it seemed worth trying again to separate the cluster from the noncluster stars. Since the quality of the pair of plates with 17 years' interval was extremely

* *Contributions from the Mount Wilson Observatory, Carnegie Institution of Washington*, No. 691.

[1] *Recherches astronomiques de l'Observatoire d'Utrecht* V 1911.

[2] *Pub. Astr. Lab. Groningen*, No. 10, 1902.

[3] *Mt. Wilson Contr.*, No. 670; *Ap. J.*, **96**, 382, 1942.

good, equal weights were assigned the two pairs. Within a circle of 10 minutes of arc around BD+56°522, 800 stars were measured. For all but 12 stars, good photographic magnitudes by P. Th. Oosterhoff were available.[4] For 320 of these, Oosterhoff's paper gives color indices.

As usual, each of the pairs of plates was measured in four positions—east, west, north, and south—in the direction of increasing reading of the micrometer screw, about four days being required to measure each pair of plates in one position. Each star was measured three times in the sequence 1–800 and then twice in the reverse order, 800–1; in this way I hoped to check any changes in the relative position of the plates during the interval of measuring. It is gratifying to state that no definite change was found during all the measures. Five extra measures were made on a few stars for which the reverse measures differed unduly from the direct measures; for the eight sets of measures the number of stars ranged from 17 to 38, or, in the mean, 3.4 per cent; of these, about one-half the extra measures were on stars brighter than the tenth magnitude or fainter than 15.5 mag., both of which groups are liable to give some difficulty in measuring.

The measured quantities were then combined into four sets: α I, α II, δ I, and δ II, I and II defining the two pairs of plates. The range in these figures showed that a simple reduction of the form $a + bx$ or $a' + cy$ might reduce the values enough to distinguish the stars which were certainly not members of the cluster. Values of a and a' were derived from stars in the central region about 3′ square, while b and c were determined from the stars in the strips about 3′ wide which were farthest east and west or north and south. Excluded were all stars brighter than 12.5 or fainter than 15.5 mag.; double stars; stars marked uncertain during the measures; and stars judged not to be members of the cluster because of a definite motion or on account of their color index. The values of a, a', b, and c, thus derived, were applied to all 800 stars and were then multiplied by 0.820 and 1.390 for I and II, respectively, in order to reduce the measured quantities to units of 0″.0001 per year.

The 409 stars between the limits 12.50 and 15.49 mag. which, from these preliminary reductions, might be members of the cluster were now divided according to their position on the plates into 45 squares of about 3 minutes of arc; and for each square the mean $\mu_{\alpha I}$, $\mu_{\alpha II}$, $\mu_{\delta I}$, and $\mu_{\delta II}$ were derived. This showed that a reduction including quadratic terms would definitely improve the results. A preliminary reduction with quadratic terms showed that 49 of the 409 stars probably had motions excluding them from membership in the cluster; finally, in order to give a fairly even distribution of the stars over the field, 60 more stars were excluded for which the agreement between the two pairs of plates was less satisfactory. This left 300 stars, probable members of the cluster, which could be used for the final determination of the constants in the equations of condition:

$$\mu = m - (a + bx + cy + dx^2 + cxy + fy^2),$$

for the four sets of measures in α and δ for both pairs of plates. The constants thus derived were substituted in the equations of condition for all 800 stars, giving $\mu_{\alpha I}$, $\mu_{\alpha II}$, $\mu_{\delta I}$, and $\mu_{\delta II}$ in units of 0″.0001 per year. It is gratifying to state that only 5 of the 300 stars used for the derivation of the constants finally turned out to have motions indicating that they might not be members of the group; in a total of 300 stars their inclusion cannot have vitiated the final motions by more than one or two times 0″.00001.

A magnitude error was evident from the beginning of the measuring. However, as by far the majority of the stars, especially of the brighter ones, must be members of the cluster, it is possible to find this error with considerable accuracy and to correct the results for it. For this purpose the mean proper motions were plotted for each magnitude, the few stars brighter than magnitude 10 being plotted on one diagram. By making a set

[4] *Ann. Sterrewacht te Leiden*, **17**, 1, 1937.

of concentric circles with radii representing motions of 3-, 4-, and 5-thousandths of a second of arc to fit over each plot, it could be decided which stars probably did not belong to the cluster; when these were omitted, together with the stars marked as uncertain during the measures and those with abnormal color indices, the mean motions were found for the different magnitudes (Table 1) and were plotted against the magnitudes. A smooth curve was drawn through these points, and from this curve the corrections in the last two columns of Table 1 were applied. In the seventh and eighth columns of Table 2 the corrected $\bar{\mu}_\alpha$ and $\bar{\mu}_\delta$ are the final values of the mean motions. The first two columns of Table 2 give the current number and the number in Oosterhoff's catalogue, with an asterisk in the first column indicating the stars used to derive the plate constants; the third and fourth columns give the right ascension and declination taken from Oosterhoff; and the fifth and sixth columns give Oosterhoff's photographic magnitude and color index, when available. If not provided by Oosterhoff, the magnitude was estimated from neighboring stars and is given to one decimal only. The positions of these stars were measured

TABLE 1

MEAN MOTION FOR DIFFERENT MAGNITUDES AND CORRECTION APPLIED

Mean Mag.	Mean μ_α	Mean μ_δ	n	Corr. μ_α	Corr. μ_δ
9.14.....	−0".0056	−0".0037	17	+0".0056	+0".0050
10.52.....	− .0048	− .0043	26	+ .0047	+ .0039
11.45.....	− .0035	− .0034	37	+ .0033	+ .0033
12.57.....	− .0019	− .0023	57	+ .0019	+ .0020
13.53.....	− .0009	− .0006	99	+ .0006	+ .0007
14.55.....	+ .0003	+ .0003	170	− .0002	− .0002
15.54.....	+ .0004	+ .0004	253	− .0006	− .0004
16.10.....	+0.0010	+0.0005	39	−0.0008	−0.0005

in tenths of a millimeter on one of the plates with respect to the nearest star and have been assigned the same Oosterhoff number as the principal star with adjunct "b" or "c." The last column, headed "Remarks," gives the number of the star in van Maanen's dissertation, *Utrecht* V; "var." indicates the two stars which Oosterhoff suspects to be variable, and "NC" or "NC?" respectively, the stars which are definitely or probably not members of the cluster.

From a comparison of the values μ_α and μ_δ for the two pairs of plates, we can find for different magnitudes the probable errors contained in Table 3. After applying a magnitude correction, the values in the second and third columns are reduced to those in the fifth and sixth columns, which are the final probable errors of the mean motions in α and δ. These results are very consistently small—in the mean 0".00065 for $\bar{\mu}_\alpha$ and 0".00069 for $\bar{\mu}_\delta$; the only values larger than 0".0010 are for the 45 stars of sixteenth magnitude.

DISCUSSION OF THE RESULTS

Comparison with "Utrecht" V.—Of the 200 stars common to *Utrecht* V and the present investigation, 16 are now included among the certainly noncluster stars and 10 are probably noncluster stars. With the accuracy reached in *Utrecht* V only 2 stars would have been recognized as noncluster stars and 5 as probably noncluster stars, while of the 12 stars, which in *Utrecht* V show a motion exceeding 0".020 and therefore might have been taken for field stars, only 6 have motions which show them not to be members of the cluster—4 definitely and 2 probably. In Figure 1 the dispersion of the motions of these 200 stars is shown; in the lower part, which represents the new motions, 154 stars fall within the central circle with a radius of 0".003. The other circle represents a radius of 0".005. The diagram shows the enormous increase in accuracy between the two sets of measures.

TABLE 2

PROPER MOTIONS OF STARS MEASURED

(Unit = 0".0001)

No.	Oosterhoff No.	α 1900 2^h	δ 1900 +56°	Phot. Mag.	Color Index	$\bar{\mu}_\alpha$	$\bar{\mu}_\delta$	Remarks	
1	360	10^m 52.2	39' 37"	13.20	-0.03	0	- 15	1076	
2	360b	52.3	39 39	14.8	.....	+ 13	- 1		
3	363	52.5	40 49	15.84	.....	- 25	- 14		
4	376	55.2	37 19	12.54	- .13	+ 21	+ 1	1081	
5•	379	56.2	38 23	14.74	.....	- 2	+ 3		
6	380	56.4	39 51	11.24	- .23	+ 15	- 29	1075	
7	381	56.6	39 39	15.87	.....	- 23	- 34		
8	382	56.8	38 33	14.84	.....	+ 21	- 4		
9•	391	58.6	41 1	15.27	.....	- 20	- 10		
10•	393	58.8	39 7	15.22	.....	- 1	- 5		
11	395	59.2	44 44	14.40	.....	+ 26	+ 7		
12	396	59.4	44 34	15.29	.....	- 3	- 10		
13	407	11 0.9	44 29	15.77	.....	- 56	- 26		NC?
14•	408	0.9	36 9	13.78	+ .09	- 23	+ 9		
15•	410	1.3	36 44	14.70	.....	- 12	- 11		
16•	413	1.8	41 53	15.33	.....	- 24	- 22		NC?
17	414	1.9	39 44	15.10	.....	+ 13	- 1		
18	416	2.0	37 59	15.92	.....	+ 14	+ 8		
19•	418	2.2	37 29	13.98	+ .22	- 9	- 11		
20	422	2.8	43 50	15.29	.....	+ 4	+ 2		
21	423	2.9	38 40	15.38	.....	- 20	0		
22	424	2.9	44 29	13.74	+ .70	+ 15	- 7		NC?
23	428	3.1	45 0	15.96	.....	+ 12	+ 2		
24•	429	3.3	42 26	14.49	.....	- 3	+ 2		
25•	430	3.4	43 6	14.24	+ .11	+ 11	- 11		
26	431	3.4	36 2	13.07	+ .34	+ 37	- 5	1084	NC?
27•	437	4.4	45 12	15.11	.....	+ 1	- 9		
28•	438	4.5	42 16	15.22	.....	- 8	- 14		
29	439	4.7	34 43	16.07	.....	- 9	- 2		
30	440	4.8	44 28	13.36	+ .72	+ 25	+ 19		NC
31•	441	4.8	43 6	15.24	.....	- 10	+ 4		
32	443	4.9	34 33	15.87	.....	+ 3	- 81		NC
33•	444	5.0	40 31	13.34	+ .15	+ 14	0	1074	
34•	450	6.6	38 44	15.50	.....	- 7	+ 12		
35	454	7.2	38 46	16.04	.....	- 23	+ 38		
36	455	7.2	41 29	13.08	.00	+ 10	- 9	1071	
37	457	7.4	44 12	16.00	.....	- 33	- 38		NC?
38	458	7.5	44 58	13.96	+ .03	+ 7	+ 5		
39	460	7.8	41 53	15.79	.....	- 28	- 8		
40•	461	7.9	35 55	15.50	.....	- 23	- 10		
41•	462	7.9	40 24	14.43	.....	- 7	- 9		
42	464	8.3	37 1	14.70	.....	- 15	- 1		
43	466	8.4	38 39	15.72	.....	- 31	+ 22		
44	467	8.8	38 30	14.70	.....	- 7	+ 1		
45	468	8.8	34 53	14.84	.....	- 12	+ 18		
46	470	9.1	40 50	14.28	.....	+377	-142		NC
47	471	9.2	41 51	15.83	.....	- 13	- 30		
48•	472	9.3	40 7	13.40	- .04	- 7	- 3		
49	475	9.4	45 56	11.38	- .21	+ 51	- 29	951	NC
50•	477	9.6	43 25	15.22	.....	+ 12	- 22		
51•	479	9.7	47 1	15.31	.....	- 4	- 7		
52	480	9.7	38 27	15.03	.....	+ 5	+ 13		
53•	489	10.7	41 24	14.53	.....	- 2	+ 10		
54	491	11.1	41 53	11.14	- .19	+ 22	- 22	967	
55	492	11.3	45 34	15.94	.....	+ 19	- 14		
56•	494	11.4	46 20	12.85	- .13	+ 9	- 3	947	
57	495	11.4	46 32	13.10	+ .08	+ 5	- 24	945	
58	499	11.9	45 14	15.04	.....	+ 1	+ 9		
59	500	11.9	42 13	15.38	.....	- 1	- 12		
60	501	11.9	42 1	15.86	.....	- 37	- 8		
61•	502	12.0	39 42	15.25	.....	- 8	- 21		
62	503	12.1	44 28	16.00	.....	- 5	+ 44		
63•	504	12.2	44 38	14.94	.....	0	- 3		
64	505	12.2	44 55	12.43	- .11	+ 18	- 19	954	
65•	509	12.7	35 28	13.11	+ .38	+ 8	+ 11	987	
66•	510	13.3	40 53	13.58	+ .08	- 8	- 8		
67	511	13.7	36 56	15.99	.....	- 7	+ 14		
68	512	13.7	34 2	15.47	.....	+ 10	- 26		
69	513	13.8	45 53	13.95	+ .17	- 15	+ 5		
70	514	13.8	41 24	15.92	.....	- 21	- 12		
71	515	13.9	46 43	12.11	- .02	+ 19	- 12	943	
72	516	13.9	44 43	16.16	.....	+ 4	- 19		
73	517	13.9	42 28	10.18	- .22	+ 22	- 40	964	NC?
74•	518	14.0	44 4	15.17	.....	- 8	- 3		
75	519	14.2	37 56	15.06	.....	+ 3	- 16		
76	520	14.5	46 10	14.63	.....	+150	- 47		NC
77	522	14.7	37 10	15.99	.....	- 20	+ 6		
78	523	14.8	41 59	14.80	.....	+ 6	+ 5		
79	527	15.3	36 2	13.16	- .03	+ 1	+ 6	986	
80•	528	15.4	45 34	14.73	.....	- 10	- 4		

TABLE 2 -- Continued

No.	Oosterhoff No.	α 1900 2^h	δ 1900 +56°	Phot. Mag.	Color Index	$\bar{\mu}_\alpha$	$\bar{\mu}_\delta$	Remarks	
81	529	11^m $15^s.4$	37' 58"	15.52	.....	- 9	+ 2		
82	530	15.7	44 45	10.28	- .29	+ 25	- 39	960	NC?
83	532	16.3	36 8	13.64	+ .30	- 12	+ 8	985	
84•	536	16.6	36 10	14.61	.....	- 4	- 2		
85	538	16.9	41 26	11.40	- .19	+ 6	- 13	970	
86	539	17.0	40 42	15.39	.....	- 28	- 22		NC?
87•	541	17.3	38 46	13.49	+ .15	+ 5	- 7	981	
88	543	17.3	41 48	15.48	.....	- 97	+ 40		NC
89	545	17.4	36 30	15.88	.....	- 15	+ 22		
90	546	17.4	44 44	15.51	.....	+ 25	+ 8		
91	547	17.4	45 13	12.42	- .04	+ 12	+ 4	953	
92	549	17.8	46 15	12.86	- .10	+ 2	- 11	948	
93	551	18.0	46 26	10.67	- .23	+ 35	- 40	946	NC?
94•	554	18.1	43 34	13.98	- .02	- 1	+ 3		
95•	555	18.1	45 23	14.27	.....	+ 7	- 4		
96•	556	18.4	37 28	14.26	.....	- 7	- 4		
97•	558	18.4	43 11	15.15	.....	- 6	+ 17		
98	563	18.6	40 59	12.24	- .16	+ 18	- 22	974	
99	569	19.1	39 16	15.77	.....	- 7	- 6		
100•	571	19.3	42 2	14.92	.....	- 8	- 6		
101	572	19.3	35 17	10.63	- .29	+ 4	+ 10	989	
102•	573	19.4	37 26	15.28	.....	+ 6	- 10		
103•	574	19.4	34 1	14.22	.....	+ 13	+ 4		
104	575	19.6	46 46	16.09	.....	- 25	- 30		
105	576	19.6	36 11	15.93	.....	- 37	- 7		
106	579	19.7	38 27	15.82	.....	+ 7	- 2		
107	580	19.8	42 39	15.87	.....	- 17	- 2		
108•	581	19.9	33 12	15.44	.....	- 7	+ 6		
109	583	19.9	43 24	15.62	.....	+ 15	+ 25		
110•	584	19.9	41 31	13.69	+ .07	- 2	+ 5		
111	585	20.0	39 22	15.62	.....	- 6	+ 13		
112•	586	20.1	46 0	14.54	.....	- 7	+ 4		
113	587	20.4	34 37	15.94	.....	- 39	- 29		NC?
114	589	20.6	38 41	15.93	.....	- 6	+ 1		
115	592	20.9	39 53	16.18	.....	- 7	+ 26		
116	594	21.2	43 10	15.04	.....	- 8	+ 16		
117•	596	21.4	35 25	12.93	- .09	+ 10	+ 11	988	
118•	597	21.4	43 53	14.09	+ .08	+ 9	+ 10		
119	598	21.7	39 58	15.34	.....	+ 2	- 4		
120	599	21.8	39 15	14.56	.....	+ 8	+ 21		
121	600	21.9	36 54	15.82	.....	- 3	- 18		
122	601	22.0	35 39	16.11	.....	- 25	- 6		
123•	602	22.0	41 14	14.51	.....	+ 12	+ 18		
124	603	22.0	45 28	14.73	.....	- 9	- 15		
125	604	22.3	34 34	10.44	+1.15	+ 46	- 5	990	NC
126•	605	22.3	46 24	14.41	.....	- 6	- 11		
127	608	22.4	42 5	15.64	.....	+ 13	- 10		
128•	609	22.4	39 42	14.55	.....	+ 10	+ 14		
129	611	22.6	32 42	12.09	+ .26	- 71	+ 88	993	NC
130	612	22.6	32 50	8.87	- .34	0	+ 74	992	
131	612c	23.3	32 45	15.6	.....	+ 17	+ 4		
132•	613	22.7	40 55	14.60	.....	+ 6	+ 4		
133•	615	22.8	42 12	15.27	.....	- 6	+ 10		
134	616	23.1	40 45	15.92	.....	- 50	- 3		NC?
135	617	23.2	43 53	14.29	.....	- 4	+ 2		
136•	619	23.3	44 44	13.20	.....	+ 15	0	957	
137	620	23.3	44 32	13.05	- .01	+ 7	- 19	958	
138	621	23.6	46 5	15.13	.....	- 13	- 7		
139	622	23.7	42 17	10.88	- .27	+ 16	+ 3	966	
140	623	23.7	39 25	12.54	- .05	+ 15	- 1	978	
141	624	23.8	34 42	15.86	.....	+ 29	- 46		NC?
142•	625	23.8	40 59	14.50	.....	+ 15	0		
143	626	23.8	48 5	12.79	- .04	- 1	- 13	937	
144	627	23.9	47 13	15.89	.....	- 7	- 25		
145	629	24.1	44 3	14.67	.....	+ 27	- 7		
146	630	24.1	43 51	15.80	.....	- 9	+ 2		
147	631	24.2	42 51	16.15	.....	- 41	+ 13		
148	637	24.5	36 23	15.88	.....	- 15	+ 7		
149	638	24.6	42 36	15.70	.....	+ 25:	+ 5:		
150	638b	24.7	42 38	15.7	.....	- 37	- 4		
151•	639	24.8	35 7	14.93	.....	+ 5	- 14		
152	641	25.0	46 29	15.42	.....	+ 1	- 13		
153	642	25.0	44 50	13.57	+ .03	- 9	+ 17	956	
154	644	25.3	41 57	15.71	.....	+ 11	+ 24		
155	646	25.4	40 18	14.94	.....	+ 18	+ 10		
156	647	25.4	40 35	12.92	+ .14	+ 12	- 8	977	
157	648	25.4	40 52	15.30	.....	+ 19	+ 13		
158	649	25.5	41 50	11.04	- .18	+ 7	- 6	969	
159•	650	25.5	42 17	15.05	.....	+ 2	+ 8		
160	651	25.5	44 0	15.71	.....	+ 16	+ 8		

TABLE 2 -- Continued

No.	Oosterhoff No.	α 1900 9^h	δ 1900 +56°	Phot. Mag.	Color Index	$\bar{\mu}_\alpha$	$\bar{\mu}_\delta$	Remarks	
161	652	11^m $25^s.6$	46' 43"	14.97	.....	+ 23	+ 18		NC?
162	654	25.8	37 23	15.92	.....	- 18	- 6		
163•	655	25.9	36 23	13.86	- .11	+ 6	+ 2		
164•	656	25.9	47 38	13.92	- .15	- 2	- 9		
165	658	26.1	47 12	11.38	- .07	+ 25	- 19	942	
166	659	26.2	40 57	13.04	+ .02	+ 1	+ 1	975	
167•	661	26.6	40 1	14.58	.....	+ 5	+ 18		
168	662	26.6	44 42	8.47	- .24	+ 51	- 21	959	
169	662b	26.6	44 48	14.3	.....	- 2	+ 4		
170	664	26.7	46 5	14.40	.....	- 2	+ 9		
171	665	26.9	46 7	14.10	.....	- 33	+ 18		NC
172•	666	27.0	34 0	14.78	.....	+ 1	- 3		
173	670	27.1	43 56	10.96	- .26	+ 17	- 27	962	NC??
174	675	27.6	42 21	13.22	+ .19	- 6	- 11	965	
175•	676	27.6	39 20	14.18	+ .23	+ 15	+ 16		
176	677	27.6	38 21	14.66	.....	+ 12	+ 3		
177	681	27.9	32 0	12.63	- .03	- 2	- 8	995	
178	683	27.9	46 38	15.92	.....	- 69	- 2		NC?
179	684	27.9	43 17	15.78	.....	- 25	0		
180	685	27.9	41 1	15.77	.....	- 19	+ 28		
181•	686	27.9	37 59	14.84	.....	- 2	- 6		
182	687	28.0	33 54	15.82	.....	- 15	- 4		
183	688	28.0	43 47	14.72	.....	- 13	+ 1		
184	689	28.2	45 23	13.35	+ .26	+ 3	+ 2	952	
185•	690	28.3	39 59	14.42	.....	- 4	+ 3		
186	692	28.6	41 17	9.54	- .33	- 5	- 18	972	
187	693	28.7	39 54	13.64	+ .09	- 3	- 1		
188	695	28.7	44 16	12.28	- .12	+ 12	- 14	961	
189•	696	28.8	47 9	14.46	+ .16	+ 12	- 14		
190	697	29.1	32 22	15.88	.....	- 79	- 10		NC
191	698	29.2	35 58	15.79	.....	- 2	+ 38		
192	699	29.4	36 3	15.92	.....	- 50	+ 8		NC?
193	700	29.4	36 31	13.13	- .08	- 12	- 1		
194•	701	29.4	39 24	14.61	.....	+ 1	+ 8		
195	703	29.5	37 57	15.59	.....	- 35	- 4		
196	704	29.6	47 29	16.29	.....	+ 21	- 14		
197	706	30.6	47 4	14.99	.....	+ 13	- 6		
198•	707	30.6	48 8	14.05	.....	0	- 6		
199•	708	30.6	41 3	14.87	.....	- 4	+ 8		
200	709	30.9	33 54	14.36	.....	+ 4	+ 11		
201	710	30.9	32 58	14.22	.....	+ 49	- 28		NC
202•	713	31.1	41 35	13.93	+ .24	+ 7	+ 9		
203	714	31.1	47 14	11.94	- .16	+ 19	- 11	941	
204•	715	31.2	42 58	14.58	.....	- 6	+ 8		
205	716	31.2	40 22	13.73	+ .10	- 4	+ 8		
206	717	31.2	44 51	9.47	- .20	+ 15	- 20	955	
207	719	31.4	42 33	15.89	.....	+ 6	+ 2		
208	720	31.7	39 12	13.80	.00	- 13	+ 6		
209	721	31.9	47 32	13.63	+ .37	- 34	- 22	939	NC?
210	724	32.2	42 40	14.21	+ .30	- 15	+ 26		NC?
211	725	32.3	45 52	11.64	- .20	+ 17	- 32	950	
212	725b	32.3	45 50	14.0	.....	- 9	+ 11		
213	728	32.4	41 1	14.91	.....	- 14	- 4		
214	730	32.5	47 41	12.92	+ .35	+ 56	- 26	938	NC
215	731	32.5	46 6	10.87	- .17	+ 34	- 2	949	NC??
216•	734	32.9	33 21	13.82	+ .05	+ 5	+ 3		
217	735	33.0	46 50	16.07	.....	- 13	+ 19		
218	736	33.1	36 56	15.51	.....	+ 5	+ 2		
219•	737	33.5	39 39	15.40	.....	- 16	+ 19		
220	740	33.8	45 1	14.11	.....	+ 10	- 1		
221	740b	33.7	45 0	15.0	.....	- 13	0		
222	741	34.0	32 15	15.17	.....	+ 12	+ 3		
223	742	34.0	49 15	16.10	.....	+ 19	- 24		
224•	743	34.3	48 8	14.64	.....	- 1	+ 13		
225•	745	34.5	36 58	15.42	.....	- 5	- 17		
226	746	34.6	38 57	12.63	- .14	+ 8	- 7	980	
227•	747	34.7	40 51	15.39	.....	- 12	+ 6		
228	749	35.1	37 39	15.07	.....	- 43	+ 17		NC
229•	751	35.3	32 54	15.12	.....	- 1	+ 31		NC?
230•	752	35.4	45 34	14.88	.....	+ 15	+ 6		
231	754	35.4	32 0	14.10	.....	+164	+ 23		NC
232•	755	35.5	44 49	13.66	+ .17	+ 6	+ 6		
233	756	35.9	40 25	15.95	.....	+ 13	+ 6		
234	757	36.3	34 23	15.70	.....	+ 6	+ 4		
235	758	36.6	47 16	15.00	.....	+ 7	- 8		
236	759	36.6	38 36	15.63	.....	+131	-136		NC
237	761	37.2	41 27	15.73	.....	- 16	+ 21		
238•	762	37.3	31 32	14.62	.....	- 15	- 9		
239	763	37.4	47 48	15.80	.....	+ 10	+ 9		
240	764	37.6	37 51	15.81	.....	- 28	- 18		

TABLE 2 -- Continued

No.	Coster-hoff No.	α 1900 2^h	δ 1900 +56°	Phot. Mag.	Color Index	$\bar{\mu}_\alpha$	$\bar{\mu}_\delta$	Remarks
241•	765	11^m $37^s.6$	45' 24"	14.27	.....	+ 1	0	
242	767	37.8	35 11	15.67	.....	+ 3	+ 16	
243	769	37.9	34 13	10.96	- .31	- 16	+ 27	991
244	770	37.9	36 46	15.88	.....	+ 14	- 52	NC?
245•	772	38.0	37 17	15.18	.....	+ 5	- 8	
246	773	38.2	43 11	15.90	.....	+ 31	+ 18	
247•	774	38.3	47 18	14.04	- .03	+ 1	- 12	
248	776	38.5	33 58	15.98	.....	+ 1	+ 5	
249	778	38.5	39 13	12.16	- .18	- 2	- 8	979
250•	779	38.6	43 18	14.98	.....	+ 11	+ 1	
251•	781	39.2	37 44	15.49	.....	- 11	+ 8	
252	782	39.2	38 17	9.60	- .25	- 6	+ 7	982
253	783	39.2	48 17	14.93	.. ..	+ 46	- 8	NC
254•	784	39.7	43 19	13.52	.00	- 5	- 1	
255	785	39.7	39 23	14.57	.....	- 10	+ 6	
256	787	39.9	36 19	15.71	.....	+ 35:	- 10:	
257•	788	40.1	38 28	15.05	.....	- 6	- 11	
258	789	40.4	49 4	11.82	- .04	+ 17	- 20	935
259•	790	40.4	40 45	13.20	+ .02	+ 7	- 3	976
260	792	40.5	45 58	13.71	+ .57	+ 63	- 85	NC
261•	793	40.5	41 26	14.09	- .02	+ 10	+ 8	
262	795	40.7	49 45	15.14	.....	+ 22	+ 14	
263	797	40.8	41 50	15.66	.....	- 33	+ 13	
264•	798	41.1	34 32	15.06	.....	- 3	- 15	
265•	799	41.1	47 37	14.12	- .02	- 4	+ 9	
266	800	41.1	42 40	12.30	- .06	+ 13	+ 7	963
267	801	41.3	38 15	12.86	- .07	+ 1	- 4	983
268	802	41.3	44 25	14.15	+ .04	+ 14	+ 1	
269	803	41.8	36 35	10.63	- .31	+ 17	+ 22	984
270	804	41.8	41 38	13.43	+ .04	- 26	+ 8	
271	805	41.9	40 33	14.99	.....	+ 23	+ 25	NC?
272	806	41.9	48 29	16.01	.....	+ 12	- 1	
273	807	42.2	39 7	13.86	+ .73	- 8	+ 2	NC?
274	808	42.2	39 24	15.84	.....	+ 26	+ 8	
275	809	42.3	39 57	15.83	.....	- 3	+ 1	
276•	810	42.4	49 40	14.45	.00	+ 2	- 3	
277•	812	42.7	38 42	13.90	+ .17	0	+ 20	
278•	813	42.7	44 47	14.54	.....	+ 4	- 4	
279•	815	42.9	46 44	14.64	.....	+ 5	- 18	
280	816	43.4	47 16	16.03	.....	+ 29	+ 12	
281•	820	43.8	39 35	13.17	- .03	+ 12	+ 19	
282	821	43.9	39 53	15.70	.....	- 1	+ 2	
283	823	44.1	35 41	16.17	.....	0	+ 15	
284	825	44.6	37 24	15.24	.....	+ 10	+ 10	
285	827	44.7	36 14	15.93	.....	+ 5	+ 2	
286	829	44.8	46 42	11.45	+ .39	+1135	-392	944 NC
287•	830	44.8	44 18	13.60	+ .07	- 10	+ 4	
288•	832	45.0	38 34	14.30	- .04	+ 22	+ 14	
289	833	45.2	44 32	15.72	.....	- 7	+ 28	
290	834	45.5	32 16	10.94	- .19	- 31	+ 38	994 NC?
291	836	45.6	38 25	15.86	.....	+ 11	+ 24	
292•	837	45.7	41 41	14.22	+ .18	- 7	- 1	
293	838	45.7	47 9	12.64	- .07	+ 20	- 18	782
294	839	46.0	49 24	9.58	- .23	+ 29	- 42	776 NC??
295•	840	46.3	31 49	15.35	.....	- 12	- 10	
296•	841	46.3	35 42	13.32	+ .15	+ 13	- 5	
297	842	46.4	38 8	13.20	+ .07	- 4	- 6	859
298	843	46.4	40 21	9.52	- .22	- 6	- 6	829
299	844	46.5	42 12	15.56	.....	+ 7	+ 8	
300•	845	46.5	42 15	14.79	.....	- 9	+ 1	
301	846	46.6	46 39	10.13	- .23	0	- 26	783
302	847	46.7	36 16	9.35	- .23	- 12	+ 22	870
303	848	46.7	41 46	15.23	.....	- 14	+ 17	
304	850	47.0	44 25	14.33	+ .42	+ 16	+ 15	
305	851	47.3	45 9	11.47	+ .44	+126	+ 96	788 NC
306	852	47.4	48 45	14.99	.....	- 12	+ 8	
307	853	47.6	35 40	16.03	.....	- 1	- 4	
308•	854	47.7	38 53	14.33	+ .08	- 4	+ 3	
309•	855	47.8	36 41	15.16	.....	+ 5	- 6	
310	856	47.9	40 32	15.64	.....	+ 19	+ 30	
311•	857	47.9	40 26	14.94	.....	- 10	+ 2	
312	858	48.1	44 41	15.50	.....	+ 30	+ 26	
313	859	48.1	39 36	10.86	- .15	+ 3	+ 12	846
314	860	48.1	33 43	11.61	+ .31	+ 51	- 32	875 NC
315	864	48.3	38 7	10.05	- .29	- 12	+ 29	860
316	865	48.3	37 41	14.20	+ .87	-113	- 47	NC
317	867	48.5	37 48	11.00	+ .34	-106	- 62	863 NC
318	868	48.5	44 17	15.71	.....	- 13	0	
319	869	48.5	39 3	12.08	+ .03	+ 13	+ 22	850
320	871	48.6	43 26	15.51	.....	+ 17	+ 4	

TABLE 2 -- Continued

No.	Oosterhoff No.	α 1900 2^h	δ 1900 +56°	Phot. Mag.	Color Index	$\bar{\mu}_\alpha$	$\bar{\mu}_\delta$	Remarks
321•	872	$11^m\ 48^s.6$	43' 19"	13.05	+ .06	- 8	- 11	792
322•	874	48.7	31 56	14.33	.....	+ 4	+ 8	
323	875	48.8	39 35	15.26	.....	+ 8	- 4	
324	876	48.8	39 42	12.75	- .01	+ 2	+ 3	845
325	878	49.1	44 37	15.70	.....	- 15	- 1	
326	879	49.1	40 56	11.57	- .23	- 9	+ 5	816
327	880	49.1	40 49	12.69	- .04	- 7	- 6	817
328	882	49.2	32 42	15.94	.....	+ 39	- 2	
329•	883	49.2	43 57	14.74	.....	- 6	+ 1	
330•	884	49.2	34 32	15.40	.....	+ 8	- 16	
331	886	49.3	42 45	15.93	.....	- 13	- 6	
332•	887	49.3	48 23	14.06	.00	+ 23	- 7	
333•	891	49.6	35 37	14.83	.....	+ 10	+ 1	
334	892	49.7	40 46	11.24	- .23	- 11	- 11	819
335	893	49.7	40 49	11.79	- .26	+ 24	+ 16	818
336	894	49.7	35 8	15.78	.....	+103	- 76	NC
337•	895	49.7	35 32	14.90	.....	+ 15	- 18	
338	896	50.0	41 55	12.53	- .06	+ 5	+ 9	801
339•	897	50.1	45 10	13.64	+ .29	+ 6	+ 10	787
340•	898	50.4	42 5	14.64	.....	+ 5	+ 3	
341	900	50.6	45 27	12.56	+ .07	- 5	- 4	786
342	901	50.7	42 26	15.01	.....	- 17	- 3	
343•	904	51.0	45 28	12.62	+ .10	+ 15	+ 3	785
344	907	51.2	40 46	12.37	- .06	- 8	- 2	821
345	908	51.2	45 11	15.84	.....	- 41	- 7	
346	909	51.3	41 55	15.32	.....	+ 3	+ 11	
347	910	51.5	32 11	15.99	.....	- 23	+ 20	
348	911	51.6	39 1	11.43	- .23	+ 7	+ 8	851
349•	914	51.7	41 59	15.27	.....	- 4	+ 4	
350	915	51.7	34 48	15.88	.....	- 1	- 12	
351	916	51.9	49 50	15.75	.....	- 56	+ 32	NC
352•	917	52.2	38 41	14.91	.....	- 4	- 1	
353	918	52.3	45 18	16.06	.....	- 6	- 1	
354	919	52.4	44 31	11.34	- .03	+ 10	- 1	791
355	922	52.4	40 39	9.73	- .26	- 20	- 12	822
356	923	52.4	39 6	13.10	- .08	- 8	- 10	849
357•	924	52.6	40 29	14.93	.....	- 2	- 23	
358	926	52.6	39 57	11.69	- .06	+ 15	- 1	840
359	929	52.7	41 45	10.45	- .25	- 5	- 3	804
360	930	52.9	41 55	12.46	- .08	+ 12	- 4	802
361	931	53.1	32 28	15.50	.....	- 11	+ 47	NC?
362•	932	53.3	34 38	12.89	- .11	- 5	- 2	872
363•	934	53.5	42 11	14.78	.....	+ 6	+ 24	
364	935	53.9	40 8	14.14	.....	+ 24	- 10	
365	936	54.1	41 21	10.52	- .26	- 15	- 11	808
366•	938	54.2	34 43	14.24	.....	+ 13	+ 14	
367	939	54.2	40 27	12.30	- .14	- 3	+ 5	827
368	940	54.3	32 3	15.82	.....	- 27	+ 8	
369•	941	54.3	41 30	15.10	.....	- 14	+ 13	
370•	942	54.4	36 48	15.26	.....	+ 18	- 9	
371	943	54.5	33 41	11.43	+ .21	+128	+ 96	876 NC
372	944	54.5	45 33	14.11	+ .45	- 90	- 55	NC
373•	945	54.7	38 24	14.95	.....	+ 10	+ 7	
374•	946	54.8	41 40	14.57	.....	+ 2	+ 7	
375	947	54.9	37 59	15.95	.....	+ 29	- 23	
376	948	55.0	41 32	15.63	.....	+ 13	+ 1	
377	949	55.1	40 39	15.63	.....	- 27	+ 10	
378	950	55.1	43 5	11.41	- .19	+ 13	- 10	794
379	952	55.2	39 56	12.08	- .03	- 14	+ 6	841
380•	953	55.3	44 54	15.06	.....	+ 5	- 13	
381	955	55.5	41 44	15.99	.....	- 7	+ 16	
382•	956	55.8	41 30	12.67	- .02	+ 18	+ 4	806
383•	957	55.8	36 1	15.23	.....	+ 2	- 2	
384•	959	56.0	39 58	12.84	- .15	- 3	+ 4	842
385•	960	56.2	39 46	13.77	+ .33	+ 6	- 4	
386•	961	56.2	34 37	14.86	.....	+ 11	+ 1	
387	963	56.3	40 34	11.08	- .24	- 16	+ 8	825
388•	964	56.3	39 16	14.55	.....	0	+ 2	
389	965	56.5	42 31	12.77	.00	- 12	+ 5	797
390•	966	56.5	39 4	14.35	.....	- 4	- 2	
391•	967	56.6	36 34	14.17	+ .10	- 4	- 1	
392	968	56.6	35 51	16.06	.....	- 32	- 8	
393	969	56.7	38 15	14.17	+1.00	- 16	+ 13	NC?
394•	970	56.7	40 58	13.95	.....	- 4	- 3	
395	971	56.7	39 14	15.91	.....	+ 11	- 41	
396	972	56.8	37 1	11.73	- .18	- 3	+ 11	867
397•	973	56.9	49 8	15.03	.....	+ 11	+ 6	
398	974	56.9	44 37	15.84	.....	- 32	- 2	
399	976	57.1	41 6	11.52	- .06	0	+ 1	812
400	977	57.1	40 29	11.19	- .12	- 6	+ 7	828

TABLE 2 -- Continued

No.	Oosterhoff No.	α 1900 2^h	δ 1900 +56°	Phot. Mag.	Color Index	$\bar{\mu}_\alpha$	$\bar{\mu}_\delta$	Remarks	
401	978	11^m 57.2	41' 43"	10.78	- .22	- 3	- 1	805	
402•	979	57.3	37 55	14.48	.....	- 1	0		
403	980	57.3	40 59	9.90	- .18	- 5	0	815	
404•	981	57.5	36 57	13.02	- .02	+ 15	0	868	
405•	982	57.7	39 43	13.98	+ .19	+ 9	+ 12		
406	984	57.9	36 39	15.34	.....	+ 12	- 8		
407	985	58.2	41 3	12.06	- .08	- 8	+ 3	813	
408	986	58.3	41 29	12.65	+ .05	+ 4	+ 3	807	
409•	987	58.3	42 15	14.86	.....	- 13	+ 16		
410•	988	58.6	38 25	12.82	+ .02	- 5	+ 5	857	
411	989	58.6	43 12	15.58	.....	- 5	- 9		
412•	990	58.6	38 43	14.53	.....	+ 1	- 14		
413	991	58.6	40 38	11.48	- .06	+ 10	- 4	823	
414	992	58.6	41 0	10.07	- .17	+ 4	- 10	814	
415•	993	58.7	36 13	13.55	+ .18	- 1	+ 9		
416•	994	58.8	43 16	15.36	.....	0	- 10		
417	995	58.9	45 17	15.72	.....	- 5	+ 24		
418•	996	58.9	45 31	15.25	.....	+ 19	+ 6		
419•	999	59.0	38 25	13.36	+ .05	+ 17	- 5	856	
420•	1000	59.0	39 22	13.28	+ .15	- 4	+ 3	848	
421	1001	59.1	36 42	10.66	- .27	- 11	+ 6	869	
422	1004	59.2	41 17	10.97	- .23	- 14	- 18	810	
423	1005	59.3	45 17	14.56	.....	- 20	+ 28		NC
424	1006	59.4	33 52	15.86	.....	+ 71	+ 4		NC
425	1007	59.6	40 41	15.53	.....	- 32	+ 2		
426•	1008	59.7	35 21	14.03	.....	+ 3	+ 3		
427	1009	59.7	32 48	15.78	.....	+ 3	+ 6		
428	1012	59.9	34 37	12.42	+ .02	- 19	0	873	
429	1014	12 0.0	38 21	13.00	- .03	- 1	+ 6	858	
430	1015	0.0	42 59	10.64	+ .09	- 3	- 10	795	
431•	1016	0.1	45 46	14.28	.....	+ 15	+ 5		
432	1017	0.1	41 48	15.60	.....	- 3	- 4		
433	1018	0.1	41 49	15.53	.....	+ 7	- 8		
434•	1020	0.2	40 36	13.75	+ .03	+ 1	- 2		
435	1021	0.2	39 35	13.07	+ .02	- 15	+ 5	847	Var?
436•	1022	0.3	45 17	13.78	.....	+ 9	+ 17		
437	1023	0.3	37 39	12.96	+ .32	- 99	- 64	864	NC
438	1025	0.5	41 34	15.82	.....	+ 9	+ 27		
439	1026	0.6	41 2	15.72	.....	- 10	+ 17		
440	1027	0.7	33 40	16.13	.....	+ 3:	+ 10:		
441•	1028	0.8	38 38	14.90	.....	+ 32	- 6		NC?
442•	1029	0.9	35 55	15.21	.....	- 10	- 3		
443	1030	0.9	41 37	16.03	.....	+ 7	- 30		
444•	1031	0.9	39 37	15.29	.....	+ 4	+ 1		
445	1034	1.1	41 54	15.31	.....	+ 16	+ 3		
446•	1035	1.2	31 0	14.34	.....	- 2	0		
447	1036	1.4	34 55	15.53	.....	+ 7	- 2		
448	1038	1.5	41 15	15.67	.....	- 39	- 3		
449•	1039	1.6	36 37	15.37	.....	+ 8	- 18		
450•	1040	1.7	44 33	14.83	+ .55	+ 4	+ 18		
451	1041	1.7	40 38	11.13	- .23	+ 19	- 6	824	
452	1046	2.2	39 56	16.03	.....	+ 19	- 18		
453	1047	2.2	37 38	12.08	- .14	+ 8	- 9	865	
454•	1049	2.3	42 59	14.01	+ .11	- 23	- 6		
455	1050	2.3	41 22	16.02		- 1	- 6		
456	1052	2.5	40 50	15.28	.....	+ 10	- 10		
457	1053	2.5	40 36	15.4	.....	+ 14	+ 2		
458	1054	2.6	41 36	14.43	.....	+112	- 22		NC
459	1055	2.6	45 31	15.48	.....	+ 26	+ 10		
460•	1056	2.7	41 8	14.73	.....	+ 7	+ 21		
461	1057	2.8	40 26	7.15	- .03	- 16	+ 37	830	
462	1057b	1.2	40 24	15.7	.....	- 25	- 18		
463	1057c	1.5	40 21	15.8	.....	+ 11	+ 12		
464•	1058	3.1	40 57	13.71	.....	+ 9	+ 7		
465•	1059	3.1	41 5	14.84	.....	- 11	+ 16		
466	1060	3.2	43 45	15.63	.....	+ 12	+ 2		
467•	1061	3.5	48 43	13.85	.00	0	+ 14		
468	1062	3.7	46 13	12.89	+ .40	+ 46	- 16	784	NC
469	1063	4.0	43 16	15.62	.....	- 7	- 12		
470	1064	4.0	39 45	14.52	.....	+ 10	+ 22		
471•	1066	4.1	42 25	13.27	+ .03	- 8	+ 9	799	
472	1069	4.2	36 43	15.32	.....	+ 24	- 34		NC
473	1070	4.2	37 22	16.02	.....	+ 25	+ 31		
474	1071	4.3	34 34	16.09	.....	+ 11	+ 32		
475•	1072	4.5	42 13	13.58	+ .27	- 1	+ 4		
476•	1073	4.5	33 29	13.07	+ .01	+ 2	+ 11	877	
477	1075	4.8	34 2	15.84	.....	+ 19	+ 30		
478•	1076	4.8	35 54	14.90	.....	- 8	0		
479	1077	4.9	41 29	13.87	+ .02	- 7	+ 4		
480	1078	4.9	39 50	10.00	- .27	- 2	- 8	839	

TABLE 2 -- Continued

No.	Oosterhoff No.	α 1900 2^h	δ 1900 +56°	Phot. Mag.	Color Index	$\bar{\mu}_\alpha$	$\bar{\mu}_\delta$	Remarks
481	1079	12^m $4^s.9$	40' 1"	15.55	.....	+ 7	+ 30	
482	1080	5.0	41 10	11.24	- .22	- 5	+ 4	811
483•	1081	5.1	41 41	14.42	.....	+ 9	- 4	
484•	1082	5.2	32 18	14.98	.....	+ 25	- 9	
485•	1083	5.2	41 15	13.31	+ .04	+ 3	+ 2	
486	1084	5.3	39 40	15.54	.....	- 26	+ 20	
487	1085	5.3	41 22	10.53	- .22	- 8	+ 2	809
488	1086	5.4	32 32	15.66	.....	- 7	+ 52	NC
489	1087	5.4	34 22	16.05	.....	- 18	- 21	
490	1090	5.5	40 21	16.03	.....	+ 43	+ 5	
491	1091	5.7	39 38	15.67	.....	- 19	- 32	
492•	1092	5.8	34 13	15.32	.....	- 3	- 19	
493•	1093	5.8	40 51	13.59	+ .10	+ 8	+ 6	
494•	1095	6.0	38 41	13.79	- .08	- 11	- 10	
495•	1096	6.0	38 54	15.31	.....	0	- 24	
496•	1098	6.1	32 57	14.29	.....	+ 2	+ 8	
497•	1099	6.2	42 38	13.37	+ .25	+ 7	+ 9	796
498•	1100	6.3	37 48	14.54	+ .21	- 11	+ 12	
499•	1101	6.6	35 43	15.28	.....	- 4	- 10	
500	1102	6.7	35 20	15.70	.....	- 32	+ 7	
501•	1105	6.9	41 0	14.07	+ .15	- 5	+ 1	
502•	1106	6.9	41 36	14.24	+ .05	+ 3	+ 6	
503•	1107	7.0	36 31	13.87	- .05	+ 7	+ 10	
504•	1108	7.1	39 55	13.93	.....	- 1	+ 6	835
505	1109	7.1	39 49	11.10	- .29	+ 4	+ 16	838
506	1110	7.1	40 1	13.47	.....	- 9	- 14	834
507•	1113	7.2	48 21	14.55	.....	+ 8	- 4	
508•	1114	7.2	36 6	12.55	- .01	+ 10	+ 6	871
509	1116	7.5	40 24	9.55	- .18	+ 9	- 4	831
510	1117	7.5	41 34	15.76	.....	+ 19	+ 8	
511•	1118	7.5	42 10	14.18	.....	+ 1	+ 19	
512	1119	7.5	47 34	13.84	+ .99	- 40	- 18	NC
513	1121	7.7	40 14	13.62	+ .24	- 17	+ 8	832
514	1122	7.8	38 32	12.37	- .01	+ 6	+ 15	855
515	1123	8.1	43 56	15.31	.....	+ 37	+ 68	NC
516	1124	8.2	46 20	15.96	.....	+ 13	- 37	
517•	1125	8.3	45 58	14.39	+ .13	- 4	+ 4	
518•	1126	8.4	37 57	12.79	- .16	- 2	+ 7	861
519•	1127	8.4	33 23	13.94	.....	+ 9	+ 1	
520	1128	8.5	38 47	12.31	+ .01	- 6	- 13	852
521•	1129	8.5	38 38	13.12	+ .05	+ 6	- 8	853
522•	1130	8.7	43 8	14.58	+ .01	+ 9	+ 7	
523•	1131	8.7	35 37	13.47	- .01	- 4	- 4	
524	1132	8.8	40 8	8.76	- .23	- 6	+ 32	833
525	1133	8.8	39 54	9.23	- .20	- 7	+ 31	837
526•	1135	9.0	33 18	14.66	.....	- 4	+ 12	
527	1136	9.0	37 16	15.56	.....	- 5	+ 4	
528	1137	9.3	36 50	15.27	.....	+ 24	+ 7	
529	1138	9.5	39 34	14.38	+1.46	- 8	+ 32	NC
530	1139	9.5	39 41	16.02	.....	+ 26	- 18	
531	1141	9.6	33 45	10.07	- .27	+ 2	+ 32	874
532	1143	9.7	46 59	15.66	.....	+ 10	- 32	
533•	1145	10.1	38 18	14.98	.....	+ 3	- 8	
534	1146	10.2	48 59	15.95	.....	- 23	- 4	
535•	1147	10.3	38 57	14.82	.....	- 10	+ 1	
536•	1148	10.4	47 50	14.29	+ .18	- 16	+ 5	
537•	1149	10.5	36 33	15.48	.....	- 11	- 4	
538	1150	10.5	44 30	13.98	+ .63	+115	- 69	NC
539	1152	10.8	39 51	14.81	.....	+ 7	+ 12	
540	1153	10.9	36 50	15.71	.....	+ 8	- 34	
541•	1154	11.0	47 46	14.80	.....	+ 15	+ 1	
542	1155	11.0	39 46	12.68	+ .12	- 5	- 11	843
543•	1157	11.4	35 39	15.11	.....	+ 10	- 9	
544	1159	11.7	35 25	16.05	.....	+ 31	+ 10	
545	1160	11.9	48 49	15.38	.....	+ 29	+ 27	NC?
546	1161	11.9	40 0	10.41	- .17	- 10	- 6	836
547	1162	12.0	42 27	7.30	- .12	+ 18	- 37	798
548	1162b	10.9	42 34	14.3	.....	+ 30	+ 16	NC?
549•	1163	12.1	39 48	15.32	.....	- 9	+ 2	
550•	1164	12.1	43 26	14.81	.....	+ 13	- 2	
551•	1166	12.4	44 52	13.34	- .07	- 17	- 1	789
552	1167	12.4	39 3	14.56	.....	- 50	+ 6	NC
553•	1171	12.5	43 21	13.98	.....	- 2	+ 3	
554	1174	13.0	47 9	11.85	- .17	+ 9	+ 3	781
555•	1175	13.1	41 33	14.67	.....	- 1	+ 11	
556•	1176	13.2	35 46	15.22	.....	+ 2	- 12	
557	1177	13.2	38 56	14.58	.....	+ 6	+ 4	
558•	1178	13.3	32 5	15.35	.....	- 16	- 5	
559•	1179	13.3	41 55	13.06	+ .06	- 4	+ 5	803
560•	1180	13.3	37 36	14.62	.....	+ 6	- 2	

TABLE 2 -- Continued

No.	Coster-hoff No.	α 1900 2h	δ 1900 +56°	Phot. Mag.	Color Index	$\bar{\mu}_\alpha$	$\bar{\mu}_\delta$	Remarks	
561	1181	12m 13s.4	40' 30"	12.76	- .11	0	- 3	826	
562	1181b	13.1	40 36	16.0	.....	- 20:	- 4:		
563•	1182	13.7	43 36	13.80	+ .26	+ 8	+ 13		
564•	1183	13.9	34 48	15.21	.....	0	- 8		
565	1184	13.9	37 35	12.26	- .11	- 10	+ 1	866	
566•	1185	13.9	37 54	13.37	+ .07	- 11	- 7	862	
567	1186	13.9	49 31	15.87	.....	+ 9	- 18		
568	1187	14.7	43 15	10.94	- .17	- 16	+ 7	793	
569	1188	14.8	33 3	15.67	.....	- 15	+ 6		
570	1189	14.8	40 56	14.46	+ .45	+131	-114		NC
571	1190	15.0	42 37	15.58	.....	- 1	+ 18		
572•	1191	15.2	38 11	14.92	.....	- 3	+ 6		
573•	1192	15.2	41 31	15.09	.....	- 18	- 6		
574	1193	15.2	37 19	15.74	.....	+ 5	+ 19		
575	1194	15.2	38 2	15.84	.....	- 11	+ 15		
576•	1195	15.3	34 45	13.53	+ .03	- 1	- 9		
577	1196	15.3	47 14	10.69	- .24	- 21	- 40	780	NC?
578•	1198	15.7	41 19	13.95	+ .11	- 3	- 3		
579	1199	15.8	37 1	16.18	.....	+ 13	- 30		
580	1201	16.0	32 3	14.42	.....	+ 63	- 21		NC
581	1202	16.2	39 48	12.28	- .04	- 17	- 12	844	
582•	1203	16.3	41 13	14.05	+ .15	- 16	+ 2		
583•	1204	16.5	46 33	13.46	+ .05	+ 7	0		
584•	1206	16.7	38 47	14.86	.....	+ 13	- 14		
585	1207	16.8	43 15	15.95	.....	- 20	+ 32		
586•	1209	17.1	35 59	14.92	.....	+ 9	+ 6		
587	1210	17.3	46 43	15.90	.....	+ 13	- 28		
588	1210b	17.1	46 46	15.9	.....	- 29	+ 6		
589•	1213	17.7	40 42	14.75	.....	0	+ 7		
590•	1214	18.0	32 48	14.99	.....	- 5	+ 14		
591•	1215	18.2	32 30	15.25	.....	0	+ 20		
592	1216	18.5	37 22	15.54	.....	- 15	- 37		
593	1217	18.5	46 37	15.61	.....	- 37	+ 12		
594	1218	18.8	40 46	16.06	.....	- 29	- 50		NC?
595	1219	18.9	34 59	15.61	.....	+ 15	- 6		
596	1221	19.4	31 54	15.75	.....	+ 15	+ 18		
597	1222	19.4	42 55	15.88	.....	- 1	- 28		
598	1223	19.4	44 36	15.99	.....	- 11	- 8		
599	1224	19.5	47 1	15.97	.....	+ 22	+ 2		
600•	1225	19.8	36 54	14.65	+ .37	- 24	- 13		
601	1227	19.9	47 43	15.88	.....	- 2	+ 2		
602	1230	20.8	34 44	15.79	.....	- 9	+ 18		
603	1232	21.0	40 48	11.44	- .16	- 28	- 7	820	
604•	1233	21.2	35 36	15.40	.....	+ 8	- 3		
605	1234	21.2	32 40	14.27	.....	+ 25	- 42		NC
606•	1235	21.3	47 38	15.25	.....	- 26	+ 12		
607	1236	21.3	44 4	15.95	.....	-117	- 30		NC
608	1238	21.6	43 4	15.86	.....	- 67	+ 24		NC
609	1239	21.8	31 8	14.57	.....	- 15	+ 44		NC
610	1240	22.0	39 55	16.07	.....	- 7	- 6		
611	1241	22.2	32 28	14.61	.....	- 1:	- 2:		
612	1242	22.6	32 33	10.71	+ .26	+118	-106	721	NC
613	1244	22.7	36 52	16.16	.....	- 27	+ 20		
614•	1245	22.7	46 24	14.88	.....	+ 2	- 6		
615	1247	23.3	44 7	15.80	.....	- 11	+ 25		
616•	1249	23.9	32 14	14.36	- .39	0	- 9		
617	1250	23.9	47 1	15.62	.....	+ 5	- 8		
618	1251	24.0	39 50	15.70	.....	+ 19	- 26		
619•	1253	24.1	46 30	13.27	+ .08	- 8	+ 6	691	
620	1254	24.1	32 24	12.71	- .04	- 15	+ 4	723	
621	1257	24.5	39 9	10.70	- .06	- 16	+ 2	706	
622	1258	24.6	33 5	12.51	+1.14	+117	+ 15	717	NC
623	1259	24.6	47 1	15.93	.....	+ 39	- 27		NC?
624•	1260	24.8	39 55	14.38	.....	- 6	- 7		
625	1261	25.0	37 0	9.94	- .22	- 25	+ 8	710	
626•	1262	25.1	42 25	14.48	+ .02	- 10	- 13		
627	1263	25.2	36 47	16.19	.....	- 9	- 21		
628•	1264	25.2	34 18	14.88	.....	- 8	+ 5		
629•	1265	25.3	42 17	14.39	+ .11	+ 4	- 7		
630	1266	25.4	45 42	12.48	.00	- 20	+ 1	695	
631•	1267	25.6	40 52	14.62	.....	- 10	- 21		
632	1268	25.6	40 37	9.62	- .16	- 26	+ 6	704	
633	1270	25.9	48 41	14.89	+ .46	+ 20	- 12		
634	1271	26.1	47 13	15.30	.....	+168	- 48		NC
635	1272	26.1	41 29	14.61	+1.17	- 30	+ 44		NC
636	1275	26.4	32 18	15.97	.....	0	- 58		NC?
637	1276	26.6	46 7	12.46	- .12	- 23	0	692	
638	1278	26.7	43 43	11.66	- .13	+ 6	0	696	
639	1280	26.9	39 14	15.72	.....	- 17	- 15		
640•	1281	26.9	41 50	14.18	.....	- 7	+ 2		

TABLE 2 -- Continued

No.	Oosterhoff No.	α 1900 2^h	δ 1900 +56°	Phot. Mag.	Color Index	$\bar{\mu}_\alpha$	$\bar{\mu}_\delta$	Remarks	
641	1282	12^m $26^s.9$	39' 23"	11.34	- .09	- 26	- 11	705	
642	1283	27.1	41 33	11.90	- .13	- 19	+ 1	701	
643	1284	27.1	42 5	12.00	+ .23	+ 22	- 13	699	NC
644•	1285	27.4	41 2	13.49	+ .14	- 15	- 11	702	
645	1286	27.5	36 43	14.15	+ .12	- 12	0		
646•	1287	27.5	40 33	15.11	.....	+ 5	- 1		
647•	1289	28.2	42 47	15.23	.....	+ 12	- 12		
648	1290	28.4	33 13	15.22	.....	+210	- 54		NC
649•	1291	28.7	38 9	15.39	.....	+ 5	+ 10		
650•	1294	29.7	44 50	15.32	.....	- 8	+ 2		
651•	1295	30.1	39 35	13.87	- .04	- 6	- 8		
652•	1296	30.2	41 52	12.87	- .06	- 5	- 12	700	
653•	1297	30.3	35 24	15.10	.....	+ 6	- 17		
654	1298	30.4	45 57	11.92	- .11	+ 2	0	694	
655	1301	30.6	31 48	15.76	.....	+ 5	- 6		
656	1304	30.8	47 27	12.87	+ .18	+ 17	- 16	689	
657•	1305	30.8	47 12	15.08	.....	- 1	+ 9		
658	1306	30.9	48 23	15.73	.....	- 17	+ 24		
659	1307	30.9	48 16	15.90	.....	+ 22	+ 46		NC?
660•	1308	31.0	36 15	13.86	+ .23	- 3	- 4		
661	1309	31.0	38 51	15.61	.....	- 17	- 14		
662•	1310	31.2	41 50	15.19	.....	- 16	+ 1		
663	1311	31.6	45 14	15.75	.....	+ 21	- 6		
664	1313	31.7	46 40	16.03	.....	- 28	- 46		NC?
665•	1316	32.1	38 31	15.09	.....	+ 13	- 21		
666	1317	32.1	42 34	15.55	.....	- 16	- 6		
667	1318	32.4	33 52	16.16	.....	+ 9	+ 26		
668•	1320	32.5	47 56	13.83	+ .15	- 2	+ 4		
669•	1321	33.2	38 12	14.38	.....	- 18	- 9		
670	1322	33.2	33 57	15.86	.....	+ 29	- 54		NC?
671	1323	33.3	49 10	15.85	.....	- 5	- 22		
672•	1324	33.3	36 42	13.90	+ .10	- 11	- 4		
673	1327	33.4	37 57	15.61	.....	- 18	- 2		
674	1328	33.6	46 23	13.70	+ .09	- 9	+ 15		
675	1329	33.7	43 41	15.54	.....	+ 6	- 24		
676	1330	33.7	43 27	15.55	.....	- 7	- 8		
677	1331	33.8	32 3	12.80	- .10	- 10	+ 1	725	
678•	1332	33.9	38 24	13.71	+ .07	- 23	- 1		
679	1333	33.9	36 35	12.78	+ .06	- 8	- 3	711	
680	1335	34.1	32 51	15.76	.....	- 67	+ 23		NC
681•	1336	34.1	47 49	15.03	.....	- 17	- 5		
682	1338	34.4	37 37	15.57	.....	- 17	- 18		
683•	1339	34.5	36 46	15.03	.....	+ 5	- 9		
684	1340	34.9	32 40	15.76	.....	- 14	- 22		
685•	1341	35.2	42 50	13.81	+ .08	- 1	- 4		
686	1345	36.0	48 31	11.58	+ .05	- 17	- 10	688	
687•	1346	36.0	48 46	13.13	- .07	+ 5	- 2	686	
688	1347	36.0	39 1	16.22	.....	+ 40	- 23		
689•	1348	36.0	31 41	14.95	.....	+ 1	+ 2		
690	1349	36.2	35 43	13.25	+ .13	- 4	- 14	714	
691•	1350	36.2	38 39	13.04	+ .01	- 1	+ 7	708	
692•	1351	36.2	41 37	15.26	.....	- 4	- 14		
693	1352	36.5	48 33	10.27	- .22	- 1	- 34	687	
694•	1354	36.6	34 19	15.37	.....	+ 14	- 8		
695•	1356	36.7	39 39	14.75	.....	+ 21	- 7		
696•	1358	37.2	36 2	12.77	+ .01	- 32	- 6	713	NC?
697	1359	37.5	39 34	14.44	+ .64	+ 81	- 39		NC
698	1361	37.6	34 57	15.79	.....	- 3	0		
699•	1362	37.9	34 6	15.24	.....	- 6	- 10		
700•	1363	38.0	41 47	14.82	.....	+ 20	- 22		
701	1364	38.1	37 52	10.12	- .18	- 45	+ 6	709	NC?
702	1365	38.3	37 16	15.61	.....	+ 7	- 14		
703	1368	38.4	45 27	15.84	.....	+ 6:	+ 14:		
704•	1369	38.4	43 33	13.99	+ .15	0	- 3		
705	1371	38.5	46 2	15.57	.....	+ 35	- 35		NC?
706•	1372	38.6	42 11	14.73	+ .25	- 13	- 1		
707	1373	38.8	37 5	15.65	.....	+ 17	- 6		
708•	1375	39.0	32 36	13.67	+ .16	- 14	+ 9		
709	1378	39.3	36 2	12.15	- .09	- 20	0	712	
710•	1380	39.4	40 55	15.36	.....	- 2	- 6		
711	1381	39.5	46 19	15.67	.....	+ 34	- 10		
712•	1384	40.0	42 43	13.44	- .02	- 16	+ 2		
713•	1388	41.0	36 43	14.25	+ .14	- 10	+ 7		
714•	1394	41.6	33 12	14.41	.....	- 7	+ 7		
715•	1395	41.6	45 14	14.69	.....	- 3	- 7		
716•	1398	41.8	42 6	15.34	.....	+ 4	- 6		
717	1399	41.8	36 42	14.40	+ .74	+392	-194		NC
718	1402	42.1	43 18	15.96	.....	+ 28	- 10		
719	1403	42.2	41 58	14.33	.....	- 6	+ 1		
720	1403b	42.1	41 59	15.2	.....	- 2	+ 9		

TABLE 2 -- Continued

No.	Oosterhoff No.	α 1900 2h	δ 1900 +56°	Phot. Mag.	Color Index	$\bar{\mu}_\alpha$	$\bar{\mu}_\delta$	Remarks	
721	1404	12m 42s.2	48' 0"	16.21	.....	- 26	+ 5		
722	1406	42.9	46 34	16.00	.....	+ 3	- 8		
723	1409	43.3	32 48	15.72	.....	- 11	+ 13		
724•	1410	43.3	45 24	14.30	- .04	- 10	- 5		
725	1412	43.4	33 36	11.56	- .16	- 13	+ 11	715	
726	141:	43.5	33 24	15.88	.....	- 23	+ 26		
727	1414	43.6	32 33	11.89	+ .33	- 14	- 70	722	NC
728	1416	43.8	33 53	14.07	.....	+ 25	- 20		NC??
729•	1418	44.0	40 14	14.81	+ .24	- 13	- 14		
730•	1419	44.0	47 48	14.48	+ .20	- 17	+ 14		var.?
731•	1422	44.4	39 1	15.42	.....	+ 20	- 15		
732	1423	44.4	40 51	15.56	.....	- 81	+ 52		NC
733•	1425	44.6	37 4	14.87	.....	- 11	+ 13		
734•	1427	44.7	34 56	14.37	+ .03	- 7	+ 15		
735•	1428	44.8	39 8	15.05	.....	- 2	- 9		
736	1432	44.9	37 54	15.65	.....	+ 17:	- 10:		
737	1434	45.5	41 24	15.75	.....	+ 23	+ 2		
738	1436	45.6	36 24	15.62	.....	- 11	- 38		
739	1438	45.8	39 0	11.42	- .17	- 32	+ 8	707	
740	1439	45.9	33 18	11.01	- .24	- 2	+ 20	716	
741•	1444	46.7	32 48	13.22	+ .12	- 4	+ 10	719	
742•	1448	47.1	40 14	14.74	+ .59	+ 17	+ 3		
743	1449	47.2	46 52	15.98	.....	- 47	+ 24		NC?
744•	1452	47.6	38 12	14.67	.....	+ 17	+ 9		
745	1453	47.7	37 5	16.19	.....	+ 37	- 25		
746•	1456	48.4	41 44	15.04	.....	+ 7	- 3		
747	1458	48.5	40 4	16.05	.....	+ 11	+ 2		
748•	1459	48.6	41 27	14.56	.....	- 18	- 7		
749•	1460	48.6	46 2	12.74	- .03	- 8	- 2	693	
750•	1461	49.2	42 29	13.43	+ .11	+ 6	+ 6		
751•	1464	49.6	47 34	13.22	- .03	+ 6	+ 2	690	
752	1465	49.8	43 25	12.85	- .04	+ 1	- 17	697	
753	1468	49.9	37 48	16.11	.....	+ 4	- 7		
754•	1469	50.0	38 52	14.34	- .13	0	+ 7		
755	1471	50.5	36 26	14.38	+ .25	+332	-229		NC
756	1473	51.0	37 6	14.55	+1.06	+ 32	+ 29		NC
757	1474	51.3	35 53	15.97	.....	- 7	- 16		
758•	1477	51.9	44 13	15.40	.....	- 24	+ 4		
759	1478	52.3	42 3	15.03	.....	+ 10	- 8		
760•	1479	52.8	34 24	13.70	- .01	- 3	- 17		
761	1480	52.8	44 2	13.88	+ .36	+ 18	+ 15		
762	1481	53.1	37 40	15.88	.....	- 11	- 31		
763	1483	53.2	33 31	15.49	.....	-115:	- 10:		NC
764•	1486	54.2	41 45	13.81	+ .03	+ 11	0		
765•	1488	54.4	36 30	14.26	+ .02	+ 5	+ 4		
766•	1489	54.4	40 52	13.35	- .02	- 2	+ 4	703	
767•	1494	55.9	42 36	14.44	+ .52	+ 13	+ 11		
768•	1498	57.0	39 18	14.30	+ .21	+ 2	+ 8		
769•	1501	57.2	46 35	15.47	.....	+ 7	0		
770	1502	57.4	36 2	15.83	.....	+ 33	- 7		
771•	1505	58.0	35 15	15.39	.....	- 2	+ 6		
772	1506	58.7	43 37	16.06	.....	+ 23	- 8		
773•	1507	59.0	46 32	14.53	+ .16	+ 10	- 22		
774•	1508	59.1	43 4	14.09	+ .16	+ 15	+ 7		
775•	1512	59.5	37 15	14.60	.....	+ 2	+ 8		
776•	1513	13 0.2	43 46	14.32	+ .10	+ 3	+ 11		
777•	1514	0.2	34 58	13.84	- .08	- 17	+ 10		
778	1515	0.4	34 40	16.00	.....	- 69	- 22		NC?
779	1516	0.4	43 39	11.21	- .12	- 35	+ 11	621	
780•	1517	0.6	40 5	14.72	- .07	+ 5	+ 6		
781	1518	0.7	37 29	15.86	.....	+ 5	- 15		
782•	1519	0.8	44 15	15.27	.....	- 12	- 2		
783	1520	0.8	45 20	15.86	.....	+ 50	- 44		NC
784•	1522	1.1	44 50	14.94	.....	- 2	- 26		
785	1525	2.2	35 42	12.01	+ .29	- 27	+ 42	632	NC?
786•	1533	2.9	41 36	14.38	+ .11	+ 8	+ 3		
787•	1535	3.2	36 36	14.27	+ .26	+ 4	- 5		
788	1538	3.7	36 55	16.27	.....	+ 29	- 18		
789	1539	3.8	39 49	11.36	- .21	- 31	+ 9	626	
790	1546	6.2	39 34	14.82	+1.09	- 26:	+ 56:		NC
791•	1552	7.3	41 20	15.16	.....	+ 16	0		
792	1557	8.0	42 2	15.91	.....	+ 11	+ 4		
793•	1562	9.1	44 17	14.22	+ .18	+ 19	+ 12		
794	1566	9.8	39 6	11.51	- .08	- 21	+ 28	629	
795•	1570	10.6	41 29	14.29	+ .19	+ 24	+ 18		NC?
796•	1573	11.6	39 48	15.23	.....	+ 2	+ 9		
797	1575	11.8	38 52	13.95	+1.52	- 41	+ 27		NC
798	1577	12.0	40 46	14.80	+1.03	+ 7	+ 42		NC
799	1586	13.4	38 16	9.13	- .25	- 74	+ 14	630	NC
800	1590	13.7	42 22	11.52	- .13	- 2	+ 28	623	

Selection of noncluster stars.—From Table 3 we see that the brightest and the faintest stars show larger probable errors, as might be expected from the increased difficulty in the measurement. In order to find which stars probably do not belong to the cluster, the motions were again plotted for each magnitude, except that stars brighter than magnitude 10 were plotted together.

In Figure 2, scatter diagrams give the motions of the stars of magnitudes 13 and 16, the magnitudes where we have the smallest and the largest internal probable errors. From these diagrams it is evident how much easier it is to distinguish between cluster and noncluster stars when the probable errors are small. For a few doubtful stars the probable errors are indicated by crosses, the length of the arms representing the probable error. Since for the noncluster stars the motions are smaller for the fainter stars and the probable error is larger, it is clearly very difficult to pick out the noncluster stars fainter than magnitude 15.5. However, from each scatter diagram we try to decide which stars

TABLE 3

PROBABLE ERRORS FOR DIFFERENT MAGNITUDES

Mag.	P.E. in μ_α	P.E. in μ_δ	n	After Corr. for Mag. Error		Cluster Stars
7, 8, 9	0".0036	0".0010	18	0".0006	0".0008	17
10	.0028	.0006	31	.0007	.0008	23
11	.0025	.0006	44	.0008	.0006	37
12	.0015	.0005	64	.0006	.0005	56
13	.0008	.0004	109	.0003	.0004	100
14	.0006	.0006	200	.0005	.0006	170
15	.0010	.0008	289	.0008	.0008	252
16	0.0013	0.0011	45	0.0010	0.0011	41
All	0".0011	0".0007	800	0".00065	0".00069	696

definitely belong to the cluster and which probably do not. For 19 of the brighter stars we have, in addition, radial velocities.[5] The radial velocity of the cluster is about −47 km/sec; star 799 = BD+56°545 must therefore be excluded, as its radial velocity from 3 Mount Wilson plates is −24 ±2 km/sec.

Altogether, 63 stars were marked as definitely not belonging to the cluster, and 41 as probably not. Besides the mean motions, two more criteria were used to determine their membership—viz., the color index and the internal agreement between the two pairs of plates. These 104 stars are shown in Figure 3 and are collected in Tables 4*a* and 4*b*, where they are arranged according to decreasing magnitude. The 4 stars at the bottom of Table 4*b* have been added later (see p. 47).

Table 5 shows the numbers of these 108 noncluster stars according to their total motion. For this purpose the correction from relative to absolute motion derived on page 33 was applied. This table is interesting because in *Utrecht* V we found that there were more field stars with motions between 0".010 and 0".019 than between 0".000 and 0".009. The fact that we now find by far the highest percentage of field stars among those with the smallest motions is undoubtedly due to the increase in the accuracy. The results are not quite comparable, because in *Utrecht* V we were not dealing with stars fainter than about magnitude 13.6; if, however, we exclude the stars fainter than this limit, the first two numbers in the next to the last column change to 72 and 21, still showing by far the largest percentage for the smallest motions. The 692 other stars which,

[5] Six of these stars had radial velocities determined at Mount Wilson. Dr. Trumpler was kind enough to send me, by letter, radial velocities for 15 and spectral types for 74 stars.

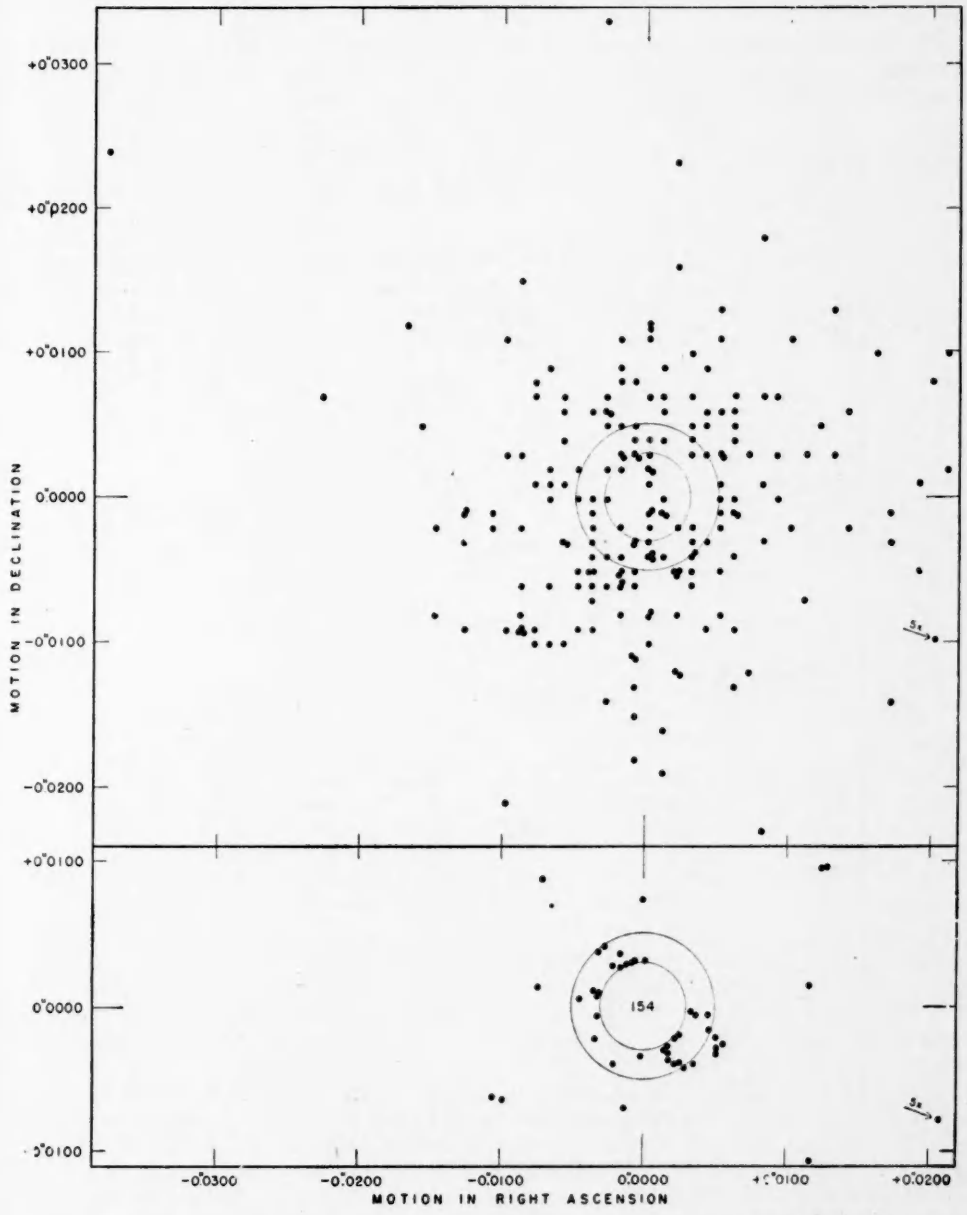

FIG. 1.—Comparison of the results derived in *Utrecht* V with those of the present paper

according to their motions, might belong to the cluster have the distribution shown in Table 6.

The distribution of these motions in α and δ is plotted in Figure 4. The error-curves in this figure are constructed from the probable errors—0".0092 for α and 0".0090 for δ—derived from the actual deviations. These values are larger than the internal errors given

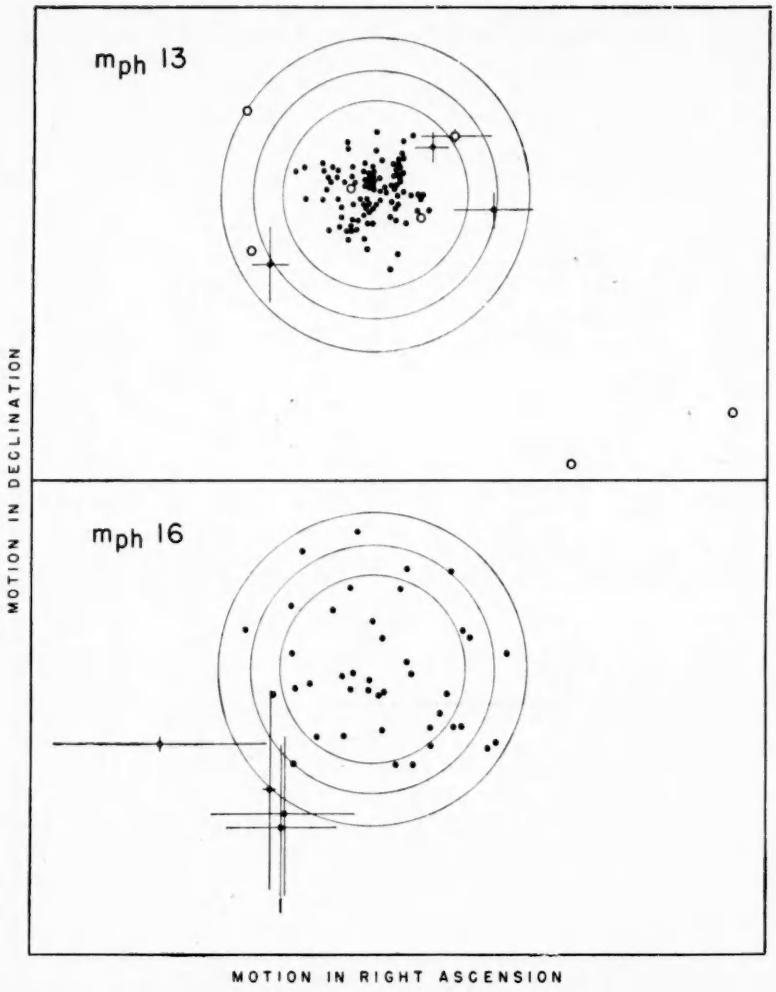

FIG. 2.—Scatter diagrams of the motions for magnitudes 13 and 16

on page 44. While in practice the external errors are always larger than the internal ones, we have here an additional circumstance which would increase the difference, viz., that undoubtedly a certain number of the stars are not really cluster stars. Another explanation would be internal motions in the cluster, which, if this were the only cause, would amount to 0".00065 in α and 0".00058 in δ.

As we shall see later, some 50 stars may still be included which probably do not belong to the cluster. This fact probably is the main cause of the discrepancy in the probable

errors. The point was investigated by scrutinizing the stars whose deviations exceed 0".0025 in either co-ordinate, in connection with the probable errors of the individual stars. But in this way we were able to exclude only 4 more stars—Nos. 173, 215, 294, and 728, given in the last four lines of Table 4*b*. It also appeared that about 70 per cent of the larger deviations come from the stars fainter than 15.5 mag. and may well be explained by the larger errors for these stars.

THE THEORETICAL NUMBER OF NONCLUSTER STARS

In my parallax work I have been accustomed to use Table 4 in *Groningen* **27** to derive the photographic magnitudes. While, as a whole, the values thus derived agree well with other sources, it is evident that at low galactic latitudes this table is less reliable, owing to the strong but uncertain amount of interstellar absorption in many parts of the galaxy. Nevertheless, we have used this table to derive the values given in Table 7 for the number of field stars in our region.

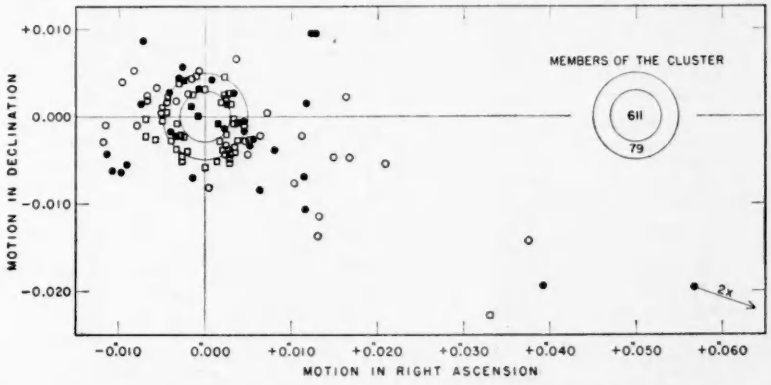

FIG. 3.—Distribution of the motions of the noncluster stars. For comparison, the distribution of the cluster stars is given to the right. In the small circle with radius 0".003 we find 611 stars; in the ring between 0".003 and 0".005, 79 stars; outside the larger circle, only 2 stars.

Another, and possibly a more reliable, determination of the number of field stars to be expected in the region measured may be derived from the counts of stars on small-scale plates. Several plates with different exposures of the region of *h* and χ Persei taken by Mr. Humason at the 10-inch photographic doublet in 1920 were available. The plate with an exposure of one hour shows stars of exactly the same limiting magnitude as the plates measured for the present paper. On this plate of Mr. Humason's I counted the number of stars in squares with sides of 2'.85 over an area 161 by 143 minutes of arc. For the central parts of both clusters, where there is a good deal of overlapping of the images on the 10-inch plates, the counts were made on the 80-foot-focus plates. The numbers of stars per square vary from 0 to 81 in the very center of *h* Persei. The mean numbers in right ascension and declination are given in Table 8 and plotted in Figure 5.

We find a slight general increase in the numbers from east to west and from north to south; but, except for the center of the field, which contains the double cluster, the figures run smoothly enough for us to conclude that over the area covered by the proper-motion field we may accept 4.90 stars per square for the field stars in the region of *h* Persei. This means that in the circle measured we should expect about 190 field stars, or 40 more than we would expect from the table in *Groningen* **27**.

TABLE 4*a*

STARS DEFINITELY NONMEMBERS OF THE CLUSTER, ARRANGED ACCORDING TO APPARENT MAGNITUDE

No.	M_{ph}	C.I.	μ_a	μ_δ
799	9.13	−0.25	−0″.0074	+0″.0014
125	10.44	+1.15	+ .0046	− .0005
612	10.71	+0.26	+ .0118	− .0106
317	11.00	+0.34	− .0106	− .0062
49	11.38	−0.21	+ .0051	− .0029
371	11.43	+0.21	+ .0128	+ .0096
286	11.45	+0.39	+ .1135	− .0392
305	11.47	+0.44	+ .0126	+ .0096
314	11.61	+0.31	+ .0051	− .0032
727	11.89	+0.33	− .0014	− .0070
643	12.00	+0.23	+ .0022	− .0013
129	12.09	+0.26	− .0071	+ .0088
622	12.51	+1.14	+ .0117	+ .0015
468	12.89	+0.40	+ .0046	− .0016
214	12.92	+0.35	+ .0056	− .0026
437	12.96	+0.32	− .0099	− .0064
30	13.36	+0.72	+ .0025	+ .0019
260	13.71	+0.57	+ .0063	− .0085
512	13.84	+0.99	− .0040	− .0018
797	13.95	+1.52	− .0041	+ .0027
538	13.98	+0.63	+ .0115	− .0069
171	14.10	.....	− .0033	+ .0018
231	14.10	.....	+ .0164	+ .0023
372	14.11	+0.45	− .0090	− .0055
316	14.20	+0.87	− .0113	− .0047
201	14.22	.....	+ .0049	− .0028
605	14.27	.....	+ .0025	− .0042
46	14.28	.....	+ .0377	− .0142
755	14.38	+0.25	+ .0322	− .0229
529	14.38	+1.46	− .0008	+ .0032
717	14.40	+0.74	+ .0392	− .0194
580	14.42	.....	+ .0063	− .0021
458	14.43	.....	+ .0112	− .0022
697	14.44	+0.74	+ .0081	− .0039
570	14.46	+0.45	+ .0131	− .0114
756	14.55	+1.06	+ .0032	+ .0029
423	14.56	.....	− .0020	+ .0028
552	14.56	.....	− .0050	+ .0006
609	14.57	.....	− .0015	+ .0044
635	14.61	+1.17	− .0030	+ .0044
76	14.63	.....	+ .0150	− .0047
798	14.80	+1.03	+ .0007	+ .0042
790	14.82	+1.09	− .0026	+ .0056
253	14.93	.....	+ .0046	− .0008
228	15.07	.....	− .0043	+ .0017
648	15.22	.....	+ .0210	− .0054
634	15.30	.....	+ .0168	− .0048
515	15.31	.....	+ .0037	+ .0068
472	15.32	.....	+ .0024	− .0034
88	15.48	.....	− .0097	+ .0040
763	15.49	.....	− .0115	− .0010
732	15.56	.....	− .0081	+ .0052
236	15.63	.....	+ .0131	− .0136
488	15.66	.....	− .0007	+ .0052
351	15.75	.....	− .0056	+ .0032
680	15.76	.....	− .0067	+ .0023
336	15.78	.....	+ .0103	− .0076
424	15.86	.....	+ .0071	+ .0004
608	15.86	.....	− .0067	+ .0024
783	15.86	.....	+ .0050	− .0044
32	15.87	.....	+ .0003	− .0081
190	15.88	.....	− .0079	− .0010
607	15.95	.....	−0.0117	−0.0030

From Figure 5 we can also derive 27′ as the approximate distance between the centers of the two clusters. The diameter of *h* Persei may be taken as 35′, although the denser part of the cluster is limited to about 25′. For the region in which the numbers of stars were counted, I have constructed the density diagram in Figure 6, which shows the extreme irregularity of the star density in this region. In order not to make this figure too irregular, the means of 9 squares, or regions 8′.55 square, were taken.

TABLE 4*b*

STARS PROBABLY NONMEMBERS OF THE CLUSTER

No.	M_{ph}	C.I.	μ_α	μ_δ
701	10.12	−0.18	−0″.0045	+0″.0006
73	10.18	−0.22	+ .0022	− .0040
82	10.28	−0.29	+ .0025	− .0039
93	10.67	−0.23	+ .0035	− .0040
577	10.69	−0.24	− .0021	− .0040
290	10.94	−0.19	− .0031	+ .0038
785	12.01	+0.29	− .0027	+ .0042
696	12.77	+0.01	− .0032	− .0006
26	13.07	+0.34	+ .0037	− .0005
209	13.63	+0.37	− .0034	− .0022
22	13.74	+0.70	+ .0015	− .0007
273	13.86	+0.73	− .0008	+ .0002
393	14.17	+1.00	− .0016	+ .0013
210	14.21	+0.30	− .0015	+ .0026
795	14.29	+0.19	+ .0024	+ .0018
548	14.30	.....	+ .0030	+ .0016
441	14.90	.....	+ .0032	− .0006
161	14.97	.....	+ .0023	+ .0018
271	14.99	.....	+ .0023	+ .0025
229	15.12	.....	− .0001	+ .0031
16	15.33	.....	− .0024	− .0022
545	15.38	.....	+ .0029	+ .0027
86	15.39	.....	− .0028	− .0022
361	15.50	.....	− .0011	+ .0047
705	15.57	.....	+ .0035	− .0035
13	15.77	.....	− .0056	− .0026
141	15.86	.....	+ .0029	− .0046
670	15.86	.....	+ .0029	− .0054
244	15.88	.....	+ .0014	− .0052
659	15.90	.....	+ .0022	+ .0046
134	15.92	.....	− .0050	− .0003
178	15.92	.....	− .0069	− .0002
192	15.92	.....	− .0050	+ .0008
623	15.93	.....	+ .0039	− .0027
113	15.94	.....	− .0039	− .0029
636	15.97	.....	.0000	− .0058
743	15.98	.....	− .0047	+ .0024
37	16.00	.....	− .0033	− .0038
778	16.00	.....	− .0069	− .0022
664	16.03	.....	− .0028	− .0046
594	16.06	.....	− .0029	− .0050
294	9.58	−0.23	+ .0029	− .0042
215	10.87	−0.17	+ .0034	− .0002
173	10.96	−0.26	+ .0017	− .0027
728	14.07	.....	+0.0025	−0.0029

I also counted the number of stars in the same region on plates taken at the 10-inch photographic doublet with an exposure of 6^m40^s, which shows stars down to about mag-

nitude 14. The diameter of *h* Persei comes out 38′, practically the same; but the curve is so much flatter that it is difficult to decide on the limits of the cluster. For the plate showing stars down to magnitude 14, we find 1.1 stars per square with sides of 2′.85, which, for the region measured, would indicate 42 field stars instead of 31.3—a gain of practically the same ratio as that for the stars of magnitude 16.1.

It would be fairly easy to ascribe this difference to the fact that in *Groningen* **27** the figures are based on the mean for all galactic latitudes and that these means must, therefore, in many regions be smaller than in others, where the absorption is less than in general. But we do not know how much absorption there is in different parts of the Milky Way. In the region under discussion Dr. Stebbins has been kind enough to determine the

TABLE 5

DISTRIBUTION OF THE MOTION OF THE FIELD STARS

Limits of μ	Noncluster	Percentage	Percentage in *Utrecht* V
0″.0000–0″.0090	79	73	19
0.0100–0.0190	22	20	39
0.0200–0.0290	3	3	25
0.0300–0.0390	0	0	10
0.0400–0.0490	3	3	4
≧0.0500	1	1	3

TABLE 6

DISTRIBUTION OF MOTION OF POSSIBLE CLUSTER STARS

Limits of μ	n	Percentage
0″.0000–0″.0009	195	28
0.0010–0.0019	279	40
0.0020–0.0029	137	20
0.0030–0.0039	65	9
0.0040–0.0049	14	2
≧0.0050	2	0

photographic absorption for 15 stars. In the mean, his result is 2.05 mag., but he finds for the two brightest stars the exceptionally high values of 2.5 and 2.6 mag. Even in the small region under investigation here, we can see a great deal of difference in the absorption east and west of the center of the field (Table 8 and the corresponding figure [Fig. 5, *a*]). We may therefore conclude that the number of noncluster stars probably exceeds 108 but is less than 190.

A first glance at Table 7 might convince us that down to magnitude 15 we have located practically all the noncluster stars and that the lack of the fainter noncluster stars might be explained either by absorption or by the fact that it is more difficult to find the fainter noncluster stars because their motions are smaller and their probable errors larger. A closer scrutiny shows another disturbing effect. For magnitude 10 we find only 2 stars which can be definitely called nonmembers of the cluster; the motions of the other 8 stars are so small that it is rather doubtful whether, in view of the smaller accuracy for the brighter stars, they can exclude the 8 stars from the cluster. This uncertainty is empha-

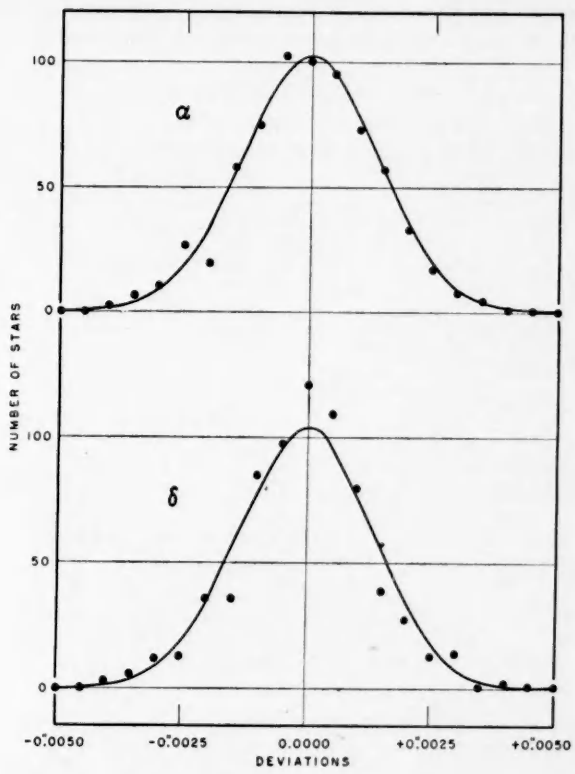

FIG. 4.—Distribution of the deviations in μ_α and μ_δ for the possible cluster stars

TABLE 7

NUMBER OF STARS OF VARIOUS MAGNITUDES TO BE EXPECTED IN THE REGION MEASURED

m_{ph}	N Theor.	Field Stars Found	Total N Obs.	Possible Cluster Stars
8	0.1	0	2	2
9	0.3	0	5	5
10	0.8	2	18	16
11	2.3	12	49	37
12	6.0	19	93	74
13	14.4	27	157	130
14	31.3	36	266	230
15	70.2	67	466	399
15.5	99.0	78	589	511
16.0	140.0	104	755	651
16.1	149.8	108	800	692

sized by the fact that for 6 of these 8 stars Trumpler gives spectra which make it possible that, after all, they are members of the cluster. Only radial velocities could decide the question.

THE FINAL MOTION OF THE CLUSTER

The motions derived are relative to the motion of the cluster. Comparing the parallactic motions of the noncluster stars with these relative motions, we would find the motion of the cluster as the difference; this method was used, for instance, in a former paper: "The Proper Motion of the Open Cluster Messier 67."[3] In the present investigation, however, some extra precautions have to be taken. The motion of star 286 is so large as to influence the mean very definitely and should, accordingly, be excluded. Moreover, in Figure 3, we see a group of 3 stars—46, 717, and 755—whose motions are so closely the same and are so different from the motions of the other stars that we are inclined to

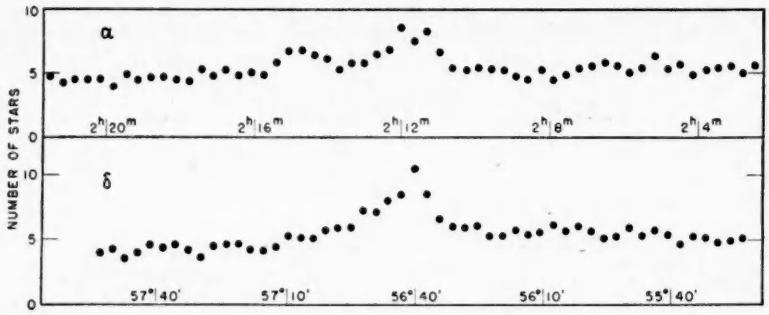

FIG. 5.—Mean number of stars in right ascension and declination per area with sides of 2'.85, in a region 161 by 143 minutes of arc around *h* Persei.

TABLE 8

MEAN STAR DENSITY PER SQUARE WITH SIDES OF 2'.85

$\alpha = 2^h21^m40^s$ to $\alpha = 2^h2^m20^s$

4.7	4.5	6.8	8.2	4.5	5.6
4.2	4.4	6.4	6.6	4.9	4.9
4.5	5.3	6.1	5.5	5.4	5.1
4.5	4.7	5.3	5.3	5.6	5.4
4.5	5.3	5.8	5.4	5.8	5.6
4.0	4.9	5.8	5.3	5.5	5.0
5.0	5.0	6.5	5.2	5.0	5.6
4.5	4.9	6.8	4.7	5.4	
4.7	5.9	8.7	4.5	6.3	
4.7	6.8	7.5	5.3	5.3	

$\delta = +57°50'$ to $\delta = +55°20'$

3.9	4.5	5.7	6.6	6.1	5.4
4.2	4.6	5.9	6.0	5.7	4.6
3.6	4.6	5.9	5.9	6.0	5.2
4.0	4.1	7.2	6.0	5.7	5.1
4.5	4.1	7.1	5.2	5.1	4.8
4.3	4.4	8.0	5.2	5.2	4.9
4.6	5.2	8.4	5.7	5.9	5.1
4.1	5.1	10.5	5.4	5.2	
3.6	5.1	8.5	5.6	5.7	

think that they form a small separate group. I have, therefore, computed the motion of the cluster, first by comparing the mean parallactic motions for different magnitudes with the corresponding motions derived here for the 107 stars of Table 4 (excluding star 286) and then for the 104 stars, excluding the little group of 3 stars with common proper motion.

Finally, since we know the parallactic motions with greater accuracy for the stars between magnitude 12.5 and 15.5, I have repeated this process, first for the 56, and then

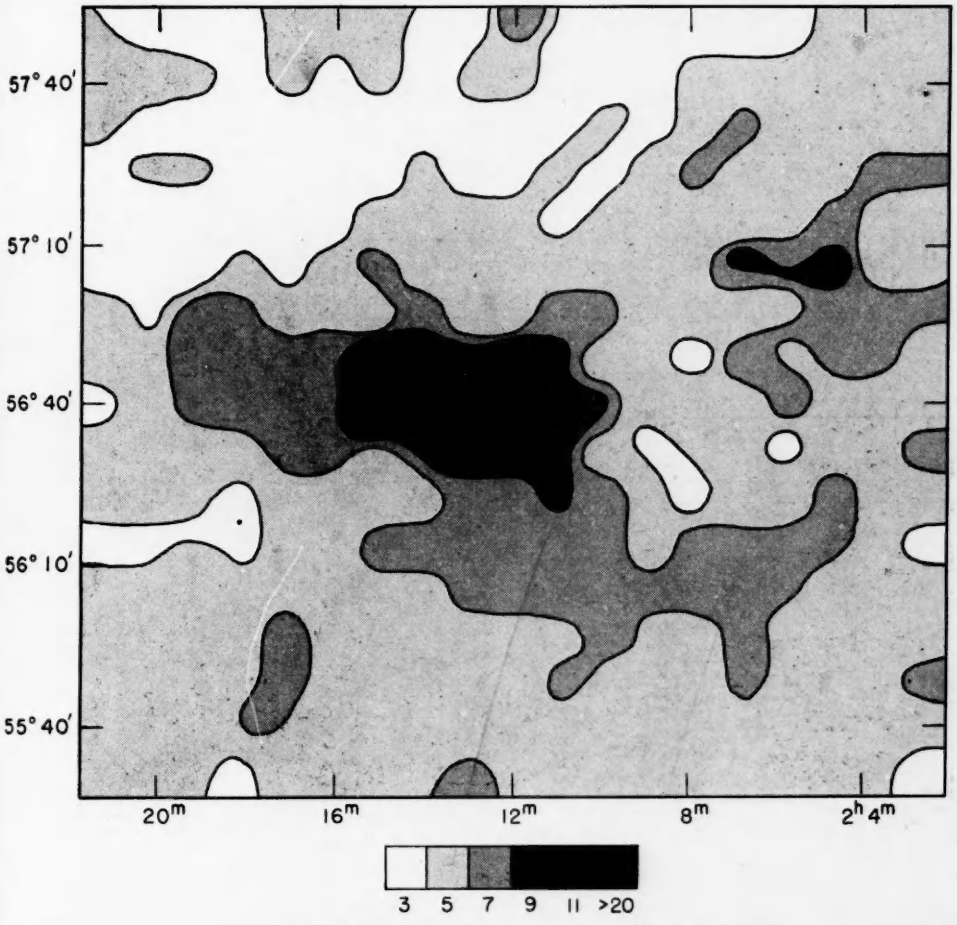

FIG. 6.—Density of stars in the neighborhood of *h* Persei

for the 53, stars between these magnitudes. The four computations give the results in Table 9 for the final motion of the cluster, which should be used to reduce the motions of Table 2 from relative to absolute.

OOSTERHOFF'S COLOR INDICES

In Oosterhoff's catalogue are color indices for 320 of the stars measured for motion in the present paper. In Figure 7 they are plotted against his magnitudes. The cluster stars are indicated by dots, noncluster stars by circles, and doubtful stars by crosses. It is clear

at once that practically all cluster stars fall on the main branch of the Hertzsprung-Russell diagram. Practically all stars falling to the right of the dotted line have proper motions and are therefore not members of the cluster. Attention should be called to a few stars which do not seem to fall in the expected positions: Nos. 461, 547, 430, 65, and 616. Stars Nos. 461 and 547 are the two brightest stars in the field, and their radial velocity is the same as that of the cluster. The fact that these two brightest stars are so close to the center of *h* Persei makes it practically certain that they must belong to the group. Their color index, however, is only slightly negative—much smaller than the fainter members of the group. Stars Nos. 430 and 65 are also located too far to the right on the diagrams;

TABLE 9

FINAL VALUES OF MOTION OF THE CLUSTER

Group	Magnitudes	μ_α	μ_δ	No. of Stars
I.....	9.1–16.1	+0".0019:	−0".0030	107
II.....	9.1–16.1	+ .0030	− .0036	104
III.....	12.5–15.5	− .0003	− .0027	56
IV.....	12.5–15.5	+0.0017	−0.0038	53
Mean.....		+0".0016±0".0005	−0".0033±0".0002	.....

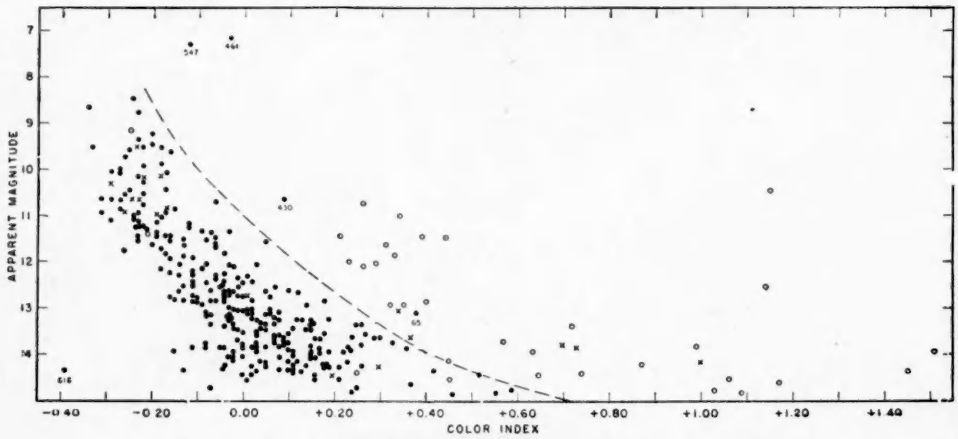

FIG. 7.—Correlation of color index and magnitude for 320 stars

their motions are small, but, of course, that fact alone does not necessarily indicate that they are members of the cluster.[6] Radial velocities for these stars would decide their membership. Star No. 616, with very small motion, has a large negative color index for its magnitude. If it is a cluster star, it would be of abnormal magnitude for its type.

Of course, several of the stars which have motions excluding them from membership in the cluster fall to the left of the dotted line in the diagram, but there is no reason why they should not do so. On the other hand, it is most interesting that practically all stars falling to the right of this curve have shown by their motions that they are not members of the group.

[6] For star No. 430 Stebbins finds an unusual absorption 1.1; this absorption also makes it improbable that the star belongs to the cluster.

THE PHOTOGRAPHIC DETERMINATION OF STELLAR PARALLAXES WITH THE 60- AND 100-INCH REFLECTORS*

NINETEENTH SERIES

ADRIAAN VAN MAANEN
Mount Wilson Observatory
Received April 5, 1944

ABSTRACT

Trigonometric parallaxes determined with the 60- and 100-inch reflectors are given for 25 fields, including 28 stars. As in the other recent series, most of the stars were placed on the program on account of their large proper motions. One star, vM-W 110, was observed as a possible white dwarf, but the negative parallax derived makes it doubtful if the absolute magnitude can be fainter than +8.

The present paper gives the results for 28 stars in 25 fields, which have recently been measured for parallax. The work has been carried out in the same way as for the previous-

TABLE 1

STELLAR PARALLAXES DETERMINED AT MOUNT WILSON

Object	α 1900	δ 1900	m_{pg}	Spectrum*	Relative Parallax	μ_α Rel.	P.E.	No. of Exp.	Instrument
L 1154-29	$0^h10^m42^s$	+12° 59′	13.5	.....	+0″.084	+0″.647	4 10	16	60″
vM-W 30	0 11 11	+15 22	15.92	.....	+ .041	+0.183	6 2	18	100
BD+61°195	0 56 19	+61 48	10.5	M1	+ .133	+0.735	10 7	18	60
Wolf 47	0 56 58	+61 50	14.5	M7	+ .109	+0.722	5 4	18	60
Ross 323	1 3 18	+30 54	15.3	.....	+ .012	+0.367	6 3	18	60
Radcl. 45, 368	1 25 21	+30 28	15.3	.....	+ .001	+0.200	5 5	20	100
Wolf 1530	1 39 42	+15 51	15.3†	.....	+ .060	−0.755	6 3	18	100
Ross 15	1 52 30	+58 1	14.0	M5	+ .074	+0.319	4 9	18	60
Ross 556	2 38 24	+25 6	12.3	M4	+ .119	+0.811	6 9	16	60
Ross 62	6 2 49	+26 35	14.9	.....	+ .039	−0.511	8 3	16	100
Ross 614	6 24 18	− 2 44	12.6	M4e	+ .233	+0.704	16 6	18	100
S.A. 55, 33	11 30 52	+29 24	15.0	.....	+ .011	+0.256	8 2	18	100
Wolf 424	12 28 24	+ 9 34	13.7	M5e	+ .239	−1.728	13 2	16	100
L 1346-53	15 58 30	+20 56	14.4	.....	+ .095	−0.928	10 10	16	60
Ross 132	17 33 26	−22 38	12.5	.....	− .006	−0.091	14 4	18	100
vM-W 110	18 36 44	− 0 1	13.13	.....	− .015	−0.053	14 6	20	100
L 997-21	19 51 24	− 1 17	14.1	A0±	+ .077	−0.463	7 9	20	100
Wolf 1130	20 2 42	+54 10	13.6	M4e	+ .045	−1.164	6 10	18	60
L 856-54 A	20 50 0	−14 26	14.5	.....	+ .063	+1.369	11 12	18	100
L 856-54 B	20 50 0	−14 26	16.2	.....	+ .080	+1.363	5 5	18	100
Wolf 1340	21 57 8	+ 0 55	10.5	M0e	+ .086	−0.466	6 1	16	60
Wolf 1561 A	22 12 6	− 9 18	14.5	M6	+ .094	−0.458	8 3	20	100
Wolf 1561 B	22 12 6	− 9 18	16.5	M7	+ .104	−0.463	7 3	20	100
vM-W 76	22 12 27	+14 52	14.60	.....	+ .050	+0.199	8 2	18	100
L789-6	22 33 0	−15 52	14.3	M5e	+ .308	+2.280	10 6	18	100
Ross 780	22 47 52	−14 47	11.5	M5	+ .183	+0.963	14 15	18	100
Ross 291	23 20 54	+23 59	15.2	.....	+ .029	+0.509	7 5	18	100
Wolf 1533	23 30 36	+ 3 18	15.2	.....	+0.025	+0.522	9 3	18	100

* The spectra are either by Mr. Humason or Mr. Kuiper.

† Wolf gives m_{pg} as 17, but counts of the number of stars give as m_{ph} only 15.3.

* *Contributions from the Mount Wilson Observatory, Carnegie Institution of Washington*, No. 692.

ly published series.[1] The results are in Table 1. One star, vM-W 110, was put on the program as a possible white dwarf, but the negative parallax derived leaves us in doubt about the absolute magnitude. All the other stars were put on the program on account of their proper motion. As in the other recent papers of this series, it was hoped to find some more stars of faint absolute magnitudes. Three stars have measurable companions (BD+61°195;[2] L 856-54; and Wolf 1561), and three others have companions which could not be measured separately (Rd 45, 368; Ross 614; and Wolf 424); the list therefore represents 31 stars. Excluding vM-W 110, 27 stars have absolute photographic mag-

TABLE 2

ADDITIONAL STARS WITH ABSOLUTE PHOTOGRAPHIC MAGNITUDES +15.0 OR FAINTER

Object	α 1900	δ 1900	m_{ph}	μ	Parallax	M_{ph}
Wolf 1530	1^h40^m	+15° 51′	15.3 vM* 17. Wolf	0″.78	+0″.063	+14.3 vM +16. Wolf
Ross 513 B	15 31	+18 3	16.5	1.18	+ .086	+16.2
Wolf 1055 B	19 12	+ 5 3	18.†	1.45	+ .172	+19.2
Wolf 1084	20 40	+54 57	16.4	1.87	+ .071	+15.7
L 856-54 B	20 50	−14 26	16.2	1.48	+ .074	+15.6
Wolf 1561 B	22 12	− 9 18	16.5	0.68	+ .101	+16.5
L 789-6	22 33	−15 52	14.3	3.27	+0.314	+16.8

* For Wolf 1530, Wolf gives m_{ph} 17, while from star counts in this field I derive m_{ph} of only 15.3.

† On *Harvard Announcement Card* No. 678 Van Biesbroeck gives the red magnitude as 18; from a letter I am allowed to quote that the color index is probably small.

nitudes fainter than +10, of which the following 6 are fainter than +15: the companion of Ross 614; both components of Wolf 424; the companion of L 856-54 and of Wolf 1561; and L 789-6. Of these six stars, only the companions of L 856-54 (Δ = 1″.6, Δm = 1.7 mag.) and of Wolf 1561 (Δ = 8″.0, Δm = 2 mag.) are new, the others having been announced before. The plates measured for L 789-6 were a new set, taken on 103 G plates with a yellow filter, while the results published in the seventeenth series were derived from E 33 plates taken without a filter. In the same series a preliminary parallax, based on 12 exposures only, had been published for Wolf 424.

In the seventeenth series a list was given of the 21 stars known to have photographic absolute magnitudes +15.0 or fainter; to these now should be added the stars in Table 2.

[1] *Mt. W. Contr.*, Nos. 111, 1916; 136, 1917; 158, 1918; 182, 1920; 204, 1921; 237, 1922; 270, 1923; 290, 1925; 321, 1926; 356, 1928; 391, 1929; 435, 1931; 468, 1933; 506, 1935; 553, 1936 (*Ap. J.*, **84**, 409); 590, 1938 (*Ap. J.*, **87**, 424); 630, 1940 (*Ap. J.*, **91**, 503); 652, 1941 (*Ap. J.*, **94**, 396).

[2] The companion of BD+61°195, Wolf 47, was placed in the center of the field; for the BD star, of mag. 10.5, about 5′ distant no sector was used; the result is that its parallax is less reliable than otherwise would have been the case.

ORBIT OF THE NINTH SATELLITE OF JUPITER*

SETH B. NICHOLSON
Mount Wilson Observatory
Received April 21, 1944

ABSTRACT

Jovicentric rectilinear co-ordinates of J IX which represent satisfactorily all the positions observed from 1938 to 1943 were computed by mechanical integration with the co-ordinates and velocities on September 28.0, 1940, U.T., as constants of integration.

Solar perturbations change the orbit so rapidly that ordinary osculating elements describe the motion of the satellite for a short time only. The mean semimajor axis is 0.1585 astronomical unit, the mean period about 758 days.

The orbit of the ninth satellite of Jupiter has been computed from observations made in the years 1938–1943. The combined attractions of Jupiter and the sun were taken into account by computing the satellite's accelerations in jovicentric rectilinear equatorial co-ordinates for 10-day intervals. In computing these accelerations, the heliocentric co-ordinates of Jupiter from *Planetary Co-ordinates*[1] *1800 to 1940* and *1940 to 1960* were used, with 0.00095479 for the mass of Jupiter in units of the sun's mass. Mechanical integration of the accelerations gave the co-ordinates of the satellite at 10-day intervals, the rectilinear co-ordinates and velocities for September 28.0, 1940, which were used as constants of integration, having been adjusted by differential corrections until all the observations were satisfactorily represented. For comparison with the observed positions, geocentric positions were computed with the geocentric co-ordinates of Jupiter interpolated from the *American Ephemeris and Nautical Almanac*.

All the observations of J IX[2] from 1938 to 1943, with their residuals from the final orbit, are listed in Table 1. The positions, referred to the equator and equinox of 1950.0, have been corrected for aberration and geocentric parallax. The observed positions are so well represented that no significant correction to the adopted mass of Jupiter is indicated. The residuals could probably be still further reduced by additional small adjustments of the integration constants; but such a revision does not seem practical unless observations covering a longer time interval are used. An improved value of Jupiter's mass might be obtained if the series of observations of J IX from 1914 to 1918 were included in the solution. Observations of J VIII over a still longer interval, 1908–1943, are also available for this problem. Before definitive results could be obtained, however, the computed co-ordinates of Jupiter would need revision. J VIII and J IX are so faint and so far from Jupiter that their positions can seldom be referred directly to the planet. The positions of J IX, which were referred to stars of the astrographic zones, should be reduced to the system used for the positions of Jupiter, before a more definitive orbit is computed. Such reductions[3] are comparable in size to the residuals in Table 1.

The ordinary elliptical elements of the jovicentric orbit of J IX vary so rapidly that they describe the motion for only a very short time. The orbit is best defined by the rectangular co-ordinates of the satellite which are given in Table 2 for every 10 days during 100-day intervals at the beginning and end of the series and for dates in 1940 near September 28.0. The unit of distance is the astronomical unit, the co-ordinates being referred to the equator and equinox of 1950.0.

*Contributions from the Mount Wilson Observatory, Carnegie Institution of Washington, No. 693.

[1] H.M. Nautical Almanac Office, London: H.M. Stationery Office, 1933 and 1939.

[2] S. B. Nicholson and Myrtle L. Richmond, *A.J.*, **48**, 129, 1939; **49**, 9, 1940; **50**, 163, 1943.

[3] *A.J.*, **49**, 9, 1940; **50**, 163, 1943.

The jovicentric path of J IX is plotted in Figure 1, projected on the plane in which the satellite was moving on September 28.0, 1940. The inclination of this plane to that of the earth's equator was 23° 39′, and the longitude of the ascending node was 129°54′, the satellite's motion being retrograde. In July, 1938, the satellite was 0.007 astronomical unit south of the orbital plane of September 28.0, 1940, and in August, 1944, it will be 0.014 north of that plane.

TABLE 1

OBSERVATIONS OF J IX

U.T.	LIGHT-TIME	α (1950.0)	δ (1950.0)	O−C	
				$\Delta\alpha$	$\Delta\delta$
1938	day				
July 30.4653	0.0241	333° 48′ 8″.6	−11° 36′ 46″.0	+0″.5	−1″.6
July 31.3014	.0240	333 42 10.6	−11 38 50.4	−0.5	−0.8
Aug. 1.4444	.0240	333 33 54.6	−11 41 41.9	−0.2	+1.0
Aug. 24.3799	.0238	330 25 59.6	−12 46 35.0	−1.4	+1.8
Aug. 25.2403	.0238	330 18 34.0	−12 49 8.6	−2.3	0.0
Oct. 21.1354	.0266	324 57 0.9	−14 36 13.0	+1.8	+1.0
Oct. 22.1285	.0267	324 56 17.4	−14 36 30.3	+2.1	+0.7
1939					
July 16.4363	.0257	9 39 14.6	+ 1 44 3.0	−0.6	−0.5
Oct. 8.3269	.0222	5 15 28.2	− 0 40 26.1	−0.6	+2.7
Dec. 15.1181	.0267	2 34 34.5	− 1 13 33.7	−1.2	+1.2
Dec. 16.1181	.0268	2 38 9.0	− 1 11 19.1	−1.2	+2.9
1940					
Sept. 9.3876	.0258	42 50 7.0	+15 29 39.8	−0.9	−0.7
Sept. 28.3965	.0244	41 38 20.4	+15 9 19.6	+0.6	+0.4
Nov. 1.2812	.0231	37 28 5.0	+13 50 39.9	−0.2	−0.2
1941					
Nov. 26.4198	.0243	79 51 16.5	+21 34 5.2	−0.9	+1.3
1942					
Feb. 17.1644	.0283	72 1 38.8	+21 26 14.6	−0.5	−1.2
Feb. 18.2326	.0284	72 3 14.9	+21 26 59.9	−1.1	−0.1
Nov. 8.4549	.0270	116 26 3.6	+21 51 1.4	+0.5	−0.9
Nov. 9.4521	.0270	116 27 42.8	+21 50 57.4	+0.5	−1.1
1943					
Jan. 6.2815	.0238	112 54 7.2	+22 25 58.7	+0.4	−0.1
Apr. 3.2271	.0288	108 53 24.0	+22 32 27.0	+1.0	+0.3
Apr. 4.1991	0.0289	108 58 18.9	+22 31 37.5	+2.6	+1.5

The variations in the ordinary elliptical orbital elements are shown in Figure 2. The elements for the interval from 1914 to 1918 were computed from unpublished co-ordinates representing the observations in that interval. Accurate co-ordinates of J IX have not been computed for the years between 1919 and 1938. The semimajor axis ranged from 0.151 to 0.168 astronomical unit, with a mean value of 0.1585. If Jupiter's attraction alone is used, the period computed for a semimajor axis of 0.1585 astronomical unit is 745.9 days; the observed mean period is 758 days. The eccentricity ranged from 0.103 to 0.415, its average value being 0.23 from 1914 to 1918 and 0.32 from 1938 to 1944. The mean eccentricity is probably about 0.275. The inclination of the orbit to the ecliptic varied rather irregularly from a minimum value of 152.5° in 1917 to a maximum of 161.2°

in 1941, with a mean value of about 157°. The changes in eccentricity and inclination from 1917 to 1941 are not secular and may be due to relatively short-period variations. The longitude of the node, Ω, increased from 310° in 1915 to 79° in 1944—a secular progression of about +4.44° per year. It may be expressed approximately by the equation

$$\Omega = 61° + 4.44° \ (t - 1940),$$

which is plotted as straight lines in Figure 2 (Ω). The longitude of perijove, π, varied from 280° to 349°, with mean values of 301° and 319° in 1916 and 1941, respectively. The

TABLE 2

EQUATORIAL CO-ORDINATES OF J IX (1950.0)

(Astronomical Units)

U.T.	x	y	z
1938			
July 21.0	+0.1257849	+0.0432244	+0.0466553
July 31.0	+ .1270190	+ .0284178	+ .0446225
Aug. 10.0	+ .1268928	+ .0132709	+ .0420833
Aug. 20.0	+ .1253119	− .0020616	+ .0390309
Aug. 30.0	+ .1221956	− .0173980	+ .0354682
Sept. 9.0	+ .1174848	− .0325301	+ .0314099
Sept. 19.0	+ .1111507	− .0472272	+ .0268850
Sept. 29.0	+ .1032033	− .0612430	+ .0219383
Oct. 9.0	+ .0936977	− .0743264	+ .0166308
Oct. 19.0	+ .0827379	− .0862345	+ .0110385
Oct. 29.0	+ .0704756	− .0967471	+ .0052494
1940			
Aug. 19.0	+ .1084655	+ .0512884	+ .0507373
Aug. 29.0	+ .1111840	+ .0355433	+ .0472814
Sept. 8.0	+ .1123735	+ .0193356	+ .0431648
Sept. 18.0	+ .1118503	+ .0028682	+ .0383837
Sept. 28.0	+ .1094518	− .0136062	+ .0329561
Oct. 8.0	+ .1050540	− .0297877	+ .0269266
Oct. 18.0	+ .0985916	− .0453399	+ .0203704
Oct. 28.0	+ .0900744	− .0599073	+ .0133933
Nov. 7.0	+ .0795987	− .0731407	+ .0061290
Nov. 17.0	+ .0673485	− .0847263	− .0012695
Nov. 27.0	+ .0535856	− .0944114	− .0086400
1944			
Mar. 1.0	− .0793209	+ .1698362	+ .0272260
Mar. 11.0	− .0695858	+ .1724022	+ .0320523
Mar. 21.0	− .0596149	+ .1742574	+ .0367591
Mar. 31.0	− .0494460	+ .1753809	+ .0413223
Apr. 10.0	− .0391182	+ .1757528	+ .0457174
Apr. 20.0	− .0286716	+ .1753550	+ .0499198
Apr. 30.0	− .0181478	+ .1741707	+ .0539044
May 10.0	− .0075900	+ .1721845	+ .0576456
May 20.0	+ .0029568	+ .1693830	+ .0611172
May 30.0	+ .0134457	+ .1657543	+ .0642929
June 9.0	+0.0238274	+0.1612885	+0.0671454

variations of π are so irregular that the indicated change of +0.7° per year may not be secular. If it is secular, the longitude of perijove may be expressed approximately by the equation

$$\pi = 318° + 0.7° \ (t - 1940).$$

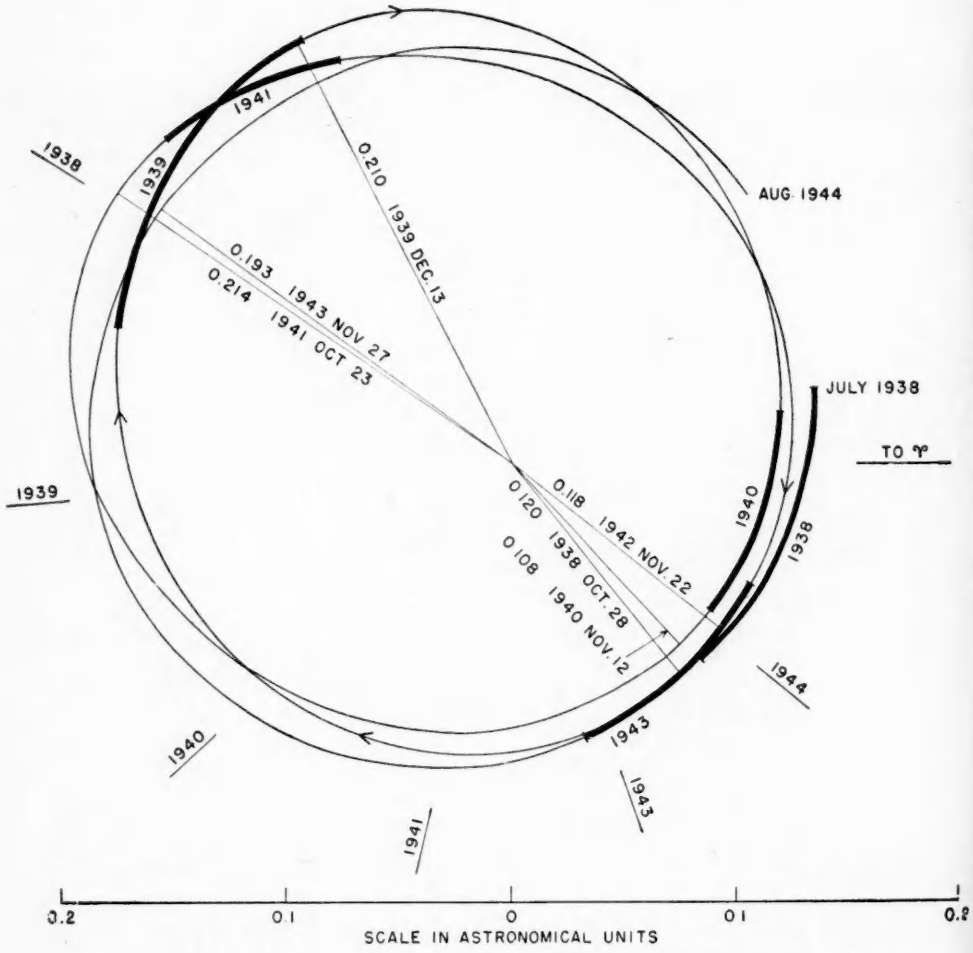

FIG. 1.—The path of Jupiter's ninth satellite projected on the orbital plane of September 28.0, 1940. The heavy lines indicate the part of the orbit in which the satellite was observed. The direction to the earth at each opposition is indicated.

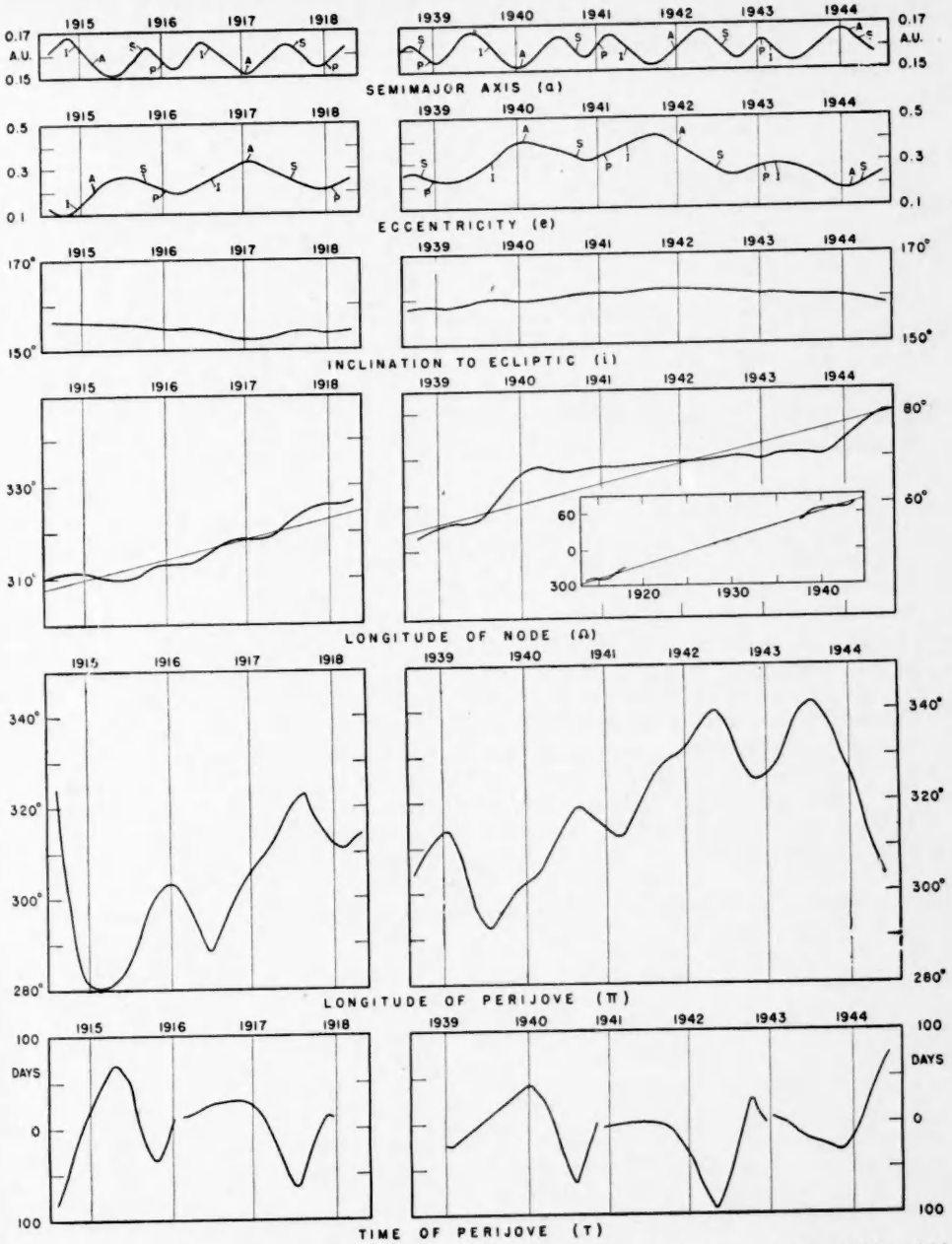

FIG. 2.—Orbital elements plotted against time. The letters, I, A, S, and P, on the plots of (a) and (e) indicate the times of inferior conjunction with the sun, apijove, superior conjunction, and perijove, respectively.

The differences between the time when the mean anomaly, M, equals zero and the time of perijove, T, calculated from the mean anomaly and the mean motion at each date are plotted in Figure 2 (T).

TABLE 3

MEAN ELEMENTS

T = January 0, 1943 $\pm$75 days	e = 0.275 $\pm$ 0.15
ω = 103° + 3.7° (t − 1940) $\pm$ 24°	a = 0.1585 $\pm$ 0.008 astronomical unit
Ω = 61° + 4.44° (t − 1940) $\pm$ 7°	P = 758 $\pm$ 25 days
i = 157° $\pm$ 5°	

The mean elements listed in Table 3 with their approximate ranges are probably of no physical significance but serve to describe the orbit roughly with the usual constants.

I am greatly indebted to Miss Myrtle L. Richmond for much of the numerical computation from which the results were derived.

THE SPECTROGRAPHIC ORBIT AND LIGHT-VARIATIONS OF η GEMINORUM

DEAN B. MCLAUGHLIN AND SUZANNE E. A. VAN DIJKE[1]
Observatory of the University of Michigan
Received April 8, 1944

ABSTRACT

A series of 144 one-prism Michigan spectrograms, taken between 1930 and 1941, and 15 earlier velocities from other observatories give the orbital elements: $P = 2983$ days; $\gamma = +17.6$ km/sec; $K = 8.8$ km/sec; $e = 0.53$; $\omega = 168°$; and $T =$ JD 2426570.

From 1928 to 1941 the light-variation was semiregular, with a period of 234 days and a range from 3.1 to 3.9 mag., though very few minima were fainter than 3.5. Irregular velocity variations are probably associated with the light-changes. Two of the deepest minima coincide with possible eclipse dates, but the evidence is inconclusive.

The well-known red variable η Geminorum[2] was placed on the Michigan spectrographic program in 1930, as one of a list of class-M variables of small range. Originally, the purpose was to investigate the relations of light- and velocity-curves of semiregular variables as a class. The star η Geminorum offered some hope of success, since it was known to have a variable radial velocity.

The supposed period of light-variation was 233 days. The spectrographic observations of the first two seasons failed to show any correlation of velocity with such a period, though the light-curve did exhibit a cycle of about that length. Instead, the spectrograms in 1930–1931 showed a steady decline of velocity from +22 to +5 km/sec. The velocity remained near the latter value until February, 1932, and then began to increase. A deep minimum of light occurred early in 1931, about the middle of the decline of velocity. Accordingly, it was suspected that η Geminorum might be the long-sought giant eclipsing variable of class M. Another light-minimum in December, 1932, after an apparent decrease of velocity, strengthened the suspicion.[3] However, subsequent observations failed to show a further decline of velocity, and the eclipse hypothesis was abandoned.

A few years later, Christie,[4] on the basis of a small number of velocities, published the following orbital elements:

$$\begin{aligned} P &= 1875 \text{ days} \\ \gamma &= +18.2 \text{ km/sec} \\ K &= 5.3 \text{ km/sec} \\ e &= 0.4 \\ \omega &= 280° \end{aligned}$$

The minimum velocity these elements would permit was +13 km/sec, as contrasted with a well-determined value of +5 km/sec from the mean of 18 Michigan plates at the minimum in 1931.

All the available observations of radial velocity are listed in Table 1. Besides 144

[1] Mr. McLaughlin is on leave from the University of Michigan, with temporary address at Harvard Observatory, Cambridge, Massachusetts. Miss Van Dijke is currently at Mount Wilson Observatory.

[2] HD 42995: 1900; $\alpha = 6^h08^m.8$; $\delta = +22°32'$; spectrum Ma (M3).

[3] McLaughlin, *Pub. A.A.S.*, **7**, 178, 1933.

[4] *Ap. J.*, **83**, 434, 1936.

Michigan observations, there are 11 from the Lick Observatory,[5] 2 from the Cape Observatory,[6] and 2 from Victoria[7]—a total of 159.

The Michigan spectrograms were taken with the one-prism spectrograph and have a dispersion of 40 A/mm at $H\gamma$. All of these prior to JD 7774, were measured by McLaughlin. All later plates were measured by Miss Van Dijke, who also measured several of the earlier ones, in order to test for systematic differences between the two measurers. No significant discordances were found.

Throughout the measures a uniform set of comparison and star lines was used, except for the omission of a few lines in the violet region on underexposed spectrograms. The residuals of the individual lines were examined on the first 20 plates; and all lines that showed appreciable systematic deviations from the mean were assigned corrected standard positions, which brought them into agreement. Care was taken to see that the lines

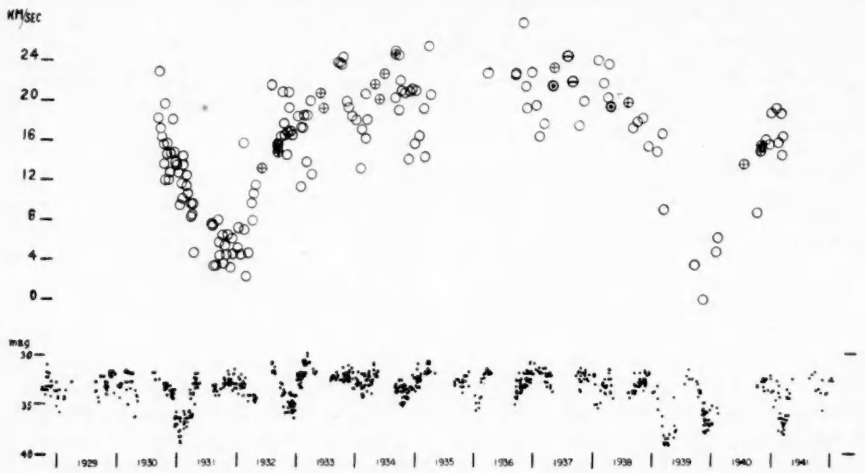

FIG. 1.—Individual observations of radial velocity and apparent magnitude (visual) of η Geminorum from 1928 to 1942. Open circles are Michigan velocities; crossed circles, Lick Observatory velocities; barred circles, Cape Observatory velocities; circled dots, Victoria velocities.

at the violet end were homogeneous with the rest of the set, so that their inclusion or omission would not introduce spurious scatter.

The Michigan velocities are plotted against date of observation in Figure 1. Upon this plot are superimposed the earlier velocities from other observatories, brought up to the cycle of 1931–1939 by application of the final adopted period. From 1930 to 1933 there was a nearly symmetrical decline and increase of velocity, and from 1933 to 1938 there was a broad flat maximum with superimposed fluctuations. A smaller number of observations in 1939 and 1940 shows that another minimum of the same shape as the first occurred at that time. Fortunately, the Lick observations from earlier cycles outline a part of the increase of velocity and fix the minimum well enough to permit improvement of the period. The value finally adopted is 2983 days. Phases expressed in thousandths of this period and reckoned from an arbitrary origin are given in the second column of Table 1.

[5] *Pub. Lick Obs.*, **16**, 87, 1928.

[6] *Cape Ann.*, **10**, Part 8, 158, 1928. Three observations are tabulated; but one, at +41.1 km/sec, has been excluded as probably in error, since it falls far outside the range of all other values.

[7] *Pub. Dom. Ap. Obs.*, **6**, 167, 1933.

TABLE 1

RADIAL VELOCITIES OF η GEMINORUM

JD	Phase	Velocity (Km/Sec)	Residuals O−C (Km/Sec)	JD	Phase	Velocity (Km/Sec)	Residuals O−C) (Km/Sec)
2415035.74*...	0.592	+15.4	+1.1	2426636.90....	0.481	+3.5	−1.1
5041.86....	.594	14.6	+0.2	6646.88....	.485	5.3	+0.4
5672.06....	.806	21.7	+1.4	6653.94....	.487	4.3	−0.7
5695.92....	.814	19.9	−0.5	6667.96....	.492	6.3	+0.9
5723.82....	.823	22.4	+1.9	6678.88....	.496	3.1	−2.7
5783.77....	.843	24.3	+3.0	6687.97....	.499	6.2	+0.1
9731.85....	.167	22.9	+1.5	6693.83....	.500	4.5	−1.7
				6724.66....	.511	5.1	−2.2
2420175.77....	.316	19.4	+1.0	6734.66....	.514	7.1	−0.6
0909.66....	.562	13.2	+0.9	6743.75....	.517	4.5	−3.5
1268.79....	.682	20.5	+2.5	6758.70....	.522	15.7§	+7.2
1287.76....	.688	19.1	+0.9	6760.74....	.523	6.9	−1.7
				6778.65....	.529	2.2	−7.0
2419816†.....	.195	23.9	+2.8	6789.68....	.533	4.6	−5.0
9839.....	.203	21.6	+0.6	6801.66....	.537	9.5	−0.5
				6814.59....	.541	7.8	−2.6
2422700.80‡...	.162	21.0	−0.4	6820.56....	.543	10.5	−0.1
3057.89‡...	.282	19.0	−0.6	6830.55....	.546	11.2	+0.3
6211.93....	.339	22.7	+5.3	6933.91....	.580	21.4	+7.8
6236.92....	.347	18.1	+1.2	6979.88....	.596	15.2	+0.7
6250.94....	.352	17.1	+0.6	6988.88....	.599	16.2	+1.5
6254.85....	.353	16.2	−0.2	7002.97....	.604	20.7	+5.7
6261.93....	.356	15.5	−0.9	7008.91....	.606	17.5	+2.4
6271.98....	.359	13.5	−2.5	7014.83....	.608	16.2	+1.0
6274.80....	.360	19.5	+3.5	7016.95....	.608	14.3	−0.9
6280.95....	.362	11.9	−4.0	7031.74....	.613	16.6	+1.1
6287.87....	.364	14.5	−1.3	7036.86....	.615	20.6	+5.0
6294.74....	.367	15.6	+0.1	7042.76....	.617	19.0	+3.4
6298.89....	.368	11.8	−3.6	7055.78....	.621	16.7	+0.9
6307.90....	.371	12.7	−2.4	7086.80....	.632	16.4	+0.1
6312.95....	.373	14.6	−0.3	7102.67....	.638	18.2	+1.7
6327.79....	.378	18.0	+3.5	7108.78....	.640	17.1	+0.5
6334.81....	.380	14.7	+0.3	7119.72....	.643	11.1	−5.6
6341.89....	.382	12.3	−1.8	7124.62....	.645	17.1	+0.3
6343.83....	.383	13.7	−0.3	7132.60....	.648	18.4	+1.5
6348.74....	.385	13.3	−0.5	7147.56....	.653	13.7	−3.3
6364.74....	.390	12.6	−0.8	7158.59....	.656	18.3	+1.1
6373.81....	.393	9.3	−3.7	7166.62....	.659	19.7	+2.4
6377.77....	.395	11.5	−1.3	7184.55....	.665	12.4	−5.1
6383.65....	.396	10.0	−2.6	7345.87....	.719	23.6	+4.7
6387.74....	.398	13.4	+1.0	7357.80....	.723	23.5	+4.5
6397.75....	.401	14.3	+2.3	7368.81....	.727	23.4	+4.4
6406.70....	.404	11.3	−0.3	7376.76....	.730	24.1	+5.0
6413.65....	.407	12.3	+1.0	7392.78....	.735	19.7	+0.5
6423.60....	.410	10.6	−0.3	7407.69....	.740	19.0	−0.3
6436.67....	.414	9.5	−0.9	7428.69....	.747	18.2	−1.2
6442.60....	.416	8.2	−2.0	7457.76....	.757	17.8	−1.8
6446.62....	.418	8.4	−1.4	7480.79....	.764	13.0	−6.8
6450.60....	.419	9.5	−0.2	7485.72....	.766	16.9	−2.9
6455.64....	.421	4.6	−4.9	7503.60....	.772	16.0	−3.9
6567.91....	.458	7.5	+2.7	7508.71....	.774	20.4	+0.5
6575.92....	.461	7.2	+2.9	7516.61....	.776	17.8	−2.2
6580.92....	.463	3.3	−1.0	7699.85....	.838	20.0	−0.7
6588.90....	.465	3.4	−0.8	7706.82....	.840	24.7	+4.0
6602.86....	.470	7.9	+3.7	7715.83....	.843	18.7	−2.1
6613.88....	.474	5.7	+1.4	7722.79....	.846	24.2	−3.4
6616.85....	.475	4.4	+0.1				
6631.89....	0.480	6.3	+1.7	7730.80....	0.848	+21.7	+0.9

*Lick Observatory. †Cape Observatory. ‡Victoria, Dominion Astrophysical Observatory. §Half-weight.

TABLE 1—*Continued*.

JD	Phase	Velocity (Km/Sec)	Residuals O−C) (Km/Sec)	JD	Phase	Velocity (Km/Sec)	Residuals O−C (Km/Sec)
2427736.80....	0.850	+20.7	−0.1	2428984.61....	0.268	+21.2	+1.2
7756.77....	.857	20.5	−0.4	9009.60....	.277	+19.8	+0.1
7774.70....	.863	13.7	−7.2	9019.58....	.280	+23.2	+3.6
7786.89....	.867	20.6	−0.4	9166.90....	.330	+16.9	−0.9
7804.60....	.873	20.9	−0.1	9197.88....	.340	+17.5	+0.2
7818.73....	.878	15.4	−5.7	9224.76....	.349	+17.8	+1.0
7826.71....	.880	20.7	−0.4	9248.93....	.357	+15.0	−1.2
7836.80....	.884	16.1	−5.0	9308.65....	.377	+14.5	−0.1
7870.69....	.895	18.9	−2.3	9344.57....	.389	+16.3	+2.9
7885.69....	.900	14.2	−7.0	9351.72....	.392	+ 8.7§	−4.5
7899.62....	.905	25.1	+3.8	9537.88....	.454	+ 3.1	−1.9
7917.60....	.911	20.2	−1.1	9579.81....	.468	− 0.4	−4.6
8267.60....	.028	22.4	+0.6	9663.67....	.496	+ 4.5	−1.3
8443.91....	.087	22.3	+0.5	9675.65....	.500	+ 5.9	−0.3
8483.96....	.101	27.5	+5.8	9928.87....	.585	+ 8.4	−5.5
8503.75....	.107	21.1	−0.6	9978.74....	.602	+15.7	+0.9
8517.91....	.112	18.8	−2.9				
8539.74....	.119	22.4	+0.7	2430006.70....	.611	+15.1	−0.2
8571.56....	.130	19.1	−2.5	0020.76....	.616	+18.3	+2.7
8590.64....	.136	16.0	−5.6	0054.70....	.627	+18.8	+2.7
8620.64....	.146	17.3	−4.3	0062.64....	.630	+15.4	−0.8
8836.98....	.219	17.1	−3.8	0072.68....	.633	+18.4	+2.1
8868.79....	.230	19.5	−1.2	0076.63....	.634	+14.2	−2.2
8954.73....	0.258	+23.7	+3.5	0083.62....	0.637	+16.0	−0.5

§ Half-weight.

All the velocities were combined into 20 normal places, which are listed in Table 2. In forming these means, equal weight was given to all velocities except for two Michigan plates of low quality, which received half-weight. The velocities from the other observa-

TABLE 2

NORMAL PLACES FOR ORBITAL SOLUTION, η GEMINORUM

Mean Phase	Mean Velocity (Km/Sec)	Residual O−C (Km/Sec)	No. of Plates	Mean Phase	Mean Velocity (Km/Sec)	Residual O−C (Km/Sec)	No. of Plates
0.058.....	22.4	+0.6	2	0.538.....	7.6	−2.5	6
.138.....	21.0	−0.6	10	.562.....	13.2	+1.0	1
.252.....	20.6	+0.3	8	.591.....	15.2	+1.0	6
.337.....	18.7	+1.2	6	.611.....	17.3	+2.0	11
.362.....	14.8	−1.0	12	.637.....	16.4	−0.1	11
.388.....	13.2	−0.3	13	.667.....	17.3	−0.2	6
.412.....	9.9	−0.7	9	.731.....	21.6	+2.4	7
.465.....	4.5	+0.2	9	.768.....	17.0	−2.8	6
.492.....	5.0	−0.4	10	.855.....	20.0	−0.9	19
0.517.....	7.9	−0.1	5	0.908.....	22.6	+1.3	2

tories are individually more accurate than those measured on the Michigan plates; but, because of the possibility of systematic differences and some remaining uncertainty in the period (and hence in the phases of the older observations), it appeared advisable to give them only the same weight as Michigan velocities.

A solution by the method of Lehmann-Filhés yielded the following orbital elements:

$$
\begin{aligned}
P &= 2983 \text{ days} \\
\gamma &= +17.6 \text{ km/sec} \\
K &= 8.8 \text{ km/sec} \\
e &= 0.53 \\
\omega &= 168^\circ \\
T &= \text{Phase } 0.459 = \text{JD } 2426570 \\
a \sin i &= 306{,}000{,}000 \text{ km}
\end{aligned}
$$

Figure 2 is a plot of the normal places and of the velocity-curve computed from the above elements. The largest deviations from the curve are due to fairly accordant groups of plates, a fact which suggests the existence of some variation of velocity in addition to

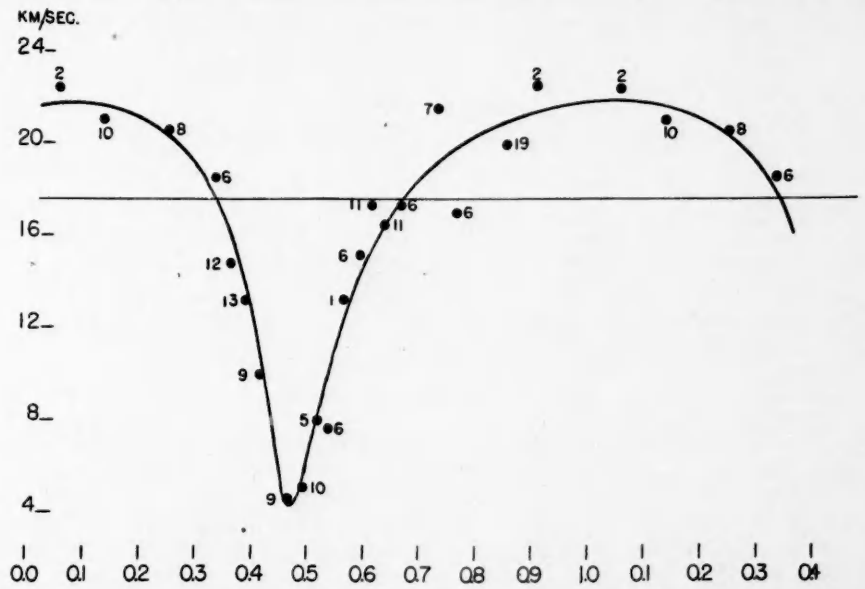

FIG. 2.—Velocity-curve and plot of normal velocities of η Geminorum. Numerals beside each dot indicate the number of observations combined into the means. Abscissae are phases in decimals of the period (2983 days).

that due to orbital motion. The last columns of Tables 1 and 2 contain the residuals of the individual observations and normals, respectively, from the computed curve. In view of the rather large scatter (probably due to secondary variations) a least-squares solution does not appear to be essential. The entire curve should be observed with higher dispersion.

The value of $a \sin i$ suggests that it may be possible to determine an astrometric orbit. The parallax is 0".013; and the apparent semimajor axis of the orbit should then be about 0".026, at least. If the mass ratio of brighter to fainter star is 2, the stars should be at least 0".12 apart at greatest elongation.

From 1928 to 1942 McLaughlin made 704 visual estimates of η Geminorum. These are plotted at the bottom of Figure 1. A well-marked variation in a period of about 234 days is evident. In most cycles the range is less than 0.5 mag. At maximum the star is commonly about 3.2 mag.; at minimum it is sometimes as bright as 3.4; and on one occasion only was it fainter than 3.8 mag.

Table 3 gives dates and magnitudes of all the minima that could be even roughly determined. Even the best (usually the deepest) are in doubt by several days. Residuals in the third column were computed from the formula

$$\text{Min.} = \text{JD } 2425634 + 234\,E\,,$$

which was determined from these observations. The maxima are usually so broad and flat that only vague determinations of their dates could be made.

The individual velocities from 1932 to 1938 show apparent systematic variations with a range of about 10 km/sec. An examination of these fluctuations in connection with the light-variations failed to reveal any correlation. Nevertheless, it appears likely that they are real. Their average deviation from the curve considerably exceeds that to be expected from measures of such a well-defined spectrum, and successive plates tend to depart in the same direction or to show a distinct trend. In contrast, the residuals of the plates taken in 1930 and 1931 are decidedly smaller and are typical of the results that can be obtained from one-prism spectra when care is taken to use uniform sets of lines.

TABLE 3

LIGHT-MINIMA OF η GEMINORUM

JD 2400000+	Mag.	O−C (Days)	Eclipse O−C (Days)	JD 2400000+	Mag.	O−C (Days)	Eclipse O−C (Days)
25,620	3.6	−14	.....	28,193	3.5	−15	.....
26,370	3.7	+34	−3	28,940	3.5	+30	.....
26,828:	3.4	+24:	.....	29,364	3.9	−14	+8
27,037	3.6	− 1	.....	29,614	3.7	+ 2	.....
27,483:	3.4	−23:	.....	30,069	3.7	−11	.....
27,726	3.5	−14	.....				

An alternative explanation of the fluctuations which must not be ignored is a possible blending of the spectrum with that of a secondary star of similar spectral class. The centers of the blended lines would be affected not only by the variation of the light of the primary star but also by the density of the exposure of the photographic emulsion. But, under either hypothesis, it is hard to see why the velocity showed no strong fluctuations in 1930 and 1931.

If η Geminorum is an eclipsing binary, mid-eclipse should occur at the middle of the descending branch of the velocity-curve, at phase 0.393. The corresponding dates are JD 6373 (1931, January 31) and 9356 (1939, April 2). Both of these dates occur close to the centers of two of the deepest observed minima in the interval 1928–1942. The corresponding residuals are entered in the last column of Table 3. The coincidence is too close to be dismissed as fortuitous, but it is far from conclusive. Other minima were almost as deep—especially two that followed the deep one of 1939. Unfortunately, the middle of the next decline of velocity in 1947 will occur almost exactly on the date of conjunction with the sun, so that a test of the eclipse hypothesis probably will have to wait until 1955. At that time, if the 234-day period holds, the predicted eclipse date should occur midway between two dates of minima in the 234-day cycle.

If the deep minima were not eclipses, their occurrence at those dates may be related to the fact that the star was nearing periastron. If we assume the 234-day variation to represent a pulsation, we may conjecture that increased tidal action near periastron might cause an increase of amplitude. This would be consistent with the occurrence of additional deep minima after the deep one of 1939. On the other hand, the system is such a wide one that the deep minima near periastron may be simply fortuitous.

COMPARISON OF THE λ 3883 *CN* BAND IN THE SPECTRA OF COMETS 1940c AND 1942g

ANDREW MCKELLAR*
Dominion Astrophysical Observatory
Victoria, B.C.
Received May 11, 1944

ABSTRACT

A comparison is made of the structure of the λ 3883 0,0 *CN* band in the spectra of Comet 1940c (Cunningham) and Comet 1942g (Whipple-Fedtké-Tevzadze). Strictly comparable spectrograms obtained with the same instrument are used. Differences in the structure of the band for the two comets are evident from wave-length measurements and on reproductions of the spectra. These differences are discussed in terms of the resonance theory of the production of the bands, taking into account the contour of the solar spectrum, as suggested by Swings. The effects of the different heliocentric distances and of the radial velocities of the comets with respect to the sun are noted. Taking into consideration these factors and the resolution used in obtaining the plates, the variations in band structures are considered as adequately explained.

The problems associated with the rotational structure and the intensity distribution within individual molecular emission bands in the spectra of comets have been considered by a number of investigators in recent years.[1–13]. No real success in accounting for the irregularities in the band profiles, particularly in the well-observed *CN* bands, was attained before 1941. At that time Swings, assuming the bands to arise as a result of pure resonance, pointed out the importance of taking account of the irregular intensity contour of the exciting solar radiation. Subsequent work[9–12] has strongly substantiated the ideas advanced by Swings. It therefore appears that not only has a satisfactory explanation of the unusual band profiles been achieved, but also the dominant role of resonance in the production of the emission bands has been demonstrated.

As a contribution to this subject it has been thought instructive and worth while to present a direct comparison of the structure of the λ 3883 0,0 *CN* band in the spectra of Comet 1940c (Cunningham) and Comet 1942g (Whipple-Fedtké-Tevzadze). Perhaps the first such comparison was that made nearly thirty years ago by V. M. Slipher[14] for Comets 1914b (Zlatinsky) and 1915a (Mellish). Unfortunately, at that time lack of knowledge of the origin of band spectra in general and of cometary bands in particular made impossible the proper interpretation of the evident differences in the bands. Even Adel's redis-

* At present on leave of absence from the Dominion Astrophysical Observatory.

[1] Bobrovnikoff, *Pub. A.S.P.*, **42**, 309, 1930, and **43**, 61, 1931; *Pub. Lick Obs.*, **17**, 121, 1930.

[2] Adel, *Pub. A.S.P.*, **49**, 254 and 276, 1937.

[3] Swings and Nicolet, *Ap. J.*, **88**, 173, 1938.

[4] Dufay, *C.R.*, **206**, 1948, 1938.

[5] Wurm, *Ap. J.*, **89**, 312, 1939; *Zs. f. Ap.*, **15**, 115, 1938.

[6] McKellar, *Pub. A.S.P.*, **52**, 283, 1940.

[7] Swings, Elvey, and Babcock, *Ap. J.*, **94**, 320, 1941.

[8] Swings, *Lick Obs. Bull.*, **19**, 131, 1941.

[9] McKellar, *Rev. Mod. Phys.*, **14**, 179, 1942.

[10] McKellar, *Ap. J.*, **98**, 1, 1943.

[11] Swings, *M.N.*, **103**, 86, 1943.

[12] McKellar, *Ap. J.*, **99**, 162, 1944.

[13] Bobrovnikoff, *Ap. J.*, **99**, 173, 1944.

[14] *Bull. Lowell Obs.*, **2**, 67, 1914, and **2**, 151, 1916.

cussion[2] of Slipher's material in 1937 was not productive of significant results, although it did stimulate interest in the problem.

When observed at Victoria, Comets 1940c and 1942g differed considerably in heliocentric distance and in radial velocity with respect to the sun, both of which are factors having a bearing on the band profiles. The plates of these comets were obtained with the same spectrograph and, in a number of cases, with the same slit-width. Data concerning the spectrograms are given in footnotes 9 and 12. While wave-length measurements on the λ 3883 *CN* band in the spectrum of Comet 1940c have been published by Swings, Elvey, and Babcock[7] and by Bobrovnikoff[13] and on this band for numerous other comets by various investigators, it was considered best for the comparison to use only the Victoria measurements. Having been obtained with one instrument and measured by one person, they are homogeneous in all important respects. The significance of this point in the present case is considerable, since the separation between adjacent lines in the *R* branch of the *CN* band (~ 0.6–0.8 A) is of the same order as the spectral purity used. Hence a small change in projected slit-width can and does have a marked effect on the resolution of band structure. Incidentally, in view of the relatively wide slits generally employed in obtaining cometary spectrograms, it has become customary to describe the spectrographic conditions by the width at the photographic plate of a monochromatic image of the slit and to use for such a description the term "spectral purity." This procedure assumes that lines have rectangular profiles and so is only an approximation to the classical spectral purity defined by Schuster, which quite properly took account of diffraction. In the latter case the focal ratio and the aperture of the collimator, among other factors, must be considered. "Spectral purity" as we have used it serves very well to indicate the general order of the resolution to be expected under conditions normally employed on cometary spectra. It is a much more significant and useful quantity than, say, the dispersion with no mention of collimator and camera focal lengths, slit-width, etc.

Reproductions of some of the spectrograms measured are shown in Plate IV, *A* and *B*. The upper and central spectra of Comets 1940c and 1942g, respectively, are strictly comparable. They were obtained under identical spectrographic conditions. The projected slit-width was 0.85 A; and, to give full data, the dispersion at λ 3880 was 57 A per millimeter, the slit-width 0.075 mm, the focal length and aperture of the collimator 114 and 6.3 cm, respectively, and of the camera, 22.8 and 7.6 cm, respectively. The lower reproduction, *C*, also of Comet 1942g, was taken under conditions similar to those used for *B*, except that the spectrograph slit was narrower, being 0.045 mm. The projected slit-width was thus only 0.50 A. The main purpose of including *C* was to show the resulting increase in resolution which is clearly evident, particularly in the nonhead-forming *R* branch. The radial velocities of Comet 1942g with respect to the earth were very closely the same when the originals of *B* and *C* were obtained. *A* has been displaced horizontally with reference to *B* and *C* an amount corresponding to the difference between the radial velocities of the two comets with respect to the observer. This is shown by the slight displacement of the upper two comparison spectra. The three cometary spectra in Plate IV should therefore be in exact alignment.

The wave-length measurements of the Victoria spectrograms are presented in Tables 1 and 2. Table 1 gives the detailed measurements of the *CN* band from seven plates of Comet 1940c. These micrometer measurements have not been previously published, although intensity profiles of this band from these same plates may be found in footnote 9. It would seem that the profiles reveal the structure of the *R* branch somewhat better than do the measurements. Table 2 contains a comparison of the wave lengths of the structural features of the λ 3883 *CN* band for the two comets. It is arranged so that the three columns A, B, and C correspond to the spectra *A*, *B*, and *C* of Plate IV. Column A consists simply of the mean wave lengths from Table 1. Columns B and C, for Comet 1942g, were

PLATE IV

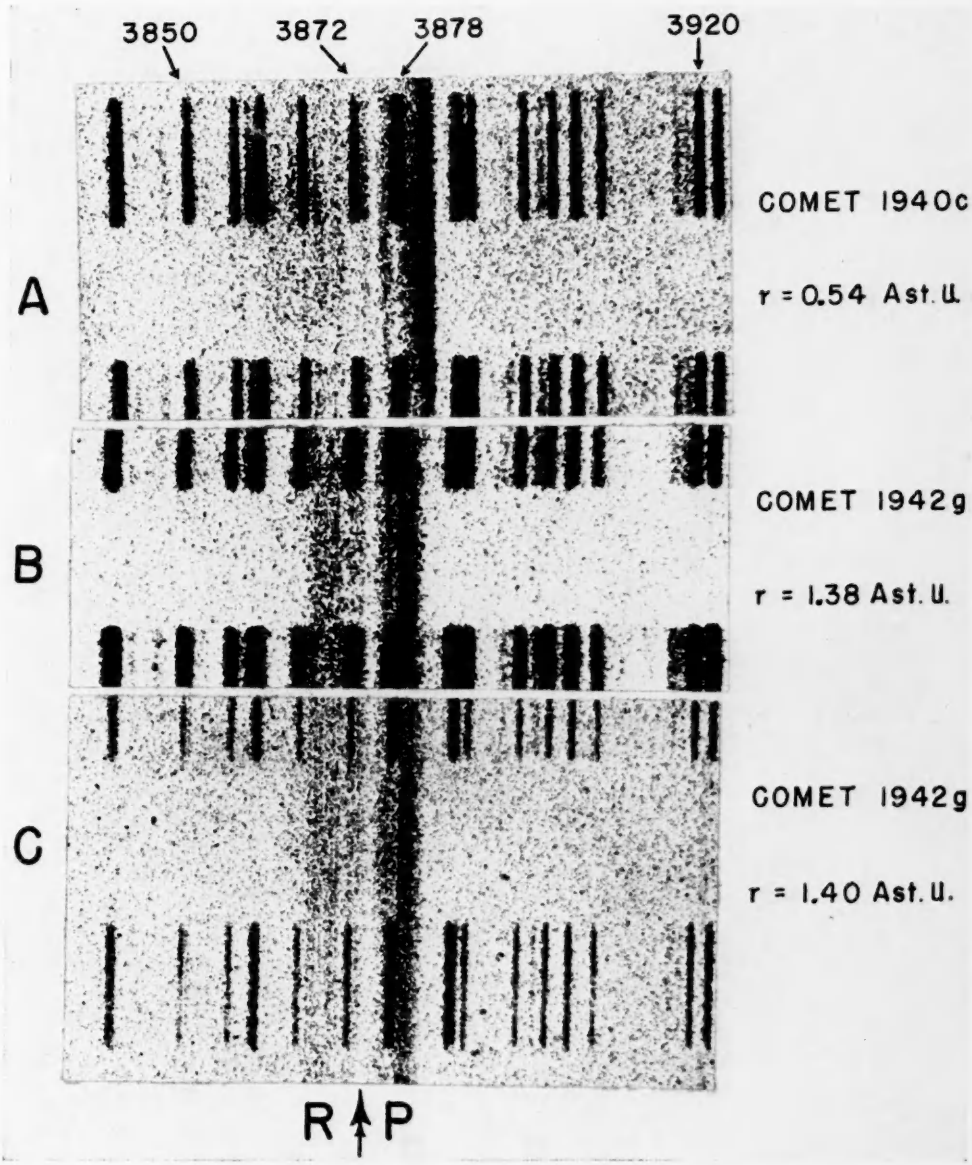

λ 3883 0, 0 *CN* Band in the Spectra of Comets 1940c and 1942g

A) Comet 1940*c*, as photographed 1941, Jan. 2.086 U.T., $r = 0.54$ a.u.
B) Comet 1942g, as photographed 1943, Feb. 24.535 U.T., $r = 1.38$ a.u.
C) Comet 1942g, as photographed 1943, Mar. 1.468 U.T., $r = 1.40$ a.u.
Projected spectrographic slit-width for *A* and *B* equals 0.85 A; for *C* equals 0.50 A

obtained from the detailed wave-length measurements already published.[15] The figures in column B are the average wave lengths from the plates of Comet 1942g taken February 24 and 27, 1943, obtained as noted above with slit-width the same as used for Comet 1940c. They may, therefore, be directly compared with the wave lengths for Comet 1940c in column A. Column C, giving the wave lengths for the plates of Comet 1942g obtained with the highest spectral purity, has been included, since it corresponds to spectrogram *C*. The identifications are not included here. They are as given in Table 2 of footnote 12.

Table 3 lists the laboratory wave lengths[16] of the lines of the 0,0 λ 3883 *CN* band, up to those involving $K'' = 25$. Lines involving higher rotational quantum states are in general not of interest in connection with cometary *CN* emission. Each line is in reality a doublet but is resolved only with the very high resolving-powers obtainable in the labora-

TABLE 1

STRUCTURE OF THE λ 3883 0, 0 CN BAND SEQUENCE IN THE SPECTRUM OF COMET CUNNINGHAM (1940c)

Spectral Feature	Dec. 9.130, 1940 $r=1.01$ Ast. Unit	Dec. 11.135, 1940 $r=0.97$ Ast. Unit	Dec. 13.112, 1940 $r=0.093$ Ast. Unit	Dec. 16.127, 1940 $r=0.87$ Ast. Unit	Jan. 1.081, 1941 $r=0.56$ Ast. Unit	Jan. 2.086, 1941 $r=0.54$ Ast. Unit	Jan. 3.086, 1941 $r=0.52$ Ast. Unit	Mean Wave Length
Violet edge of emission	.....	.....	.....	.....	.....	3858.7	.....	3858.7
Center of broad emission maximum	3866.95	3868.43	3868.39	3868.69	3867.29	67.85	.....	(3867.57(2dd) for $r=0.54$ astr. unit) (3868.12(2dd) for $r=0.94$ astr. unit)
Narrow minimum of intensity	69.73	.....	69.43	.....	69.79	68.97	.....	3869.48
Maximum of intensity	.....	.....	.....	.....	70.87	70.39	69.53	3870.26(2−d)
Deep minimum of intensity	72.03	72.13	.....	72.36	72.51	72.53	72.18	3872.29
Sharp maximum of intensity	73.96	73.61	73.93	73.52	74.00	73.95	73.72	3873.81(1+)
Very deep minimum (band origin)	75.46	75.36	75.26	75.36	75.01	75.37	75.08	3875.27
Sharp maximum of intensity	76.75	76.99	76.78	76.82	76.67	76.80	76.63	3876.78 (5)
Deep minimum of intensity	78.17	78.30	78.23	78.30	78.11	78.22	78.08	3878.20
Subsidiary maximum of intensity	.....	.....	.....	.....	79.39	.....	79.36	3879.38 (4)
Minimum of intensity	.....	.....	.....	.....	79.99	.....	80.03	3880.01
Center of main *P* branch maximum	80.69	80.85	80.78	81.02	82.08	82.35	82.13	3882.19 (10d)
Red edge of band (band head)	82.85	82.46	82.84	82.41	82.91	82.97	82.86	(3882.64 for $r=0.94$ astr. unit) (3882.91 for $r=0.54$ astr. unit)

tory. These wave lengths have been given to indicate the closeness of their spacing and hence to enable one to appreciate the conditions under which the identifications of emission features in cometary *CN* bands are made. Also they provide the material upon which critical examination and judgment of the validity of any such identifications can be based.

The most obvious difference apparent between the *CN* bands in *A* and *B*, both from Plate IV and from Table 2, is in the wave-length range covered by the emission. For Comet 1940c, both the *R* and the *P* branches extend outward from the band origin (marked by an arrow head) much farther than for Comet 1942g, and the main maxima of intensity in both branches of the band are more distant from the band origin for the former comet. This results from a different distribution of molecules among the rotational states of *CN* in the two cases. For Comet 1940c the maxima in the distribution are at about $K'' = 20$ and $K'' = 13$ for $r = 0.54$ and $r = 0.92$, respectively, while states up to $K'' = 25$ are appreciably populated. For Comet 1942g the maximum of intensity occurs about $K'' = 10$, and emission occurs out to states corresponding to $K'' = 13$. This effect, in turn, can be considered a consequence of the different "rotational" temperatures of

[15] See footnote 12, Table 2.

[16] Uhler and Patterson, *Ap. J.*, **42**, 434, 1915; Jenkins and Wooldridge, *Phys. Rev.*, **53**, 137, 1938.

TABLE 2

COMPARISON OF STRUCTURE OF λ 3883 *CN* BAND FOR COMETS 1940c AND 1942g

SPECTRAL FEATURE	A Mean λ, Comet 1940c (Projected Slit-Width = 0.85 A)	B Mean λ, Comet 1942g (Projected Slit-Width = 0.85 A)	C Mean λ, Comet 1942g (Projected Slit-Width = 0.5 A)
Violet edge of emission	3858.7	.....	3866
Emission line	.....	.....	66.18 (0+)
Emission line	.....	.....	66.89 (1s)
Emission line	67.57 (2dd*) $r=0.54$	.....	67.68 (1+s)
Emission line	68.12 (2dd) $r=0.94$	3868.86 (3+dd)	68.44 (1+s)
Narrow minimum of intensity	69.48	.....	.....
Emission line	70.26 (2−d)	.....	70.04 ($1\frac{1}{2}$s)
Emission line	.....	.....	70.71 ($1\frac{1}{2}$)
Marked minimum of intensity	72.29	71.51	71.54
Emission line	.....	.....	72.06 (1s)
Emission line	.....	.....	72.47 ($1\frac{1}{2}$)
Emission line	73.81 (1+)	72.94 (2−d)	73.47 (1−s)
Emission line	.....	.....	74.25 ($\frac{1}{2}$−)
Deep minimum (band origin)	75.27	74.82	74.95
Definite maximum of intensity	76.78 (5)	77.41 (5d)	77.30 (4d)
Marked minimum of intensity	78.20	78.46	78.52
Subsidiary maximum of intensity	79.38 (4)	.....	.....
Subsidiary minimum of intensity	80.01	.....	80.11
Center of main *P* branch maximum	82.19 (10d)	80.11 (9d)	80.16 (8d)
Red edge of band (band head)	82.64 for $r=0.94$ 82.91 for $r=0.54$	81.57	81.57

* "d" indicates diffuse, and "dd" very diffuse, emission; "s" indicates sharp emission feature.

TABLE 3

LABORATORY WAVE LENGTHS OF THE λ 3883 *CN* BAND LINES UP TO $K''=25$

Line	λ	Line	λ	Line	λ	Line	λ
R(25)	3853.49	*R*(11)	3866.82		Band origin	*P*(14)	81.32
(24)	54.57	(10)	67.62	*P*(1)	3875.77	(15)	81.59
(23)	55.62	(9)	68.41	(2)	76.31	(16)	81.88
(22)	56.66	(8)	69.18	(3)	76.84	(17)	82.10
(21)	57.69	(7)	69.92	(4)	77.35	(18)	82.32
(20)	58.68	(6)	70.67	(5)	77.83	(19)	82.52
(19)	59.67	(5)	71.37	(6)	78.30	(20)	82.70
(18)	60.63	(4)	72.06	(7)	78.75	(21)	82.85
(17)	61.57	(3)	72.74	(8)	79.19	(22)	82.99
(16)	62.49	(2)	73.36	(9)	79.58	(23)	83.10
(15)	63.39	(1)	74.00	(10)	79.97	(24)	83.19
(14)	64.30	*R*(0)	74.61	(11)	80.33	(25)	83.26
(13)	65.15			(12)	80.67	Band head	83.40
(12)	65.99			(13)	81.00		

the two comets. Spectrogram *A* was taken when Comet 1940c was at a heliocentric distance $r = 0.54$ astronomical unit, whereas *B* was obtained when the heliocentric distance of Comet 1942g was 1.38 astronomical units. A difference in effective temperature is therefore not surprising. To present actual figures, the profile representative of spectrogram *A* has been found to correspond to a temperature of about 435° K,[9] while for spectrogram *B*, the corresponding figure is estimated as about 200° K. These temperatures are in fair accord with figures obtained from the equation $T = 300\, r^{-\frac{1}{2}}$° K (*r* being the heliocentric distance in astronomical units). This expression is readily derivable for ideal black bodies in the radiation field of the sun. The general effect noted in this paragraph has been mentioned and discussed a number of times recently[3,4,9,12] and may now be taken as well established. It alone would seem to be sufficient to account for all the difference, already referred to, observed by Slipher between the *CN* bands in Comets 1914b and 1915a. He had photographed these at heliocentric distances of 0.67 and 1.52 astronomical units, respectively. His spectrograms were not obtained with sufficient spectral

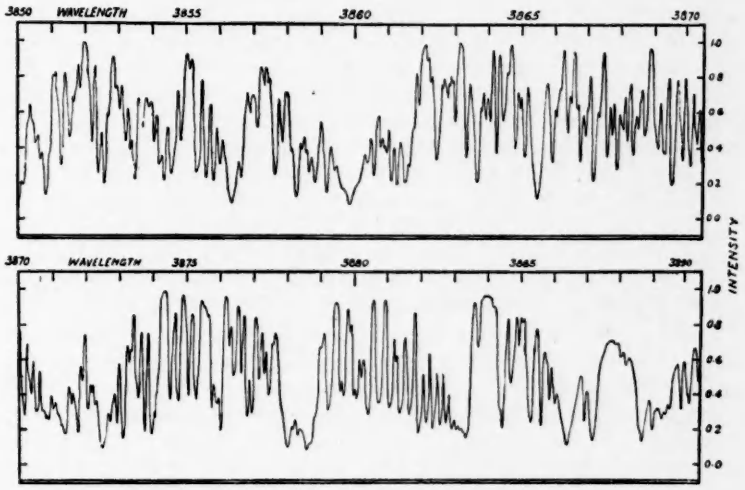

FIG. 1.—Contour of solar spectrum

purity to reveal the structure shown in Plate IV and discussed in the following paragraphs. The variation in extent and general intensity distribution with heliocentric distance is observed not only for the bands of different comets as above but also for the same comet at different points in its orbit.[9] The study of as many cases as possible corresponding to a large range of heliocentric distances should be carried out, extending the earlier work of Dufay.[4] In so doing, there should be taken into account the factors influencing detailed fine structure, as discussed below.

The second main topic concerns the local irregularities of the intensity profile of the *CN* band in the spectra of the two comets. As intimated in the introduction, these irregularities follow from the uneven intensity contour of the solar spectrum, if the bands are considered to be produced by a pure resonance mechanism, sunlight being the exciting radiation.[8,9,11] The contour of the solar spectrum[17] in the region of λ 3883 is shown in Figure 1. It is of assistance in following the present discussion.

In all three spectrograms of Plate IV the structural features most plainly seen are the definite minima at λ 3878 in the *P* branch and at λ 3872 in the *R* branch, one on each

[17] See Minnaert, Mulders, and Houtgast, *Photometric Atlas of the Solar Spectrum*, Utrecht, 1940.

side of the band origin. As an example, their *raison d'être* may profitably be considered in detail. These are the minima discussed by Swings in connection with his original explanation of the band structure.[8]

In the λλ 3883–3860 region the outstanding and most sharply defined absorption feature in the solar spectrum is the one at λ 3878.4, made up of two very intense *Fe* lines at λ 3878.0 and λ 3878.7. The wider minimum centered at about λ 3872 is also a strong one. In a cometary head, *CN* molecules in the rotational quantum states $K'' = 5$, $K'' = 6$, and $K'' = 7$ of the ground electronic and vibrational states would be capable of absorbing solar radiation of wave lengths λλ 3877.83, 3878.30, and 3878.75 in the *P* branch, and λλ 3869.92, 3870.67, and 3871.37 in the *R* branch. All of these lie within the above minima in the solar spectrum. Such absorption would be the means of populating upper states having $K' = 4$, $K' = 5$, $K' = 6$, $K' = 7$, and $K' = 8$, mainly those with $v' = 0$. Then, upon the return of the molecules to the normal state, emission such as that observed in cometary bands would ensue. It is seen that the lack of solar radiation of the above wave lengths would result in an underpopulation of the upper rotational states listed, compared with those adjacent to them, then to a lack of intensity for the emission lines originating from these states, and, finally, to the observed minima of intensity in the cometary *CN* bands. One means of testing the validity of this hypothesis is to examine the band structure for two comets having different velocities with respect to the sun. The data in Table 2 can be used for this purpose. The mean radial velocity of Comet 1940c with respect to the sun over the relevant period of time was −33 km/sec, while for Comet 1942g it was +7 km/sec. Thus compared to the case of Comet 1940c, the solar spectrum was effectively shifted for Comet 1942g toward longer wave lengths by an amount corresponding to 40 km/sec or, at λ 3880, by 0.52 A. The observed wave lengths of the minima in the *CN* emission bands should therefore be correspondingly affected. If we assume that nearly all the effect is due to the sharp, deep solar line at λ 3878, the minimum in the *P* branch should be shifted 0.52 A to the *red* and that in the *R* branch 0.52 A to the *violet* for Comet 1942g relative to 1940c. The actual shifts, from the comparable columns A and B of Table 2, are 0.26 A and 0.78 A, in the correct senses, for the two branches. The mean value is 0.52 A, which is in excellent agreement with that predicted, even fortuitously so, considering that the band consists of discrete lines close together rather than an actual continuum.

The less apparent minima in the cometary bands could likewise be compared. This was done, effectively, in the photometric study of the bands for Comets 1939d and 1940c, where quantitative photometric evidence of the validity of this resonance mechanism was found.[9,11] So it appears that differences in detailed structure of the bands in different comets can be satisfactorily accounted for on the basis of the resonance hypothesis of their origin. To demonstrate this fully, a spectrophotometric study of the band or bands is necessary, and the following points must be taken into consideration: (1) the distribution of molecules among the rotational levels of the normal state (by using a Maxwell-Boltzmann distribution at an "effective" temperature or by any more suitable distribution; indeed, the study may be designed to obtain the distribution from the band structure[10]); (2) the contour of the exciting solar radiation, as shifted by the radial velocity of the comet; and (3) the spectral purity used in obtaining the cometary spectrum.

In his recently published article[13] on the spectrum of Comet 1940c, it is unfortunate that Bobrovnikoff did not take into consideration the above factors. With projected slit-width at λ 3880 equal to 1.46 A, despite his dispersion being relatively great (16.1 A/mm), it was manifestly impossible to resolve any of the individual *CN* lines listed in Table 3 above. Therefore, in suggesting, as he did, that the identifications given in his Table 2 had no significance whatever as identifications of individual band lines, he was undoubtedly correct. However, the statement that neither his nor any observational material yet obtained is adequate to settle the matter of the band structure is misleading. On the contrary, it seems certain that any structure yet observed in this band (and for at

least fifteen comets between 1907 and the present time sufficient resolving-power has been used to provide some evidence of structure) can be satisfactorily accounted for on the basis of the resonance hypothesis of its origin in combination with the three points noted in the previous paragraph. It appears most desirable to apply these methods to the study not only of the *CN* bands but to all cometary emission bands, including the Swan system of C_2.

A further point regarding the *CN* identifications given by Bobrovnikoff requires comment. He has identified the four emission features measured between λ 3856 and λ 3868 with the 1,1 *CN* band, which has its head at λ 3871. This identification, despite the fact that it has been given by many investigators of cometary spectra over the last thirty or forty years, is almost certainly erroneous. The 1,1 band must be a great many times fainter than the 0,0 band in sources at the low excitation temperatures of comets. Even at an excitation temperature of 5900° K, it has been measured[18] as merely one-half the intensity of the 0,0 band. Therefore, only on extremely strongly exposed or overexposed cometary spectrograms might the 1,1 band be expected to occur with sufficient strength to be detected. Actually, the emissions measured in the λλ 3855–3874 region are normally due to the *R* branch of the 0,0 *CN* band. If the *P* branch is present between λ 3875 and λ 3883, the *R* branch of this same band simply must appear. As shown on the intensity profiles of this region for Comets 1939d and 1940c,[9] obtained from spectrograms as strong as those of Plate IV, there is no evidence of the 1, 1 band. All the emission over the λλ 3855–3874 region is fully accounted for by the *R* branch of the λ 3883 0,0 *CN* band.

[18] Ornstein and Brinkman, *Kon. Akad. v. Wetensch. Amsterdam*, **34**, 33, 1931.

ON THE RADIATIVE EQUILIBRIUM OF A STELLAR ATMOSPHERE. II

S. CHANDRASEKHAR
Yerkes Observatory
Received May 11, 1944

ABSTRACT

In this paper a new method is described for solving the various problems of radiative transfer in the theory of stellar atmospheres. The basic idea consists in expressing the integral (proportional to the density of radiation) which occurs in the equation of transfer as a sum according to Gauss's formula for numerical quadratures and replacing the integrodifferential equation by a system of linear equations. General solutions of this linear system can readily be written down, and this enables one to obtain solutions for the various problems to any desired degree of accuracy.

The method has been applied in detail to the problem considered in the earlier paper, and the first four approximations explicitly found. The corresponding laws of darkening have also been determined. An interesting by-product of the investigation is a new and entirely elementary proof of the exact Hopf-Bronstein relation, giving the boundary temperature in terms of the effective temperature.

1. *Introduction.*—In an earlier paper[1] it was shown how successively higher approximations to the solution of the equation of transfer

$$\mu \frac{dI}{d\tau} = I - \tfrac{1}{2}\int_{-1}^{+1} I\, d\mu \tag{1}$$

can be obtained by expanding I in terms of spherical harmonics in the form

$$I(\tau, \mu) = \sum_{l=0}^{\infty} I_l(\tau) P_l(\mu). \tag{2}$$

More recently an important investigation by G. C. Wick[2] has come to the author's notice in which an alternative method for solving equations similar to (1) has been developed. It is the object of this paper to describe Wick's method in its astrophysical context and to show its particular adaptability for solving the standard problems of radiative transfer in the theory of stellar atmospheres.

2. *The outline of the method.*—Wick's basic idea consists in expressing the integral on the right-hand side of equation (1) as a sum, using for this purpose Gauss's formula for numerical quadratures.[3] Thus, denoting by $\mu_{-n}, \ldots, \mu_{-1}, \mu_1, \ldots, \mu_n$, and $\mu_{-i} = -\mu_i$ the $2n$ real roots of the Legendre polynomial $P_{2n}(\mu)$ of order $2n$, we can write, according to Gauss,

$$\int_{-1}^{+1} I(\tau, \mu)\, d\mu \simeq \sum_{j=-n}^{+n} a_j I(\tau, \mu_j), \tag{3}[4]$$

[1] *Ap. J.*, **99**, 180, 1944. Referred to hereafter as "I."

[2] *Zs. f. Phys.*, **120**, 702, 1943.

[3] See, e.g., P. Frank and R. V. Misses, *Differentialgleichungen der Physik*, **1**, 394, New York, 1943.

[4] Note that the summation on the right-hand side does not include the term $j = 0$.

where the a_j's are certain weight factors. It may be further noted that

$$a_j = a_{-j}\,; \qquad \mu_j = -\mu_{-j}\,. \tag{4}$$

It is known that for a given number of subdivisions of the interval $(-1, +1)$ Gauss's choice of the points μ_j and the weights a_j yields the best value for the integral in the sense that for any *arbitrary* polynomial of degree $4n - 1$, the formula (3) is *exact*. In particular,

$$\sum_{j=1}^{n} a_j \mu_j^m = \int_0^1 \mu^m d\mu = \frac{1}{m+1}. \tag{5}$$

Accordingly, the representation of the integral as a finite sum of the form (3) can be made as accurate as may be desired by choosing n sufficiently large.

In the "nth approximation" we therefore replace equation (1) by the linear system of ordinary equation of order $2n$:

$$\mu_i \frac{dI_i}{d\tau} = I_i - \tfrac{1}{2}\Sigma a_j I_j \qquad (i = \pm 1, \ldots, \pm n), \tag{6}$$

where, for the sake of brevity, we have written I_i for $I(\tau, \mu_i)$. Further, in equation (6) the summation over j is extended over all the positive and negative values.

3. *The general solution of the system of equations (6).*—We shall now find the different linearly independent solutions of the system (6) and later, by combining these, obtain the general solution.

First, we shall seek a solution of (6) of the form

$$I_i = g_i e^{-k\tau} \qquad (i = \pm 1, \ldots, \pm n), \tag{7}$$

where the g_i's and k are constants, for the present unspecified. Introducing equation (7) into equation (6), we obtain the relation

$$g_i (1 + \mu_i k) = \tfrac{1}{2}\Sigma a_j g_j\,. \tag{8}$$

Hence,

$$g_i = \frac{\text{constant}}{1 + \mu_i k} \qquad (i = \pm 1, \ldots, \pm n), \tag{9}$$

where the "constant" is independent of i. Substituting the foregoing form for g_i in equation (8), we obtain the following equation for k:

$$1 = \tfrac{1}{2}\Sigma \frac{a_j}{1 + \mu_j k}. \tag{10}$$

Remembering that $a_{-j} = a_j$ and $\mu_{-j} = -\mu_j$, we can re-write equation (10) as

$$1 = \sum_{j=1}^{n} \frac{a_j}{1 - \mu_j^2 k^2}. \tag{11}$$

It is thus seen that k^2 must satisfy an algebraic equation of order n. However, since

$$\sum_{j=1}^{n} a_j = 1 \tag{12}$$

(cf. eq. [5]), $k^2 = 0$ is a solution of equation (11). Accordingly, equation (10) has only $2n - 2$ distinct roots, which occur in pairs

$$\pm k_\alpha \qquad (\alpha = 1, \ldots, n-1). \tag{13}$$

And, corresponding to these $2n-2$ roots, we have $2n-2$ independent solutions of equation (6). To complete the solution we notice that equation (6) admits of a solution of the form

$$I_i = b(\tau + q_i) \qquad (i = \pm 1, \ldots, \pm n), \quad (14)$$

where b is an arbitrary constant. For, inserting the form (14) for I_i in equation (6), we find that

$$\mu_i = q_i - \tfrac{1}{2}\Sigma a_j q_j ; \quad (15)$$

and this can be satisfied by

$$q_i = \mu_i + Q \qquad (i = \pm 1, \ldots, \pm n), \quad (16)$$

where Q is an arbitrary constant. Thus, the system (6) allows the solution

$$I_i = b(\tau + Q + \mu_i) \qquad (i = \pm 1, \ldots, \pm n), \quad (17)$$

where b and Q are two arbitrary constants.

Thus, combining solutions of the form (7) and (17), we have the general solution

$$I_i = b\left\{\sum_{a=1}^{n-1}\left[\frac{L_a e^{-k_a\tau}}{1+\mu_i k_a} + \frac{L_{-a}e^{+k_a\tau}}{1-\mu_i k_a}\right] + \mu_i + Q + \tau\right\}, \quad (18)$$

where b, $L_{\pm a}$, $(a = 1, \ldots, n-1)$, and Q are $2n$ arbitrary constants.

4. *The solution of equation (1) satisfying the necessary boundary conditions.*—For the astrophysical case under consideration the boundary conditions are[5] that none of the I_i's increase exponentially as $\tau \to \infty$ and that, further, there is no incident radiation on the surface $\tau = 0$. The first of these conditions implies that in the general solution (18) we omit all the terms in exp $(+k_a\tau)$. Thus,

$$I_i = b\left\{\sum_{a=1}^{n-1}\frac{L_a e^{-k_a\tau}}{1+\mu_i k_a} + \mu_i + Q + \tau\right\} \quad (i = \pm 1, \ldots, \pm n). \quad (19)$$

Next the nonexistence of any radiation incident on $\tau = 0$ requires that

$$I_{-i} = 0 \quad \text{at} \quad \tau = 0 \quad \text{and for} \quad i = 1, \ldots, n, \quad (20)$$

or, according to equations (4) and (19),

$$\sum_{a=1}^{n-1}\frac{L_a}{1-\mu_i k_a} + Q = \mu_i \qquad (i = 1, \ldots, n). \quad (21)$$

These are the n equations which determine the $(n-1)$ constants L_a and the further constant Q. The constant b is left arbitrary; and this, as we shall presently show, is related to the constant net flux in the atmosphere.

Now the net flux is defined in terms of F, where

$$F = 2\int_{-1}^{+1} I\mu\, d\mu . \quad (22)$$

Expressing the integral on the right-hand side as a sum over the $I_i\mu_i$'s according to Gauss's formula and using the solution (19) for the I_i's, we find

$$F = 2b\left\{\sum_{a=1}^{n-1} L_a e^{-k_a\tau}\sum_i \frac{a_i\mu_i}{1+\mu_i k_a} + \sum_i a_i\mu_i^2 + (Q+\tau)\sum_i a_i\mu_i\right\}. \quad (23)$$

[5] Cf. I, p. 182.

On the other hand (cf. eq. [5]),

$$\Sigma a_i \mu_i^2 = \tfrac{2}{3} \qquad \text{and} \qquad \Sigma a_i \mu_i = 0 \,. \tag{24}$$

Moreover,

$$\left.\begin{aligned} \Sigma \frac{a_i \mu_i}{1+\mu_i k_a} &= \frac{1}{k_a} \Sigma a_i \left(1 - \frac{1}{1+\mu_i k_a}\right) \\ &= \frac{1}{k_a}\left(2 - \Sigma \frac{a_i}{1+\mu_i k_a}\right), \end{aligned}\right\} \tag{25}$$

which vanishes according to equation (10). Hence,

$$F = \tfrac{4}{3} b = \text{constant} \,; \tag{26}$$

i.e., b is related to the constant net flux, as stated.

In terms of our solution for the I_i's we can obtain a convenient formula for J defined by

$$J = \tfrac{1}{2} \int_{-1}^{+1} I \, d\mu = \tfrac{1}{2} \Sigma a_i I_i \tag{27}$$

in our present approximation. We have

$$J = \tfrac{1}{2} b \left\{ \sum_{a=1}^{n-1} L_a e^{-k_a \tau} \sum_i \frac{a_i}{1 + \mu_i k_a} + \sum_i a_i \mu_i + (Q+\tau) \sum_i a_i \right\}; \tag{28}$$

or, according to equations (5), (10), (24), and (26), we have

$$J = \tfrac{3}{4} F \left(\tau + Q + \sum_{a=1}^{n-1} L_a e^{-k_a \tau} \right). \tag{29}$$

If we express J in its "normal" form (cf. I, eq. [47]),

$$J = \tfrac{3}{4} F (\tau + q[\tau]) \,, \tag{30}$$

we have

$$q(\tau) = Q + \sum_{a=1}^{n-1} L_a e^{-k_a \tau} \,. \tag{31}$$

Finally, we may note that, according to the solution (29) for J, we have the law of darkening (cf. I, eq. [49]):

$$I(0, \mu) = \tfrac{3}{4} F \left(\mu + Q + \sum_{a=1}^{n-1} \frac{L_a}{1 + k_a \mu} \right). \tag{32}$$

This completes the solution. The clear superiority of our present method over our earlier one of expanding I in terms of spherical harmonics is apparent. It is to be particularly noted that, in contrast to our earlier method, we can now write down the formal solution for any order of approximation quite generally.

5. *The first, second, third, and fourth approximations.*—We shall now obtain in their numerical forms the first four approximations to the solution for J and the corresponding laws of darkening.

i) *The first approximation.*—The first approximation is obtained by choosing $n = 1$, in which case

$$a_1 = a_{-1} = 1 \qquad \text{and} \qquad \mu_1 = -\mu_{-1} = \frac{1}{\sqrt{3}}. \tag{33}$$

There is no nonzero root for equation (10), and equation (21) now implies that

$$Q = \mu_1 = \frac{1}{\sqrt{3}}. \tag{34}$$

Accordingly,

$$q(\tau) = \frac{1}{\sqrt{3}} \tag{35}$$

and

$$I(0, \mu) = \tfrac{3}{4} F\left(\mu + \frac{1}{\sqrt{3}}\right). \tag{36}$$

It is remarkable that in the very first approximation our method predicts a boundary value for $q(\tau)$ which is in *exact* agreement with the Hopf-Bronstein value (cf. I, eq. [73]). Actually, as we shall presently show (see § 6 below), this is identically the case in *all* approximations; and, consequently, we have here an essentially new and "elementary" proof of the Hopf-Bronstein relation.

One further remark about this first approximation may be made. The differential equations for I_1 and I_{-1} are

$$\left.\begin{aligned} \frac{1}{\sqrt{3}} \frac{dI_1}{d\tau} &= I_1 - \tfrac{1}{2}(I_1 + I_{-1}), \\ -\frac{1}{\sqrt{3}} \frac{dI_{-1}}{d\tau} &= I_{-1} - \tfrac{1}{2}(I_1 + I_{-1}), \end{aligned}\right\} \tag{37}$$

which are essentially the equations of Schwarzschild's first approximation.[6] However, the difference is that on the left-hand sides of the foregoing equations we now have $1/\sqrt{3}$ instead of the usual $1/2$. It is interesting to speculate that, had Schwarzschild used our present systematic method, based on Gauss's formula, he might have discovered the exact boundary temperature some twenty-five years before Hopf and Bronstein!

ii) *The second approximation.*—To obtain the second approximation we have to choose for the μ_i's the zeros of $P_4(\mu)$ and the corresponding weight factors. We have[7]

$$\left.\begin{aligned} a_1 = a_{-1} &= 0.652145\,; \qquad \mu_1 = -\mu_{-1} = 0.339981\,, \\ a_2 = a_{-2} &= 0.347855\,; \qquad \mu_2 = -\mu_{-2} = 0.861136\,. \end{aligned}\right\} \tag{38}$$

Equation (11) reduces to

$$\mu_1^2 \mu_2^2 k^2 = a_1 \mu_1^2 + a_2 \mu_2^2 = \tfrac{1}{3}\,. \tag{39}$$

Hence,

$$k_1 = \frac{1}{\sqrt{3}\mu_1\mu_2} = 1.972027\,. \tag{40}$$

Solving for Q and L_1, we find

$$Q = 0.694025\,; \qquad L_1 = -0.116675\,. \tag{41}$$

[6] Cf. E. A. Milne, *Handb. d. Ap.*, **3**, No. 1, 114–116, Berlin: Springer, 1930.

[7] A. N. Lowan, N. Davids, and A. Levenson, *Bull. Amer. Math. Soc.*, **48**, 739, 1942.

Accordingly, on this approximation

$$q(\tau) = 0.694025 - 0.116675e^{-1.97203\tau} \tag{42}$$

and

$$I(0, \mu) = \tfrac{3}{4}F\left(\mu + 0.694025 - \frac{0.116675}{1+1.97203\mu}\right). \tag{43}$$

iii) *The third approximation.*—We now have

$$\left.\begin{aligned} a_1 = a_{-1} = 0.467914\ ; &\quad \mu_1 = -\mu_{-1} = 0.238619\ , \\ a_2 = a_{-2} = 0.360762\ ; &\quad \mu_2 = -\mu_{-2} = 0.661209\ , \\ a_3 = a_{-3} = 0.171324\ ; &\quad \mu_3 = -\mu_{-3} = 0.932470\ . \end{aligned}\right\} \tag{44}$$

The equation for k^2 reduces to

$$0.02164502k^4 - 0.254545k^2 + \tfrac{1}{3} = 0\ , \tag{45}$$

the positive roots of which are

$$k_1 = 3.202945 \quad \text{and} \quad k_2 = 1.225211\ . \tag{46}$$

Solving for Q, L_1, and L_2, we find

$$Q = 0.703899\ , \quad L_1 = -0.101245\ , \quad L_2 = -0.02530\ . \tag{47}$$

Hence,

$$q(\tau) = 0.703899 - 0.101245e^{-3.20295\tau} - 0.02530e^{-1.22521\tau} \tag{48}$$

and

$$I(0, \mu) = \tfrac{3}{4}F\left(\mu + 0.703899 - \frac{0.101245}{1+3.20295\mu} - \frac{0.02530}{1+1.22521\mu}\right). \tag{49}$$

iv) *The fourth approximation.*—To obtain the fourth approximation we have to choose for the μ_i's the roots of $P_8(\mu)$ and the corresponding weight factors. We have

$$\left.\begin{aligned} a_1 = a_{-1} = 0.362684\ ; &\quad \mu_1 = -\mu_{-1} = 0.183435\ , \\ a_2 = a_{-2} = 0.313707\ ; &\quad \mu_2 = -\mu_{-2} = 0.525532\ , \\ a_3 = a_{-3} = 0.222381\ ; &\quad \mu_3 = -\mu_{-3} = 0.796666\ , \\ a_4 = a_{-4} = 0.101229\ ; &\quad \mu_4 = -\mu_{-4} = 0.960290\ . \end{aligned}\right\} \tag{50}$$

The equation for k^2 reduces to

$$0.00543900k^6 - 0.1284982k^4 + 0.422222k^2 - \tfrac{1}{3} = 0\ , \tag{51}$$

the positive roots of which are

$$k_1 = 4.45808\ ; \quad k_2 = 1.59178\ ; \quad k_3 = 1.10319\ . \tag{52}$$

The constants Q, L_1, L_2, and L_3 were found to be

$$\left.\begin{aligned} Q = 0.706920\ ; &\quad L_1 = -0.083921\ ; \\ L_2 = -0.036187\ ; &\quad L_3 = -0.009461\ . \end{aligned}\right\} \tag{53}$$

Accordingly,

$$q(\tau) = 0.70692 - 0.08392e^{-4.45808\tau} - 0.03619e^{-1.59178\tau} - 0.00946e^{-1.10319\tau} \tag{54}$$

and

$$I(0,\mu)=\tfrac{3}{4}F\left(\mu+0.70692-\frac{0.08392}{1+4.45808\mu}-\frac{0.03619}{1+1.59178\mu}-\frac{0.00946}{1+1.10319\mu}\right). \quad (55)$$

In Tables 1 and 2 we have tabulated the functions $q(\tau)$ and $I(0,\mu)/F$ according to our second, third, and fourth approximations. It is also seen that, in agreement with our

TABLE 1

THE FUNCTION $q(\tau)$ DERIVED ON THE BASIS OF THE SECOND, THIRD, AND FOURTH APPROXIMATIONS (EQS. [42], [48], AND [54])

τ	$q(\tau)$			τ	$q(\tau)$		
	Second Approximation	Third Approximation	Fourth Approximation		Second Approximation	Third Approximation	Fourth Approximation
0.00	0.5774	0.5774	0.5774	0.90	0.6743	0.6898	0.6933
.05	.5883	.5938	.5974	1.0	.6778	.6924	.6954
.10	.5982	.6080	.6139	1.2	.6831	.6959	.6987
.15	.6072	.6202	.6274	1.4	.6867	.6982	.7008
.20	.6154	.6307	.6386	1.6	.6891	.6997	.7024
.25	.6228	.6398	.6479	1.8	.6907	.7008	.7035
.30	.6295	.6477	.6557	2.0	.6918	.7016	.7044
.35	.6355	.6544	.6621	2.2	.6925	.7021	.7050
.40	.6410	.6603	.6676	2.4	.6930	.7025	.7055
.50	.6505	.6698	.6761	2.6	.6933	.7028	.7058
.60	.6583	.6770	.6823	2.8	.6936	.7031	.7064
.70	.6647	.6824	.6870	3.0	.6937	.7033	.7065
0.80	0.6699	0.6866	0.6905	∞	0.6940	0.7039	0.7069

TABLE 2

THE LAWS OF DARKENING GIVEN BY THE SECOND, THIRD AND FOURTH APPROXIMATIONS (EQS. [43], [49], AND [55])

μ	$I(0,\mu)/F$		
	Second Approximation	Third Approximation	Fourth Approximation
0.0	0.4330	0.4330	0.4330
0.1	0.5224	0.5285	0.5319
0.2	0.6078	0.6164	0.6205
0.3	0.6905	0.7003	0.7046
0.4	0.7716	0.7819	0.7861
0.5	0.8515	0.8620	0.8660
0.6	0.9304	0.9410	0.9449
0.7	1.0088	1.0193	1.0231
0.8	1.0866	1.0970	1.1007
0.9	1.1640	1.1743	1.1779
1.0	1.2411	1.2513	1.2548

earlier remarks, $q(0)$ agrees with the exact value $1/\sqrt{3}$ in all our approximations. (For a proof of this relation see § 6 below.) Moreover, a comparison of the law of darkening on our fourth approximation with the exact values given in I, Table 2, indicates that in this approximation we have reached an over-all accuracy of about one part in two hundred.

6. *A proof of the Hopf-Bronstein relation* J (0) = ($\sqrt{3}/4$) F.—In the preceding section we have verified that $q(0)$ agrees with the Hopf-Bronstein value $1/\sqrt{3}$ in all the four approximations we have numerically worked out. We shall now show how this result can be demonstrated to be quite generally and rigorously true. In order to do this, we start by considering the function

$$S(\mu) = \sum_{a=1}^{n-1} \frac{L_a}{1 - k_a\mu} + Q - \mu . \tag{56}$$

According to the boundary conditions (21),

$$S(\mu_i) = 0 \qquad (i = 1, \ldots, n) . \tag{57}$$

This fact enables us to determine $S(\mu)$ explicitly. For, by multiplying equation (56) by the function

$$R(\mu) = (1 - k_1\mu)\ (1 - k_2\mu) \ldots . (1 - k_{n-1}\mu) , \tag{58}$$

we obtain a polynomial of degree n in μ which vanishes for $\mu = \mu_i$, $i = 1, \ldots, n$. Accordingly, $S(\mu)R(\mu)$ cannot differ from the polynomial

$$P(\mu) = (\mu - \mu_1)\ (\mu - \mu_2) \ldots . (\mu - \mu_n) \tag{59}$$

by more than a constant factor; and this factor can be determined by comparing the coefficients of the highest power of μ (namely, μ^n) in $P(\mu)$ and $S(\mu)R(\mu)$. In the former it is unity, while in the latter it is

$$(-1)^n k_1 k_2 \ldots . k_{n-1} . \tag{60}$$

Hence,

$$S(\mu) = (-1)^n k_1 k_2 \ldots . k_{n-1} \frac{P(\mu)}{R(\mu)} . \tag{61}$$[8]

From equations (31), (56), and (61) we now conclude that

$$q(0) = \sum_{a=1}^{n-1} L_a + Q = S(0) = (-1)^n k_1 k_2 \ldots . k_{n-1} \frac{P(0)}{R(0)} . \tag{62}$$

On the other hand, according to our definitions of the functions $P(\mu)$ and $R(\mu)$,

$$P(0) = (-1)^n \mu_1 \mu_2 \ldots . \mu_n ; \qquad R(0) = 1 . \tag{63}$$

Hence,

$$q(0) = k_1 k_2 \ldots . k_{n-1} \mu_1 \mu_2 \ldots . \mu_n . \tag{64}$$

We shall now show how the quantity on the right-hand side of equation (64) can be explicitly evaluated from the equation for the roots $k_1, \ldots, k_{n-1}$. We have (eq. [11])

$$1 = \sum_{j=1}^{n} \frac{a_j}{1 - k^2\mu_j^2} . \tag{65}$$

Multiplying this equation by the product of the factors $(1 - k^2\mu_1^2), \ldots, (1 - k^2\mu_n^2)$, we obtain

$$\left.\begin{aligned} (-1)^{n-1} \mu_1^2 \mu_2^2 \ldots . \mu_n^2 k^{2n} + \ldots . - \sum_{i=1}^{n} a_i \left(\sum_{j=1}^{n} \mu_j^2 - \mu_i^2 \right) k^2 + \sum_{i=1}^{n} \mu_i^2 k^2 \\ + \sum_{i=1}^{n} a_i - 1 = 0 ; \end{aligned}\right\} \tag{66}$$

[8] This relation can be used for a direct evaluation of the constants L_a without going through a routine solution of linear equations (21).

or, using equation (5), we have

$$(-1)^{n-1}\mu_1^2\mu_2^2 \ldots . \mu_n^2 k^{2n-2} + \ldots . + \tfrac{1}{3} = 0 . \tag{67}$$

Hence the product of the roots $k_1^2 \ldots . k_{n-1}^2$ is given by

$$k_1^2 k_2^2 \ldots . k_{n-1}^2 = \frac{1}{3\mu_1^2\mu_2^2 \ldots . \mu_n^2} \tag{68}$$

or

$$k_1 k_2 \ldots . k_{n-1} = \frac{1}{\sqrt{3}\mu_1\mu_2 \ldots . \mu_n} . \tag{69}$$

Combining equations (64) and (69), we have

$$q(0) = \frac{1}{\sqrt{3}} , \tag{70}$$

a result which is thus seen to be true in all orders of approximation. We therefore conclude that equation (70) represents an exact relation.

Finally, it is to be noted that equations (30) and (70) imply that

$$J(0) = \frac{\sqrt{3}}{4} F , \tag{71}$$

which is the well-known relation of Hopf and Bronstein.

7. *Further applications of the method.*—Our analysis in the preceding sections has demonstrated the extreme simplicity with which solutions accurate to any desired extent can be obtained. But the usefulness of the method is by no means limited to the particular problem which has been considered. Indeed, the possible applications of the method are so numerous that it would hardly be possible to consider all of them within the limits of a single paper. We shall therefore content ourselves with a brief consideration of two further standard problems in the theory of radiative transfer, postponing to a later occasion the more detailed discussion of the various solutions.

i) *The radiative equilibrium of a planetary nebula.*[9]—As was first pointed out by Ambarzumian, the equation of transfer for the "ultraviolet" radiation (i.e., radiation beyond the head of the Lyman series) consistent with Zanstra's theory is

$$\mu \frac{dI}{d\tau} = I - \tfrac{1}{2} p \int_{-1}^{+1} I \, d\mu - \tfrac{1}{4} p S e^{-(\tau_1 - \tau)} , \tag{72}$$

where p is a certain factor less than unity, τ_1 the optical thickness of the nebula for the ultraviolet radiation, and πS the amount of ultraviolet radiant energy incident on each square centimeter of the inner surface of the nebula (i.e., at $\tau = \tau_1$).

Again, in equation (72), we approximate the integral occurring on the right-hand side by a sum according to Gauss's formula for numerical quadratures. And in this manner we replace equation (72) by the system of $2n$ linear equations

$$\mu_i \frac{dI_i}{d\tau} = I_i - \tfrac{1}{2} p \Sigma a_j I_j - \tfrac{1}{4} p S e^{-(\tau_1 - \tau)} \quad (i = \pm 1, \ldots . , \pm n) , \tag{73}$$

in the nth approximation. We shall now briefly indicate how the general solution of this linear system of equations can be obtained.

[9] For earlier discussions of this problem see V. A. Ambarzumian, *Pulkovo Obs. Bull.*, No. 13, and *M.N.*, **93**, 50, 1931; also S. Chandrasekhar, *Zs. f. Ap.*, **9**, 266, 1935.

Setting

$$I_i = S\left[g_i e^{-k\tau} + h_i e^{-(\tau_1-\tau)}\right] \quad (i = \pm 1, \ldots, \pm n) \quad (74)$$

in equation (73) (where g_i, h_i, and k are constants), we find

$$g_i(1 + k\mu_i) = \tfrac{1}{2}p\Sigma a_j g_j \quad (75)$$

and

$$h_i(1 - \mu_i) = \tfrac{1}{2}p\Sigma a_j h_j + \tfrac{1}{4}p\,. \quad (76)$$

Equation (75) implies that

$$g_i = \frac{\text{constant}}{1 + \mu_i k} \qquad (i = \pm 1, \ldots, \pm n) \quad (77)$$

and that k is a root of the equation

$$1 = p\sum_{j=1}^{n} \frac{a_j}{1 - \mu_j^2 k^2}\,. \quad (78)$$

Since $p < 1$, the foregoing equation admits of $2n$ distinct roots, which occur in pairs as

$$\cdot \pm k_\alpha \qquad (\alpha = 1, \ldots, n)\,. \quad (79)$$

Considering next equation (76), we observe that h_i must be expressible in the form

$$h_i = \frac{\beta}{1 - \mu_i} \qquad (i = \pm 1, \ldots, \pm n)\,, \quad (80)$$

where β is a constant which must, in turn, be so chosen that

$$\beta = \tfrac{1}{2}p\beta\Sigma \frac{a_j}{1 - \mu_j} + \tfrac{1}{4}p\,. \quad (81)$$

Hence,

$$\beta = \tfrac{1}{4}p \frac{1}{1 - p\sum_{j=1}^{n} \frac{a_j}{1 - \mu_j^2}}\,. \quad (82)$$

Accordingly, the general solution of equation (73) can be written in the form

$$I_i = S\left\{\sum_{\alpha=1}^{n}\left[\frac{L_\alpha e^{-k_\alpha\tau}}{1 + \mu_i k_\alpha} + \frac{L_{-\alpha} e^{+k_\alpha\tau}}{1 - \mu_i k_\alpha}\right] + \frac{p\,e^{-(\tau_1-\tau)}}{4(1 - \mu_i)\left(1 - p\sum_{j=1}^{n} \frac{a_j}{1 - \mu_j^2}\right)}\right\}, \quad (83)$$

where $L_{\pm\alpha}$, $\alpha = 1, \ldots, n$, are $2n$ constants of integration. For the problem under consideration the solution (83) becomes determinate when the boundary conditions at $\tau = \tau_1$ and at $\tau = 0$ are taken into account. These are

$$I_i = I_{-i} \quad \text{at} \quad \tau = \tau_1 \quad \text{for} \quad i = 1, \ldots, n \quad (84)$$

and

$$I_{-i} = 0 \quad \text{at} \quad \tau = 0 \quad \text{for} \quad i = 1, \ldots, n\,. \quad (85)$$

The conditions (84) arise from the geometry of the problem, as was first pointed out by Milne,[10] while the conditions (85) arise from the nonexistence of any radiation incident on $\tau = 0$. The explicit form which these conditions take can be readily written down in

[10] *Zs. f. Ap.*, **1**, 98, 1930.

terms of the general solution (83). We shall not continue with this discussion further, but it is apparent how solutions of any desired degree of accuracy can be obtained in this manner.

ii) *The standard case in the theory of the formation of absorption lines.*—In a standard notation[11] the equation of transfer appropriate for this problem is

$$\mu \frac{dI_\nu}{dt_\nu} = I_\nu - \frac{(1-\epsilon)\,\eta_\nu}{2\,(1+\eta_\nu)} \int_{-1}^{+1} I_\nu d\mu - \frac{1+\epsilon\eta_\nu}{1+\eta_\nu}(a_{\nu_0} + b_{\nu_0} t_\nu) \,. \tag{86}$$

In the "standard case" the ratio η_ν of the line to the continuous absorption coefficients is assumed to be constant. Suppressing the suffix ν and introducing the quantity

$$\lambda = \frac{1+\epsilon\eta}{1+\eta} \,, \tag{87}$$

we can re-write equation (86) more conveniently in the form

$$\mu \frac{dI}{dt} = I - \tfrac{1}{2}(1-\lambda) \int_{-1}^{+1} I d\mu - \lambda\,(a + bt) \,. \tag{88}$$

In the nth approximation we replace the foregoing equation by the system of linear equations

$$\mu_i \frac{dI_i}{dt} = I_i - \tfrac{1}{2}(1-\lambda)\,\Sigma a_j I_j - \lambda\,(a+bt) \quad (i = \pm 1, \ldots, \pm n) \,. \tag{89}$$

Proceeding as before, we verify that the solution of this system appropriate for the problem on hand is

$$I_i = \sum_{\alpha=1}^{n} \frac{L_\alpha e^{-k_\alpha t}}{1+\mu_i k_\alpha} + (\mu_i b + a + bt) \quad (i = \pm 1, \ldots, \pm n) \,, \tag{90}$$

where the k_α's are the n positive roots of the equation

$$1 = (1-\lambda) \sum_{j=1}^{n} \frac{a_j}{1-\mu_j^2 k^2} \tag{91}$$

and the L_α's ($\alpha = 1, \ldots, n$) are the n constants of integration to be determined by the boundary conditions

$$\sum_{\alpha=1}^{n} \frac{L_\alpha}{1-\mu_i k_\alpha} + a = \mu_i b \qquad (i = 1, \ldots, n) \,. \tag{92}$$

Again solutions to any desired degree of accuracy can be obtained.

In conclusion, we should further like to point out that the methods developed in this paper can readily be applied also to problems in which the scattering does not take place isotropically, as, for example, in the case of scattering by free electrons. But we postpone a discussion of this problem to a later occasion.

I am indebted to Miss Frances Herman, who carried out the numerical work involved in the preparation of Tables 1 and 2.

[11] See, e.g., B. Strömgren, *Ap. J.*, **86**, 1, 1937.

ON THE ABSORPTION CONTINUUM OF THE NEGATIVE OXYGEN ION

RUPERT WILDT AND S. CHANDRASEKHAR
Leander McCormick Observatory and Yerkes Observatory
Received May 23, 1944

ABSTRACT

A new determination of the electron affinity of oxygen (3.07 e.v.) suggests that the ionization continuum of O^- in the photographic ultraviolet region becomes so strong in late K and M stars that its contribution to the monochromatic absorption coefficient cannot be neglected. The influence of O^- on the Rosseland mean is insignificant. A discontinuity in the spectra of M giants, first observed by Lindblad, is tentatively identified with the absorption edge of O^- near λ 4050. The theoretical strength of the Lindblad discontinuity depends on the abundance ratio of atomic oxygen to atomic hydrogen, which in M stars varies with the pressure-sensitive shift of the dissociation equilibrium of the several hydrides and oxides. The result is a positive absolute magnitude effect for the Lindblad discontinuity. The differential of free-oxygen abundance implied by Lindblad's spectrophotometric observations agrees as to order of magnitude with that predicted by Russell from the dissociation equilibrium in giant and dwarf stars of the oxygen branch.

The stability of the negative ion of atomic oxygen has long been known from its frequent appearance in the mass spectrograph. From an analysis of experiments on electron collisions in molecular oxygen, W. W. Lozier[1] assigned to the oxygen atom an electron affinity of 2.2 ± 0.2 e.v. This figure warranted the conclusion that the negative oxygen ion could be dismissed as of little consequence for the continuous absorption coefficient of stellar atmospheres. Recently D. T. Vier and J. E. Mayer[2] have announced a considerably higher value for the electron affinity of oxygen, viz., 3.07 ± 0.08 e.v. The authors are unable to advance any explanation of the divergence of this figure from Lozier's smaller one. However, they place great confidence in their experimental method, which had previously been applied, by Mayer and several collaborators, to the various halogens and had given consistent results. Accepting the verdict of Vier and Mayer, it appears that in the late-type stellar atmospheres the continuous absorption in the photographic ultraviolet region contributed by the negative oxygen ions approaches that of the negative hydrogen ions and may even overtake the latter for the M stars. This surmise rests on a comprehensive discussion of the structure and of the absorption coefficient of O^- given by D. R. Bates and H. S. W. Massey.[3] The following remarks are necessarily of a tentative nature and are mainly intended to stress the astrophysical importance of a more detailed study of the negative oxygen ion.

The ground state of O^- has the configuration $(1s)^2(2s)^2(2p)^5$ and is a $^2P^o$ term. Lozier's experiments and later ones by H. D. Hagstrum and J. T. Tate[4] furnished evidence of the existence in O^- of a stable excited state closely adjacent to the ionization continuum. The nature of this state, whose configuration may be either $(1s)^2(2s)^2(2p)^6$ or $(1s)^2(2s)^2(2p)^4(3s)$, has been debated at length by Bates and Massey. Although they could not decide between the two possibilities, they favor the second assumption. For the computation of the ionization equilibrium in first approximation the existence of this excited state may be disregarded. The Saha equation for O^- then reads:

$$\log_{10}\frac{p_O \cdot p_e}{p_{O^-}} = -3.07\,\frac{5040}{T} + 2.5\log_{10}T - 0.48 + \log_{10}\frac{2\cdot 9}{6}.$$

[1] *Phys. Rev.*, **46**, 268, 1932.
[2] *J. Chem. Phys.*, **12**, 28, 1944.
[3] *Phil. Trans. R. Soc.*, A, **239**, 269, 1943.
[4] *Phys. Rev.*, **59**, 354, 1941.

The last two terms practically cancel, 9 and 6 being the statistical weights in the ground state of O and O^-, respectively. Writing the Saha equation for H^- with L. R. Henrich's[5] new value of the electron affinity,

$$\log_{10}\frac{p_H \cdot p_e}{p_{H^-}} = -0.75\,\frac{5040}{T} + 2.5\log_{10} T + 0.12\,,$$

the abundance ratio of the negative ions of oxygen and hydrogen is found to be

$$\log_{10}\frac{p_{O^-}}{p_{H^-}} = \log_{10}\frac{p_O}{p_H} + 2.32\,\frac{5040}{T} + 0.12 = \log_{10} A + B(T)\,.$$

The abundance ratio A (by numbers of atoms) is not known with great accuracy, but $A = 10^{-3}$ may be regarded as a conservative estimate.[6] Strictly speaking, A is not the abundance ratio of oxygen to hydrogen, as commonly understood, but the ratio of atomic oxygen to atomic hydrogen. This distinction becomes important at the lowest temperatures encountered in stellar atmospheres, at which the numbers of free atoms are appreciably reduced by molecular association. The table below gives for two different values of A the $\log_{10}(p_{O^-}/p_{H^-})$ and reveals how with decreasing temperature the abundance of O^- overtakes that of H^-, equality being attained approximately at $T = 4000°$ K with $A = 10^{-3}$, and even at solar temperature, on the perhaps rather extreme assumption of $A = 10^{-2}$. It should be noted that this effect is independent either of the electron pressure or of the total pressure but that it is a function of A and T only.

$5040/T$	0.6	0.8	1.0	1.2	1.4	1.6	1.8	2.0
$T°$ K	8400	6300	5040	4200	3600	3150	2800	2520
$B(T)$	+1.51	+1.98	+2.44	+2.90	+3.37	+3.83	+4.30	+4.76
$\log_{10}\frac{p_{O^-}}{p_{H^-}}$ $A=10^{-3}$	−1.49	−1.02	−0.56	−0.10	+0.37	+0.83	+1.30	+1.76
$\log_{10}\frac{p_{O^-}}{p_{H^-}}$ $A=10^{-2}$	−0.49	−0.02	+0.44	+0.90	+1.37	+1.83	+2.30	+2.76

Figure 1 reproduces the absorption coefficients (absorption cross-sections per ion) of H^- and O^- according to Henrich and to Bates and Massey, respectively. In O^- the existence or otherwise of a stable excited state belonging to the configuration $(1s)^2(2s)^2(2p)^4(3s)$ has a pronounced influence on the processes of electron capture by the oxygen atom and of photoelectric ionization of the negative ion. For details the memoir of Bates and Massey should be consulted. They give two curves for the absorption coefficient, marked A and B, corresponding to different assumptions as to the nature of the excited state. As their computations were based upon an electron affinity of 2.2 e.v., it was necessary to transform their results to the new value of 3.07 e.v., using formula (19) of their paper. Since the original data were available only in the form of graphs, no great accuracy can be claimed for this procedure, but Figure 1 is believed to be sufficiently illustrative. Approaching the ionization limit of O^- (near λ 4050) from the ultraviolet, the absorption coefficient tends to zero in case A, while it remains finite in case B (the original graph B contradicts the statement, made by Bates and Massey in the text, that the absorption cross-section tends to infinity as the frequency tends to the value at the ionization limit; but the origin of this discrepancy remains obscure). Hence, in case B we would expect to observe in stellar spectra near λ 4050 a rather conspicuous discontinuity not unlike the one at the Balmer limit, provided that the fraction p_{O^-}/p_{H^-} is much greater than 1—say, perhaps, greater than 5. In case A the rise of the O^- curve toward ultraviolet would

[5] *Ap. J.*, **99**, 59, 1944.

[6] A. Unsöld, *Zs. f. Ap.*, **21**, 76, 1941.

reduce the decline of the H^- curve, and at a short distance from the ionization limit a strong absorption continuum would result for, say, p_{O^-}/p_{H^-} greater than 10, i.e., at temperatures lower than about 3000° K. These inequalities are subject to a moderate upward revision, because Henrich's absorption coefficient of H^- is believed to be systematically too small from λ 4000 toward the ultraviolet. The physical mechanism distinguishing case *B* is a resonance phenomenon arising when a $(2p)^4(3s)^2P$ level of O^- exists with zero binding energy relative to the ^3P normal state of the oxygen atom. Whether or not this state of affairs actually prevails in the negative ion is of no great consequence for the interpretation of M-type spectra, as proposed below. The principal difference con-

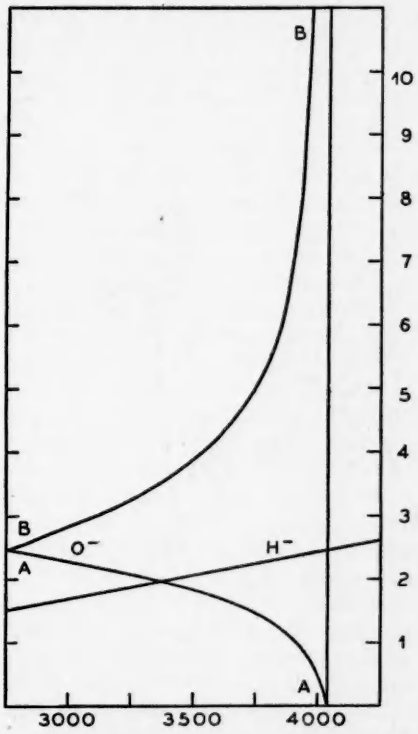

FIG. 1.—Ordinates: absorption cross-sections per ion; H^- unit 10^{-17} cm², O^- (*A* and *B*) unit 10^{-18} cm². Abscissas: angstrom units.

sists in the greater relative abundance of oxygen required in order to produce the O^- continuum in case *A*, for which, moreover, the absorption edge at λ 4050 would be less sharply defined than in case *B*.

B. Lindblad[7] made a spectrophotometric comparison between λ 5100 and λ 3700 of the two M stars HD 95735, dM2, and HD 120933, gM2. His monochromatic magnitude differences (including an arbitrary zero-point correction of 0.12 mag.) are plotted in Figure 2 on a $1/\lambda$ scale, and some similar data by Y. Öhman[8] are added to cover completely the blue-green region of the spectrum. This permits the disturbing influence of

[7] *Stockholm Obs. Ann.*, **12**, No. 2, 1935.

[8] *Stockholm Obs. Ann.*, **12**, No. 8, 1936.

the MgH bands in the dwarf to be eliminated. A straight line is drawn through Öhman's undisturbed points, representing the relative spectrophotometric gradient, namely,

$$0.921\,\frac{d\,(m_d - m_g)}{d\,\frac{1}{\lambda}} = \frac{c_2}{T_d} - \frac{c_2}{T_g} = -0.55\,.$$

A parallel translation of Öhman's gradient, so as to fit Lindblad's points near λ 4500, reveals a strong absorption continuum in the giant, extending from about λ 4100 far into

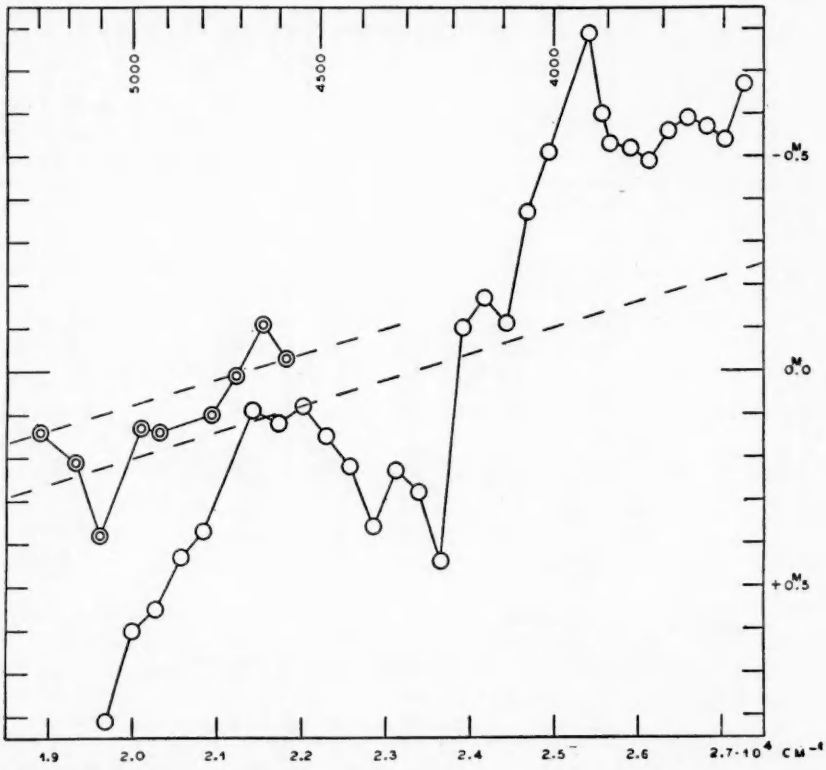

FIG. 2.—Ordinates: magnitude differences (dM2−gM2), according to Lindblad (*op. cit.*, Table 6, represented by single circles) and to Öhman (*op. cit.*, Table 6, represented by double circles). Abscissas: wave numbers (cm^{-1}).

the ultraviolet. That this is not an isolated instance is qualitatively demonstrated by a series of low-dispersion spectrograms of 12 M dwarfs and 16 M giants, which were obtained with quartz optics at the aluminized 60-inch Mount Wilson reflector.[9] On these spectrograms it was an easy matter to separate the giants from the dwarfs, on account of a striking difference in the appearance of the ultraviolet continuum. In the dwarfs the photographic density of the continuous spectrum steadily and slowly decreases from a maximum in the blue toward the ultraviolet limit; in the giants there is a marked drop between λ 4100 and λ 4000, or so, and no further recovery at shorter wave lengths down to λ 3300, where the spectra fade out. From exposure ratio scales it was estimated that

[9] R. Wildt, *Ap. J.*, **84**, 335, 1936; *Mt. W. Contr.*, No. 551.

the discontinuity near λ 4000 is of the order of 0.5 mag., a figure that agrees well with Lindblad's photometry. All these spectra were photographed on infrared sensitive plates, and from the strength of the simultaneously recorded infrared maximum, near λ 8500, it was possible to estimate a crude color equivalent. Several pairs of dwarfs and giants, selected for equal apparent visual magnitude, proved to have nearly the same integrated infrared intensity but were readily distinguished by the weakness of the ultraviolet in the giants. This was taken to indicate that the surface temperatures of these pairs do not differ markedly and that a peculiar absorption mechanism located in the atmospheres of the giants is responsible for their low ultraviolet intensities. Unfortunately, similar observations of pairs of K stars were not undertaken at that time. While this sample of M stars actually investigated is admittedly small, it may be regarded as representative of the M stars at large, pending evidence to the contrary. In other words, what may be called, for sake of brevity, the "Lindblad discontinuity" and the "Lindblad continuum" are assumed to be typical features of the giant M spectra.

The relation between color and effective temperatures observed among G and F stars cannot, as yet, be predicted from theory, though steady progress in this direction has been made through the efforts of Williamson and Henrich. This problem will be even harder to solve for the K and M stars, because of purely observational difficulties. In their spectra the crowding of lines and bands makes it exceedingly difficult to define clearly what should be regarded as continuous background, but this dilemma can perhaps be circumvented by differential spectrophotometric observations of dwarfs and giants having the same spectral type. Such observations, i.e., of the very sort Lindblad and Öhman have carried out, should eliminate in the first approximation the disturbing influence of the line and band absorption and, therefore, should lend themselves to a test of the theory of the continuous absorption coefficient by way of the absolute-magnitude effects it implies. Now, according to the current theory of the atmospheric absorption coefficient, for temperatures lower than 5000° K the contribution of atomic hydrogen to the opacity becomes negligibly small and the parameter, $k_\nu/\bar{k}$, which determines the intensity distribution in the continuum, is a function only of the temperature, since for H^- both k_ν and $\bar{k}$ are proportional to the electron pressure. Consequently, the relative spectrophotometric gradient, dwarf *minus* giant, should be a function only of the difference of the effective temperatures, which are marked among the K stars and seem to disappear at M0, according to G. P. Kuiper's[10] study of the temperature scale. On the other hand, the difference in color temperature between K dwarfs and giants to be expected on the current theory ought to be small, on account of the slight dependence of the variation of $k_\nu/\bar{k}$ with temperature in the relevant range. But the observed differences in color temperatures between dwarfs and giants are considerable for late G and K stars, and this throws some doubt on the adequacy of the current theory, operating with H^- as the only source of continuous absorption.

With the recognition of the Lindblad discontinuity as a typical feature of the M giants in general, it becomes practically certain that another absorption mechanism besides the photoelectric ionization of H^- must be introduced for these stars into the theory of the continuous spectrum. The tentative identification of this new agent with the negative ion of atomic oxygen seems natural at this stage. While the final test of this conjecture must await a quantum mechanical analysis of the structure of O^- going beyond the work of Bates and Massey, some astrophysical consequences of the proposed identification will be taken up here. With H^- and O^- operating jointly, the parameter $k_\nu/\bar{k}$ would still be independent of the electron pressure. Therefore, no Lindblad discontinuity could appear in the giants, because the dwarfs and giants of the early subdivisions of class M are supposed to have nearly the same effective temperatures, unless oxygen were much more abundant in the giants than in the dwarfs. The giants are now widely held to be a cosmogonically distinctive group of stars, and there is no a priori reason to reject the hy-

[10] *Ap. J.*, **88**, 429, 1938.

pothesis that they might be richer in oxygen than the main-sequence stars. Fortunately, there is no need to rely on this rather special hypothesis. It is mentioned here merely because a true cosmic difference in abundance may be superimposed upon, and hard to disentangle from, an apparent difference in the abundance of free atomic oxygen, such as is bound to result from the greater amount of oxygen that is locked up in molecules in the M dwarfs, in consequence of their higher mean atmospheric pressure. This effect is very conspicuous in H. N. Russell's[11] diagrams illustrating the shift of the dissociation equilibrium as function of the atmospheric temperature, both for giant and for dwarf stars. According to Russell's graphs, the abundance factor $A = p_O/p_H$, as used above, is constant in the giants at temperatures higher than 2500° K. But in the dwarfs, A has fallen at 2800° K to one-tenth of its value at 3150° K, above which temperature it is constant. This means that with decreasing temperature the giants become relatively richer in free atomic oxygen. Conversely, the dwarfs become poorer in negative oxygen ions. Of course, Russell's figures are subject to change on altering the composition of the model atmosphere, but the qualitative characteristics of his diagrams are expected to be conserved. The differential of oxygen abundance required to produce a Lindblad discontinuity of 0.5 mag. can be estimated with the help of G. Burkhardt's[12] table, which gives the monochromatic flux averaged over the stellar surface as function of the two variables $k_\nu/\bar{k}$ and $h\nu/kT_e$. Regarding case A, with $T_e = 3150°$ K and $A = 10^{-3}$ for the dwarfs, it seems that A would have to be larger by a factor of the order of 5 in the giants. For case B the absorption of O^- near the ionization limit is so much stronger that a smaller A could be chosen for the dwarfs, and yet in the giants the required oxygen abundance would have to be greater by a small factor only, perhaps of the order of 2. No great precision can be attained in making these estimates, among other reasons because the choice of the correct value for $\bar{k}$ is a matter of some difficulty, as will be explained presently. Notwithstanding that, it appears safe to say that the interpretation of the Lindblad discontinuity proposed here does not imply an unreasonably large difference in oxygen abundance between giants and dwarfs. Incidentally, it may be noted that the influence of O^- on the computation of $\bar{k}$ is quite insignificant, since the frequency dependent weight factor entering the Rosseland mean is small in the ultraviolet.

In order to make the estimates just described, $\bar{k}$ was computed for $T = 3150°$ K by adding the absorption coefficients for the bound-free (Henrich) and free-free (Wheeler and Wildt) transitions of H^-, with the result $\bar{k} = 0.95 \cdot 10^{-18}$ cm^2 (this is the Rosseland mean of the absorption cross-section, not the mass absorption coefficient). This figure is predominantly determined by the high transparency to the infrared side of the ionization limit of H^-, as will be apparent from the nature of the Rosseland mean as a harmonic mean. Specifically, $k_\nu/\bar{k}$ assumes the values of 7.5 and 0.15 at the frequencies 7000 and 6000 cm^{-1}, respectively, which would entail an immensely strong emission on the infrared side of the ionization limit of H^-. Burkhardt's table does not extend beyond $k_\nu/\bar{k} = 0.5$, but it can be inferred that near λ 16,000 the energy-curve of the M stars should rise steeply toward the infrared by many magnitudes. This conclusion is certainly contradicted by the few known infrared energy-curves of late-type stars,[13] though the resolving-power of these measurements was rather small. This, then, brings to light a serious deficiency of the present theory of the continuous absorption coefficient, as far as the low-temperature range is concerned. There does not seem to exist any grave "infrared problem" at solar temperatures. For the contribution of the free-free transitions of H^- varies ever so little with temperature, while the absorption from bound-free transitions mounts rapidly with falling temperature. In order to stop this infrared leakage at low temperatures, some new absorption mechanism affecting primarily the infrared would have to be found. Further

[11] *Ap. J.*, **79**, 281, 1934; *Mt. W. Contr.*, No. 490.

[12] *Zs. f. Ap.*, **13**, 56, 1936.

[13] C. G. Abbot, *Ap. J.*, **69**, 293, 1929.

discussion of this point would go beyond the scope of this paper, but it is well to remember that the free-free absorption coefficient of H^- has been derived from an approximate theory.

Finally, the splitting of the giant branch into two parallel sequences—the oxygen and the carbon stars—is of particular interest in the context considered here. The study of the low-dispersion spectra of 16 carbon stars[9] disclosed an important difference between the spectral classes R and N as regards their ultraviolet continuum, which is very strong in the former and excessively weak in the latter (for the prototype, 19 Piscium, it was estimated from exposure ratio scales that the energy-curve drops by about 2.5 mag. near λ 4000).[14] These observations lead to some speculations on the atmospheric opacity of late-type stars, in so far as it is caused by continuous molecular absorption. It is now necessary to re-examine this situation with reference to the continuous absorption produced by negative ions, but such an attempt would be unprofitable at this time for lack of many requisite data. The negative ion of atomic carbon appears with great strength in the mass spectrograms. Quantum mechanical estimates have indicated for carbon an electron affinity of about 1 e.v. However, this result may be off by 100 per cent or more, as experience from similar computations for other negative ions has taught.

[14] A further factor which may be of importance in this connection is the systematic difference of temperature which appears to exist between the R and the N stars (cf. P. C. Keenan and W. W. Morgan, *Ap. J.*, **94**, 501, 1941).

STUDIES OF FAINT B-TYPE STARS. II*

DANIEL M. POPPER[1]
McDonald Observatory and Berkeley, California
Received April 14, 1944

ABSTRACT

Radial velocities and spectral types are listed for 150 B-type stars between magnitudes 8 and 12. The combined observations of this paper and of *McDonald Observatory Contribution* No. 35 are shown graphically.

The observations of B-type stars published in *McDonald Observatory Contribution* No. 35[2] have been extended by obtaining spectrograms of 150 additional stars, making a total of 268 stars. An attempt has been made to distribute the observations uniformly along the available portion of the Milky Way (see Figs. 1–3). The improvement in distribution over that of the first paper alone is due in a large measure to lists of B stars from unpublished sections of the *Henry Draper Extension*, made available through the courtesy of Dr. Shapley, Dr. Bok, and Mrs. Mayall, of the Harvard College Observatory. These lists include stars in three regions of galactic longitude: 180°–190°, 320°–340°, and 20°–40°. A few stars were chosen from the Cape catalogue of faint stars.[3] A second spectrogram was obtained for each of 13 stars observed by O'Keefe.[4] The remaining sources of material are listed in paper I.

Two spectrograms, having a dispersion 76 A/mm at $H\gamma$, were obtained for each star, with the exception of 24 stars with poor lines and of 2 stars for which insufficient observing time was available. The average exposure time for a star of given magnitude was decreased by hypersensitization of the emulsion.

MAGNITUDES

Although material has been obtained for the determination of magnitudes and colors of the stars, as well as additional material for some of the stars in paper I, I have not had the opportunity of reducing it. This material consists of photographic and photovisual plates taken with the 6-inch UV camera and of the spectrograms themselves, from which colors are to be determined (see paper I for a discussion). For 63 of the stars of this paper, however, photographic magnitudes and colors had been obtained by Seyfert in the program for the earlier paper. In this sense he is a collaborator, and I wish to express my indebtedness to him. His colors are not published here, since it is desirable to combine them with the colors from the spectrograms. Reliable photographic magnitudes are also available for 25 of the remaining stars. Of these, 10 are stars from the *Bergedorfer Spektral-Durchmusterung*, while 15 magnitudes were obtained from the colors and visual magnitudes of Stebbins, Huffer, and Whitford.[5]

The magnitudes of the 43 remaining stars for which photographic magnitudes are listed in Table 2 were taken from the catalogues listing the stars as B stars or from the CPD (*Durchmusterung* stars between −20° and −36°). For these latter, corrections to

* *Contributions from the McDonald Observatory, University of Texas*, No. 92.

[1] On leave of absence for war research.

[2] Seyfert and Popper, *Ap. J.*, **93**, 461, 1941. Referred to as "I."

[3] *Catalogue of 20,554 Faint Stars*, Observatory of the Cape of Good Hope, 1939.

[4] *Ap. J.*, **94**, 353, 1941.

[5] *Ap. J.*, **91**, 20, 1940.

the magnitudes were applied as given in *Harvard Ann.*, **80**, 256, 1917. For 19 of the BD stars, only approximate visual magnitudes are available. These were obtained from the BD and are corrected according to published tables.[6]

SPECTRAL TYPES

Classification of the spectra is discussed in the earlier paper. As a check on the consistency of the spectral types, a random selection of 45 of the spectrograms of that paper was reclassified along with the spectrograms of this paper. The systematic difference averages 0.1 spectral subdivision, while the differences taken without regard to sign average 0.5 subdivision. The star HD 123884 of paper I should be classified cB9 instead of cB6.

The use of the intensity ratio of the helium lines λ 3964 and λ 4026 continues to be a useful criterion for luminosity classification on our spectrograms of stars from types B1 to B4. The explanation suggested in paper I for the relative strengthening of λ 3964 in c stars is incorrect. The true reason is probably that this line is lost in the wing of $H\epsilon$ in the spectra of main-sequence stars.

TABLE I

LUMINOSITY CLASSIFICATION ACCORDING TO MORGAN, KEENAN, AND KELLMAN

TYPE	McDONALD		
	c	c⁻	Normal
O9.5	.....	.....	I–III
B0	.....	.....	I–III
B0.5	I	II	III–IV
B1	I–II	III	V
B2	I	III	V
B3–A0	I	.....	V

An attempt is made in Table 1 to correlate the luminosity classes used here with those of Morgan, Keenan, and Kellman.[7] Blank spaces occur in the table where luminosity classes are not used in the McDonald classification. A few B0 stars were observed which belong in class V. For these the remark is entered, following Table 2, that the spectrum is similar to that of τ Sco. In these spectra the *Si* IV lines are much stronger than those of *Si* III, but the ratio of *Si* IV to *H* is considerably smaller than for normal B0 stars.

RADIAL VELOCITIES

As in paper I, a correction of −2.1 km/sec has been applied to all measured velocities in order to reduce them to the system of Moore's catalogue.[8] When the difference in velocity from two spectrograms exceeds five times the larger probable error of measurement, the comment "Velocity variable?" has been appended to Table 2. It is not implied that all the other stars have constant velocities. A few stars are common to our list and to that of Neubauer.[9] These are indicated in the remarks at the end of Table 2. They are too few in number for a statistical comparison.

[6] Pannekoek, *Pub. Astr. Inst. Univ. Amsterdam*, No. 1, 1924.

[7] *An Atlas of Stellar Spectra*, Chicago: University of Chicago Press, 1943.

[8] *Lick Obs. Pub.*, Vol. **18**, 1932.

[9] *Ap. J.*, **97**, 300, 1943.

TABLE 2

OBSERVATIONS OF B STARS

STAR	α 1900	δ 1900	l	b	m_{pg}	SPECTRUM	STAR VEL. (KM/SEC)	K-LINE VEL. (KM/SEC)	REMARKS
	Part I								
8-1454	0^h50^m1	+61° 13′	91	− 1	11.10	O7	−24eF	−54eF	
8-1105	1 1.2	+60 6	93	− 2	11.50	c⁻B2	−33dB	−12bB	
8-640	1 4.8	+59 7	93	− 3	11.50	B2.5	−12cA	−25bC	
8-1675	1 5.4	+61 23	93	0	11.80	B1	−52cA	−41cA	
8-1779	1 12.6	+61 18	94	− 1	11.90	B3	−46dD	− 8bA	R
236800	1 30.1	+59 26	96	− 2	9.58	B3	−25cC	−15dB	
236961	2 17.7	+57 1	103	− 3	9.41	B1	−34eA	+15d	
237015	2 45.0	+59 57	105	+ 2	9.05	B4	−15dA	+ 5eB	
9-274	2 52.2	+59 6	106	+ 1	11.00	B4n	−44eC	+ 4bA	
9-53	3 0.2	+58 55	107	+ 2	11.04	A2p	+28cB	Stellar	R
9-106	3 5.2	+58 34	108	+ 2	10.51	B1n	− 9eE	−30cC	
232999	4 37.0	+50 21	123	+ 4	9.77	cB2	+ 1bA	−15bB	
242926	5 16.1	+33 13	141	0	9.28	O7.5	− 8eC	− 9cC	
243780	5 21.4	+21 25	152	− 6	9.94	B3+F8	+21cB	−12bB	R
243827	5 21.7	+33 15	142	+ 1	10.89	c⁻B2	+66dC	−34e	
245770	5 32.7	+26 16	149	− 1	9.73	B1neα	+ 6dE	+ 1aC	R
246901	5 38.3	+33 29	144	+ 3	8.68	cB1+K	− 1bA	+ 2cA	R
247331	5 40.2	+25 30	151	0	8.73	B3neγ	−14dB	+19e	R
248893	5 48.0	+22 6	155	0	10.0	B0	+23cB	+12bA	
250980	5 58.1	+ 9 40	166	− 5	9.18	B2neβ	− 1cA	+ 2aB	R
251204	5 59.0	+23 24	155	+ 2	10.4	B0	+ 7dD	.....	
253021	6 5.7	+21 40	157	+ 3	10.2	B2	.... f	+33d	R
254428	6 11.2	+13 32	165	0	9.13	B0.5	+18aA	+15bB	
254577	6 11.8	+22 26	157	+ 5	9.5	B0	+18eC	− 6aB	
255191	6 14.0	+24 17	156	+ 6	10.7	cB1	+24cD	+20e	
256 .7	6 18.6	+ 8 21	170	− 1	9.72	B2eγ	+11eD	+26aB	R
256 25	6 19.1	+19 54	160	+ 5	9.70	O5.5	+38dA	+36bA	
258982	6 26.2	+ 6 14	173	0	9.6	B2	+62cF	+16cC	R
259597	6 28.1	+ 8 24	171	+ 1	8.60	B3neγ	+37fF	+19aA	
259828	6 28.8	+ 8 11	172	+ 1	11.06	B5	+11dB	+46d	
+0°1576	6 39.7	+ 0 42	179	0	9.33	O9	+41cC	+30bB	
236775	6 41.5	+ 5 42	175	+ 3	10.56	B3	+38eB	+29bA	
+0°1627	6 44.2	+ 0 50	180	+ 1	9.42	B2	+12dE	+29bD	R
+0°1638	6 45.1	+ 0 33	180	+ 1	10.03	O8n	+46eD	+49bA	
+1°1560	6 46.8	+ 1 29	180	+ 2	9.63	B2n	+24eD	+27b	
−1°1471	6 52.0	− 1 38	183	+ 2	10.13	B1	+75dA	.....	
−3°1668	6 52.9	− 3 38	185	+ 1	9.76	B3	+45cA	+23cB	
−2°1892a	6 57.4	− 2 51	185	+ 3	10.43	B3	+42cC	+27e	R
−4°1806a	7 0.1	− 4 5	186	+ 3	10.55	B3	+68dC	.....	R
−3°1746	7 2.6	− 3 56	186	+ 3	10.61	B5eγ	+65cA	.....	R
55885	7 9.8	−15 13	197	− 1	8.90	B(5)neβ	+57eA	+58cA	R
123-602	7 12.1	−14 54	197	0	10.5	B5	+33dC	+45bD	
123-1955	7 23.4	−15 11	198	+ 2	9.69	O7	+54dB	+32aB	
62413	7 38.7	−27 11	210	− 1	10.29	B4eα	+39cA	+25aA	R
63290	7 43.0	−27 41	212	0	9.46	cB1	+43aA	+25dB	

TABLE 2—*Continued*

Star	α 1900	δ 1900	l	b	m_{pg}	Spectrum	Star Vel. (Km/Sec)	K-Line Vel. (Km/Sec)	Remarks
	Part I—*Continued*								
148-732	7h56m4	−30° 27′	215	+ 1	11.3	B7	+ 6eC	.....	
148-1118	7 59.4	−31 26	217	+ 1	11.4	B4	+ 8fC	.....	
148-1662	8 3.3	−30 1	216	+ 2	11.1	B8	+20eA	Stellar	
148-2127	8 7.1	−31 49	218	+ 2	11.1	B9	+ 2cA	Stellar	
−44°4543	8 31.1	−44 41	231	− 2	10.4	B0	+44dF	.....	
172-1522	8 43.7	−45 57	233	− 1	9.45	B1	+57dF	+31e	R
172-1753	8 46.5	−44 12	232	0	9.9	B0	+27dA	.....	
−46°4786	8 53.5	−46 40	235	0	9.9	B1	+22eB	.....	
−47°4551	8 54.5	−47 21	236	0	9.0	O7	−13fB	.....	
78959	9 5.9	−43 29	234	+ 3	9.6	B0.5	+44bA	+28dD	
124448	14 8.6	−45 49	286	+13	9.7	Bp	−65aA	−46b	R
144695	16 2.0	−49 41	300	0	9.6	O9	0eF	.....	
−46°10590	16 3.4	−46 43	302	+ 2	10.2	O9	−19eE	.....	
150197	16 34.3	−47 22	305	− 2	9.32	O8	− 2cD	−33cA	
150475	16 36.1	−37 39	313	+ 4	8.60	O8.5	−22cB	− 8cC	R
151018	16 39.6	−45 42	307	− 2	9.2	B0	−48cC	.....	
151300	16 41.4	−47 0	306	− 3	9.53	O6	−47dA	.....	
180-1052	16 50.1	−43 34	310	− 2	9.21	B0	−27dB	−27bA	
155959	17 9.6	−40 46	314	− 3	9.0	B0.5	−13eC	−24bA	
156134	17 10.7	−35 27	319	0	8.50	c⁻B0.5	−22dD	+56cF	R
157-521	17 25.1	−31 16	324	0	11.0	B4	− 2eB	.....	
−33°12155	17 25.7	−33 16	323	− 1	10.0	O8	−22cC	−11d	
−34°11820	17 29.2	−34 34	322	− 3	10.8	B1	−32cB	0cB	R
−33°12242	17 29.6	−33 49	322	− 2	10.3	cB0.5	−31bA	−21cB	
−35°11760	17 31.2	−35 20	321	− 3	9.9	cB5	+ 7cB	0c	R
160730	17 36.4	−24 15	331	+ 2	10.24	O8	−72eC	.....	
−35°11892	17 38.7	−35 22	322	− 5	9.8	B3	−53eD	−24bC	
−24°13687	17 52.0	−24 49	333	− 2	10.3	B2	−22aB	− 9bC	
165049	17 59.0	−15 22	342	+ 2	8.20	c⁻B1.5	−24bB	−17aA	R
165319	18 0.3	−14 12	342	+ 2	8.40	B0	+30aC	− 9aC	R
165517	18 1.2	−25 7	333	− 4	8.70	B0	−48dF	+10cB	R
−22°12627	18 3.6	−22 21	336	− 3	10.2	B2	−10cB	.....	
166188	18 4.4	−18 13	340	− 1	9.10	B2neβ	+25cE	−16cB	R
166418	18 5.4	−16 44	341	0	8.30	B0	+36cD	−24bB	R
166611	18 6.3	−26 45	332	− 5	9.68	B1	−23dA	+17aA	
134-464	18 6.4	−14 32	343	0	9.93	B0.5	−14eB	+20e	
−20°5043	18 8.1	−20 20	338	− 3	9.7	O7	+28dA	+49e	
−20°5061	18 9.7	−20 44	338	− 3	9.6	B5n	..... f	+15cA	
167451	18 10.2	−13 36	344	0	9.00	cB1	−13bF	− 2aA	R
134-1269	18 10.5	−14 39	344	0	9.83	B1	−28cA	+ 2c	
168352	18 14.1	−17 7	342	− 2	8.90	B2	−16bA	−29aA	R
134–2076	18 14.6	−15 6	344	− 1	9.76	B0	+21dA	−12bF	
168607	18 15.5	−16 25	343	− 2	9.73	cB8eγ	−30bF	+ 2cF	R
168625	18 15.5	−16 25	343	− 2	9.55	cB2	− 4bA	−13dA	
−20°5108	18 16.4	−20 7	340	− 4	9.4	B0.5	+17cA	+13aA	

TABLE 2—*Continued*

Star	α 1900	δ 1900	l	b	m_{pg}	Spectrum	Star Vel. (Km/Sec)	K-Line Vel. (Km/Sec)	Remarks
				Part I—*Continued*					
134-2608	18h18m2	−14° 12′	345	− 2	10.37	B0.5	+23cA	− 6bA	
169754	18 21.1	−11 25	348	− 1	9.50	B0.5	+11dF	+17d	R
230373	18 55.9	+12 59	14	+ 2	10.65	B7n	+ 1dD	− 4cA	
+22°3559	18 57.5	+22 26	22	+ 6	(10.4)	B3	−19aA	+ 6bB	
177812	19 1.1	+ 3 6	5	− 3	9.10	cB1.5	+40bC	+14aB	R
+24°3632	19 1.8	+24 39	24	+ 7	(10.4)	cB8	0eE	Stellar	
230705	19 2.5	+18 29	19	+ 4	11.26	B3	+ 5cA	−11bA	
230780	19 4.7	+14 58	16	+ 2	10.8	B5	−26dD	−60e	R
231564	19 24.8	+12 22	16	− 4	10.8	c−B1	+25dE	+28aA	
+23°3730	19 36.0	+23 47	27	0	(9.2)	cB8	+17bA	Stellar	
+22°3781	19 38.8	+23 2	27	− 1	(10.0)	O9	+ 4cA	− 8e	
+22°3782	19 38.9	+23 3	27	− 1	(9.0)	O9	+20cA	.....	
+23°3759	19 41.0	+23 48	28	− 1	(9.1)	B0	−21eB	+26cB	
+25°3952	19 41.5	+25 7	29	− 1	(10.0)	O8	+ 7dC	.....	
+29°3732	19 41.9	+30 1	33	+ 2	(9.7)	B2	+ 5eA	+ 4c	
+22°3836	19 46.8	+22 35	28	− 3	(9.3)	cB1	+ 4bB	+ 9aA	
+29°3842	19 56.6	+30 6	35	− 1	(10.4)	B1	+14bC	−12aC	R
+21°4017	19 57.1	+21 59	28	− 5	(10.4)	B0	+30dA	−15aB	
+28°3598	19 59.1	+28 25	34	− 2	(10.0)	B0	−13bD	+ 1bC	R
227415	20 0.1	+35 16	40	+ 1	10.00	B0	−25dE	−22bA	R
+31°3921	20 0.3	+31 52	37	− 1	(8.7)	B0.5	+34cC	− 7dA	
227607	20 2.0	+36 14	41	+ 2	10.00	B3	+ 5dC	− 8bB	R
227704	20 2.9	+34 38	39	+ 1	8.43	B0	−24bB	−28bA	
+19°4293	20 3.7	+19 12	27	− 8	(10.5)	B8	−20eD	Stellar?	
227836	20 4.3	+35 50	41	+ 1	9.60	Bve	−25aA	−37cC	R
+23°3915	20 6.9	+23 27	31	− 7	(9.7)	B5n	+26eD	− 6c	
+29°3944	20 9.8	+29 24	36	− 3	(10.0)	B5	−10dA	.....	
228461	20 10.4	+37 56	43	+ 1	9.46	B1	+ 6cB	−26bB	
229049	20 17.4	+38 42	44	0	10.36	B0	−17bA	− 3bB	R
40-1659	20 44.3	+45 14	53	+ 1	11.10	B4	−13dC	− 6aA	
18-390	21 17.1	+59 34	67	+ 7	10.80	B2	−49dC	−39e	
235618	21 43.5	+54 53	66	+ 1	10.05	B1	− 5dA	.....	
240171	22 58.5	+56 36	76	− 3	9.1	B2.5	−19cB	−12cA	
240311	23 24.9	+59 3	80	− 2	10.70	B6	−12dA	−42e	R
				Part II					
8-1680	1 5.8	+61 47	93	0	11.10	B(5)neα	− 6e	−37d	R
8-1720	1 8.4	+61 25	93	0	11.20	B(4)neα	−69f	.....	R
237056	2 55.0	+57 7	108	0	9.17	B1neα	−21e	−26c	
232774	3 12.9	+51 42	113	− 4	9.17	B(5)n	....f	+ 8c	
246579	5 36.7	+33 23	149	− 3	9.95	B5n	....f	.....	

TABLE 2—*Continued*

STAR	α 1900	δ 1900	l	b	m_{pg}	SPECTRUM	STAR VEL. (KM/SEC)	K-LINE VEL. (KM/SEC)	REMARKS
	Part II—*Continued*								
247795	5^h42^m6	+31° 48′	145	+ 3	9.38	B(4)neβ	....f	+28d	R
248434	5 45.7	+21 31	155	− 1	10.5	B(5)neγ	−63f	−18c	R
250163	5 54.4	+19 11	158	− 1	10.2	Bneβ	....f	.....	R
251696	6 0.9	+23 12	155	+ 3	10.1	B5n	+58f	+36c	
253339	6 6.9	+24 4	155	+ 4	10.6	B3neβ	....f	+49e	R
264600	6 44.2	+ 6 19	175	+ 4	10.90	Bn	....f	+35c	R
−5°1971	7 2.4	− 5 4	187	+ 3	10.18	B(5)neβ	+69f	+23c	R
+1°1699	7 2.7	+ 1 53	181	+ 6	(9.3)	B4n	+99e	+13c	
62780	7 40.5	−26 43	210	− 1	8.96	Bneβ	+73e	+44c	R
63150	7 42.3	−36 16	219	− 5	8.7	Bneβ	....f	.....	
64639	7 49.7	−24 33	210	+ 3	9.59	Bneγ	....f	.....	R
172-880	8 37.5	−45 44	233	− 2	9.63	Bneβ	+78f	.....	R
80834	9 16.9	−41 45	234	+ 6	10.0	Bneγ	....f	+20d	R
−40°10757	16 42.3	−40 38	311	+ 1	9.8	B(3)n	....f	.....	
−25°12556	17 54.2	−25 14	333	− 2	11	B1	+19e	+ 8d	R
−25°12786	18 2.5	−25 22	333	− 4	10.8	B5n	−42f	.....	
167722	18 11.4	−19 46	339	− 3	9.20	B3n	− 3f	− 3c	R
134-1627	18 12.2	−13 53	344	0	10.91	cB4	− 8d	.....	R
+19°4266	19 59.1	+19 42	27	− 7	(10.5)	Bn	....f	− 9b	
228041	20 6.2	+35 12	40	0	9.20	Bneβ	....f	−22b	R
+32°3749	20 9.8	+32 15	39	− 2	(10.4)	O(8)neγ	....f	.....	R

NOTES TO TABLE 2

8-1779 Velocity variable?

9-53 Type cA2 from *H* and *Ca* II; but *Si* II, *Fe* II, and *Mg* II not visible.

243780 Composite spectrum. The continuous spectra of the two stars appear to be approximately equal at λ 4250. Color index approximately +1.2 mag. Velocity mainly from F-type lines.

245770 MWC 507.

246901 Composite spectrum. The continuous spectra appear to be approximately equal at λ 4600. Color index about +0.9 mag. Velocity from both B- and K-type lines.

247331 MWC 513.

250980 MWC 518.

253021 Double lines.

256577 MWC 525.

258982 Velocity variable?

+0°1627 Velocity variable?

−2°1892a 4′ north of −2°1892.

−4°1806a 3′ sf −4°1806.

−3°1746 MWC 544.

55885 MWC 550.

62413 MWC 568.

172-1522 Velocity variable?

124448 See *Pub. A.S.P.*, **54,** 160, 1942, for a brief description of the spectrum of this star. *Hδ* and *Hγ*, if present, must be weaker than 0.2 equivalent angstroms. This upper limit was set by comparing spectrograms of HD 124448 and of ρ Leonis with a dispersion of 26 A/mm at *Hγ*. E. G. Williams has published intensities of numerous lines in the spectrum of ρ Leonis (*Ap. J.*, **83,** 83, 1936). The radial velocity is based on 5 spectrograms.

150475 Magnitude from Stebbins, Huffer, and Whitford.

156134	Magnitude from Stebbins, Huffer, and Whitford.
−34°11820	Velocity variable?
−35°11760	Probable *Hα* emission.
165049	Magnitude from Stebbins, Huffer, and Whitford. Velocities by Neubauer: stellar, -17 ± 1; K line, −10.
165319	Velocity variable? Magnitude from Stebbins, Huffer, and Whitford.
165517	Velocity variable? Magnitude from Stebbins, Huffer, and Whitford.
166188	Velocity variable? MWC 282. Magnitude from Stebbins, Huffer, and Whitford. Velocity by Neubauer: -23 ± 2.
166418	Magnitude from Stebbins, Huffer, and Whitford. Velocities by Neubauer: stellar, $+6\pm2$; K line, −20.
167451	Velocity variable? Magnitude from Stebbins, Huffer, and Whitford. Velocity by Neubauer: -5 ± 4 (var).
168352	Magnitude from Stebbins, Huffer, and Whitford. Velocities by Neubauer: stellar, -28 ± 2; K line, −30.
168607	MWC 291. This star and HD 168625 are the very red stars near M 17 (*Pub. A.S.P.*, **52**, 401, 1940).
169754	Magnitude from Stebbins, Huffer, and Whitford. Velocity by Neubauer: $+35\pm16$ (var).
177812	Magnitude from Stebbins, Huffer, and Whitford.
230780	Velocity variable? This star was erroneously announced to have *Hα* in emission (MWC 613). It should be removed from the list in *Ap. J.*, **98**, 153, 1943.
+29°3842	Velocity variable?
+28°2398	Velocity variable?
227415	Spectrum similar to that of τ Sco. Magnitude from Stebbins, Huffer, and Whitford.
227607	Velocity variable?
227836	MWC 628. Spectrum peculiar and variable. See note in *Ap. J.*, **98**, 153, 1943. Magnitude from Stebbins, Huffer, and Whitford.
229049	Spectrum similar to that of τ Sco.
240311	*Si* II lines strong.
8-1680	*He* lines sharp. MWC 421.
8-1720	MWC 422.
247795	MWC 514.
248434	MWC 515.
250163	MWC 517.
253339	MWC 522.
264600	Probable *Hα* emission. The region of *Hα* is not included on our spectrogram.
−5°1971	MWC 543.
62780	MWC 573.
64639	MWC 576.
172-880	MWC 578.
80834	MWC 580.
−25°12556	Insufficient time to obtain a second spectrogram.
167722	Magnitude from Stebbins, Huffer, and Whitford.
134-1627	Insufficient time to obtain a second spectrogram.
228041	MWC 330. Magnitude from Stebbins, Huffer, and Whitford.
+32°3749	MWC 631. The only lines visible are *He* II 4686 and *C* III + *O* II 4650.

THE TABLE OF OBSERVATIONS

The table of observations (Table 2) is divided into two parts. In Part I are listed data for the 124 stars for which two (in a few cases more) spectrograms have been obtained. Part II contains data for 26 additional stars with only one spectrogram per star. Nearly all the stars of Part II have poor lines.

The first column of the table gives the designation of the star. For most of the stars this is the HD, BD, or CoD number. HD numbers larger than 225300 are to be found in the *Henry Draper Extension* (*Harvard Ann.*, Vol. **100**). The CoD stars south of −40° are listed as B stars in the Cape catalogue of faint stars.[3] The rest of the BD and CoD stars are from unpublished portions of the *Henry Draper Extension*. Hyphenated designations refer to Selected Area and star numbers as found in the *Bergedorfer Spektral-Durchmusterung* (northern declinations) or in the *Potsdamer Spektral-Durchmusterung* (southern declinations). The 1900 positions of the BD and CoD stars are the BD and CoD positions corrected for precession. The positions for the other stars were taken from

the catalogues listing them as B stars. Galactic co-ordinates (fourth and fifth columns) were interpolated from the Lund Observatory table.

The reliable photographic magnitudes, probably good to 0.1 mag. for the most part, are listed to two decimals. These include Seyfert's observations, the Bergedorf stars, and

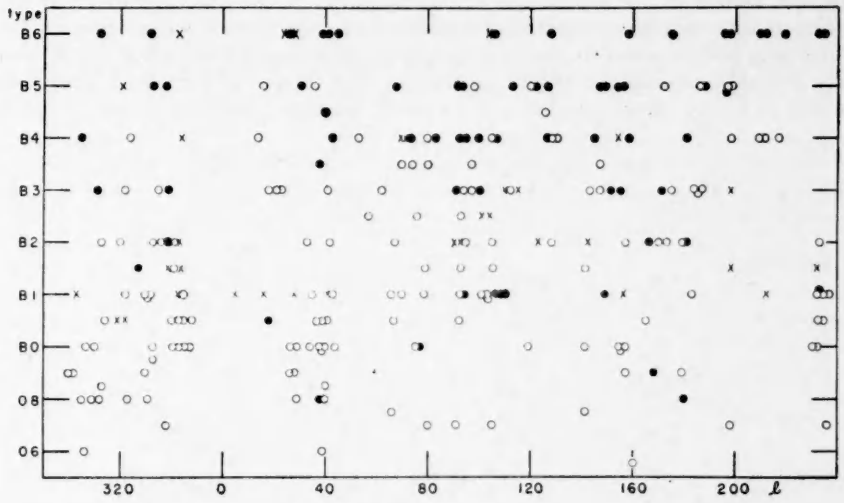

FIG. 1.—Distribution of spectral types of B stars. ○ = main-sequence stars; ● = n stars; × = c stars. Unclassified Bn stars and c stars later than B5 are shown at B6.

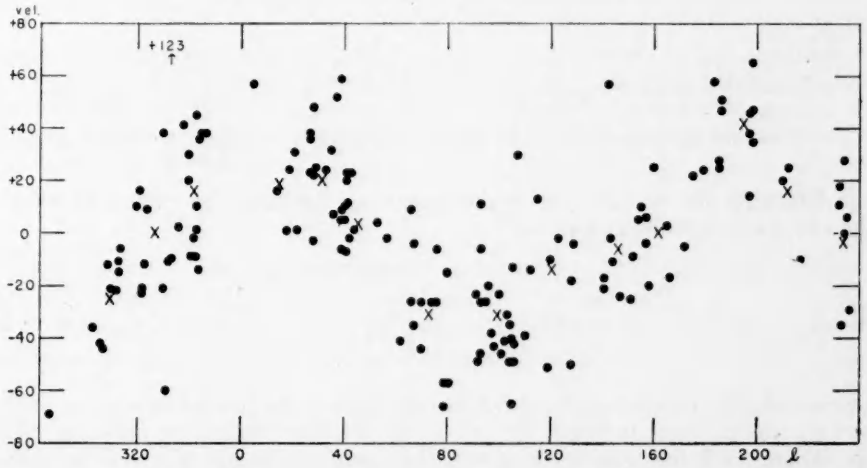

FIG. 2.—Stellar radial velocities corrected for the sun's motion and for $\cos^2 b$. × = normal points

stars observed by Stebbins, Huffer, and Whitford. A zero has been arbitrarily added in the second decimal place for stars of the last two groups (see the discussion of magnitudes above). Magnitudes in parentheses are adjusted visual magnitudes from the BD. The remaining magnitudes, given to 0.1 mag., are photographic magnitudes from the *Henry Draper Catalogue* and the *Extension* or from the *Potsdamer Spektral-Durchmusterung* or are corrected values from the CPD.

The spectral types are listed in the seventh column. The Greek letter appended to the type of a Be star indicates the highest member of the Balmer series visible in emission. The radial velocities given in the eighth (stellar) and ninth (K-line) columns are the weighted means of the measures decreased by 2.1 km/sec. The small letters following the velocities are indications of the "quality" of the spectrograms and of the K line. The quality of a spectrogram is proportional to the sum of the weights of the lines and inversely proportional to the probable error of measurement. For the K lines the quality depends only on the weight of the line. The letter "a" denotes highest quality. Estimates of K-line intensities, listed in paper I, have not been continued. The capital

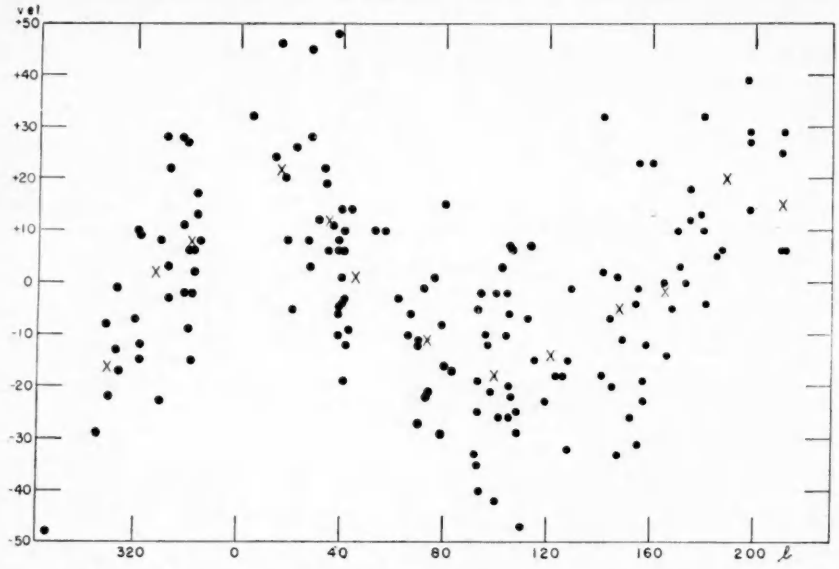

FIG. 3.—K-line velocities corrected for the sun's motion and for $\cos^2 b$. × = normal points

letters following the velocities show the agreement between the measured velocities of the two spectrograms, as follows:

Letter.....	A	B	C	D	E	F
P.e. (km/sec)..	0–±4.0	±4.1–±8.0	±8.1–±12.0	±12.1–±16.0	±16.1–±20.0	>20.0

The probable error is taken as one-third the difference of the two measures, as in paper I. Where no capital letter is listed, the published velocity depends on only one spectrogram. Where no K-line velocity is given, the spectrograms are too weak to show it. An "R" in the last column refers to a remark in the notes following the table.

DISCUSSION

Since the material is incomplete as regards magnitudes and colors, an analysis of the data has not been attempted. Some of the observations are shown graphically. These plots include the observations from both papers, I and II. Main-sequence stars later than B5 are omitted. The inhomogeneity of the observational material may introduce systematic effects.

Figure 1 shows the distribution of spectral types along the galactic plane. There is an apparent concentration of earlier types toward the galactic center and a minimum of Bn stars in that direction. In Figure 2 are plotted the stellar velocities corrected for the sun's motion among the near-by stars and for the $\cos^2 b$ term of galactic rotation. The

TABLE 3

NORMAL VELOCITIES*

STELLAR			K LINE		
l	Stars	Vel. (Km/Sec)	l	Stars	Vel. (Km/Sec)
310	9	−23	310	6	−16
327	12	0	328	11	+ 2
342	14	+16	342	13	+ 7
15	6	+19	17	7	+21
33	17	+22	36	18	+11
46	10	+ 4	46	10	+ 1
73	13	−29	74	14	−11
100	23	−31	100	25	−18
121	8	−13	122	9	−14
147	10	− 6	148	12	− 5
164	8	+ 2	166	12	− 1
195	12	+42	189	10	+20
212	3	+16	211	4	+15
234	7	− 1			

* The individual velocities are corrected for the sun's motion and for $\cos^2 b$.

153 velocities with probable errors less than 12 km/sec are shown. In forming the normal points, velocities with probable errors in classes A, B, and C are given weights 4, 3, and 2, respectively. Figure 3 is a similar plot for 153 K-line velocities from the two papers. A few stars with strong K lines are included for which only one spectrogram was obtained. The normal velocities are listed in Table 3.

RECENT PROGRESS IN ASTROPHYSICS

AN UPPER LIMIT FOR THE MASS OF THE LUNAR ATMOSPHERE

Most astronomers are of the opinion that the moon is completely devoid of any atmosphere. Russell, Dugan, and Stewart[1] estimate that the barometric pressure on the moon probably does not exceed 10^{-5} of that of air at the surface of the earth. The principal evidence on this point is given by the absence of any obscuration or blurring of the formations seen near the edge of the moon. Others have argued that previous observational tests were not sufficiently accurate to exclude an atmosphere whose density at the surface of the moon is less than about 10^{-4} or 10^{-5} of the atmosphere of the earth.[2] The kinetic theory of atmospheric dissipation does not remove the uncertainty: the heavier gases can probably remain on the surface of the moon long enough to permit the existence of a very tenuous atmosphere at the present time.

An important contribution toward the solution of this question has just arrived in the form of a paper by Professor V. G. Fessenkoff entitled "On the Mass of Moon's Atmosphere."[3] The purpose of this paper is to develop a more refined method of estimating the amount of gas on the moon's surface than has been available in the past. Fessenkoff points out that the older methods were inaccurate. They depended essentially upon measures of the general or selective absorption of starlight near the edge of the moon or of the effect of horizontal refraction caused by a hypothetical atmosphere. Fessenkoff mentions observations of purported cloud formations by F. Vaughn and by W. H. Pickering, but he considers them to be inconclusive and perhaps produced by peculiar properties of diffuse reflection at the surface of the moon.

The new method is extremely simple. Fessenkoff examined with a piece of polaroid filter the faintly luminous area near the center of the moon, on the dark side of the terminator, at first and at last quarters. The surface brightness of this area is considerable, and the test for polarization by rotating the polaroid presents no great difficulty. Fessenkoff found no change in the surface brightness as the polaroid was turned, and he concludes—presumably on the basis of laboratory tests—that the ratio of the brightnesses at radial and at tangential orientations of the axis of the polaroid cannot be in excess of $n = 1.04$.

If the diffuse light which Fessenkoff observed had been produced in its entirety by "twilight" in the lunar atmosphere, the polarization should have been complete, because the phase angle at first and at last quarters is 90°. But the light is mostly caused by scattering in the earth's atmosphere—that is, by an ordinary lunar halo, and perhaps by a small amount of the earth-lit surface of the moon. This background illumination should be almost completely unpolarized. If we designate this background surface brightness as b and the hypothetical polarized light of the lunar twilight as c, we have

$$n = \frac{\frac{1}{2}b + c}{\frac{1}{2}b} \quad \text{or} \quad \frac{c}{b} = \frac{1}{2}(n - 1).$$

If L is the amount of solar radiation received by a unit of surface on the moon oriented at right angles to the radiation, ρ is the density of the lunar atmosphere, and μ is the co-

[1] *Astronomy*, **1**, 170, Boston: Ginn & Co., 1926.

[2] R. K. Marshall, *Pop. Astr.*, **51**, 421, 1943.

[3] *Astr. J. Soviet Union*, Vol. **20**, No. 2, p. 1, 1943.

efficient of scattering, then the surface brightness of an element of the moon located on the dark side of the terminator is

$$\mu L \rho dh .$$

Integrating this over the entire thickness of the lunar atmosphere and designating by m the mass of a vertical column of unit cross-section, we find that

$$\mu L m = \tfrac{1}{2} (n - 1) b .$$

The quantity b was determined by Fessenkoff in the following manner. He measured the surface brightness of the sky in the vicinity of the sun and found it to be twice that of a standard plane white surface illuminated by the sun. He next computed the ratio between the surface brightness of the solar halo and that produced by a source whose stellar magnitude is 14.17 mag. fainter than the sun but which has a similar distribution of light over its surface. He then computed the difference arising from the facts that the lunar observations were made near the terminator and the moon was at first or at last quarter. Since the surface brightness of the solar halo in terms of the brightness of the standard surface depends upon the scattering power of air and upon the mass of the terrestrial atmosphere, he obtains an expression for b which involves this mass, M. It is assumed that the coefficients of scattering, per unit mass, in the atmosphere of the moon, μ, and in the atmosphere of the earth, μ_1, are the same. The final result is an expression for the ratio of the two masses

$$\frac{m}{M} = 0.196 \times 10^{-4} (n - 1) .$$

From the observations, $n - 1 < 0.04$. Hence,

$$\frac{m}{M} < 10^{-6} .$$

OTTO STRUVE

A. UNSÖLD'S WORK ON THE SPECTRUM OF THE B0 STAR τ SCORPII

During the last two years the *Astrophysical Journal* has printed comprehensive reviews of important astrophysical papers which are not generally accessible to American scientists. Among the least accessible papers are three contributions by A. Unsöld which appeared in Volumes **20** and **21** of the *Zeitschrift für Astrophysik* and were dated by the author April 23, 1941, June 7, 1941, and January 19, 1942. The first two arrived in this country some time before December, 1941, in the form of page proofs; the last has been made available to me through the Committee for the Distribution of Astronomical Literature, which was organized by the American Astronomical Society.

The purpose of Unsöld's work was to determine the chemical composition of the reversing layer of a main-sequence star of spectral class B. Furthermore, Unsöld hoped to obtain a picture of the physical conditions in the outer layers of such a star and to determine the temperature, the electron pressure, the total gas pressure, and the surface gravity. Such an investigation had previously been attempted only in the case of the sun, for which Russell's well-known paper and, more recently, B. Strömgren's work[1] have provided the necessary data. Since the appearance of Unsöld's work, several other stars have been discussed in a similar manner by Greenstein (α Carinae) and Aller (α Canis Majoris and γ Geminorum). Strömgren's paper was not known to Unsöld until his own investigation had been completed. The information which may be obtained from a B star differs in important ways from that provided by the sun. The B star's spectrum shows strong lines of several light elements, such as *He* and *Ne*, which are not observable in the sun. Hence the B star provides the abundances of a group of elements which re-

[1] *On the Chemical Composition of the Solar Atmosphere: Festschrift for E. Strömgren*, Copenhagen, 1940.

main undetermined in the work of Russell and of Strömgren. The atomic transitions which correspond to the lines of a B-type star take place between relatively high levels. For many of these the oscillator strengths may be estimated from the known hydrogen values.

The material used by Unsöld consisted of five coudé spectrograms of τ Scorpii obtained at the McDonald Observatory in May, 1939. The dispersion of these spectrograms, taken on film, is 1.93 A/mm at λ 3930 and 2.64 A/mm at $H\gamma$. The definition of these spectrograms was not particularly good in all regions because the curvature of the plateholders had not then been accurately determined. But the dispersion is so large that sections of fine definition yielded many important lines. For the ultraviolet region Unsöld used four McDonald Cassegrain quartz spectrograms whose dispersion is 40 A/mm at λ 3934. These plates are of the finest quality. All spectrograms were standardized with a tube sensitometer equipped with several filters. The calibrations of the sensitometer marks and their effective wave-length ranges were accurately determined by Unsöld. The exposure times were made long enough to avoid any serious photometric errors arising from lack of equality of the exposure times.

The principal result of Unsöld's first paper is a table of several hundred equivalent widths and about one dozen central intensities of all measurable lines between λ 3323 and λ 6563. A comparison with the results by E. G. Williams for a considerable number of lines suggests that the equivalent widths obtained with the smaller dispersions are about 20–25 per cent larger than those obtained with the coudé dispersion. The central intensities listed are those which are not appreciably affected by the instrumental distortion of the line contours.

The second paper starts with a discussion of the central intensities. The central absorptions (1 *minus* central intensity) of all lines measured—*H* and *He* I—are almost identical: they cluster around $R_c = 45$ per cent of the intensity of the adjoining continuous spectrum, irrespective of whether the line is one of *H* or of *He* I and irrespective of whether the line has a large *f*-value ($H\beta$) or a small *f*-value (*H* 10). There may be a small change with wave length. Unsöld suggests that for λ 4860 we have $R_c = 40$ per cent and for λ 4000, $R_c = 45$ per cent. Although Unsöld does not say so, there are several other lines which are slightly affected by the instrumental distortion but whose contours can be corrected for the known properties of the spectrograph. It is probable that all such lines would conform to the relation established by Unsöld. For the fainter lines it is, of course, impossible to establish reliable instrumental corrections.

All the lines used by Unsöld for the determination of R_c correspond to transitions between high-energy levels. It is reasonable that these lines are produced in the manner described as "true absorption" by Schwarzschild and as "local thermodynamic equilibrium" by Milne. Hence the central intensities of these lines are not zero, as they would be for "pure scattering," but correspond to the boundary temperature T_0 of the star or to the intensity of the continuous spectrum at the extreme limb of the star. The central intensities of the lines determine the limb darkening of τ Scorpii.

If the central line intensities are interpreted in this way, they can be used to determine the value $\bar{\kappa}/\kappa_\nu$, namely, the ratio of the Rosseland mean of the continuous absorption coefficient to the particular value of the absorption coefficient which corresponds to that ν at which the central intensities have been measured. The intensity of the continuous radiation observed at the surface of the star is

$$I(0, \theta) = \int_0^\infty J(\tau)\, e^{-\tau_\nu \sec\theta} d\tau_\nu \sec\theta .$$

The *Ergiebigkeit* $J(\tau)$ depends upon the temperature, which in turn increases with $\tau = \int \kappa dt$. The intensity can be shown to depend upon the ratio $\bar{\kappa}/\kappa_\nu$, except at the limb, where $\theta = \pi/2$ and the radiation depends only upon the limiting temperature T_0. When

$\bar{\kappa}/\kappa_\nu \ll 1$, the continuous radiation at the center of the disk corresponds to a temperature which is not much greater than T_0. Hence, the central intensities of the lines would be high; the darkening at the limb is small. On the other hand, an increase in $\bar{\kappa}/\kappa_\nu$ corresponds to a deepening of the absorption lines. Unsöld has made use of the well-known tables by G. Burkhardt[2] which give the ratio of the radiative flux $F\nu$, or of the average intensity of the disk of the star, to the flux in the center of a very strong absorption line $F_{\nu,0}$ which corresponds to the intensity of the continuous radiation at the limb. The tables (which were somewhat extended by Dr. Burkhardt for the purpose of Unsöld's investigation) give $F_\nu/F_{\nu,0}$ as a function of $\alpha = h\nu/kT_e$ and of $\bar{\kappa}/\kappa_\nu$. The quantity α is approximately 1.2 for the values $\lambda = 4860$ and $\lambda = 4000$ and for the temperature $T_e = 27{,}000°$ of a B0 star. The ratio $F_\nu/F_{\nu,0}$ is equal to the observed quantity $1/(1 - R_c)$. Hence, Unsöld was able to derive $\bar{\kappa}/\kappa_\nu = 2.4 \pm 0.3$. This ratio may be compared to Unsöld's theoretical ratio $\bar{\kappa}/\kappa_\nu < 0.5$, which he had previously derived for a reversing layer consisting mostly of hydrogen. The discrepancy between the observed and the predicted values of $\bar{\kappa}/\kappa_\nu$ constitutes one of the most remarkable results of the second paper in the series. It shows that the observed lines, shallow as they are, are not shallow enough to satisfy the elementary theory derived for a reversing layer consisting mostly of hydrogen. Incidentally, a somewhat similar result has since been obtained by Greenstein and by others for several A-type stars. The solution of this interesting problem constitutes the major portion of Unsöld's third paper.

In the remainder of the second paper he discusses in great detail the various elements observed in τ Scorpii. This section occupies 43 pages.

The H lines yield the value $N_{0,2}H$, the number of atoms in the neutral state and in the second energy level. For the higher members of the series the absorbing layer may be regarded as "thin," and $N_{0,2}H$ is found from the expression

$$A_\lambda = \frac{\pi e^2}{mc^2} \lambda^2 f N_{0,2}H; \qquad \log N_{0,2}H = 15.78 .$$

An independent confirmation is obtained from the drop at the Balmer limit:

$$\log N_{0,2}H = 15.97 .$$

Unsöld adopts $\log N_{0,2}H = 15.90$. He next determines the electron density from the number of observable H lines, using for this purpose the formula of Inglis and Teller:

$$\log N_e = 14.55 .$$

Another value of N_e is obtained from the Stark broadening of $H\beta$, $H\gamma$, and $H\delta$. If the normal field (in the terminology of Holtsmark) is

$$F_0 = 2.61\, e\, N^{2/3} \text{ el. st. units} ,$$

then in the wings the absorption coefficient of a broadened line is

$$k(\Delta\lambda) = C \frac{F_0^{3/2}}{\Delta\lambda^{5/2}} .$$

The constants C depend upon the known f-values and upon the quantities $\Sigma I_\kappa n_\kappa^{3/2}$, which measure the intensities of the Stark components multiplied by certain integers involving the quantum numbers of the two levels. The values of C are given in Unsöld's book. The optical depth at a certain distance $\Delta\lambda$ from the center of the line is

$$x_\nu = k(\Delta\lambda)\, N_{0,2}H .$$

[2] *Zs. f. Ap.*, **13**, 56, 1936.

Unsöld makes use of the semiempirical expression extensively used by him in previous work,

$$R = \left\{ \frac{1}{x_\nu} + \frac{1}{R_c} \right\}^{-1} ,$$

and substitutes $R_c = 0.45$, $\log N_{0,2}H = 15.90$. Integration then gives

$$A_\lambda = \int_{-\infty}^{+\infty} R \, d(\Delta\lambda) .$$

Unsöld justifies the use of $N = 1.5N_e$ and obtains $\log N_e = 14.40$. The mean of the two determinations is $\log N_e = 14.48$.

For the lines of *He* I Unsöld has proceeded essentially as in the case of *H*. He has determined $\log NH[2^3P^o]$ as for a thin layer and has then plotted these values for each series against the principal quantum number of the upper term. These curves tend to level off for large n, as the case of a thin layer is actually approached with increasing quantum number. It must be pointed out that the results are not very definite: different series approach different limiting values of $NH[2^3P^o]$. In particular, Unsöld remarks that the two series $2^3P^o-n^3D$ and $2^1P^o-n^1D$ give smaller values than the other series. But there is no great difference between those series whose lower terms are metastable and those whose lower terms have strong transitions to term 1^1S. Unsöld concludes that there are no effects of dilution of radiation. He adopts an average limiting value

$$\log NH[2^3P^o] = 14.95 .$$

It is my impression that the divergence of the individual series in Unsöld's Figure 5 (our Fig. 1) constitutes one of the most interesting unsolved problems in astrophysics. It is unimportant for the determination of the *He* abundance—Unsöld's principal task—but it promises to throw new light upon the puzzling question of the *He* I anomaly which has only in part been solved by Goldberg.[3]

Although Unsöld does not mention this question, it may be of interest to discuss it briefly. It was found many years ago that the *He* I lines $2^1P^o-n^1D$ decrease in intensity more rapidly than the lines $2^3P^o-n^3D$, as we move from subdivision B2 toward hotter or toward cooler stars. This phenomenon is most pronounced in the O-type supergiants. The O-type main-sequence stars show it somewhat less conspicuously. In the cooler stars, of type B8, there is no appreciable difference between supergiants and main-sequence stars. In stars with shells, like ϕ Persei, ζ Tauri, and γ Cassiopeiae as observed in 1940, the ratios of the *He* I intensities are greatly influenced by the dilution effect. The most notable feature in these stars is the relative strength of *He* I 3965 ($2^1S-4^1P^o$). The members of this series are not much broadened by Stark effect. The discussion by Unsöld suggests that there is no striking enhancement of this series in τ Scorpii and, consequently, no dilution effect. This agrees with the conclusion of Goldberg, who used Williams' measures in many B stars. In favor of the interpretation of the *He* I anomaly as an effect of the curve of growth is the remarkable fact that the observed maximum ratio (*He* I triplets/*He* I singlets) is about 8, according to Williams, while the ratio of the corresponding *f*-values is 10. There can be no question now that, after the shell stars have been excluded, the *He* I anomaly is produced by the saturation of some *He* I lines at and near subdivision B2. But it is not yet clear whether this will fully account for the difference between supergiants and main-sequence stars in the O and B0 subdivisions. Nor is there any certainty that the limiting value of $\log NH[2^3P^o]$ for large n is the same in Unsöld's diagram for the three series $2^1S-n^1P^o$, $2^1P^o-n^1D$, and $2^3P^o-n^3D$. It would be of great interest to examine a similar diagram for an early-type supergiant like 19 Cephei. The difficulty in dealing with the dilution effect has been that we have been compelled, in the past, to rely upon comparisons of shell spectra with spectra of

[3] *Ap. J.*, **89**, 623, 1939.

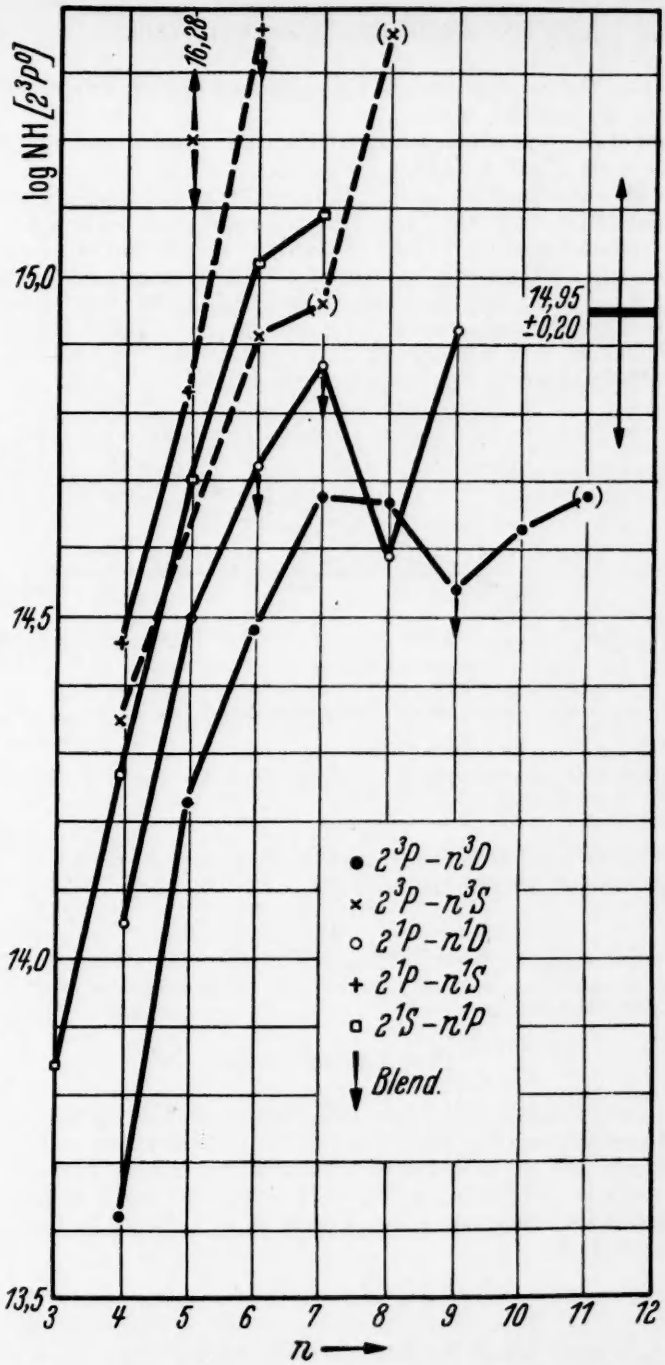

FIG. 1.—The ordinates are the logarithms of the numbers of the helium atoms in state 2^3P^o, computed from the observed equivalent widths of lines of different series under the assumption of a thin absorbing layer. The abscissae are principal quantum numbers n. Since the stronger *He* I lines are saturated near their centers, the assumption is not correct; and the points representing each series should asymptotically approach the same limiting value for large n. Unsöld adopts for this value $\log NH[2^3P^o] = 14.95 \pm 0.20$. But the individual series differ appreciably; for example, series (2^3P^o–n^3S) gives a lower limiting value than series (2^3P^o–n^3S). The meaning of these discrepancies is not clear. It probably does not seriously affect the adopted value of $NH[2^3P^o]$.

normal supergiants. The question has not been answered whether or not in a supergiant the dilution effect is completely absent.

The discussion of *He* II, which is greatly influenced by Stark broadening, follows that of *H*. The result is $\log N_{1,3}H \geqslant 12.64$.

For the other elements Stark broadening is unimportant and Unsöld's procedure consists in (*a*) the determination of the *f*-values from the spectroscopic data for the various terms, (*b*) the computation of $\log (1/R_c) \cdot (f/\Delta\omega_D)$, (*c*) the plotting of a curve of growth giving $\log (1/R_c) \cdot (A_\lambda/2\Delta\lambda_D)$ as a function of $(1/R_c) \cdot (f/\Delta\omega_D)$, and (*d*) the determination of $\log (1/R_c) \cdot (NHf/\Delta\omega_D)$ and $\log NH$ by obtaining the best possible fit of the observed curve with a theoretical curve computed for the required approximate temperature. The tables are very complete, and the extensive data on *f*-values should be of great value to other workers in this field.

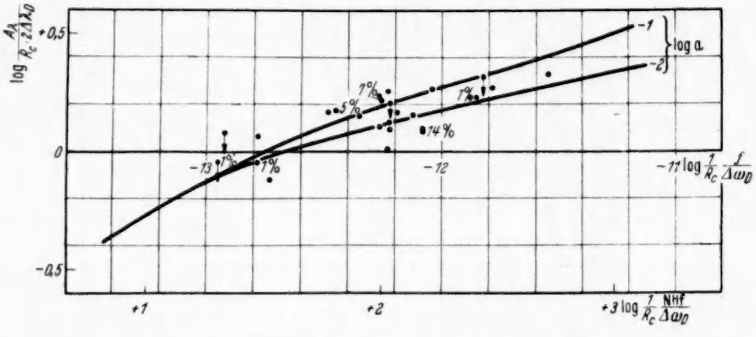

FIG. 2.—The curve of growth as determined by the lines of *O* II. The diagram is used to determine the damping constant.

The lines of *O* II are numerous enough and strong enough to permit a determination of the damping constant. Unsöld finds (Fig. 2):

$$\log a = \log \frac{\gamma}{\Delta\omega_D} = -1.5 .$$

There is no noticeable turbulence:

$$\xi_t < 2.6 \text{ km/sec} .$$

The next step in the discussion is to determine the temperature, by assuming the value $\log N_e = 14.48$ derived from the Stark effect of the hydrogen lines and by making use of the ionization equation for those elements for which two stages of ionization had been observed. The result is $T = 28{,}150° \pm 750°$ K. This temperature corresponds to a mean value of τ at which the absorption lines are formed. It is related to the effective temperature by the relation

$$T^4 = \tfrac{3}{4} T_e^4 \{ \bar{\tau} + q(\bar{\tau}) \} .$$

This value of T, combined with N_e, gives $P_e = 3.07 \pm 0.25$.

The ionization equation can next be used to determine those values of $N_r H$ which had not been observed. The sum of all these values for each element gives the relative abundances. The total gas pressure at the bottom of the atmosphere is

$$P_g = g \Sigma N H \mu m_H ,$$

and the mean pressure is approximately

$$\bar{P}_g \approx \tfrac{1}{2}P_g = 2P_e .$$

Hence,

$$4P_e = g\Sigma N H \mu m_H ,$$

from which Unsöld finds

$$\log g = 4.93 \pm 0.40 .$$

Russell's[4] mean value for main-sequence B stars is $\log g = 3.90$. Hence, τ Scorpii must be regarded as a star of lower-than-average luminosity. The spectrographic value agrees well with the known absolute magnitude of the star, -2.4 mag. The latter gives $\log g = 4.4$.

The abundances derived by Unsöld for τ Scorpii are shown in Figure 3, together with Goldschmidt's abundances in meteorites, Russell's values for the sun, and Bowen and Wyse's values for the planetary nebula NGC 7027.

The high abundances of helium and of neon are particularly interesting. The ratio $\log (H/Mg) = 4.24$ demonstrates the high abundance of hydrogen with respect to the metals. Unsöld finds

$$\text{(by numbers of atoms)} \quad H:He:R = 85:15:0.24 ,$$
$$\text{(by mass)} \quad H:He:R = 57:40:3 .$$

The third paper of the series is devoted entirely to a discussion of the continuous spectrum of τ Scorpii. Unsöld had found in the second paper that the central absorptions of all strong lines are of the order of $R_c = 45$ per cent. The usual theory of the continuous spectrum then leads to a determination of κ/κ_ν. This latter value can also be computed if we know the various mechanisms of continuous absorption in the reversing layer of τ Scorpii. The value determined from the observations was 2.4; that determined by the theory is of the order of 0.5. The two values are not compatible, and an explanation must be found for the discrepancy. One possibility would have been the existence of an unknown source of continuous absorption. With the proper distribution in ν such an additional mechanism could increase the value of κ/κ_ν and bring about a reconciliation of the observations with the theory. Unsöld made every effort to discover such a hidden mechanism but came to the conclusion that it does not exist.

He next investigated whether the various approximations in the theory of the continuous spectrum could account for the discrepancy. The Kirchhoff-Planck function $E(\bar{\tau})$ is expressed in the following manner:

$$E(\bar{\tau}) = \tfrac{3}{4}F\{\bar{\tau} + q(\bar{\tau})\} .$$

The average intensity for the entire star disk, F_ν, is then found from

$$\tfrac{1}{2}F_\nu = \int_0^\infty E_\nu(\bar{\tau})\, K_2(\tau)\, d\tau ; \qquad K_2(\tau) = \int_1^\infty \frac{e^{-w\tau}}{w^2}\, dw .$$

The optical depths $\bar{\tau}$ and τ are related by

$$d\tau = \frac{\kappa_\nu}{\bar{\kappa}}\, d\bar{\tau} .$$

In the center of a strong absorption line $\kappa_\nu/\bar{\kappa} \to \infty$ and

$$\tfrac{1}{2}F_{\nu,\,0} = E_\nu(0) \int_0^\infty K_2(\tau)\, d\tau = \tfrac{1}{2}E_\nu(0) .$$

[4] *Ap. J.*, **78**, 239, 1933.

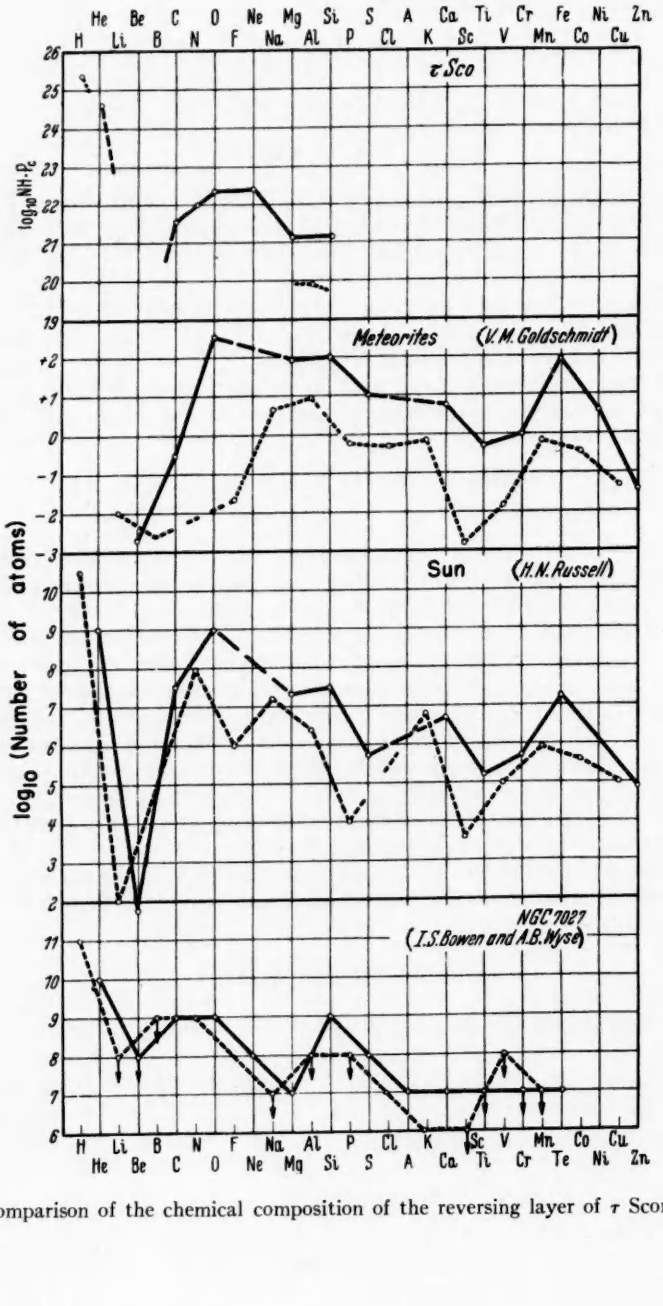
He Be C O Ne Mg Si S A Ca Ti Cr Fe Ni Zn
H Li B N F Na Al P Cl K Sc V Mn Co Cu
τ Sco
log10 NH·Pc
Meteorites (V. M. Goldschmidt)
Sun (H. N. Russell)
NGC 7027
(I. S. Bowen and A. B. Wyse)
log10 (Number of atoms)
H Li B N F Na Al P Cl K Sc V Mn Co Cu
He Be C O Ne Mg Si S A Ca Ti Cr Te Ni Zn

FIG. 3.—Comparison of the chemical composition of the reversing layer of τ Scorpii with that of other sources.

The observed central intensity is

$$1 - R_c = \frac{F_{\nu,0}}{F_\nu}.$$

For the theoretical computation of the ratio $F_{\nu,0}/F_\nu$ a knowledge of $q(\bar{\tau})$ is required. Following the usual practice, Unsöld had made the following assumptions:

1. The effect of scattering is negligible, as compared to that of absorption.
2. κ_ν/κ is independent of the depth.
3. In the computation of $q(\bar{\tau})$ the variation of κ_ν with ν may be neglected.

With these assumptions the approximations of Eddington and of Milne give

$$q(\bar{\tau}) = \tfrac{2}{3}.$$

Exact values, with the same assumptions, were obtained by Hopf for $q(0)$ and $q(\infty)$. With the same assumptions Unsöld found that the effective optical depth with respect to κ_ν, at which the lines of τ Scorpii are formed, is

$$\tau_0 = R_c = 0.40.$$

The same optical depth with respect to $\bar{\kappa}$ is, of course,

$$\bar{\tau}_0 = \tau_0 \frac{\bar{\kappa}}{\kappa_\nu} = 1.00.$$

The quantum theory of the absorption coefficient (shown in the form of two convenient diagrams for τ Scorpii and for a giant of similar temperature) gives for $\kappa_\nu/\bar{\kappa}$ at several wave lengths:

λ	3150	3650 −	3650 +	4700
$\kappa_\nu/\bar{\kappa}$	2.85	3.55	1.63	2.26

and $\bar{\tau}_0 = 0.055$. These values are not compatible with those obtained from the observations. Unsöld attributes this to assumption (3) in the computation of $q(\bar{\tau})$ and finds the answer to his puzzle in papers by Chandrasekhar[5] and by Hopf.[6] As was first pointed out by Chandrasekhar, the blanketing effect produced by the absorption lines in the solar spectrum produces a marked change in $q(\bar{\tau})$ and, consequently, also in the ratio $F_{\nu,0}/F_\nu$. In τ Scorpii the blanketing effect is produced by the strong Lyman continuous absorption, together with continuous ultraviolet absorption of *He* and He^+. Following the methods of Chandrasekhar and of Hopf, Unsöld has computed $q(\bar{\tau})$ as modified by the blanketing effect and has obtained new values for $F_{\nu,0}/F_\nu$ which agree perfectly with those derived from the observed central intensities of the lines in τ Scorpii.

It may be concluded that the theory of the continuous absorption in a star like τ Scorpii is now adequately known. It consists of the continuous absorptions of *H*, *He*, and He^+ and of Thomson scattering by free electrons. It is of fundamental importance that the blanketing effect must be taken into consideration for the computation of $q(\bar{\tau})$ and hence for the distribution of temperature with $\bar{\tau}$. As Unsöld remarks, the high opacity of the reversing layer in the region of the Lyman continuous absorption acts as a barrier against the outward-moving flux of radiation. At the same time the outward radiation of the star from the boundary must correspond at least to the black-body radiation for T_0. Radiative equilibrium can be maintained only by a lowering of T_0 if the effective temperature T_e is given. This means that the blanketing effect will tend to make the central intensities smaller than they would be without this effect.

OTTO STRUVE

[5] *M.N.*, **96**, 21, 1936.

[6] *M.N.*, **96**, 522, 1936.

NOTES

NOTE ON THE EPOCH OF THE NEXT SUNSPOT MAXIMUM

After the last sunspot maximum, which occurred in April, 1937, solar activity decreased so slowly that Wolf's smoothed relative numbers did not fall below a quarter of their last maximum value (119.2) until July, 1942. Such a slow decrease was predicted in 1940 by the writer;[1] the probability of this prediction, as computed[2] from the probability laws of sunspot variations which I published in the September, 1942, issue of this *Journal*, was very high, viz., 0.98.

In view of the slow decline of this sunspot cycle, one could easily suppose that the interval between the last sunspot maximum and the next one would be relatively long. The probability laws of sunspot variations, however, do not support this supposition; they rather indicate that this interval will be shorter than its average value of 11.1 years. This result can be obtained in the following way (the notations are the same as those in my previous paper on probability laws of sunspot variations, as mentioned above):

Since the "period of low activity" began in July, 1942, the interval between July, 1942, and the epoch of the next sunspot maximum will be equal to $t_l + t_r$, where t_l denotes the length of the period of low activity preceding the new sunspot cycle and t_r the length of the reduced period of rising in the new sunspot cycle. If t_l and t_r are expressed in months, the interval from the last maximum to the next one will be equal to $63 + t_l + t_r$, because 63 months had elapsed from April, 1937, to July, 1942. Since 11.1 years are equal to about 133 months, it follows that, if $t_l + t_r < 70$, the next sunspot maximum would be distant from its predecessor by less than 11.1 years. If prob $[t_l + t_r < 70]$ denotes the probability that in the new spot cycle $t_l + t_r$ will be less than 70 months, the probability laws of sunspot variations yield the following equation:[3]

$$\text{prob}\,[t_l + t_r < 70] = \tfrac{1}{2} + \tfrac{1}{2} \sum_{\delta=0}^{\infty} \left\{ P(\delta) \sum_{d=0}^{\infty} P(d)\, \text{erf}\,(0.36d + 0.144\delta + 0.184) \right\},$$

where the function $P(x)$ is defined by

$$P(x) = \text{erf}\,(0.16x + 0.08) - \text{erf}\,(0.16x - 0.08).$$

As $P(x)$ decreases rapidly when x increases, only a few terms of the sums in the above equation need be calculated. The calculation yields

$$\text{prob}\,[t_l + t_r < 70] = 0.95.$$

Thus one can expect with the high probability of 19 to 1 that the interval from the last sunspot maximum to the next one will be shorter than its average value of 11.1 years, i.e., that the next maximum will occur before May, 1948.

W. GLEISSBERG

ISTANBUL UNIVERSITY OBSERVATORY
January 1944

[1] *Observatory*, **63**, 218, 1940. [2] *Pub. Istanbul U. Obs.*, No. 15, p. 8, 1941.

[3] For brevity the proof of this equation is not given here. The easiest way to deduce it from the probability laws of sunspot variations is to make use of the reasoning in *Pub. Istanbul U. Obs.*, No. 15, 1941.

REVIEWS

Marine and Air Navigation. By JOHN Q. STEWART and NEWTON L. PIERCE. Boston: Ginn & Co., 1944. Pp. xii+472. $4.50.

In the actual welter of new books on navigation appearing currently, this outstanding work by Stewart and Pierce providentially comes at the climactic moment when the United States of America is being forced to take its position as the foremost air and sea power. It seems inevitable that we shall need to train and employ, perhaps for generations, great numbers of navigators for our navy, merchant marine, and air fleets.

Because of its scope, its mathematical rigor, its "complete coverage," its distinctive character, and its literary value, this book should and will be used as a text for full-year college courses in liberal arts. Career men and women in navigation and others will take such courses in their general educational programs. The book will doubtless be adopted for many wartime training classes.

The book is well produced. Scores of beautiful halftone plates and hundreds of graphs and figures on excellent paper illuminate the text. It is the largest book on navigation which the writer has seen, and every part is significant. It is intensely modern. The traditional mathematics of works on navigation is omitted, except for defining essential quantities. Every operation has been reduced to the use of tables and graphical methods.

The observations of celestial objects for the determination of the latitude and longitude of the observer are the same for sea, air, and land. The authors recognize this and write accordingly. From there on, they proceed to teach and illustrate the multifarious additional problems and practices which belong to each field. These naturally differ greatly. No stronger evidence of completeness, rigor, and practicalness of this notable book needs to be given than the following: A full page of acknowledgements lists specifically 79 persons—from the present Secretary of the Navy, through the ranks of naval officers and authors, to typists and readers. Not only has the book survived the resulting veritable barrage of criticism, checking, and suggestion, but it has appeared as a book which even the layman can read with enthusiastic interest.

The tang of the sea is there. The vivid personality of the salty seaman is there. The tacit remonstrance is there against the reduction of the ancient art, romance, and philosophy of seafaring, and the very modern art of airfaring, to a set of colorless impersonal tables.

Stewart and Pierce have written a book which will inevitably become a classic. It is recommended without any hesitation to everyone who has an interest in any branch of navigation.

OLIVER JUSTIN LEE

Dearborn Observatory

Basic Marine Navigation. By BART J. BOK and FRANCES W. WRIGHT. Boston: Houghton Mifflin Co., 1944. Pp. viii+421. Book, $4.50; kit, $1.70.

Up-to-date texts on navigation are highly welcome to both teachers and students. One of the most recent, *Basic Marine Navigation*, by Bok and Wright, answers all the requirements of a very satisfactory textbook and should provide much relief to those struggling with texts either inadequate or poorly suited to the usual college background.

Basic Marine Navigation is a thorough, well-arranged treatment of all phases of marine navigation. It is well illustrated, and the style is clear and simple. Navigational aids (with good illustrations), charts and publications, the lead and the log, the compass and its errors, compass compensation, tides and currents (with detailed, step-by-step explanation of the tables), piloting, dead reckoning, maneuvering board (brief treatment), marine meteorology (good, short explanation), the sextant, celestial navigation, time and the nautical almanac, navigation by the sun and stars, the astronomical triangle and its solution by HO 208, 211, and 214 are the sub-

jects covered. A chapter on emergency and lifeboat navigation is a unique feature of the book and contains the best treatment that I have seen. The book displays the trends of modern navigation; current practice, rather than involved theory, is emphasized. A kit of practice chart material is also furnished.

The book seems to me to be one of the three best texts now available. The others are: *Marine and Air Navigation*, by Stewart and Pierce (Ginn & Co.), and recent editions of *Navigation and Nautical Astronomy*, by Dutton (United States Naval Institute). In my opinion, the only possible criticism—and it is not a serious one—is the complete absence of air navigation from any navigation text, whether or not its aim is, as in this case, to specialize entirely upon the marine aspect of the subject. Cases often arise in which the marine navigator has to be acquainted with air navigation. Furthermore, many of the methods used in air navigation are becoming part of marine navigation. Bubble octants and air almanacs, for example, are often useful aboard surface vessels and in some cases may be used for surface navigation almost as much as the conventional marine methods.

It is understood, of course, that the above opinions are those of the writer and are not necessarily those of the Navy Department.

J. CUFFEY
Lieutenant, U.S.N.R.

United States Naval Academy